5-2016

# TRIM24 orchestrates metabolic reprogramming and EMT in Breast Cancer

Kaushik Thakkar

# TRIM24 ORCHESTRATES METABOLIC REPROGRAMMING AND EMT IN BREAST CANCER

**By**

**Kaushik Thakkar, MS**

APPROVED:

_____

**Michelle C. Barton, PhD**

_____

**Pierre McCrea, PhD**

_____

**Sendurai Mani, PhD**

_____

**Xiaobing Shi, PhD**

_____

**Jianping Jin, PhD**

_____

APPROVED:

_____

**Dean, The University of Texas**

**Graduate School of Biomedical Sciences at Houston**

**TRIM24 ORCHESTRATES METABOLIC REPROGRAMMING AND EMT IN BREAST CANCER**

A

**THESIS (DISSERTATION)**

Presented to the Faculty of

The University of Texas

Health Science Center at Houston

and

The University of Texas

MD Anderson Cancer Center

Graduate School of Biomedical Sciences

in Partial Fulfillment

of the Requirements

for the Degree of

**DOCTOR OF PHILOSOPHY**

By

**Kaushik Thakkar, M.S.**

Houston, Texas

May 2016

# Dedication

To all my family, my mentors, my teachers, and my friends

for their love, teaching, and support.

## Acknowledgments

I would like to express my deepest gratitude to the many people who have helped me throughout my PhD education. Without their teaching, advice, encouragement and support, I would not have been able to complete my dissertation.

I am extremely thankful to my advisor, Dr. Michelle C. Barton, for the opportunity to learn and mature in experimental knowledge, critical thinking and communication. She has opened up many opportunities in my research, inspired and assisted me tremendously in the past five years. I am thankful for her patience, encouragement, and the freedom to pursue my research interest in her laboratory.

I would like to acknowledge members of my present and past committees, for their patience, guidance, scientific discussion, intuitive comments and time commitment: Drs. Pierre McCrea, Sendurai Mani, Xiaobing Shi, Jianping Jin, Don Gibbons and Jessica Tyler. I would also like to thank present and past members of Barton laboratory, who have assisted in my experiments, inspired my research, and encouraged me, especially when my goals seem impossible to accomplish. I would specially like to thank Drs. Srikanth Appikonda and Abhinav Jain, for their guidance and support throughout my PhD.

My gratitude is also extended to all my friends and collaborators. It is truly a great privilege to have the opportunity to work with them and become their friends. I sincerely thank Dr. Xiaohua Su, Dr. Avinash Venkatnarayan, Dr. Liem Pham, Dr. Martha Stampher, Erin Williams, Esmeralda Pena and Roxsan Manshouri for providing

reagents and expertise. Moreover, I would like to extend my special thanks to all my teachers, professors and friends who have given me excellent teaching, valuable advice and offered very strong support. I would specially like to thank Dr. Nilesh Dagia, for his guidance and mentorship, and for convincing me to pursue PhD in Biomedical sciences in the US as a career. I would also like to thank my friends in the Graduate school Atanu Paul, Sangita Pal, Aundrietta Duncan, Niza Nemkul, Amanda Haltom, Avinash Venkatnarayan, Mayur Gadkari, Shhyam Moorthy, William Munoz and Vinay Nath for their support and encouragement.

I am very grateful to every one in my graduate school (The University of Texas Graduate School of Biomedical Sciences), my department (MD Anderson Cancer Center, Department of Epigenetics and Molecular Carcinogenesis) and Genes and Development Graduate Program for providing me with the education, training and helping me in my study. I especially thank Center for Cancer Epigenetics, CPRIT, T. C. Hsu Memorial Fellowship, Seahorse and many other fellowship foundations and sponsors for giving me the opportunity to pursue my graduate study and my dream to find a cure for cancer.

Last but not least, I am deeply grateful to everyone in my family, especially my parents, my wife (Neha Tandon), my brother, my parents-in-law, my grand parents, my uncles, my aunts, and cousins for their unconditional love, care, advice, encouragement, and strong support. They shared my successes, happiness, and challenges along the way of my career and life. Without them, I would not have been able to complete this project and pursue my dream. There are not enough words or ways to express my deepest gratitude to each and every one of my family.

# TRIM24 orchestrates metabolic reprogramming and EMT in breast cancer

**Kaushik Thakkar, MS**

**Advisory Professor: Michelle C. Barton, PhD**

In this dissertation, I report the oncogenic functions of an epigenetic regulator Tripartite Motif Protein 24 (TRIM24) coupled with metabolic reprogramming and epithelial mesenchymal transition (EMT) in breast cancer. TRIM24 was first established by our laboratory as a previously unknown negative regulator of p53 via its RING domain, as a co-regulator of nuclear receptors and a PHD/Bromodomain reader of specific histone modifications. TRIM24 expression correlates with poor prognosis of breast cancer, but the mechanisms of TRIM24-mediated oncogenesis are unknown. In the first part of my thesis, I found that TRIM24 is aberrantly expressed in early stages of breast cancer progression. Ectopic expression of TRIM24 induces malignant transformation of immortalized human mammary epithelial cells (TRIM24-iHMECs) and efficient growth of intermediate to high-grade xenograft tumors.

TRIM24 induces gross metabolic changes in the iHMECs with increased glycolysis and TCA cycle along with glucose uptake. TRIM24 causes deregulation of c-Myc and p53, the two key players that regulate cancer metabolism. TRIM24 is directly recruited to the promoters of several metabolic genes such as *GLUT1*, *IDH1*, *IDH2* and *c-Myc*. Our hypothesis is that direct activation of various glucose metabolism genes by TRIM24 coupled with deregulation of key players of metabolism is critical for TRIM24-mediated oncogenic transformation in breast cancer.

TRIM24 is over-expressed in several cancers; however, a detailed analysis of how TRIM24 promotes tumorigenesis with progression to metastasis has not been elucidated. Prior to the metastatic progression of a tumor, cancer cells undergo a transition from an epithelial to a mesenchymal phenotype; termed as epithelial-mesenchymal transition (EMT). In the second part of my thesis, I found that TRIM24 is a driver of EMT in breast epithelial cells.

Upon TRIM24 over-expression in MCF10A cells, a mesenchymal-like change in the cellular morphology was observed. TRIM24-MCF10A cells exhibited marked decrease of E-cadherin and acquisition of various mesenchymal markers such as N-cadherin, fibronectin and vimentin. Similarly, upon TRIM24-knockdown in mesenchymal cells MDA-MB-231 and MDA-MB-468, there is reversal of EMT gene signature. Gene expression analysis of TRIM24-OE MCF10A cells further confirmed that EMT was among the top pathways that were enriched. Additionally, TRIM24 may be involved in direct transcriptional regulation of EMT genes as suggested by TRIM24-ChIP analysis and the presence of Histone H3 – K23 acetylation (H3K23ac) signature, for which the TRIM24-Bromodomain acts as a histone reader, at several EMT genes in MDA-MB-468 cells. We propose that aberrant expression of TRIM24 impacts a network of transcription regulatory factors and pathways to induce EMT and cancer metastasis.

For effective reduction of cancer mortality, it is very critical to intervene in the critical transition of non-invasive ductal carcinoma to extremely lethal invasive breast cancer. Our preliminary analysis suggests that TRIM24 plays a critical role in mechanisms involving both primary and metastatic cancer. Future studies will be focused to develop a better understanding of molecular mechanisms of TRIM24' oncogenic function and will pave the way for developing therapeutic opportunities by targeting TRIM24.

# Table of Contents

## List of Figures

## List of Tables

## List of Appendices

## List of Abbreviations

| | |
|---|---|
| 2-NBDG | 2-(N-(7-nitrobenz-2-oxa-1,3-diazol-4-yl)amino)-2-deoxyglucose |
| ATCC | American Type Culture Collection |
| cDNA | complementary deoxyribonucleic acid |
| CMV | Cytomegalo virus |
| ChIP | Chromatin Immunoprecipitation |
| CIN | Chromosomal instability |
| DMEM | Dulbecco's Modified Eagle Medium |
| DMSO | Dimethyl sulfoxide |
| DNA | Deoxyribonucleic acid |
| ECAR | Extracellular Acidification Rate |
| EMT | Epithelial-mesenchymal transition |
| ER | Estrogen receptor alpha |
| FCCP | Carbonyl cyanide 4-(trifluoromethoxy)phenylhydrazone |
| GSEA | Gene Set Enrichment Analysis |
| IHC | Immunohistochemistry |
| iHMEC | isogenic Human mammary epithelial cells |
| MDACC | M.D. Anderson Cancer Center |
| mRNA | messenger ribonucleic acid |
| NP-40 | Nonidet P40 |
| OCR | Oxygen Consumption Rate |
| OXPHOS | Mitochondrial respiration or oxidative phosphorylation |
| OE | Over-expression |
| qRT-PCR | quantitative Realtime Polymerase Chain Reaction |

| | |
|---|---|
| RNA | Ribonucleic acid |
| RBCC | RING- B-box and Coiled coil |
| shRNA | short hairpin ribonucleic acid |
| TCA | Tricarboxylic Acid cycle |
| TIF1 | Transcription Intermediary Factor 1 |
| TRAP | Transcription Factor Affinity Prediction analysis |
| TRIM | Tripartite motif containing family of proteins |

# Chapter 1: Introduction

# Chapter 1: Introduction

## 1.1 Breast cancer:

Breast cancer is the most common malignant disease of Western women and it is the second leading cause of cancer-related deaths after lung cancer [1]. It is estimated that approximately 234,190 Americans will be diagnosed with invasive breast cancer and about 40,730 Americans will die of the disease in 2015-16. It is alarming to find out that the lifetime risk of breast cancer for American women has risen from 1 in 11 in the 1970s to 1 in 8 in 2013, which is attributed to shifting breast cancer risk factor demographics and the increased use of screening mammography [1].

Breast tumors are highly heterogeneous and are composed of multiple subtypes with distinct morphologies and clinical implications [2]. Breast tumors are classified based on three different criteria: (i) histology into ductal or lobular carcinomas, (ii) differentiation state/gene expression profiles into luminal and basal-like subtypes, and (iii) the expression of receptors such as estrogen (ER), progesterone (PR) and HER2 (human epidermal growth factor receptor 2) into ER+, HER2+, and ER– PR– HER2− (triple-negative breast cancer, TNBC) subtypes. Expression patterns of the ER+ and HER2+ tumors both have luminal features, however TNBCs show significant but not complete overlap with basal-like subtype [3]. One of the key reasons for a decrease in mortality rates of breast cancer patients is the widespread use of mammography that has led to increased diagnosis of early stage disease, including ductal carcinoma *in situ* (DCIS). Systematic characterization of breast cancer genomes has identified that somatic mutations in only three critical genes (TP53, PIK3CA and GATA3) occurred at more than 10% incidence across all breast cancers [3].

Classification of breast tumors based on hormone receptor and HER2 status and the use of antihormonal and HER2-targeted therapy, respectively, are among the first examples for molecular-based classification and personalized cancer treatment that made a significant difference in clinical outcomes. Three main groups of medications used for adjuvant therapy of breast cancer include hormone-blocking agents, chemotherapy and monoclonal antibodies [4]. Blocking of estrogen action can be achieved by using selective estrogen receptor modulators (SERMs) such as tamoxifen, which compete with estradiol for binding to ERα, and which induce an alteration of ERα's conformation that is not conducive for activation. Selective ERα down-regulators (SERDs) such as fulvestrant induce destabilization and degradation of ERα. Finally, another way to block ERα action is to reduce the production of estrogen in peripheral tissues and within the tumor using inhibitors of aromatase, an enzyme which synthesizes estrogens from testosterone and androstenedione [5].

For almost three decades in both early and advanced breast cancer patients, tamoxifen has been the mainstay of endocrine therapy and remains to date the most successful targeted breast cancer therapy. However, it is unclear if aromatase inhibitors (AI) offer advantages over tamoxifen as adjuvant treatments for postmenopausal women [6]. The results of the Arimidex, Tamoxifen Alone or in Combination (ATAC) trial [7], and the International Breast Cancer Study Group's Breast International Group (BIG) 1-98 trial [8] showed small but significant improved efficacy of AIs, and in general fewer side effects.

Chemotherapy is primarily used for ER- breast tumors and for patients in advance stages of breast cancer. Combinatorial chemotherapy is the preferred option and it involves use of cyclophosphamide along with doxorubicin ('AC' regime) or

cyclophosphamide along with methotrexate and flurouracil ('CAT' regime) [9]. For HER2+ breast tumors, trastuzumab, a HER2-specific monoclonal antibody has improved the 5-year disease free survival to about 87% [10].

**1.2 Cancer metastasis and EMT:**

Cancer progression involves the following steps: adenoma, carcinoma *in situ* and invasive carcinoma at the primary tumor site, (Fig. 1) [11]. A portion of cancer cells disseminate from the primary tumor, adapt and grow at a secondary site or organ other than the primary tumor sites, the phenomena is termed as 'cancer metastasis'. The distribution of tumors and the sites of tumor growth are not a chance event, but it is determined by the amount of 'seeds' (the cancer cells) on the 'congenial soil' (the destination organ for metastasis) as postulated by the Dr. Stephen Paget in 1989 [12]. Approximately 90% of breast cancer-related deaths are caused by metastasis not by primary tumor [13]. Hence, for effective reduction of cancer mortality, it is very critical to intervene in the critical transition of non-invasive ductal carcinoma to extremely lethal invasive breast cancer. The pathogenesis of cancer metastasis consists of sequential steps such as migration, invasion, proliferation and angiogenesis [14].

Epithelial to mesenchymal transition (EMT) is a fundamental biological process and plays a critical role in morphogenic processes of the developing embryo, wound healing and organ fibrosis [15]. Tumor cells frequently use EMT to gain migratory and invasive properties in order to relocate and eventually form distant metastasis [16]. During EMT, the cancer cells undergo aggressive behavioral changes; acquiring a spindle-shape, loss of desmosomes and adherens junctions (such as E-cadherin, ZO-1, occludins, and claudins), increased expression of mesenchymal markers (such as N-

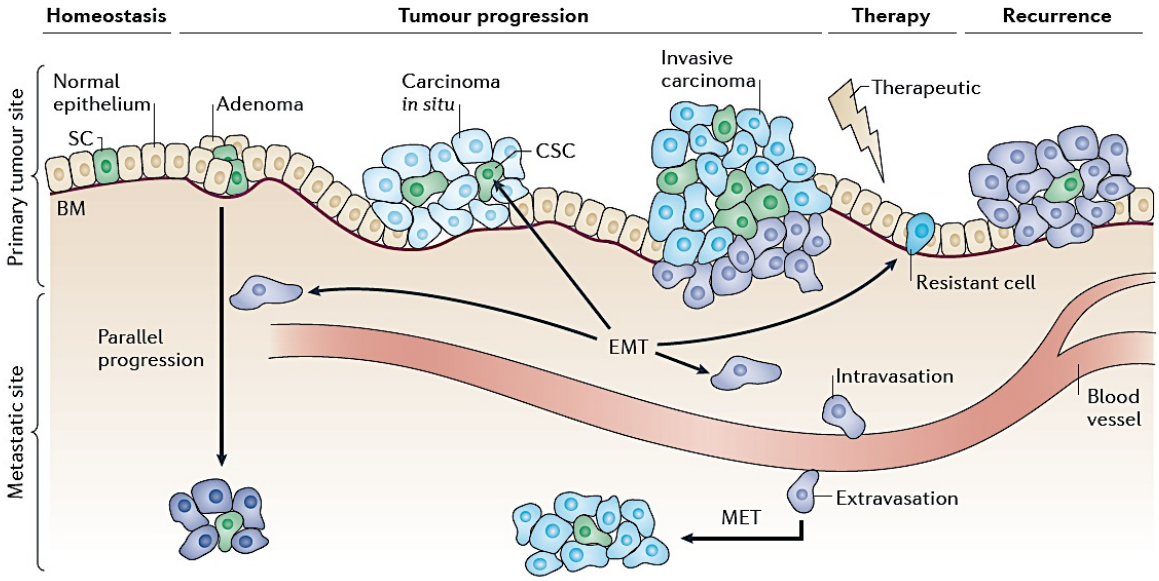


**Figure 1: Role of EMT in cancer progression.**

A primary tumor needs to undergo Epithelial to mesenchymal transition (EMT) in order to metastasize from a primary to a distant site.

(Figure is taken with permission from Craene B.D. and Berx, G. Regulatory networks defining EMT during cancer initiation and progression. Nat. Rev Cancer. 2013; 13: 97-110.) License Number: 3777250370389

cadherin, fibronectin and vimentin) and secretion of proteolytic enzymes, such as matrix metalloproteases, in order to clear the extracellular matrix (ECM) and exhibit increased migratory properties (Fig. 2) [15]. Of note, cancer cells undergoing EMT exhibit increased chemotherapy resistance, decreased apoptosis and have traits similar to stem cells [17].

Both intrinsic and extrinsic stimuli are known to induce in EMT in cancer. Microenvironment, one of the key extrinsic stimuli, is composed of ECM, myofibroblasts, cancer-associated fibroblasts, immune cells and several secretory factors such as hepatocyte growth factor, epidermal growth factor, Wnt, transforming growth factor-β, Hedgehog and various cytokines such as interleukin-6 and tumor necrosis factor-β [18]. A cohort of transcription factors including those of the Snail, Twist and Zeb families are known to orchestrate the process of EMT [19]. These transcription factors have unique tissue-specific expression profiles and are known to control the expression of each other and cooperate functionally at target genes [20]. EMT transcription factors in concert not only repress epithelial genes but also activate mesenchymal genes, and often the same transcription factor is responsible for both activation and repression [11].

EMT transcription factors recognize E-box DNA sequences located near the transcription start site of *CDH1* gene, and recruit various co-factors and histone deacetylases to transcriptionally repress *CDH1*. Notably, SNAI1 induces recruitment of HDAC1 and HDAC2 to induce repressive histone modifications at the *CDH1* promoter and likewise, ZEB1 cooperates with deacetylase SIRT1 at the *CDH1* promoter leading to deacetylation of histone H3 and reduced binding of RNA polymerase II [11]. In addition, various histone modifiers are linked to SNAI1 activity such as the

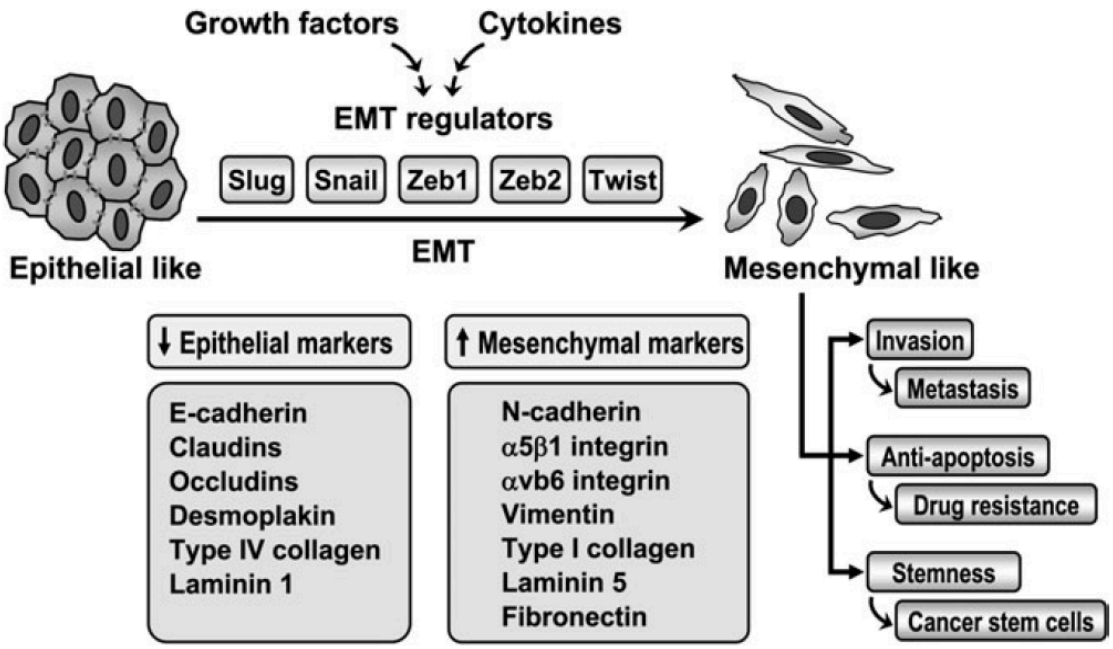


**Figure 2: An overview of regulators of EMT**

The EMT regulators transform the cancer cells from epithelial-cell like to mesenchymal-cell like with suppression of epithelial markers and expression of mesenchymal markers. The final effects on cancer cells are cancer metastasis, drug resistance and with features of cancer stem cells.

**(**Figure is taken with permission from Shih JY, Yang PC. The EMT regulator slug and lung carcinogenesis. Carcinogenesis. 2011 Sep;32(9):1299-304.) License Number: 3777750872518

methyltransferase EZH2, SUZ12 and G9a (EHMT2) [11]. Similarly, TWIST induces another repressive histone mark H4K20 monomethylation by recruiting the methyltransferase SET8 at E-cadherin promoters [21]. On the other hand, in head and neck carcinoma, expression of BMI1 is activated by TWIST1 and they both subsequently coordinate to repression of E-cadherin and p16 by recruiting the PRC2 complex [22]. Interestingly under hypoxic conditions, the hypoxia inducible factor (HIF1a) induces EMT and tumor metastasis by enhancing TWIST expression [23]. The ZEB family of transcription factors recruits co-repressors such as C-terminal binding protein (CTBP) or chromatin remodeling protein, BRG1 [24]. Additionally, ZEB1 may also interact with p300/CBP-associated factor (PCAF) and p300 and form a transcriptional activation complex [25]. Therefore, similar to SNAI1 and TWIST, ZEBs function as transcriptional repressors or activators by binding to E-boxes and recruit corresponding complexes, ultimately repressing epithelial junction and polarity genes and activating mesenchymal genes that contribute to EMT.

**1.3 Cancer cells and deregulated metabolism:**

In the second cancer hallmarks review published by Drs. Hanahan and Weinberg, ‘metabolic reprogramming’ is recognized as one of the key hallmarks of cancer [26]. Multiple research groups are trying to understand how a tumor evolves metabolically in order to adapt to the uptake of novel nutrients or microenvironment. However, because of the complex wiring of metabolic circuits and the constant evolution of metabolic switching, it has been difficult to completely characterize cancer metabolism. Current research is focused on understanding how to restrict nutrient consumption in these cancer cells or ways to deplete the nutrient uptake to starve

these cells, which would ultimately cause reduced proliferation and growth of the tumor. Additionally, identification of novel regulators of cancer metabolism and uncovering their mechanism of action are critical.

Normal cells convert glucose to pyruvate that is later converted to acetyl-CoA to fuel the tricarboxylic acid cycle (TCA cycle). NADH and FADH2 generated at the end of TCA cycle then provide electrons to the mitochondrial respiratory chain and ultimately each glucose molecule can produce up to 36 molecules of ATP. In normal cells, glycolysis is prioritized only when oxygen supply is limited. In contrast, cancer cells preferentially use glycolysis even in normoxic conditions; this phenomenon was discovered by Dr. Otto Warburg and is termed as 'Warburg effect' (Fig. 3) [27]. Hence, glycolysis in tumor cells is termed as 'aerobic glycolysis' to distinguish from the normal anaerobic glycolysis of healthy cells [28].

Glycolysis only generates 2 ATP per glucose molecule as compared to 36 ATP for each glucose molecule catabolized by mitochondrial respiration; hence, cancer cells have to compensate for the lower efficacy of energy production. They do this partly by up-regulating the expression of glucose transporters such has GLUT1 and GLUT4, to uptake more glucose and a majority of other glycolytic enzymes [29]. Oncogenes such as Ras, Myc, and HIF-1α are reported to be master inducers of cancer glycolysis [30]. Elevated transcriptional activity of c-Myc and HIF-1$\alpha$ along with p53 loss/mutation is responsible for enhancing expression of glycolytic enzymes. The majority of glycolytic gene promoters have consensus binding motifs of Myc and HIF-1α. In normoxia, c-myc promotes expression of glycolytic genes, whereas when cells are in hypoxic HIF-1α is activated that allows tumors to continuously drive glycolysis to not only support proliferation but also accelerated biosynthesis [31].

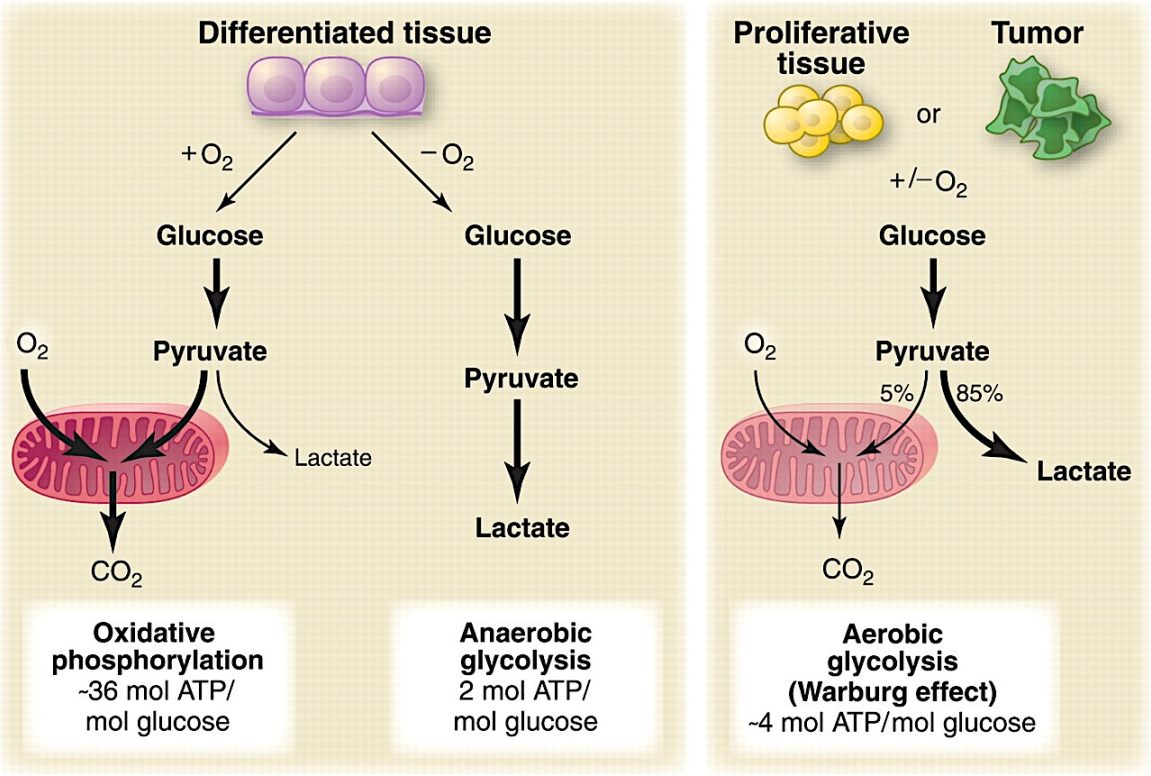


**Figure 3: Tumor metabolism and Warburg effect**

Normal differentiated tissues or cells, utilize glucose as an energy source through the glycolysis pathway and enter into Kreb's cycle to produce more energy through oxidative phosphorylation. On the contrary, cancer cells, consume increased amounts of glucose and switch to produce lactate without entering oxidative phosphorylation. Cancer cells are dependent on this switch to aerobic glycolysis for proliferation

(Figure is taken with permission from Vander Heiden, M.G., Cantley, L.C. and Thompson, C.B. Understanding the Warburg effect: The metabolic requirements of cell proliferation. Science. 2009; 324(5930):1029-1033.) License Number: 3777851053796

In contrast, the tumor suppressor p53 inhibits glucose uptake by directly inhibiting the transcription of glucose transporter GLUT1 and GLUT4 [32]. Fructose 2,6-bisphosphate functions as an allosteric activator of PFK1, a major glycolytic enzyme. Fructose 2,6-bisphosphate is produced by PFK2 from fructose 1-phosphate. p53 induces the expression of *TIGAR* and TIGAR significantly slows down tumor glycolysis by converting fructose 2,6-bisphosphate back to fructose 1-phosphate [33]. Hence, one of the key molecular interactions that define the status of cancer metabolism is that of p53, c-Myc and HIF-1$\alpha$.

As per the Warburg hypothesis, it was erroneously believed that mitochondrial metabolism is inconsequential for the metabolic demands of actively proliferating cancer cells. Recent studies, provide ample genetic evidence that mitochondria are indeed essential for tumorigenesis [34]. Further, it is proposed that tumors are metabolically heterogeneous (Fig. 4). The bulk of tumor cells, exhibit aerobic glycolysis (Warburg effect) and there is a small population of slow-cycling tumorigenic cells that are dependent on OXPHOS activity. The slow-cycling cells are proposed to be the cells that are resistant to various cytotoxic treatments [35].

**1.4 TRIM family and TRIM24:**

The TRIpartite Motif (TRIM) containing family of proteins consists of about 71 proteins that have the signature tripartite, 'RBCC', motif of RING-finger domain, one or two zinc binding motifs named B-boxes, and an associated Coiled-Coil region. On the basis of differences in their C-terminal domain structure, the TRIM proteins can be classified into 11 different sub-families (Fig. 5). Most of the TRIM family proteins act as

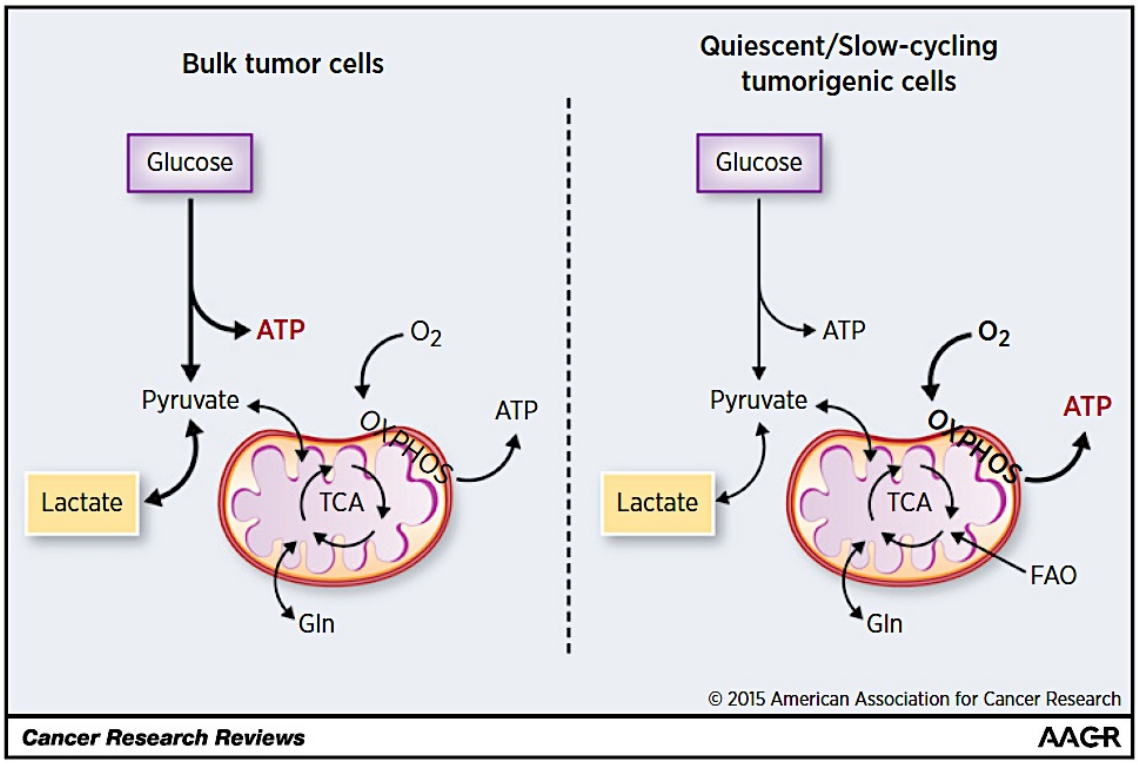


**Figure 4: Diverse metabolism in different population of cancer cells**

Different subpopulations of cancer cells coexist in tumors, contributing to functional heterogeneity. Rare tumorigenic cells exist in a quiescent/ slow-cycling state and are intrinsically resistant to cytotoxic treatments. Importantly, with respect to other cells inside the tumor, they seem to rely on a different metabolic program to maintain their energetics. In contrast to the bulk tumor, slow-cycling tumorigenic cells are more dependent on mitochondrial respiration (OXPHOS) and have impaired glycolytic capacity.

(Figure is taken with permission from Viale A, Corti D, Draetta GF. Tumors and mitochondrial respiration: a neglected connection. Cancer Res. 2015 Sep 15;75(18):3685-6.) License Number: 3777860586185

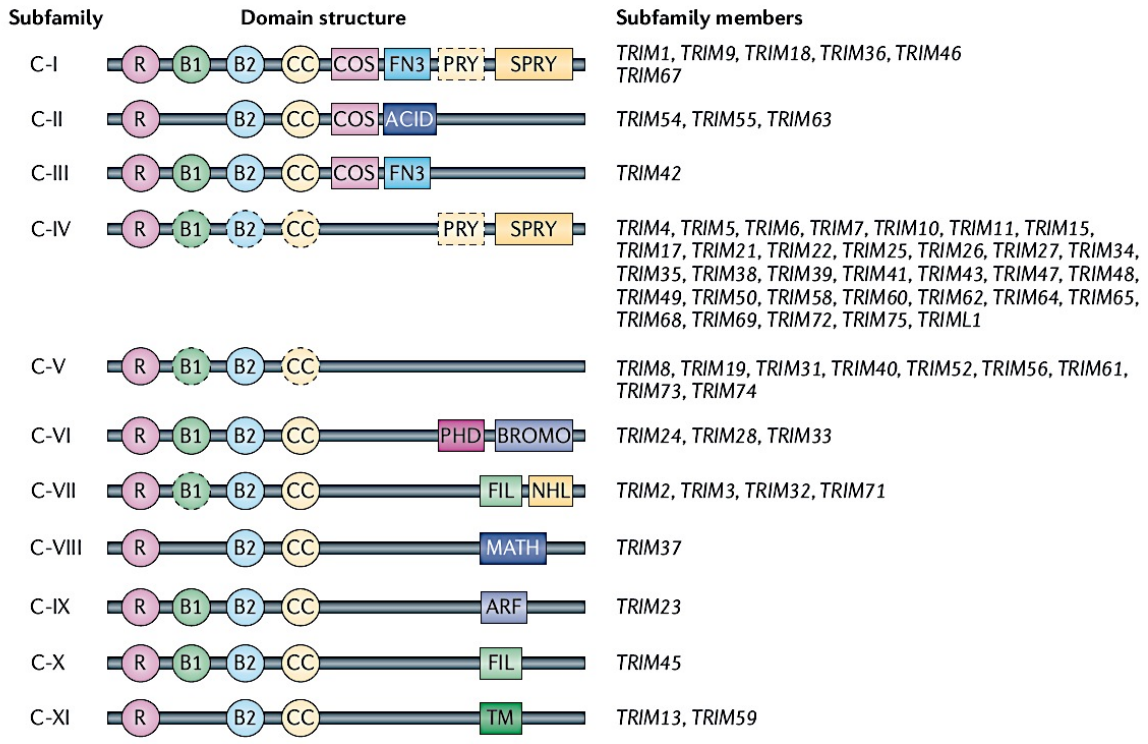


**Figure 5: The TRIM family of proteins.**

Based on protein structure the TRIM family of proteins is classified into nine eleven different sub-families. Almost all members have a RING-finger domain (R), one or two B-box domains (B) and a coiled-coiled domain (CC).

(Figure is taken with permission from Hatakeyama S. TRIM proteins and cancer. Nat Rev Cancer. 2011 Oct 7;11(11):792-804.) License Number: 3777250370389

E3-ubiquitin ligases and they function in various cellular processes, including regulation of protein stability, transcription, cell proliferation and apoptosis [36].

The Transcription Intermediary Factor (TIF1) sub-family is a unique sub-family of TRIM proteins that in addition to the N-terminal RBCC motif contains a tandem PHD-Bromodomain at the C-terminus. TRIM24 (TIF1$\alpha$) is the founding member of the TIF1 sub-family, which includes TRIM28 (TIF1$\beta$), TRIM33 (TIF1$\gamma$) and TRIM66 (TIF1$\delta$) [37]. Generally, a PHD-domain interacts with methylated lysines of histones, whereas the Bromo-domains interact with acetylated lysines of histones [38, 39]. Various members of TIF1 sub-family play key roles in regulating epigenetic mechanisms of transcriptional regulation that involve histone modifiers, nuclear receptors and heterochromatin binding proteins [37].

Oncoprotein T18 was one of the very first reports of TRIM24, in which it was found to be a fusion partner along with B-Raf protein. T18 had the first 332 amino acids of TRIM24 in its N-terminus and B-Raf protein at the C-terminus [40]. Using yeast two-hybrid screens, it was shown that mouse heterochromatin protein 1 alpha (mHP1a) interacts with TRIM24 via mHP1 chromo-shadow domain [41]. As the name suggests, HP1 proteins are associated with formation of heterochromatin and inhibition of gene expression. Using luciferase reporter assays, it was shown that interaction of TRIM24 and mHP1a associated with gene repression. In contrast, another group showed that TRIM24 exhibits its transcription repression activity in the absence its HP1-binding region in a similar reporter system [42]. Bonus, a *Drosophila* homolog of TIF1 proteins, is essential for development and interacts with various nuclear receptors such as betaFTZ-F1 and DHR3 [43]. Of note, the N-terminal RBCC motif of Bonus is essential for its transcriptional repression activity, but not the HP1-binding region and the C-

terminal PHD/Bromo domain. Hence, whether an HP1 interaction is essential for TRIM24-mediated gene regulation is not clear.

In contrast, TRIM24 localization studies reveal that TRIM24 associates with euchromatin of interphasic nuclei, and is not associated with condensed chromatin and metaphase chromosomes [44]. TRIM24 physically interacts with arginine methyltransferase 1 (CARM1) and glucocorticoid receptor-interacting protein 1 (GRIP1) to enhance transcriptional activation mediated by nuclear receptors [45]. TRIM24 knockdown is reported to diminish transcriptional activation mediated by GRIP1 and AR. Additionally, TRIM24 also reportedly interacts with several chromatin remodeling proteins. In mouse development during the zygote stage, TRIM24 is localized to transcriptional active sites co-occupied by SNF2H and BRG-1 that are known chromatin-remodeling proteins [46]. Notably, TRIM24 depletion caused mislocalization of RNA Pol-II, BRG-1 and SNF-2 and down-regulation of their target genes in the zygote. Hence, these results suggest that TRIM24 may play an active role in transcriptional activation.

TRIM24 acts a transcriptional co-regulator by virtue of its LXXL motif by which it interacts with various nuclear receptors such as RAR$\alpha$, Vitamin D3, androgen and estrogen receptors (Fig. 6). TRIM24 modulates the transcriptional activity of various nuclear receptors either positively or negatively in a ligand dependent manner. In prostate cancer cells, TRIM24 directly interacts with a histone acetyltransferase, TIP60, a coactivator of androgen receptor (AR) [47]. Additionally, TRIM24 also binds to bromodomain-containing 7 (BRD7), a corepressor of AR and negative regulator of cell proliferation. Thus, TRIM24 regulates AR-mediated transcription through crosstalk between TIP60 and BRD7 in prostate cancer [47].

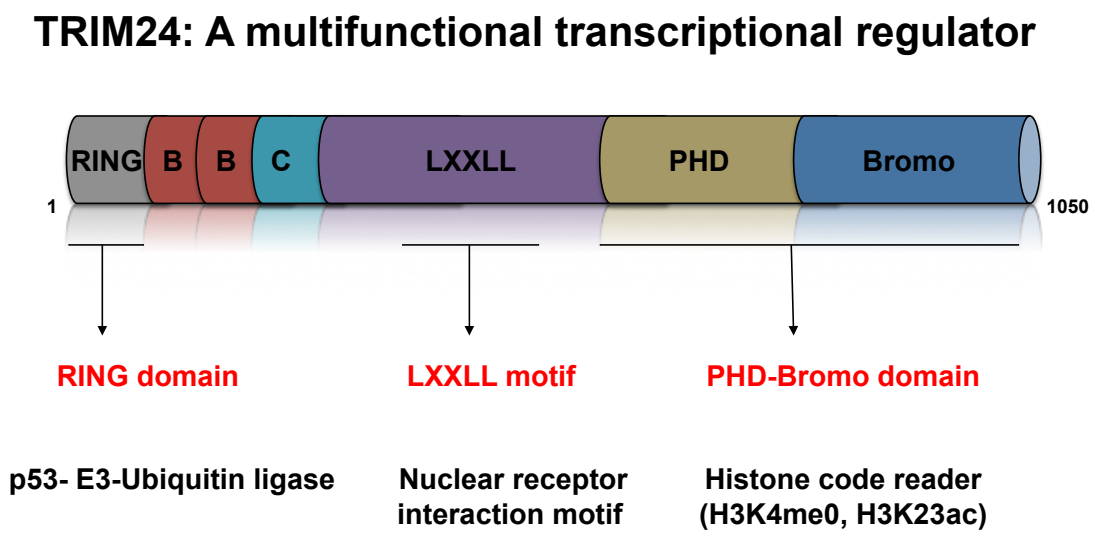


**Figure 6: TRIM24 protein structure**

Diagram of TRIM24 protein structure and domains, along with its known functions.

In a mouse model targeting exon 4 of TRIM24 for germline deletion *Trim24*$^{dlE4/dlE4}$, it was discovered that RAR-mediated signaling was reactivated, through re-expression of RARα and repressed genes in the liver, leading to eventual HCC [48]. Additionally, TRIM24 was shown to suppress HCC progression by inhibition of the IFN/STAT pathway via RAR dependent regulation of the Stat1 promoter [49]. Based on analysis of this mouse model, it was suggested that TRIM24 is a liver-specific, retinoid-dependent tumor suppressor [48]. However, recent evidence suggests that *Trim24*$^{dlE4/dlE4}$ mice retain normal levels of *Trim24* RNA lacking exon 4 and are not null of TRIM24 in liver [50]. Our laboratory generated a new mouse model for complete TRIM24 knockdown by targeting exon 1 of TRIM24 (*TRIM24*$^{dlE1/dlE1}$). It was found that *TRIM24*$^{dlE1/dlE1}$ mice have a significant depletion of visceral fat and spontaneously develop liver steatosis, fibrosis and ultimately hepatocellular carcinoma. In the murine liver, TRIM24 acts as a transcriptional co-repressor by repressing hepatic lipid accumulation, inflammation, and damage [51].

Based on multiple studies it can be concluded that TRIM24 plays a dual role of transcriptional co-activator and transcriptional co-repressor, and its role is dependent on the tissue type and associated complexes. Interestingly, it has been reported that TRIM24 may phosphorylate various transcription factors by acting as a protein kinase *in vitro* [52]. However, based on protein sequence analysis TRIM24 contains no conserved characteristics of protein kinase domains and there are no reported *in vivo* substrates.

Our laboratory identified TRIM24 as a p53-interacting protein, upon purification of an endogenous TAP-tagged version of p53 in embryonic stem cells (ES cells) [53]. Knockdown of TRIM24 ortholog, bonus, in *Drosophila* induces apoptosis. Further,

mosaic analysis in *Drosophila* depleted in the TRIM24 ortholog, bonus, shows that p53 could rescue apoptosis of imaginal disc cells. Similarly, TRIM24 knockdown in breast cancer cell lines (MCF7) results in p53-depedent apoptosis [53]. Additional studies in MCF7 breast cancer cell lines, which harbor wild-type p53, showed that TRIM24 responds to stress and damage by negatively regulating p53 through an autoregulatory feedback loop. It was found in response to DNA-damage the TRIM24-p53 interaction is disrupted due to ATM-mediated TRIM24 phosphorylation. In turn, the damage-activated p53 binds to p53 response elements on TRIM24 gene and induces TRIM24 gene expression. Finally, the newly synthesized TRIM24 terminates the DNA damage response by targeting phosphorylated-p53 for proteasomal-mediated degradation. This feedback loop was found to be independent of MDM2 and dependent upon direct binding of p53 to p53 response elements (p53 REs) in the distal promoter region of TRIM24 [54].

The aforementioned studies provide genetic evidence that TRIM24 acts as a tumor suppressor in murine liver, but there are multiple studies that provide evidence that TRIM24 acts as an oncogene in various cancers such as in prostate cancer [47], breast cancer [55, 56], non-small cell lung cancer [57], head and neck carcinoma [58], colorectal cancer [59], gastric cancer [60], glioblastoma [61], bladder cancer [62] and even human hepatocellular carcinoma [63] (Table 1). Expression of TRIM24 has been reported to correlate negatively with survival of breast cancer patients [55, 56]. Molecular and three-dimensional structural analysis showed that TRIM24 via its tandem PHD-Bromo domain acts as a dual histone code reader of H3K4me0 and H3K23ac. It was found that TRIM24 binds estrogen receptor and chromatin (at specific

| Cancer | Human/ Mouse | Oncogene/Tumor Suppressor | Clinical data | Mechanism | Ref. |
|---|---|---|---|---|---|
| HCC | Mouse | Tumor Suppressor | No | RAR-a corepressor | [48, 51] |
| Breast | Human | Oncogene | Yes | ER-a coactivator | [55] |
| NSCLC | Human | Oncogene | Yes | NA | [57] |
| HNSCC | Human | Oncogene | Yes | NA | [58] |
| CRC | Human | Oncogene | No | NA | [59] |
| Gastric | Human | Oncogene | Yes | NA | [60] |
| GBM | Human | Oncogene | Yes | PIK3CA/Akt | [61] |
| Bladder | Human | Oncogene | Yes | NA | [62] |
| HCC | Human | Oncogene | Yes | NA | [63] |

**Table 1: List of various studies of TRIM24 in different cancers**

histone modifications mentioned above) to activate estrogen-dependent genes associated with tumor development and cell proliferation [55]. Hence, by reading a non-canonical histone signature the PHD-Bromo domain of TRIM24 provides a structural rationale for gene regulation, establishing a novel route by which histone readers may influence pathogenesis of cancer.

Similar to other correlations in human cancers, it was found that TRIM24 expression positively correlates with glioma malignancy and it is a marker of poor prognosis for patients with newly diagnosed glioblastoma (GBM) [61]. TRIM24 expression is critical for efficient cell proliferation, cell cycle progression, and *in vivo* tumor growth in GBM. These authors showed that TRIM24 directly activates *PIK3CA* gene expression in a PHD-Bromo domain dependent manner. Intriguingly, TRIM24-mediated regulation of the PI3K/AKT/NF-$\kappa\beta$ pathway induces the expression of DNA repair gene $O^6$-methylguanine-DNA methyltransferase (MGMT) and induces chemoresistance to temozolomide in GBM cells [61].

Although, it has yet to be determined if TRIM24 can target mutant p53 for proteasomal-based degradation, in a very elegant study it was found that TRIM24 may be part of a protein complex responsible for conversion of mutant p53 conformation to its WT form [64]. The studies were done in mouse embryonic stem cells harboring mutant p53 (ES-cells$^{mutp53}$) that remained pluripotent and had a normal karyotype as compared to ES-cells knocked out of p53. In ES-cells$^{mutp53}$, the mutant p53 was transcriptionally active in response to DNA-damage and activated canonical p53-target genes such as p21 and btg2. Among the network of proteins identified by MS-based interactome analysis of p53, in addition to TRIM24, was CCT complex, USP7, Aurora kinase and Nedd4 [64].

To summarize, there are several reports of TRIM24 association with poor prognosis and survival in various cancers [55, 56]. TRIM24 regulates gene expression by acting either as transcriptional activator or repressor. However, whether TRIM24 plays a causal role in malignant transformation during tumor development and progression has yet to be studied. Further, the mechanisms involved in potential TRIM24-mediated tumor initiation and progression are unknown.

# Chapter 2: Materials and methods

# Chapter 2: Materials and methods

The contents of this chapter are based on Pathiraja TN, Thakkar KN, Jiang S, Stratton S, Liu Z, Gagea M, Shi X, Shah PK, Phan L, Lee MH, Andersen J, Stampfer M, Barton MC. TRIM24 links glucose metabolism with transformation of human mammary epithelial cells. Oncogene. 2015 May 28; 34(22): 2836-45.



## 2.1 Cell culture

Previously established HMEC cultures, 184D (normal pre-stasis [65]), 184B-7p (abnormal, post-stasis [65]), 184A1 (Immortal non-malignant[66]) and 184AA2 (Immortal malignant [67]) were cultured in M87A medium with 0.1% AlbuMAX bovine serum albumin (Invitrogen) and 0.1 nmol/L oxytocin (Bachem) as described [65]. MCF10A cells were cultured as described [68]. Human breast cancer cell lines (MCF-7, MDA-MB-231, MDA-MB-468, and SKBR3) from ATCC were cultured according to the supplier’s protocols. For transient knockdown experiments, TRIM24 (L-047483-00) and non-silencing control (D-00120-01-20) small interfering RNAs (siRNAs) (Dharmacon) were transfected at 100 nM for 48 hours using Lipofectamine RNAiMAX reagent (Invitrogen) as per manufactures instructions.

### 2.2 Cell proliferation, soft agar colony formation, and cell-cycle analysis

For cell proliferation (7500 cells in 24 well plate, in triplicates) and XTT assays (500 cells in 96 well plates, in quadruplets), respective cell numbers were seeded and counted every 2 days for upto 6 days (Beckman Coulter counter). For soft agar colony formation, 5000 cells were seeded in 1.5 ml of respective medium with 0.35% low-melting-temperature agarose (BD Biosciences) overlying 1.5 mL of 0.7% low-melting agarose in 6-well plates and incubated at 37°C for 14 days. For cell-cycle analysis, cells were washed and fixed with 70% ethanol for 1 hour at 4°C and stained with propidium iodide at a concentration of 50 µg/mL, along with RNase A (100 U/mL), prior to analysis using Flow cytometry and ModFit software program (Verity Software House).

### 2.3 Generation of stable cells

TRIM24 full-length coding sequences were amplified from the vector pCMV-XL4-hsTRIM24 (OriGene Technologies) using gene-specific primers (Appendix 1), digested with *Xba*I and *Pml*I and cloned into pEntry4-FLAG vector [69]. TRIM24 coding sequences and FLAG-only sequences were transferred to pLenti-PGK-Neo-DEST [69] using Gateway cloning (Invitrogen). Lentiviruses containing culture supernatants were prepared as described [55]. Briefly, 800 ng of clone/vector DNA were transfected into HEK293T cells with packaging vectors pPAX2 and pMD2 (800 ng each) using Effectene (Qiagen) according to manufacturer's instructions. After 48 hours, target cell line was transduced using virus-containing culture supernatants with 8 µg /mL Polybrene (Sigma). After 48 hours, cells were selected using 700 µg/mL G418

(Stratagene) for 10 days. Stable cell lines, ectopically expressing *TRIM24* or FLAG only were maintained in regular culture medium containing 200 µg/ml G418.

### 2.4 Quantitative real-time PCR (qRT-PCR)

Total RNA was isolated with TRIzol reagent (Invitrogen) and qRT-PCR analysis was performed as described [55]. Primers used are listed in Appendix 1.

### 2.5 nCounter analysis

A panel of 420 breast cancer associated genes was used for nCounter analysis (NanoString Technologies) [70]. Three biological replicates of RNA from TRIM24 and Control iHMECs (100ng each) were processed according to the manufacturer's recommendations (http://www.nanostring.com). Data were analyzed using the nSolver digital analyzer software program (http://www.nanostring.com/products/nSolver). Differentially expressed genes were identified using the Student *t*-test: genes with expression significantly ($p < 0.05$) up- (fold change ≥ 1.2) or down-regulated (fold change ≤ 0.8) were identified. Unsupervised hierarchical clustering of differentially expressed genes was performed using the GENE-E software program (http://www.broadinstitute.org/cancer/software/GENE-E/) and a Euclidean distance matrix. Gene Ontology (GO) category (http://www.geneontology.org/) enrichment analysis and KEGG pathway analysis were done using the Database for Annotation, Visualization and Integrated Discovery (DAVID) (http://david.abcc.ncifcrf.gov/) [71].

### 2.6 Immunoblotting and Immunohistochemistry

Immunoblotting of proteins in TRIM24 and Control iHMECs was performed using standard techniques with antibodies listed in Appendix 2. Immunohistochemistry (IHC) of breast tumor arrays, BR2082 (US Biomax) and BR1503 (US Biomax), was performed, as described [55], using a VECTASTAIN Elite ABC Kit and a DAB Detection Kit (Vector Laboratories) with an anti-TRIM24 antibody (1:200 dilution; Proteintech). IHC staining data for ER, PR, and ErbB2 were available and TRIM24 staining was quantified using the Allred scoring method (for details of the Chi-square method and calculations please see Appendix 3) [72].

### 2.7 Metabolic experiments and glucose uptake

The extracellular acidification rate (ECAR) and oxygen consumption rate (OCR) of TRIM24 and Control iHMECs were measured using an $XF^e96$ Extracellular Flux Analyzer (Seahorse Bioscience) as described [73]. Briefly, 50,000 cells were seeded into $XF^e96$ tissue culture plates in quadruplicate and ECAR and OCR measured under basal conditions and after sequential treatment of the cells with Oligomycin (1 μM), FCCP (Carbonylcyanide p-trifluoromethoxyphenylhydrazone, 500 nM) and Rot + Ant [Rotenone (1 μM) + Antimycin A (1 μM)]. Cells were trypsinized and counted using a Coulter counter (Beckman Coulter) and the cell count used for normalization purposes. For glucose uptake assays, a non-metabolic fluorescent-labeled glucose (2- NBDG) was used. iHMECs were seeded in the regular HMEC medium for 24h and just prior to performing the assay were washed with glucose-free medium. Cells were incubated with glucose-free medium, containing 120 μM 2-NBDG (Invitrogen) for 0.5h, 1.0h, 1.5h and 2h, followed by FACS analysis.

### 2.8 Xenograft experiments

Female athymic Nu/Nu mice (age 6–8 weeks) were housed under pathogen-free conditions. 1 million TRIM24 iHMECs or Control iHMECs suspended in 50 µl of serum free DMEM were co-injected subcutaneously with 50 µl of high concentration Matrigel (BD Biosciences); 10-15 mice were injected for each cell line. Tumor sizes were measured weekly by caliper for up to 64 days and xenograft volume calculated as previously described [74]. All procedures were approved by the University of Texas M D Anderson Cancer Center Institutional Animal Care and Use Committee and performed with veterinary supervision.

### 2.9 The Cancer Genome Atlas data and statistical methods

The Cancer Genome Atlas – Breast invasive carcinoma (TCGA-BRCA) data on RNA expression (Level 3) of Breast invasive carcinoma patients (1008) and normal tissues (92) in terms of RSEM (RNA-seq by Expectation-Maximization) were downloaded from the Broad Institute TCGA Firehose Genome Data analysis center pipeline (standard data run 2013/11/14). 950 of 1008 BRCA samples had PAM50 subtype information available. Gene set enrichment analysis (GSEA) was run with default parameters with TRIM24 expression levels as phenotype and C2 (canonical pathways) gene sets. GSEA with patient samples limited to Basal subtypes and TRIM24 expression as phenotype gave very similar results.

### 2.10 Invasion and migration assays

Cells were resuspended in 500 µl serum-free media and seeded in a 24-well Transwell or Matrigel plate (BD Biosciences, pore size 8 µm) at a concentration of (5 to 7.5) x $10^4$

per well. 750 μl of DMEM/ RPMI supplemented with 10% FBS was added to the lower chamber and cells were allowed to migrate or invade for 16 h in 5% $CO_2$ at 37°C. Migrating cells were stained with 0.1% crystal violet. Non-migrating cells were removed using a cotton swab. Migrated cells were quantified based on five microscopic fields at a 4X magnification and results were represented as mean ± standard deviation and student's t-test was performed for statistical significance. Each assay was performed in triplicates.

**2.11 Acini formation assay**

The overlay method of acini formation assay for MCF10A cells was performed as described [68]. Briefly, 40ul of growth-factor reduced matrigel (BD Biosciences – No. 354230) was added to each well of an eight-well glass chamber slide (Fisher – 1256518) and spread evenly in the well using the P-200 tip (the slides can be assembled on ice). MCF10A cells were trypsinized and resuspended in 2 ml of Resuspension medium and spun down for 3 min at 150g in a tissue culture centrifuge. The cells were then mixed in assay medium without EGF and mixed 10-25 times to obtain a single-cell suspension. 25,000 cells per ml cells were mixed 1:1 with assay medium containing 4% matrigel and 10 ng/ml of EGF (usually 1ml of each). 400 μl of this mixture was plated on the top of solidified matrigel in each well of the chamber slide. Final concentration of cells is 5000 cells per well in assay medium containing 2% matrigel and 5 ng/ml EGF. Cells are allowed to grow in 5% $CO_2$ humidified incubator at $37^oC$ for 10-12 days and the cells are refed with fresh assay medium containing 2% matrigel and 5 ng/ml EGF every 4 days.

### 2.12 Experimental lung metastasis studies

To determine the experimental metastatic potential of cells, 5 x $10^5$ MDA-MB-231 control-shRNA (GIPZ) and TRIM24-shRNA (GIPZ) cells labeled with RFP-firefly luciferase were injected into NOD/SCID mice via the tail vein. SCID Mice were assessed weekly for presence of lung metastasis after the intraperitoneal injection of D-Luciferin (Fisher – PI88293). *In vivo* bioluminescence was assessed using the IVIS imaging system 200 series (PerkinElmer), approximately 10 mins post-injection. Until about 6-7 weeks, mice were monitored for lung metastasis weekly and were euthanized after 7 weeks. Lungs were removed surgically and fixed using Bouin's fluid and the number of lung tumor nodules was counted and subjected to hematoxylin and eosin staining thereafter. Lungs were also stained for RFP and TRIM24 to ascertain the presence of MDA-MB-231 cells and TRIM24 expression, respectively. All procedures were approved by the University of Texas M D Anderson Cancer Center - IACUC and performed under proper supervision of veterinary personnel.

### 2.13 HTG EdgeSeq analysis

mRNA expression profiling of 2,560 genes was done using the HTG EdgeSeq Oncology Biomarker Panel assay. The assay uses an NGS-based gene expression system powered by HTG EdgeSeq chemistry. Samples were processed according to the manufacturer's recommendations (http://www.htgmolecular.com/science/sample-prep). Differentially expressed genes were identified using the Student t-test: genes with expression significantly ($p < 0.05$) up- (fold change ≥ 1.2) or down-regulated (fold change ≤ 0.8) were identified. Gene Ontology (GO) category enrichment analysis and KEGG pathway analysis were done using the molecular signatures database (MSigDB) [75].

### 2.14 Chromatin immunoprecipitation (in breast cancer cells)

Chromatin immunoprecipitation (ChIP) is routinely used in our laboratory [55]. Briefly for chromatin immunoprecipitation, cells are harvested and then cross-linked with formaldehyde for 10 min and neutralized with glycine. Cells are lyzed with 1 mL Cell Lysis Buffer (5mM PIPES pH 8.0, 85mM KCl, 0.5% NP-40, fresh protease inhibitors) for 15 minutes. After sonication, the tubes are spun. Supernatant is transferred to a new tube to check for fragment size. Lysates are divided and diluted using ChIP Lysis Buffer. Immunoprecipitation is performed overnight with specific antibodies. The next day, Protein A Sepharose beads (GE Health) are incubated with antibody/protein bound complexes for 2 hr at 4°C. Then, Protein A beads are washed and re-suspended and incubated with RNase A for 30 min at 37°C and then Protease K for 2 hours at 55°C. The crosslinks are reversed by incubating the samples at 65°C overnight. The next day, protein /antibody bound DNA fragments are extracted with Phenol/Chloroform. qPCR analyses are performed to analyze specific antibody- and protein-bound.

### 2.15 Co-immunoprecipitation

Cells were lysed in NTEP buffer (25mM Tris-HCl pH 7.5, 150mM NaCl, 5mM EDTA, 0.5% NP-40) for 30 minutes at cold room. Using high-speed centrifugation, 14,000rpm for about 10 minutes, the cell lysate is spun down. Protein concentration was measured with BCA assay. 500 μg of cell lysate was pre-cleared by incubating with Protein A sepharose beads (GE health). 500 μg cell lysate was used to incubate per respective antibody overnight in the cold room. Then, protein A Sepharose beads (GE Health) were added for additional 2 hours incubation. After extensive washing, 35 μl SDS

loading dye was added into the beads, the beads was boiled for 5-10 minutes to elute the protein complex. Elute was then subject to western blot in various percentage of SDS-PAGE gels.

**2.15 Karyotyping**

a) Protocol for Chromosome preparation:

Exponentially growing cells were exposed to Colcemid (0.04 µg/ml) for one hour at 37°C and to hypotonic treatment (0.075 M KCl) for 20 minutes at room temperature. Cells were fixed in a methanol and acetic acid (3:1 by volume) mixture for 15 minutes, and washed three times in the fixative. Slides were prepared by dropping 50-100 µl the cell suspension on wet slides and air-dried.

b) Protocol for G-banding:

Slides were baked at 90° C for 3 hours. They were then treated with trypsin (200µl of 40X trypsin +1X HBSS, pH 7) for 2.5 ~ 3.5 minutes. Stained in 8% Giemsa staining solution for 3 ~ 4 minutes. Images were captured using Nikon 80i microscope equipped with Spectral Karyotyping software from Applied Spectral Imaging (ASI, Vista, CA). 15-20 metaphases were karyotyped from each cell line.

*Karyotyping was performed at MD Anderson Cytogenetics Core

**2.16 Immunofluorescence**

Cells were grown on a sterile glass cover slips or slides overnight in 37$^{o}$C/5% $CO_2$ incubator. Slides were then rinsed briefly with PBS and cells were fixed by incubation with 1% formalin in PBS for 10 minutes. Slides were then rinsed three times

with PBS. Incubate with primary antibody for 1 hour at room temperature or overnight at 4$^{o}$C. Optimal antibody concentration is usually from 1-10ug/ml in PBS-BSA. Wash three times with PBS. Incubate with conjugated secondary antibody for 45 minutes. Again, optimal antibody concentration is usually from 1-10ug/ml in PBS-BSA. Wash three times with PBS. Mount aqueous coverslip

# Chapter 3: TRIM24 links glucose metabolism with transformation of Human mammary epithelial cells

# Chapter 3: TRIM24 links glucose metabolism with transformation of Human mammary epithelial cells

The contents of this chapter are based on Pathiraja TN, Thakkar KN, Jiang S, Stratton S, Liu Z, Gagea M, Shi X, Shah PK, Phan L, Lee MH, Andersen J, Stampfer M, Barton MC. TRIM24 links glucose metabolism with transformation of human mammary epithelial cells. Oncogene. 2015 May 28; 34(22): 2836-45.



## 3.1 Introduction and Rationale

Recent studies indicate that specific members of the tripartite motif (TRIM) protein family, characterized by conserved amino (N)-terminal zinc-finger domains of a RING-type E3 ubiquitin ligase, B-boxes and coiled coil, are important regulators of carcinogenesis [36]. Among these, we identified TRIM24, as a previously unknown E3-ubiquitin ligase of p53 in embryonic stem cells and breast cancer cell lines, and as a histone reader that activates estrogen-dependent genes associated with cellular proliferation and tumor development [53, 55, 76]. Of note, we and others reported that high expression of TRIM24 is associated with poor prognosis and survival in breast cancer patients [55, 56]. However, whether TRIM24 plays a causal role in malignant transformation of breast epithelial cells during breast tumor development and progression has yet to be studied. Further, the mechanisms involved in potential TRIM24-mediated breast tumor initiation and progression are unknown.

### 3.2 Aberrant expression of TRIM24 during breast cancer progression

To determine whether TRIM24 expression in breast tissues was deregulated during breast cancer progression, we performed IHC-staining to detect TRIM24 protein expression in a human tissue microarray (BR2082, US Biomax) consisting of samples of normal breast tissue, atypical ductal hyperplasia, intraductal breast carcinoma, and invasive breast carcinoma. We detected low TRIM24 protein expression in normal breast tissue but high expression in atypical ductal hyperplasia and carcinoma (Fig. 7A), suggesting that TRIM24 expression is deregulated in breast cancer and likely early in progression. We then examined the expression of TRIM24 in 1008 breast cancer patients and 92 normal samples from The Cancer Genome Atlas – Breast invasive carcinoma (TCGA-BRCA) dataset. We found the TRIM24 was significantly upregulated in breast invasive carcinoma patients (p-value: 1e-16, Fig. 7B) and its expression in paired samples was greater than 1.5 fold in 40 out of 106 (37.8%) patients (Fig. 8A).

Next, we assessed whether high levels of TRIM24 expression were associated with any specific breast cancer sub-type by using the TCGA-BRCA dataset and by performing TRIM24-IHC in an array of tissue samples from 72 breast cancer cases. In the TCGA-BRCA dataset, the PAM50 (Prediction analysis of Microarray – 50 genes expression signature[77]) breast-cancer subtypes showed different distribution in TRIM24 high expressing versus low expressing patients (p-value: 1.32e-07). The basal subtype (Odds ratio: 1.98, p-value: 3.8e-04) was significantly over-represented in the TRIM24 high expressing patients, followed by HER2 (Odds ratio: 1.78, p-value: 0.03) and Luminal B subtype (Odds ratio: 1.4, p-value: 0.047); whereas, the Luminal A subtype (Odds ratio: 0.43, p-value: 1.46e-08) was significantly under-represented (Fig. 7C). For details of the intersection of PAM50 and TRIM24-expression analysis, please

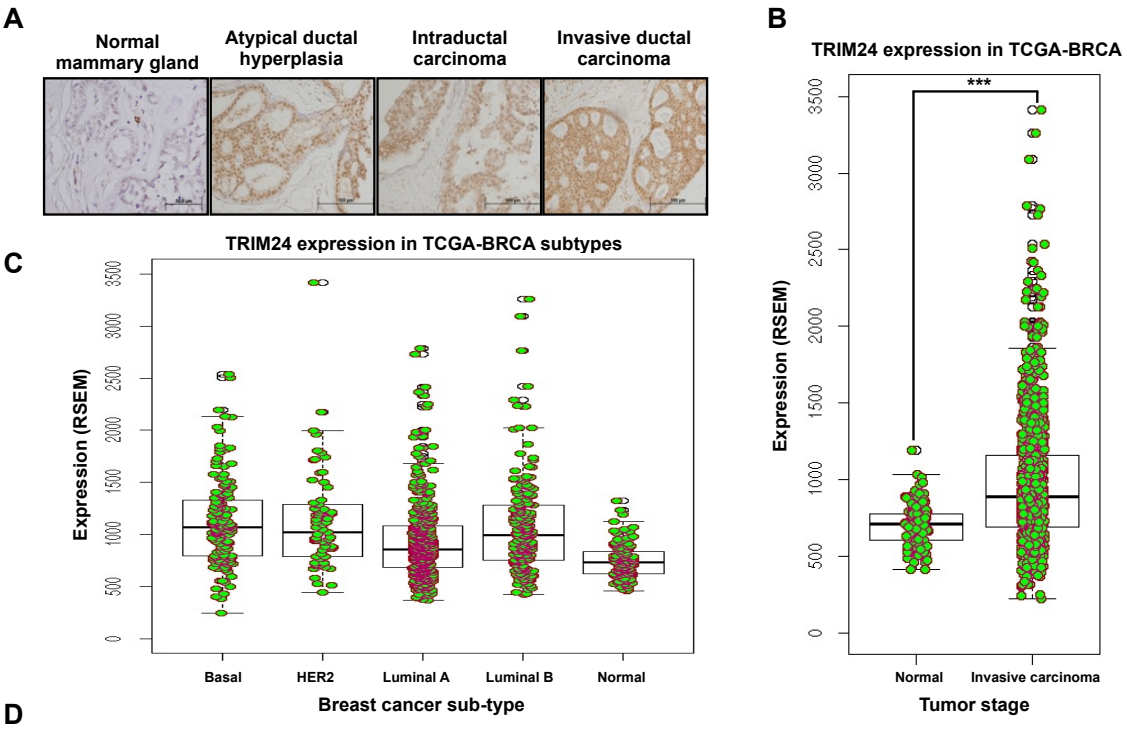


| Breast tissue Array type | TRIM24 | | | P-value |
|---|---|---|---|---|
| | Low | Intermediate | High | |
| ER - (n=43)<br>ER + (n=29) | 15<br>3 | 22<br>12 | 6<br>14 | **0.003** |
| PR - (n=48)<br>PR + (n=24) | 14<br>4 | 24<br>10 | 10<br>10 | 0.160 |
| HER2 - (n=22)<br>HER2 + (n=50) | 14<br>4 | 8<br>26 | 0<br>20 | **<0.0001** |
| p53 - (n=40)<br>p53 + (n=32) | 12<br>6 | 16<br>18 | 12<br>8 | 0.378 |
| Ki67 - (n=22)<br>Ki67 + (n=50) | 8<br>10 | 7<br>27 | 7<br>13 | 0.181 |

**Figure 7: Aberrant expression of TRIM24 during breast cancer progression**.

A, TRIM24-Immunohistochemical (IHC) staining was performed on a breast tissue array (BR2082, US Biomax) with tissues from different stages of breast cancer progression such as normal mammary gland, atypical ductal hyperplasia, Intraductal carcinoma and invasive ductal carcinoma, B, Distribution of TRIM24 expression (p-value:1.32e-07) in TCGA breast invasive carcinoma patients (1008) and normal tissues (92) and C, in PAM50 breast cancer subtypes (950). D, TRIM24 expression in breast tissue array (BR1503, US Biomax) by Allred score (left), Correlation of TRIM24

expression with ER, PR, HER2, p53, and Ki67 (right and bottom left, as assessed by IHC). ***$p < 0.001$.

A

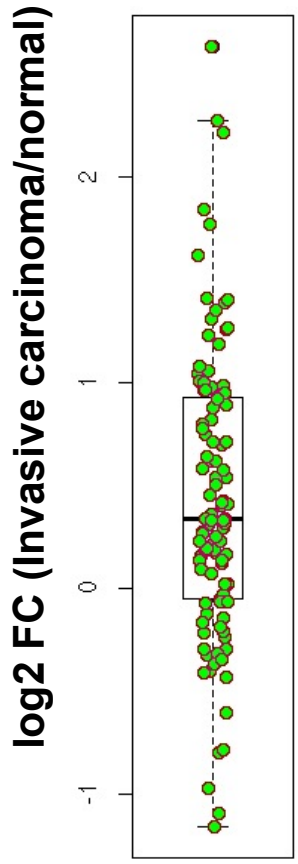


- Fold change > 0 for 78 of 106 (73%) patients with paired profiles
- 40 out of 106 (37.8%) patients have fold change > 1.5

B

**Top 30% vs. Bottom 70%**

| TRIM24 => | High Exp | Low Exp |
|---|---|---|
| LumA | 107 | 325 |
| LumB | 77 | 117 |
| Basal | 66 | 74 |
| Her2 | 31 | 36 |

**p-value**: 1.32e-07

| TRIM24 => | High Exp | Low Exp |
|---|---|---|
| LumA | 107 | 325 |
| Not LumA | 174 | 227 |

**p-value**: 1.46e-08; **Odds ratio**: 0.43

| TRIM24 => | High Exp | Low Exp |
|---|---|---|
| Lum B | 77 | 117 |
| Not LumB | 204 | 435 |

**p-value**: 0.047; **odds ratio**: 1.40

| TRIM24 => | High Exp | Low Exp |
|---|---|---|
| Basal | 66 | 74 |
| Not Basal | 215 | 478 |

**p-value**: 3.8e-04; **Odds ratio**: 1.98

| TRIM24 => | High Exp | Low Exp |
|---|---|---|
| Her2 | 31 | 36 |
| Not Her2 | 250 | 516 |

**p-value**: 0.03; **Odds ratio**: 1.78

**Key:**
**LumA**: ER+, PR+, HER2-; **LumB**: ER+, PR+, HER2+
**HER2**: ER-, PR-, HER2+; **Basal**: ER-, PR-, HER2-

**Figure 8: Aberrant expression of TRIM24 in paired samples of invasive carcinoma and classification based on breast cancer-subtypes**

A, Distribution of TRIM24 expression in TCGA breast invasive carcinoma patients in 106 paired samples; B, Distribution of TRIM24 expression in TCGA breast invasive carcinoma patients based on PAM50 breast cancer subtypes (950). TRIM24 high-expression patients were defined as 30% of patients with high TRIM24 expression. The

p-values suggest enrichment of a particular subtype in TRIM24 high-expressing patients

see Fig. 8B. In the breast cancer tissue array (BR2082, US Biomax), TRIM24 expression stratified into three classes: low (score, 0-2), undetectable to low expression in few foci (25%); intermediate (score, 3-5), abundant foci with expression in nuclear and cytoplasmic compartments (47%); and high (score, 6-8), abundant foci with high expression in nuclei (28%, Fig.6D). Of note, chi-square testing identified a statistically significant positive correlation of TRIM24 expression with ErbB2 (HER2) expression ($p < 0.0001$) and ER ($p = 0.003$) – Appendix 3.

To estimate a timeline for deregulation of TRIM24 expression in breast cancer cells during malignant transformation, we used an isogenic human mammary epithelial cells (iHMECs) model that facilitates assessment of molecular changes from the earliest stages of human breast carcinogenesis (Fig. 9A). In this model, the transformation of normal, finite lifespan iHMECs to malignant cells requires overcoming two distinct senescence-associated barriers to immortality [78, 79]. The first, a stress-associated barrier called stasis, is overcome or bypassed in cultured iHMECs by inactivation of the RB pathway, commonly through loss of $p16^{ink4a}$ expression [65, 66, 80, 81]. iHMECs that escape stasis undergo further proliferation before encountering the second, more stringent barrier to immortality due to critically shortened telomeres [81]. In rare instances, cells that gain telomerase expression escape this barrier and acquire immortal potential. Additional perturbations, such as insertional mutagenesis of p53 [67] or transduction of specific oncogenes [82] can confer malignant properties to the immortally transformed cells. We found that endogenous TRIM24 expression increases at both RNA and protein levels early in the transformation process, after stasis is overcome (184B-7p [65, 78]), and continues to be highly expressed in the immortalized HMEC lines 184A1[66] and 184AA2[67] (Fig. 9B). Strikingly, TRIM24 expression was even more highly up-regulated in MCF-7 cells (p53 wild type and ER positive),

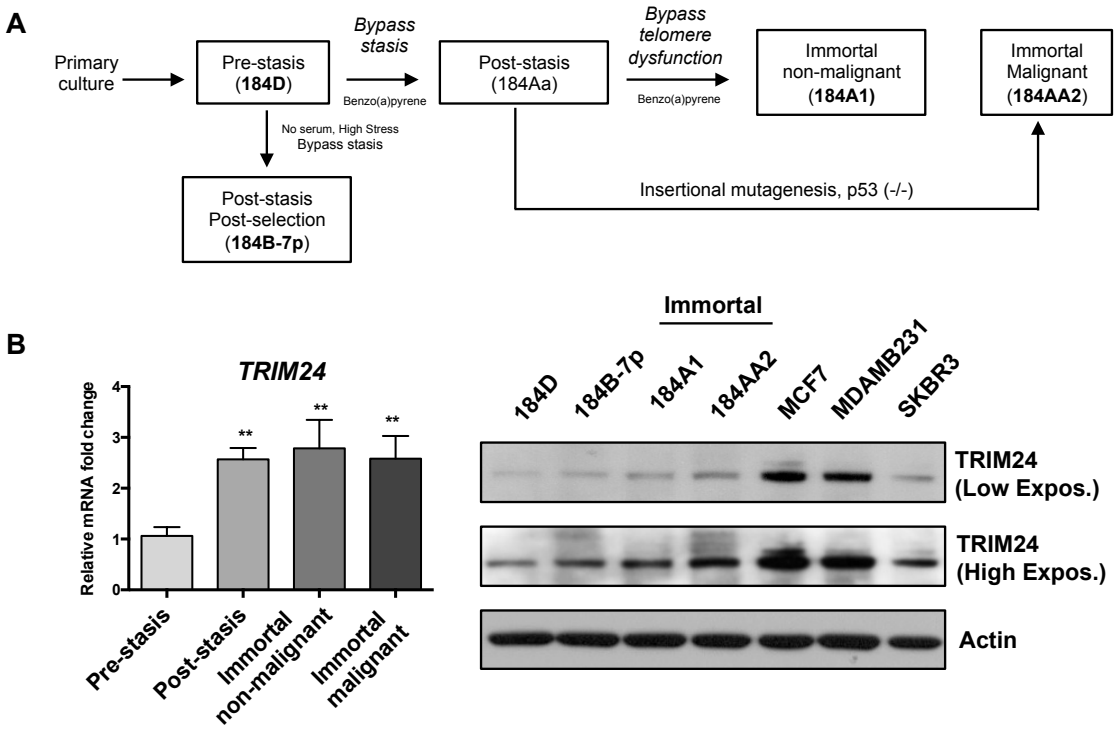


**Figure 9: Aberrant expression of TRIM24 in an isogenic HMEC model**

A, Schematic of the isogenic HMEC model showing transition of the cells from finite-lifespan cells to immortal and malignant cells. B, TRIM24 mRNA (left) and protein (right) expression in HMEC lines transitioning from “normal” finite-lifespan cells before stasis to immortal and malignant cells. Data are averages from three biological replicates ± standard deviation (SD). **p < 0.01.

MDAMB231 (p53- mutant and triple negative) and SKBR3 (p53-mutant and HER2 positive) cultured lines of breast tumor-derived cells (Fig. 9B). Thus, the progressive stages of breast cancer in human patient tumor samples and immortalization of isogenic HMEC lines support a correlation between TRIM24 expression and loss of normal, cellular homeostasis.

### 3.3 TRIM24 drives iHMEC transformation and survival

To answer the critical question of whether TRIM24 causes malignant transformation of iHMECs, we induced ectopic expression of TRIM24 in the non-malignant, immortal 184A1 HMEC (iHMEC) line. Analysis of stable control- (FLAG-only) and TRIM24-expressing, lentiviral-transduced iHMEC pools from two independent experiments (TRIM24-1 and TRIM24-2) showed increased TRIM24 expression at both the RNA and protein level, compared to control pooled cells (Fig. 10A). Of note, we see a corresponding decrease in p53 protein expression in both TRIM24-1 and TRIM24-2 iHMECs suggesting that the ectopically expressed TRIM24 is enzymatically active [53]. The growth rates of TRIM24-1 and TRIM24-2 iHMECs were significantly higher than control vector-transduced iHMECs, suggesting increased proliferation (by cell count see Fig. 10B; by XTT assay see Fig. 10C). Consistent with this, both TRIM24-1 and TRIM24-2 iHMECs exhibited significant enrichment of cells in the S and $G_2$/M phases of the cell cycle, compared to control cells enriched in $G_1$, indicating rapid cell-cycle progression as a result of TRIM24 expression (Fig. 10D, for flow data see Fig. 11).

To assess the oncogenic potential of TRIM24-iHMECs, we examined their ability to grow in an anchorage-independent manner in soft agar. Our control iHMEC line failed to form colonies in soft agar, whereas TRIM24-iHMECs formed colonies comparable in

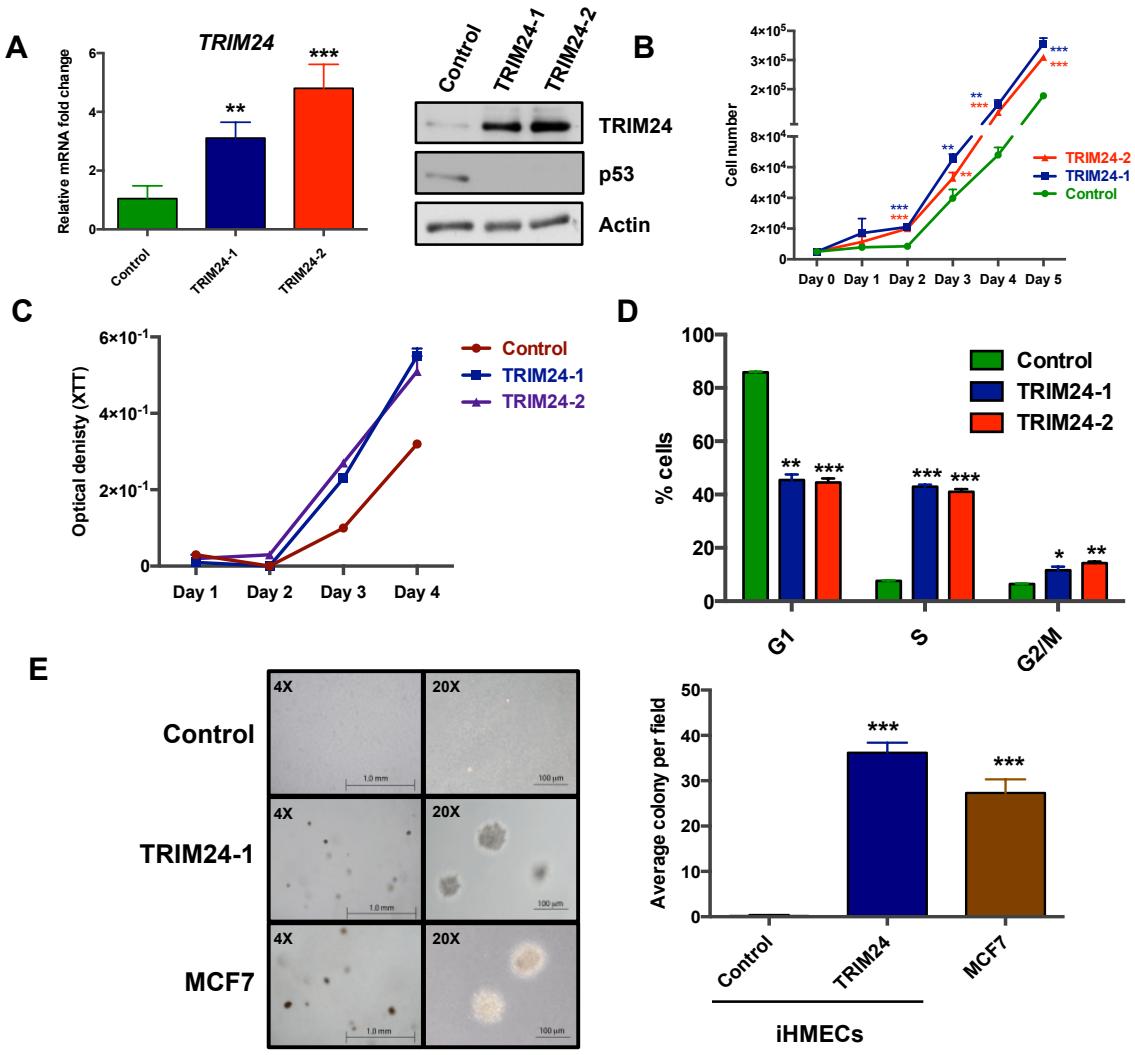


**Figure 10: TRIM24 drives iHMEC transformation and survival.**

A, qRT-PCR analysis of TRIM24 mRNA and Immunoblot of TRIM24 and p53 in Control, TRIM24-1, and TRIM24-2 iHMECs. B & C, Cell proliferation analysis of Control, TRIM24-1, and TRIM24-2 iHMECs by cell count and XTT-based analysis. C, Cell-cycle analysis of Control, TRIM24-1, and TRIM24-2 iHMECs. D, Anchorage-independent proliferation of Control iHMECs, TRIM24-1 iHMECs, and MCF-7 cells as determined using a soft agar colony formation assay (left) and quantification of the colonies per field ± SD (right). The data are averages from two replicates ± SD. *p < 0.05; **p < 0.01; ***p < 0.001.

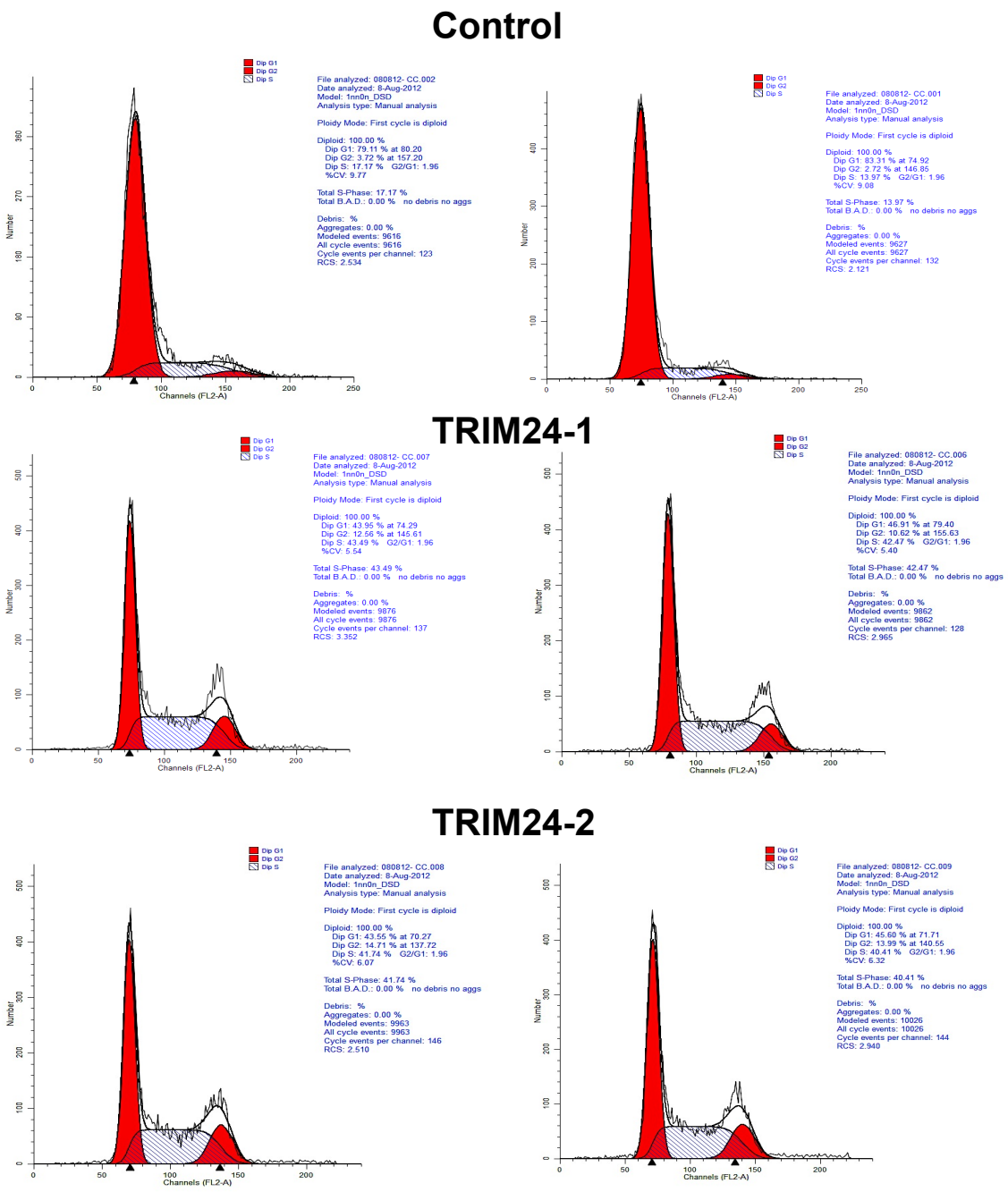


**Figure 11: Graphical representation of cell cycle changes in control vs TRIM24-iHMECs**

Flow data for cell cycle analysis of Control, TRIM24-1 and TRIM24-2 iHMECs.

size and number to colonies of MCF-7 cells used as a positive control (Fig. 10E). Thus, ectopic expression of TRIM24 confers anchorage-independent growth to iHMECs, suggesting that TRIM24 over expression is sufficient to induce malignant transformation of immortal, nontumorigenic HMECs.

### 3.4 TRIM24 regulates multiple cancer-associated pathways and promotes a glycolytic and TCA-cycle gene signature in HMECs

To understand the mechanisms of TRIM24-induced transformation of iHMECs, we analyzed the gene expression profiles of 420 cancer-associated genes in TRIM24-iHMECs and control iHMECs using the nCounter analysis system. This analysis identified 233 genes (55% of the total) that were significantly changed suggesting that TRIM24 mediated deregulated expression of cancer-relevant genes. Expression of 127 (30%) of these genes was upregulated, whereas 106 genes (25%) were downregulated (Appendix 4). Unsupervised hierarchical clustering of the 233 differentially expressed genes clearly distinguished the control and TRIM24-iHMECs (Fig. 12A), supporting TRIM24-mediated transformation of iHMECs via effects on cancer-associated genes and pathways.

TRIM24 induced expression of genes frequently altered in cancers, including *PTEN*, *NRAS*, *KRAS* and others that enrich amongst multiple cancer pathways (see Appendix 5 and 6). Additionally, TRIM24 up-regulated genes are significantly enriched ($p \leq 0.05$) in functional pathways that impact metabolism and growth, including the citrate cycle (TCA), ErbB, insulin, mitogen-activated protein kinase (MAPK) and mTOR signaling and cell cycle regulation (Fig. 12B). The highly significant pathways downregulated by

B

| Up-regulated Pathways | P-value |
|---|---|
| Citrate cycle (TCA cycle) | 2.1E-08 |
| ErbB signaling pathway | 1.1E-07 |
| Insulin signaling pathway | 9.7E-06 |
| MAPK signaling pathway | 0.000087 |
| Cell cycle | 0.0009 |
| mTOR signaling pathway | 0.0015 |

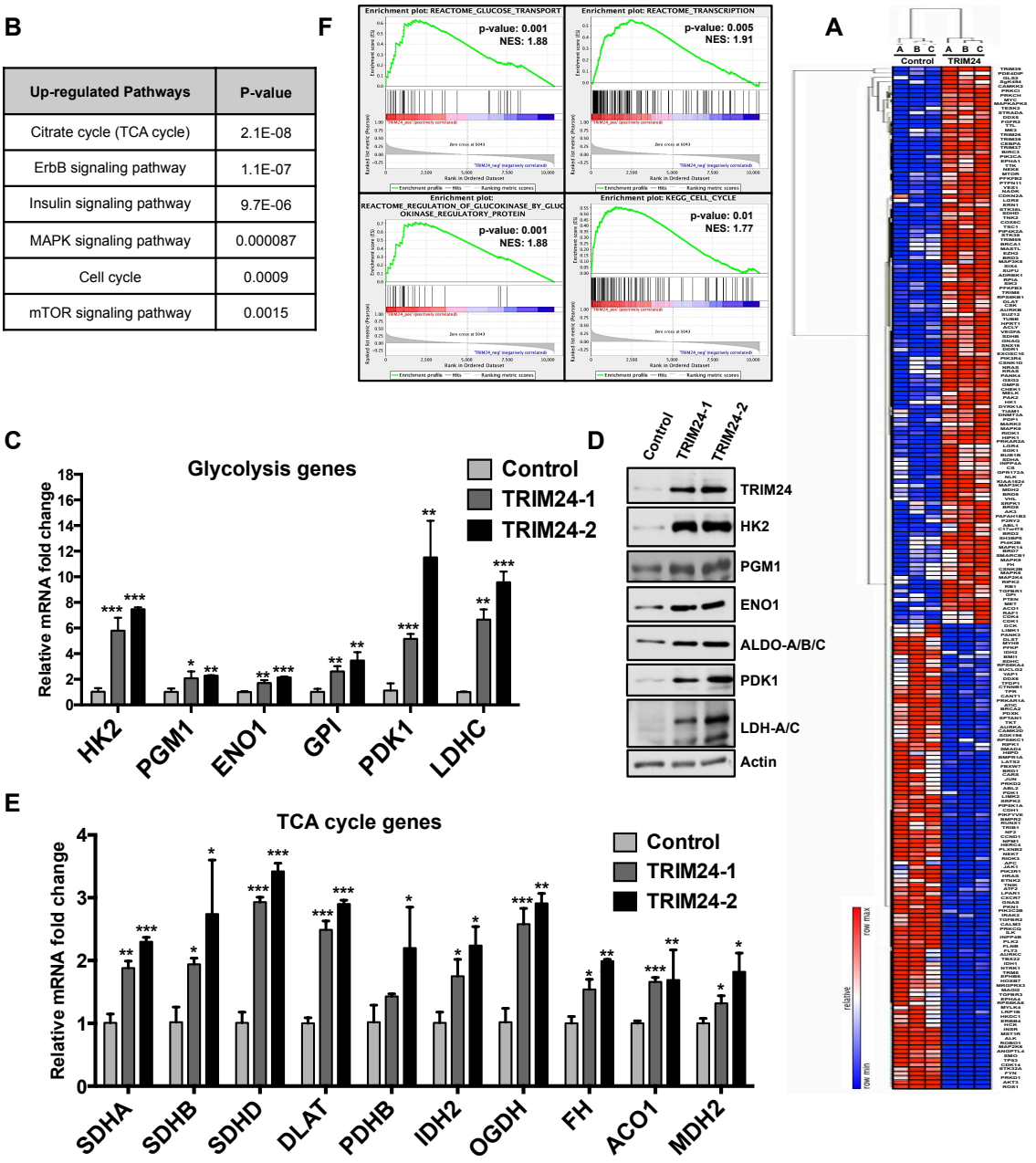


**Figure 12: Regulation of multiple cancer-associated pathways in iHMECs by TRIM24.**

A, Heat map showing unsupervised hierarchical clustering of 233 differentially expressed genes in TRIM24-1 compared to the Control. B, Table showing the list of Upregulated pathways associated with Growth and Metabolism in TRIM24-iHMECs C, qRT-PCR analysis of Glycolytic genes in Control, TRIM24-1, and TRIM24-2 iHMECs showing upregulation of their expression. D, Immunoblot for various Glycolytic proteins

in Control, TRIM24-1, and TRIM24-2 iHMECs. E, qRT-PCR analysis of TCA-cycle genes in Control, TRIM24-1, and TRIM24-2 iHMECs. The data are averages from three biological replicates ± SD. F, GSEA profiles of different pathways positively correlated to TRIM24 expression in TCGA-BRCA dataset. NES: Normalized Enrichment Score. *p < 0.05; **p < 0.01; ***p < 0.001.

TRIM24 expression includes TP53, representing a breadth of cancer types and pathways, as well as members of the ErbB pathway (see Appendix 5 and 6).

Analysis of individual glycolytic regulatory genes uncovered a glycolytic signature, specific to TRIM24-iHMECs versus control, marked by increased Hexokinase 2 (*HK2)*, Phospho-glutamase 1 (*PGM1)*, Enolase 1 (*ENO1)*, Glucose-6-phosphate isomerase (*GPI*), Pyruvate dehydrogenase kinase 1 (*PDK1*), and Lactate dehydrogenase C (*LDHC)* mRNA expression (Fig. 12C). Gene expression changes were reflected in elevated HK2, PGM1, ENO1, PDK1, and LDHC protein expression, along with elevated Aldolase A (Aldo) protein (Fig. 12D). HK2 is a key enzyme involved in tight regulation of glycolysis via catalysis of individual, irreversible steps of glucose to glucose-6-phosphate and phosphoenolpyruvate to pyruvate [83].

Additionally, we found that expression of TCA-cycle genes was also higher in TRIM24-1 and TRIM24-2 iHMECs compared to control iHMECs. Succinate dehydrogenase complex, subunits A, B, and D (*SDHA*, *SDHB* and *SDHD*); dihydrolipoamide S-acetyltransferase (*DLAT*); isocitrate dehydrogenase 2 (*IDH2*); oxoglutarate dehydrogenase (*OGDH)*; aconitase 1 (*ACO1*); malate dehydrogenase 2 (*MDH2*) and fumarate hydratase (*FH*) were among the TCA-associated genes with up-regulated expression (Fig. 12E). Collectively, these results suggest that TRIM24 expression in iHMECs and subsequent transformation rely on increased glucose metabolism to meet the higher energy demands of increased growth and proliferation. This metabolic shift is marked by up-regulation of both glycolysis and expression of TCA-cycle genes.

To determine if these findings are relevant to human breast disease, we assessed whether TRIM24 expression correlated with altered expression of glucose metabolism genes in human breast tumors using TCGA-BRCA expression data and Geneset

enrichment analysis (GSEA) on invasive breast carcinoma samples. Consistent with our *in vitro* findings, we found that the glucose transport pathway (p-value: 0.001, Normalized Enrichment Score (NES[75]): 1.88) was among the top 10 pathways positively correlated with TRIM24 expression (Fig. 12F). For a complete list of enriched pathways please see Appendix 7. Thus, TRIM24 has a significant and/or strong tendency to be co-expressed with genes that regulate glucose metabolism in breast tumors, supporting clinical relevance of our findings.

### 3.5 TRIM24 expression results in diverse metabolic states and increased glucose uptake in iHMECs

To determine the functional impact that TRIM24 expression has on cellular metabolism, we examined the two main bio-energetic pathways: oxidative phosphorylation (OXPHOS) and glycolysis. The rate of oxygen consumption by cells (OCR) is an indicator of mitochondrial respiration [73]. Additionally, cells generate ATP via glycolysis (the conversion of glucose to lactate) independently of oxygen. Measurement of the lactic acid produced indirectly via protons released into the extracellular medium, which causes acidification of the medium surrounding the cells, provides the extracellular acidification rate or ECAR [73]. Previous studies suggest that maintenance of high reserve mitochondrial capacity is a major factor that defines the vitality and/or survival of cancer cells [84].

To examine the bio-energetic phenotype of TRIM24-iHMECs and control iHMECs, we measured respiration, glycolysis rate and ATP turnover in the cells in response to pharmacological modulators of glucose metabolism (Fig. 13A and B). TRIM24-1 and TRIM24-2 iHMECs exhibited higher basal ECARs and OCRs compared to control

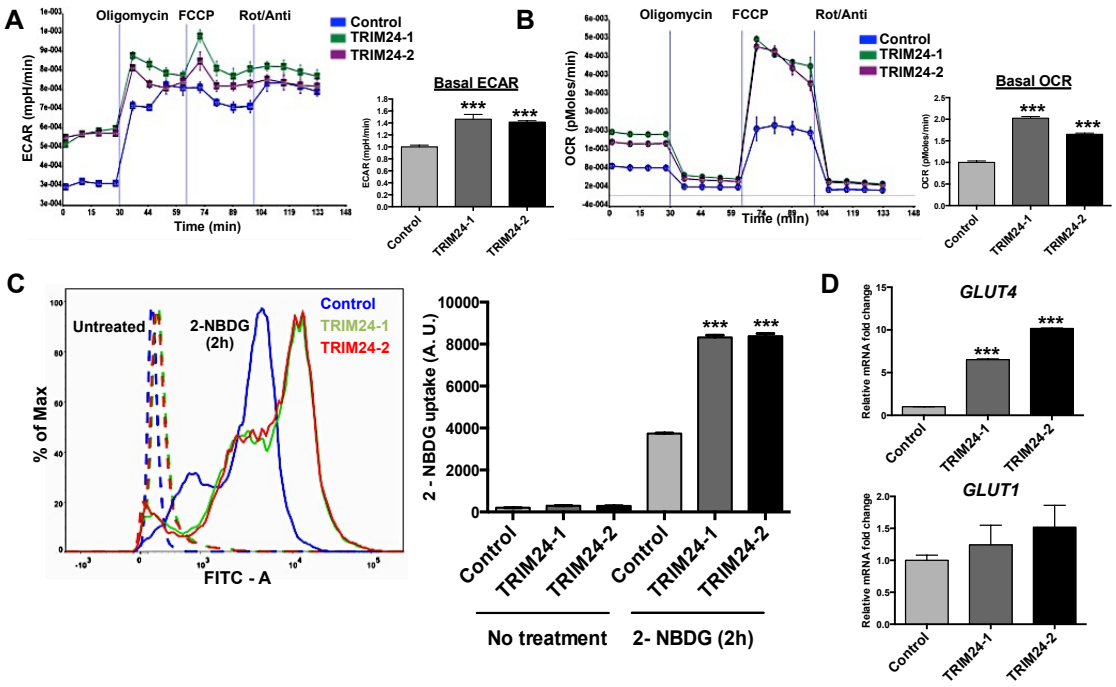


**Figure 13: TRIM24 leads to diverse metabolic states and increased glucose uptake.**

A and B, Extracellular Acidification rate (ECAR) and Oxygen Consumption Rate (OCR) in the presence of Oligomycin (1 μM), FCCP (Carbonylcyanide p-trifluoromethoxyphenylhydrazone, 500 nM) and Rot + Ant [Rotenone (1 μM) + Antimycin A (1 μM) measured using an XF$^{e}$96 Extracellular Flux Analyzer (Sea-horse) for Control, TRIM24-1 and TRIM24 iHMECs. Both ECAR and OCR were normalized using cell number. C, 2-NBDG (Florescent Glucose) uptake assay for Control, TRIM24-1, and TRIM24-2 iHMECs for 0 hours (untreated) and 2 hours. Florescent intensity curves of the 2-NBDG uptake are shown. D, qRT-PCR analysis of GLUT4 and GLUT1 mRNA expression in Control, TRIM24-1, and TRIM24-2 iHMECs. The data are averages from three biological replicates ± SD. ***$p < 0.001$.

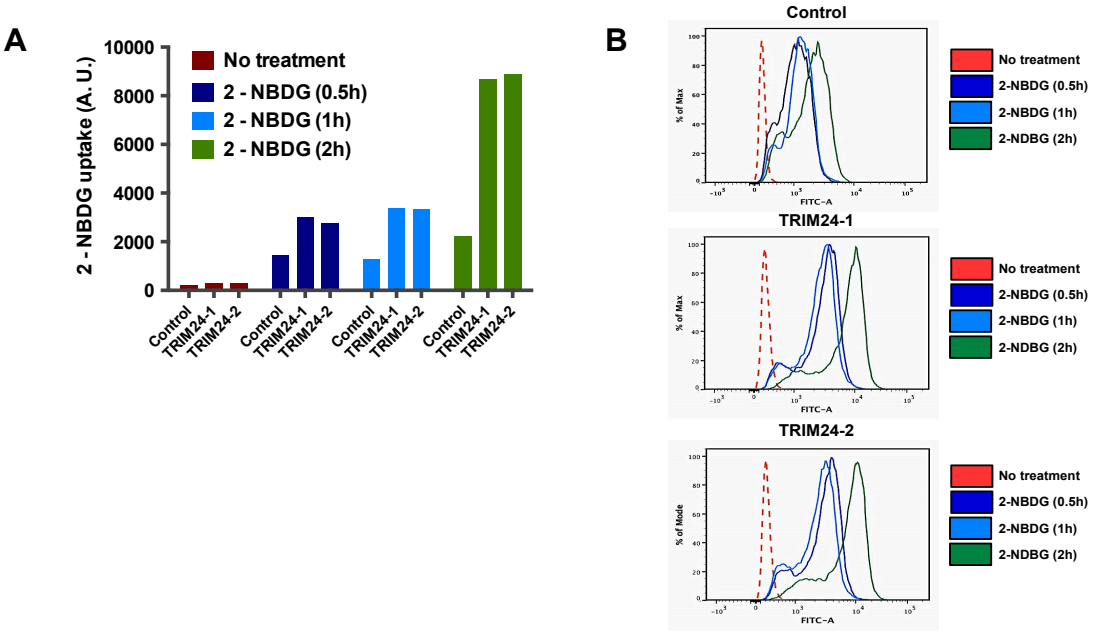


**Figure 14: Glucose uptake time course for control vs TRIM24-iHMECs as measured by FACS**

A and B, 2-NBDG (glucose) uptake assay for Control, TRIM24-1, and TRIM24-2 iHMECs for 0h (untreated), 0.5h, 1h and 2 h respectively. Bar graphs (A) and Florescent intensity curves (B) of the 2-NBDG uptake are shown.

iHMECs, suggesting increased basal glycolysis and mitochondrial respiration, respectively. We then metabolically perturbed the cells by treating the cells with compounds that shift the bio-energetic profiles of the cells. Oligomycin, an inhibitor of the mitochondrial ATP synthase, triggered a robust increase in lactic acid production (Fig. 13A), expressed as changes in ECAR levels in control and TRIM24-iHMECs. After uncoupling the proton gradient in the electron transport chain from oxidative phosphorylation by treating the cells with FCCP, TRIM24-1 and TRIM24-2 iHMECs had much higher reserve mitochondrial capacities than did control iHMECs (Fig. 13B). With these effects on metabolism, TRIM24-iHMECs are more responsive to stress under conditions of increased energy demand, compared to control iHMECs. Taken together, our findings suggest that ectopic expression of TRIM24 in iHMECs leads to increased basal glycolysis and basal mitochondrial respiration in parallel with an increased reserve of mitochondrial capacity.

Next, we studied whether the altered bio-energetic states of TRIM24-iHMECs result in increased glucose uptake by these cells. We compared control and TRIM24-iHMECs using the fluorescent 2-deoxyglucose analog (2-NBDG) staining. Our results indicated higher glucose uptake in both TRIM24-1 and TRIM24-2 iHMECs, compared to control iHMECs, further confirming the increased glycolytic state of TRIM24-transformed cells. (Fig. 13C and Fig. 14A-B). Consistent with this, we observed significantly increased glucose transporter protein *GLUT4* gene expression and measurable *GLUT1* activation in TRIM24-iHMECs (Fig. 13D).

### 3.6 TRIM24 causes deregulation of two key players of cancer metabolism

p53 and c-Myc are two important regulators that determine the fate of cellular metabolism. The tumor suppressor p53 regulates energy metabolism by lowering rates of glycolysis and inducing mitochondrial respiration. *GLUT1* and *GLUT4* are direct p53 direct targets of transcriptional regulation [85]. p53 indirectly represses GLUT3 by repressing NF-κβ gene expression [86]. p53 induces the expression of *TIGAR* (TP53-inducible glycolysis and apoptosis regulator) and TIGAR significantly slows down tumor glycolysis by converting fructose 2,6-bisphosphate back to fructose 1-phosphate [33]. Fructose 2,6-bisphosphate functions as an allosteric activator of PFK1, a major glycolytic enzyme. Fructose 2,6-bisphosphate is produced by PFK2 from fructose 1-phosphate. Additionally, p53 indirectly represses activation of several glycolytic enzymes by activating miR-34a [87]. The net result of constitutive p53 activation is primarily to direct the glycolytic flux towards pyruvate that can then enter the TCA cycle.

In contrast, the oncogene c-Myc is known to upregulate glycolysis, glutaminolysis and mitochondrial biogenesis in cancer cells. c-Myc directly upregulates the expression of HK2, PFK1, TPII, LDHA and several others in the glycolytic pathway. The majority of glycolytic enzymes contain c-Myc binding motifs in their gene promoters [88]. Two major glutamine reporters, ASCT2 and SN2, are trans-activated by c-Myc in several tumors [89]. GLS1, one of the major enzymes responsible for glutaminolysis, is indirectly upregulated by c-Myc suppressing miR-23a/b [90]. c-Myc regulates expression of several nuclear-encoded genes critical for mitochondrial growth and biogenesis. Mitochondrial transcription factor A (TFAM), a critical regulator of mitochondrial DNA replication and transcription, is trans-activated by c-Myc [91].

Interestingly, in TRIM24-iHMECs there is a significant induction of c-Myc mRNA and protein expression with concomitant decrease in p53 protein levels (Fig. 15). Induction of c-Myc and degradation of p53 in TRIM24-iHMECs may explain the dual induction of glycolysis and TCA cycle in these cells. Whether or not TRIM24 directly regulates expression of genes associated with metabolism or does indirectly by regulating p53 and c-Myc needs to be determined.

### 3.7 TRIM24 regulates expression of several genes associated with glucose metabolism in multiple breast cancer lines

We asked whether TRIM24-mediated regulation of glycolytic and TCA-associated genes is widespread amongst various cellular models of breast cancer by assessing multiple, established cell lines derived from breast tumors. Transient knock down of *TRIM24* (siTRIM24) expression in MCF-7 (luminal), MDA-MB-231 (triple-negative), and SKBR3 (*HER2*-positive) indicated that depletion of *TRIM24* down-regulated *GLUT1*, *ACO1*, *IDH1*, *IDH2*, *PGM1*, and *OGDH* expression in MCF-7 cells (Fig. 16A & Fig. 17). Moreover, expression of *GLUT1*, *ACO1*, *IDH1*, and *IDH2* was likewise decreased in MDA-MB-231 and SKBR3 cells treated with TRIM24 siRNA, suggesting that regulation of specific metabolic genes by TRIM24 is conserved, albeit to varying levels. We then checked for expression of the aforementioned metabolic genes in the isogenic panel of HMECs. Interestingly, we found that the endogenous expression pattern of *ACO1* and *IDH2* parallels endogenous TRIM24 expression and follows an upward trend along the transformation process, and *OGDH* and *HK2* gain highest expression in the immortalized malignant HMECs (Fig. 16B). Taken together, these results suggest that

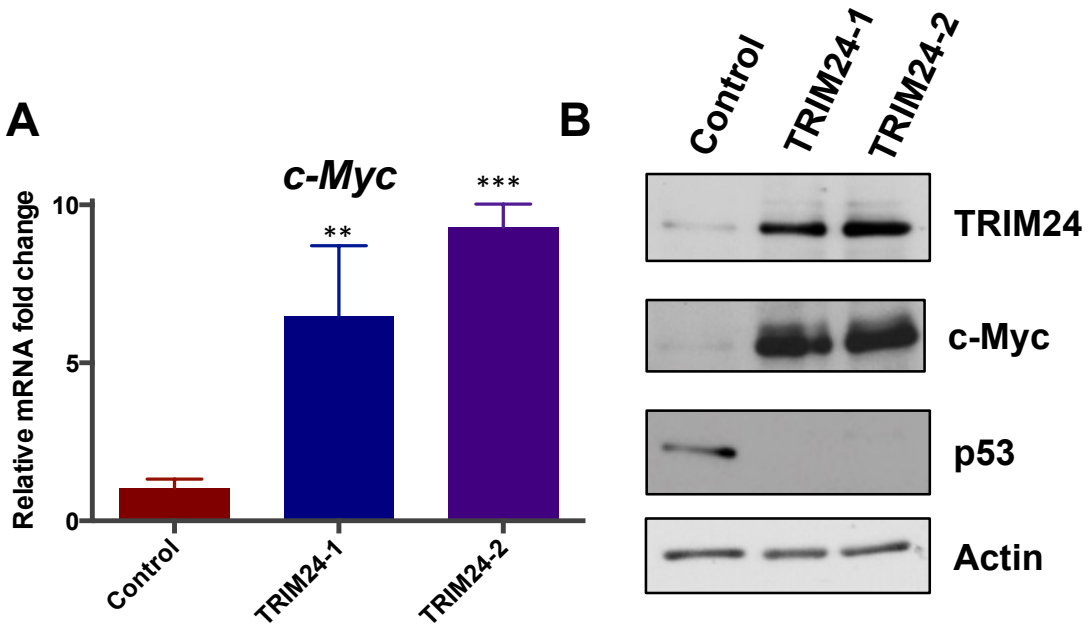


**Figure 15: TRIM24 induces deregulation of two key players of cancer metabolism**

A & B, qRT-PCR analysis of cMyc mRNA (A) and Immunoblot of TRIM24, c-Myc and p53 in Control, TRIM24-1, and TRIM24-2 iHMECs. The data are averages from three biological replicates ± SD. *$p < 0.05$ and **$p < 0.01$.

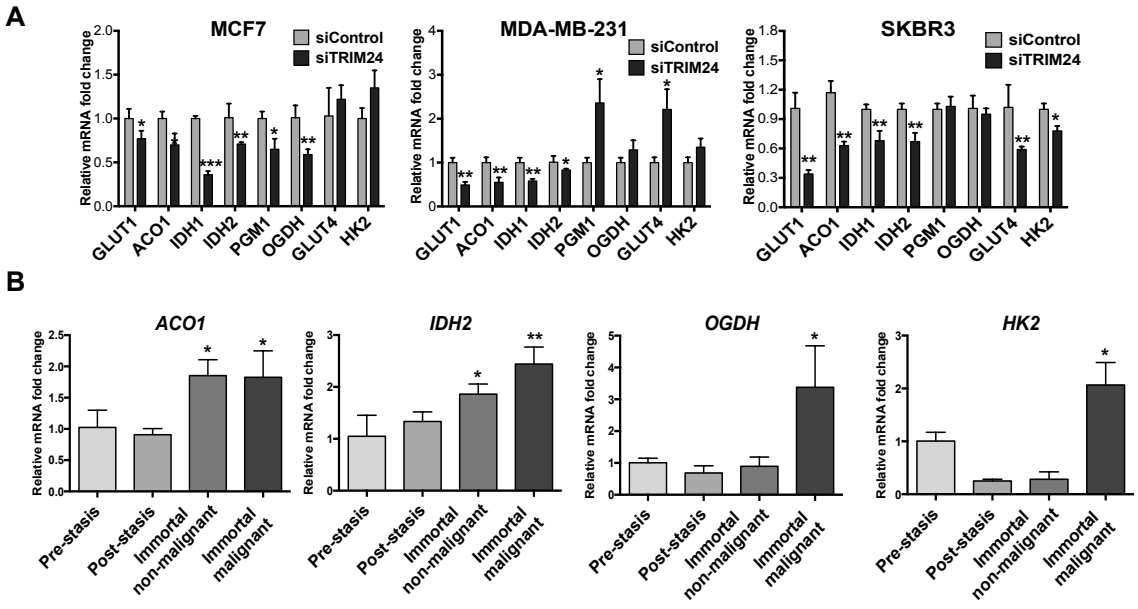


**Figure 16: TRIM24 regulates expression of several genes associated with glucose metabolism in multiple breast cancer subtypes**

A, MCF-7, SKBR3 and MDA-MB-231 cells were transfected with siControl or siRNA against TRIM24 (siTRIM24) and harvested 48 hours later. Effect of TRIM24 knockdown on expression of a glucose metabolism gene panel (by qRT-PCR analysis) is shown. The data are averages from three replicates ± SD. *$p < 0.05$; **$p < 0.01$; ***$p < 0.001$. B, mRNA expression for ACO1, IDH2, OGDH and HK2 in HMEC lines transitioning from normal finite-lifespan pre-stasis cells to abnormal finite post-stasis, non-malignant immortal and malignant cells. The data are averages from three biological replicates ± SD. *$p < 0.05$ and **$p < 0.01$.

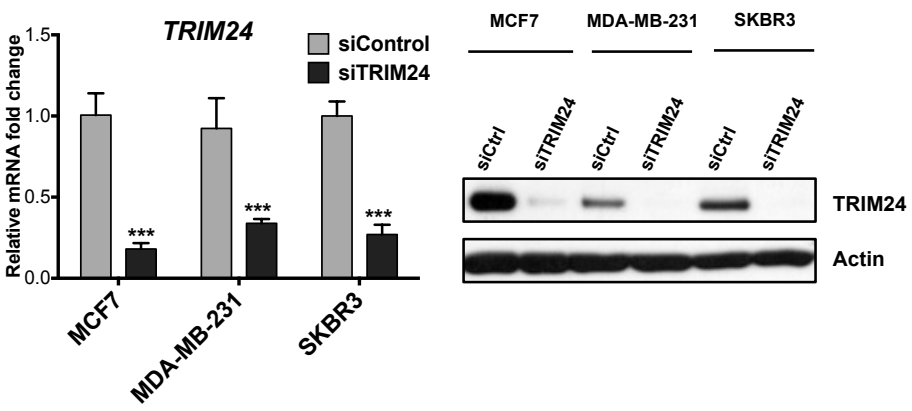


**Figure 17: siRNA based TRIM24 knockdown in multiple breast cancer cell lines**

TRIM24 RNA and protein levels in various breast cancer cell lines MCF-7, SKBR3 and MDA-MB-231 cells were transfected with siControl or siRNA against TRIM24 (siTRIM24). TRIM24 RNA (by qPCR) and protein expression (by Western) are shown.

TRIM24-mediated deregulation of glucose metabolism is a relatively global phenomenon that occurs in multiple breast cancer subtypes.

### 3.7 TRIM24-HMECs form intermediate to high-grade tumors in nude mice

We assessed the impact of *TRIM24* expression in iHMECs by *in vivo* xenograft formation. To this end, we injected female nude mice subcutaneously with either Control or TRIM24-iHMECs in 50% high concentration matrigel. TRIM24-1 and TRIM24-2 xenografts displayed significantly higher xenograft volume as compared to their control counterparts (Fig. 18A and Fig. 19A-C). H&E staining showed that xenograft tumors from TRIM24-iHMECs contained intermixed neoplastic epithelial cells and fibrous tissue in various proportions (Fig. 18B, left panel), whereas no epithelial cells were detected in xenografts from Control-iHMECs (Fig. 18C and Fig. 19D-E). TRIM24-expressing, neoplastic epithelial cells formed tumors that reflect a spectrum of low, intermediate and high-grade malignancy (Fig. 18B, left panel). The expression levels of TRIM24 in these tumors correlated with the malignancy grade, as shown by TRIM24-IHC (Fig. 18B, right panel). The grade of malignancy was based on the degree of cellular atypia, anysokaryosis and degree of vascularization (Fig. 19F-H and Appendix 8). Of note, about 60-70% of the tumors formed with TRIM24-iHMECs were either intermediate or high grade (Fig. 18C) with the proportion of epithelial cells in the subcutaneous tumors at 30-40% (Fig. 18D and Fig. 19E), compared to xenografts of Control-iHMECs that consisted of fibrous tissue only (Fig. 19E and Appendix 8). Taken together, these data indicate that over expression of TRIM24 can confer *in vivo* tumorigenic growth of iHMECs.

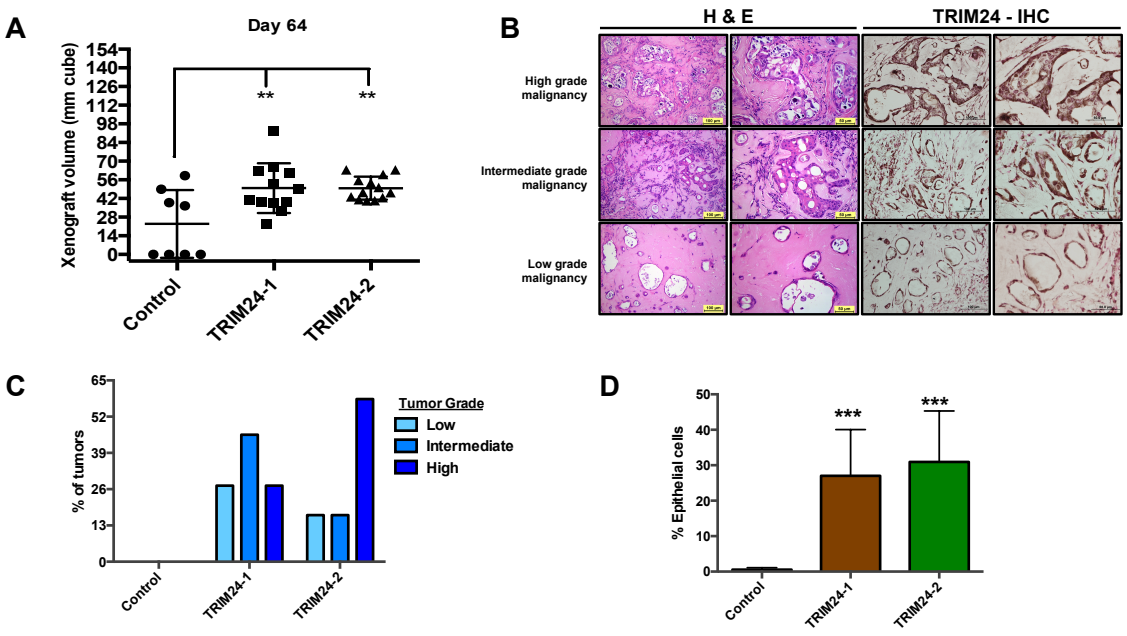


**Figure 18: TRIM24-HMECs form intermediate to high-grade tumors in nude mice**

A, Tumor volume after 65 days post-injection of Control and TRIM24-iHMECs in nude mice. **p < 0.01 (all compared to Control). B, H&E Staining and TRIM24-IHC for various grades of tumors obtained from nude mice injected with TRIM24-iHMECs. C, Distribution of various grades of tumors from mice injected with either Control or TRIM24-iHMECs. D, Distribution of epithelial cells in tumors from mice injected with either Control or TRIM24-iHMECs.

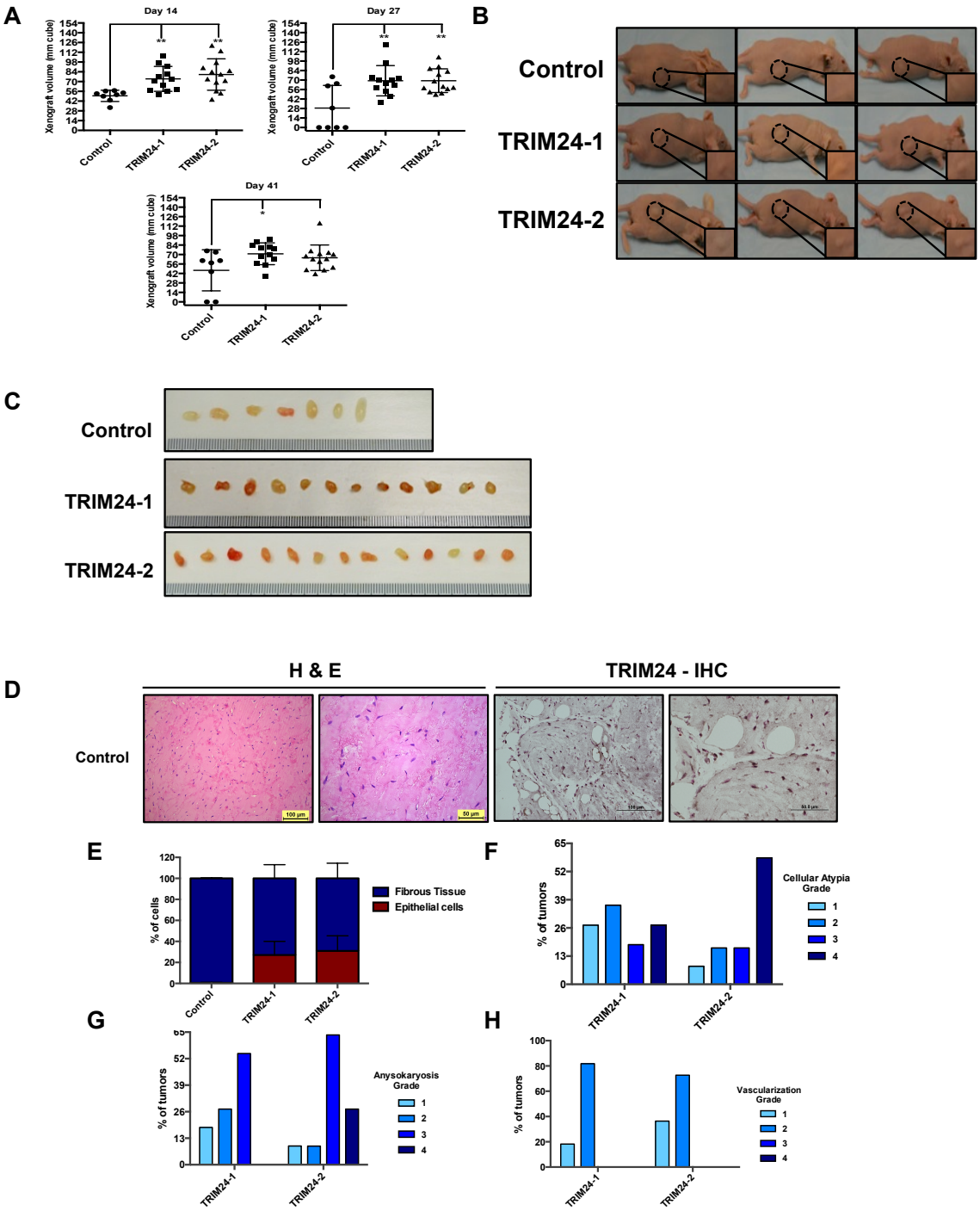


**Figure 19: Characterization of xenograft tumors formed by control and TRIM24-HMECs**

A, Tumor volume post-injection of Control and TRIM24-iHMECs in nude mice after Day 14, Day 27 and Day 41. *$P < 0.05$, **$P < 0.01$ (all compared to Control). B, Images

from mice injected with Control or TRIM24-iHMECs (showing tumors). C, Tumors obtained from mice injected with Control or TRIM24-iHMECs

D, H&E Staining and TRIM24-IHC for a representative tumor obtained from mice injected with Control-iHMECs. E, Percentage of Epithelial cells v/s fibrous tissue in tumors obtained from mice injected with Control or TRIM24-iHMECs. F, G and H, Cellular atypia grade, Anysokaryosis grade and Vascularization grade of tumors obtained from mice injected with Control of TRIM24-iHMECs.

### 3.8 TRIM24 directly regulates expression of various metabolic genes

To elucidate critical targets of TRIM24-induced transformation, previously published TRIM24 ChIP-seq (in MCF7 cells) was intersected with the transcriptional signature obtained after TRIM24-overexpression in iHMECs. Interestingly, several metabolic genes were bound by TRIM24. Recruitment of TRIM24 at several of these metabolic genes was confirmed by TRIM24-ChIP followed by qPCR in MCF7 cells. As shown in Fig. 20, TRIM24 is recruited to the promoters of several metabolic genes such as *GLUT1*, *IDH1* and *IDH2*. Hence, it is clear that *GLUT1*, *IDH1* and *IDH2* are direct TRIM24 targets.

Next, in order to determine which transcription factor(s) may help recruit TRIM24 at these metabolic genes, transcription factor affinity prediction (TRAP) analysis was performed. In TRAP analysis, it was found peroxisome proliferator activated receptor-γ (PPARγ) was among the top-three transcription factors to be significantly enriched at TRIM24-binding sties (Fig. 21). One of the key players that regulates adipogenesis and whole-body lipid metabolism is PPARγ [92]. In addition, it is also crucial for controlling gene networks involved in glucose homeostasis including increasing the expression of GLUT4 and c-Cbl associated protein (CAP)[92]. Intriguingly, in breast cancer cells ER-α physically associates with PPARγ and functionally interferes with PPARγ signaling [93]. Future studies will investigate the crosstalk between TRIM24, PPARγ and ER-α by co-immunoprecipitation and ChIP assays to confirm their recruitment and mechanism of action at various metabolic genes.

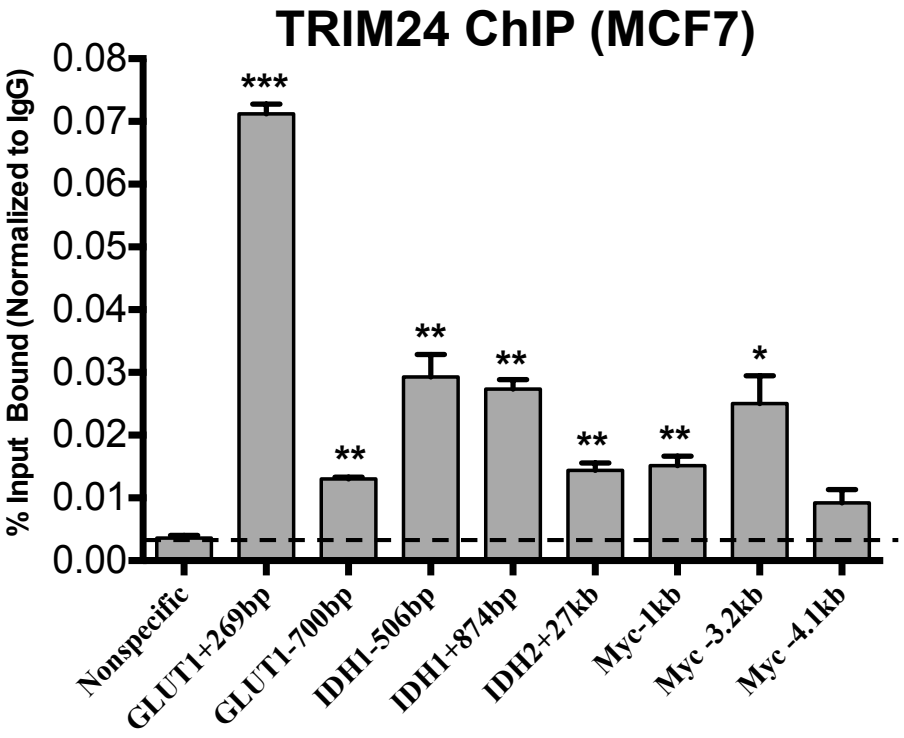


**Figure 20: TRIM24 ChIP in MCF7 cells**

TRIM24 ChIP confirms recruitment of TRIM24 at various metabolic genes such as *GLUT1*, *IDH1* and *IDH2*, and c-Myc along with previous assessment of gene expression to show direct impact of TRIM24 binding. *$P < 0.05$, **$P < 0.01$ and ***$P < 0.001$ (TRIM24 ChIPs done by Sabrina Stratton).

A

| Rank | Gene | Matrix ID | Chi-Square | P value | Adjusted P value |
|---|---|---|---|---|---|
| 1 | **ESR1** | MA0112.2 | 95.9 | 1.99e-13 | 2.35e-11 |
| 2 | **ESR2** | MA0258.1 | 87.8 | 6.25e-12 | 3.69e-10 |
| 3 | **PPARG** | MA0066.1 | 61.5 | 2.87e-07 | 1.13e-05 |
| 4 | NFE2L2 | MA0150.1 | 39 | 0.0011 | 0.0324 |
| 5 | RORA1 | MA0071.1 | 37.4 | 0.00182 | 0.043 |

B

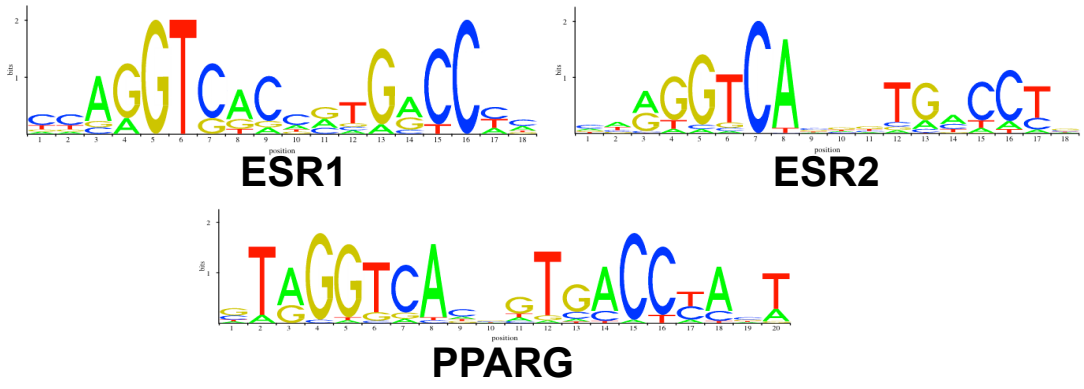


**Figure 21: TRAP analysis of TRIM24-binding peaks in MCF7 cells**

A. Table showing Top 5 hits of Transcription factor affinity prediction of TRIM24 binding peaks in MCF7 cells. B. Binding motifs of Top 3 hits viz. ESR1, ESR2 and PPARG. (Bio-informatic analysis done by Whijae Roh).

### 3.8 Effect of TRIM24 over-expression on HMEC cell size and karyotype

Interestingly, H&E staining of TRIM24-iHMECs, showed that TRIM24-iHMECs were much bigger in size (Fig. 22A) and the overall nuclear to cytoplasmic ratio was very high in these cells. Also, when an equal number (4 million) of control and TRIM24-iHMECs were spun down in a 15ml tube, the pellet formed by TRIM24-iHMECs occupied much more area (Fig. 22B).

Since, TRIM24-iHMECs are much bigger in size and exhibit all of the hallmarks of transformed cells, we determined if there was any change in the chromosome number upon TRIM24 overexpression. We performed a karyotype analysis in control and TRIM24-iHMECs and found that the majority of TRIM24-iHMECs were aneuploid with an average of 74-76 chromosomes per cell; the control-iHMECs had a normal karyotype with close to 46 chromosomes per cell (Fig. 23). In both TRIM24-iHMECs clones, increased chromosome copies (tri-, tetra- and penta- somy) and chromosomal rearrangements and translocations were observed with high frequency. A high frequency of mutated chromosomes (M) was also observed in TRIM24-iHMECs.

### 3.9 Effect of dual TRIM24-BRPF1 Bromodomain inhibitor on glucose metabolism

As discussed previously, TRIM24 contains a tandem PHD and Bromo-domain in the C-terminus that reads a non-canonical histone signature (H3K4me0 and H3K23ac). Because of the druggability of bromodomain-containing proteins, the TRIM24-bromo-domain offers a potential therapeutic for epigenetic regulation [94]. As part of the drug discovery program at the MD Anderson Cancer Center, a highly potent and selective dual TRIM24-BRPF1 bromodomain inhibitor (IACS-9571) was developed with an ITC $K_d$ = 31 nM for TRIM24 and ITC $K_d$ = 14 nM for BRPF1 [95].

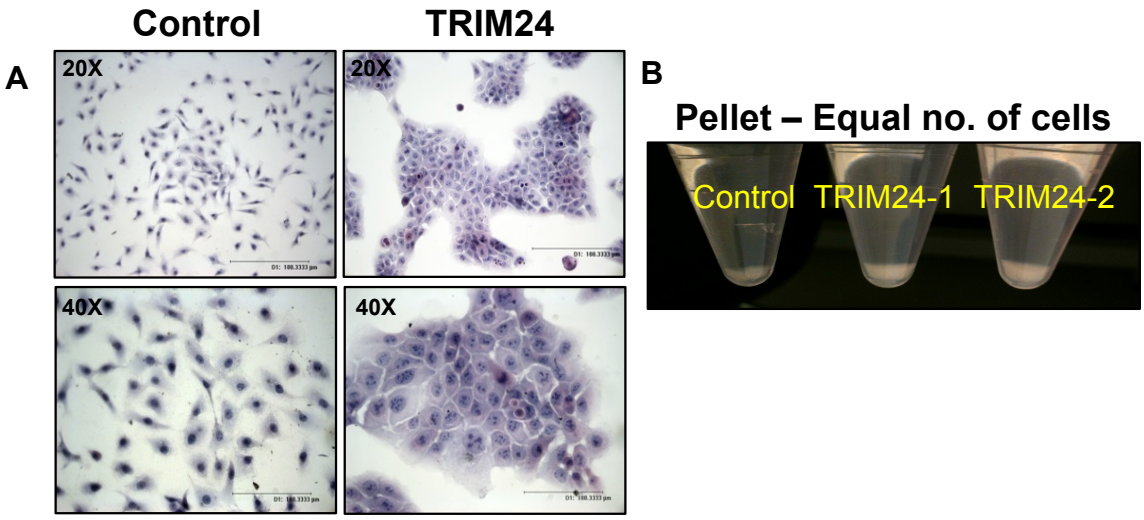


**Figure 22: TRIM24-iHMECs are bigger in size**

A. Bright light images of H&E staining of control and TRIM24-iHMECs. B. Bright light image of 15ml tube (bottom) after spinning down equal number (4 million) of control and TRIM24-iHMECs.

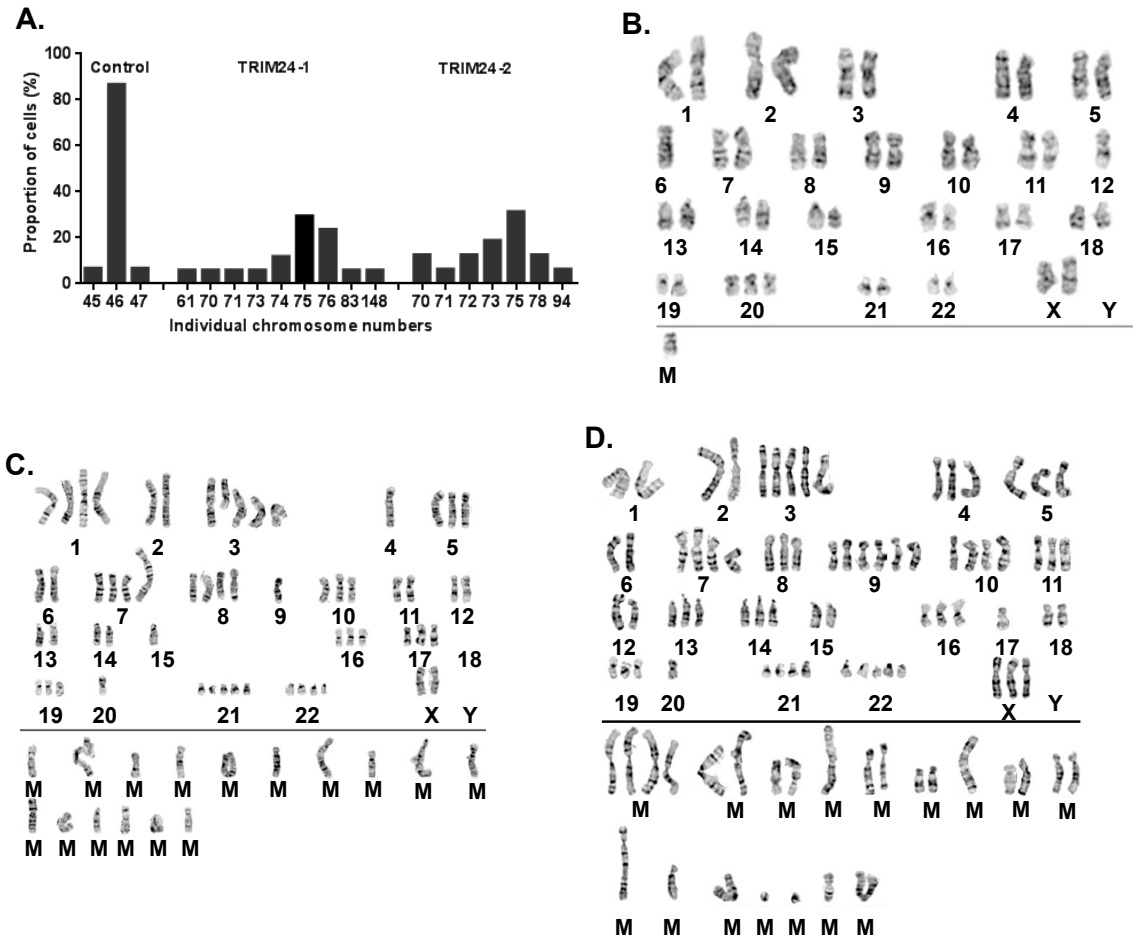


**Figure 23: Over-expression of TRIM24 in HMEC stable cell lines causes aneuploidy.**

A. Individual chromosome numbers from metaphase spreads of immortalized stable HMEC line in control or stably over-expressing TRIM24 (TRIM24-1, TRIM24-2) were analyzed (n=100). B. Representative images of G-band karyotype in control HMEC, showing the 46 chromosomes with haploid 6 and trisomy 20 that is similar to the previous published data. (C, D) Over-expression of TRIM24 in immortalized HMEC is sufficient to induce chromosome instability (CIN): Representative images of G-band karyotypes in TRIM24-1 and -2.

In order to determine if TRIM24-bromodomain function is critical for regulating glucose metabolism in breast cancer, MCF7 cells were treated with IACS-9571 for 48 h (1 μM and 5 μM). The mRNA expression of several metabolic genes was evaluated by RT-qPCR. Interestingly we found that expression of several genes associated with glucose metabolism was downregulated upon treatment with IACS-9571 (Fig. 24). These results suggest that interaction of TRIM24 with chromatin via its bromodomain may be critical for regulating glucose metabolism in breast cancer. However, the effect of IACS-9571 on glucose metabolism needs to be tested in additional breast cancer cell lines. In the future, TRIM24-overexpressing stable cells with a bromodomain chromatin-binding mutant of TRIM24 will be generated and tested for various hallmarks of transformation and changes in glucose metabolism to clearly define the role of the TRIM24 bromo-domain in regulating cancer metabolism.

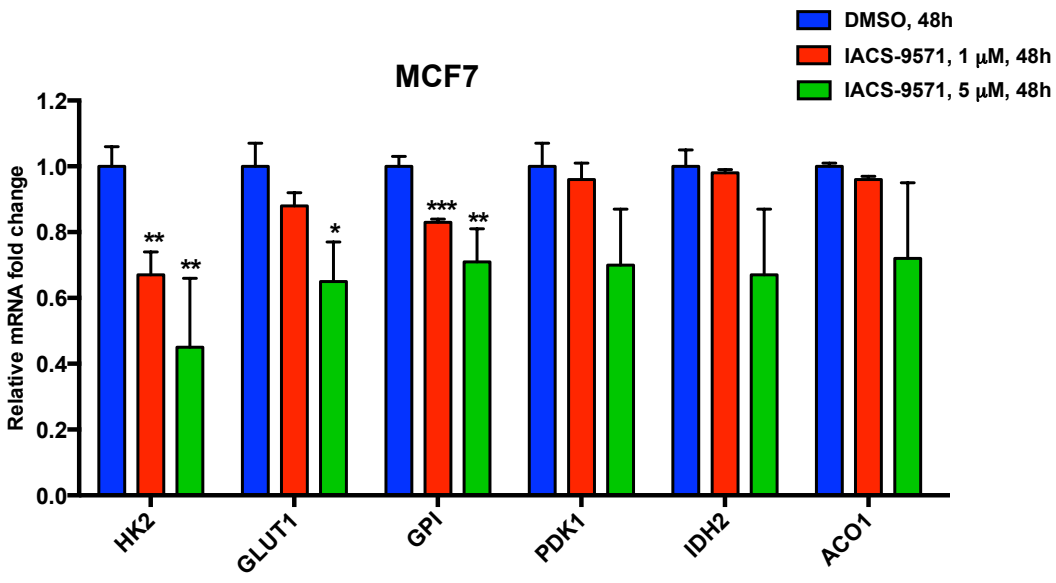


**Figure 24: Effect of TRIM24-bromodomain inhibition on glucose metabolism in breast cancer**

RT-qPCR data of various glucose metabolism genes after treatment of MCF7 cells with respective concentration of IACS-9571.

# Chapter 4: TRIM24 acts as a novel regulator of Epithelial Mesenchymal Transition (EMT) in breast cancer

# Chapter 4: TRIM24 acts as a novel regulator of EMT in breast cancer

## 4.1 Introduction and Rationale

TRIM24 is a multi-domain protein that i) negatively regulates p53 via its RING domain, ii) interacts with estrogen receptor (ER) via an LXXLL motif, and iii) recruits transcription factors to chromatin as a histone reader with PHD-Bromodomains that recognize H3K4me0/H3K23ac [96]. Recently, aberrant over-expression of TRIM24 in cancers of multiple origins, including prostate cancer [47], breast cancer [55, 56], non-small cell lung cancer [57], head and neck carcinoma [58], colorectal cancer [59], gastric cancer [60], glioblastoma [61] and human hepatocellular carcinoma [63] has been reported. My previous work showed that TRIM24 expression caused major shifts in metabolism and promoted transformation of immortalized human mammary epithelial cells [97]. However, a detailed analysis of how TRIM24 promotes tumorigenesis with progression to metastasis has not been elucidated.

Metastasis is multi-step process consisting of migration of cancer cells from the primary tumor, followed by local invasion, intravasation, extravasation and finally colonization of cancer cells at distant organs. Each step of metastasis involves a series of specific cell-to-cell interactions and activation of different signaling pathways [16]. Prior to metastatic progression of a tumor, cancer cells undergo a transition from an epithelial to a mesenchymal phenotype; the process is called the epithelial-mesenchymal transition (EMT). My preliminary analysis shows that TRIM24 is a driver of EMT. During the EMT process, epithelial cells lose cell polarity, disassemble their cell-cell adhesion machinery and acquire cell motility. The EMT process is marked by loss of E-cadherin and acquisition of various mesenchymal markers such as N-cadherin and vimentin, as a result of activation of transcription factors such as Snail,

Slug, Twist and ZEB1/ZEB2 [16]. I hypothesize that aberrant expression of TRIM24 impacts a network of transcription regulatory factors and signaling pathways to induce EMT and metastasis in breast cancer.

### 4.2 TRIM24 induces a mesenchymal-phenotype in breast epithelial cells

MCF10A cells exhibit multiple characteristics of normal breast epithelium such as an absence of anchorage-independent growth, hormone-dependent and growth factors for survival and proliferation and absence of tumorigenicity in xenograft studies in mice [68]. To further understand the mechanism of TRIM24-mediated oncogenesis, TRIM24 (FLAG-tagged, wild-type) was stably overexpressed in MCF10A. Overexpression of TRIM24 was confirmed by RNA (RT-qPCR) and protein (immunoblotting) analyses (Fig. 25A). Interestingly, TRIM24-expression substantially altered the morphology of MCF10A cells, resulting in decreased clustering, loss of cell-cell contacts and increased mesenchymal-like morphology (Fig. 25B).

In order to determine if TRIM24-overexpression induced EMT, RNA and protein expression analyses of known EMT markers were performed. Gene and protein expression analysis revealed an EMT signature, specific to TRIM24-overexpressing MCF10A cells versus vector only cells, marked by decreased E-cadherin (*CDH1*), and increased N-cadherin (*CDH2*), Fibronectin-1 (*FN1, mRNA*), Snail Family Zinc Finger 1 (SNAI1, protein), Snail Family Zinc Finger 2 (*SNAI2* aka *Slug, mRNA*) and Vimentin (VIM, protein) (Fig. 26C-D). Loss of E-cadherin (CDH1) in TRIM24-overexpressing MCF10A cells was further confirmed by immunofluorescence staining. As shown in Fig. 24E, TRIM24-OE MCF10A cells have no detectable expression of CDH1 (red), whereas vector MCF10A cells show very high expression of CDH1.

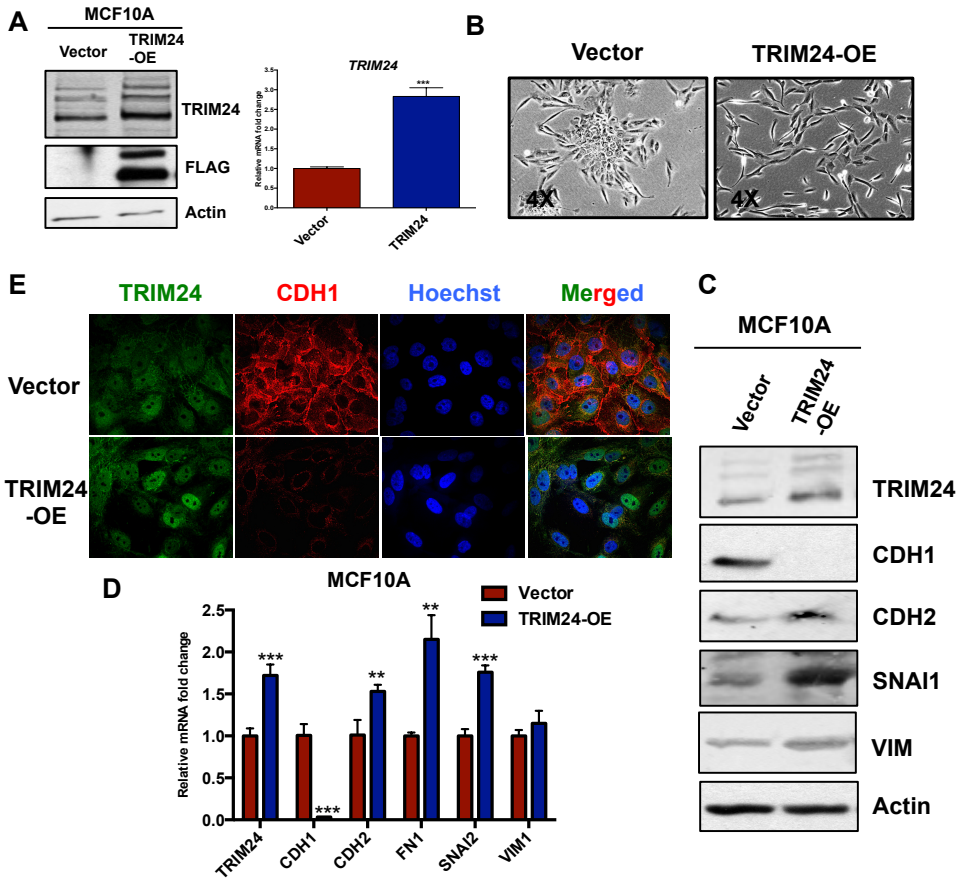


**Figure 25: TRIM24 induces EMT signature in breast epithelial cells**

A, qRT-PCR analysis of TRIM24 mRNA and Immunoblot of TRIM24 and actin in vector and TRIM24-OE MCF10A cells. B, Bright light images of vector and TRIM24-OE MCF10A cells. C & D, qRT-PCR and Immunoblot analysis of TRIM24, CDH1, CDH2, SNAI1, VIM and Actin in vector and TRIM24-OE MCF10A cells. E, Immunofluorescence analysis of TRIM24 (green) and CDH1 (red) in vector and TRIM24-OE MCF10A cells The data are averages from two replicates ± SD. *p < 0.05; **p < 0.01; ***p < 0.001.

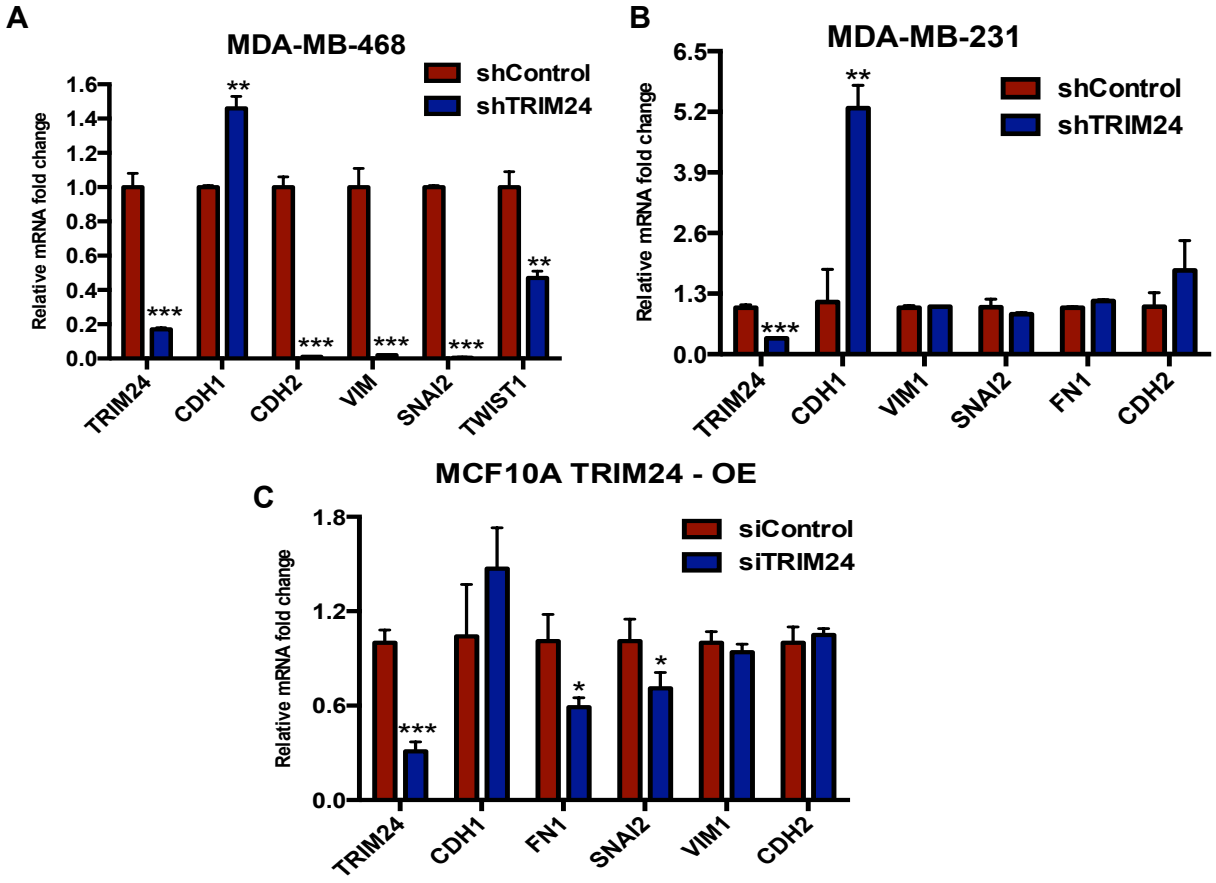


**Figure 26: TRIM24 regulates EMT-target gene expression in breast epithelial cells**

A, B & C, qRT-PCR analysis of TRIM24, CDH1, FN1, SNAI2, VIM1 and CDH2 mRNA in MDA-MB-468 (A) and MDA-MB-231 (B) – shControl and shTRIM24, and MCF10A TRIM24-OE (C) – transfected with siControl or siTRIM24, respectively. The data are averages from two replicates ± SD. *p < 0.05; **p < 0.01; ***p < 0.001.

The effects of TRIM24-mediated regulation of EMT markers were also observed after stable depletion of TRIM24 (shTRIM24) in triple-negative breast cancer cells (MDA-MB-468 and MDA-MB-231) (Fig. 26A-B). Interestingly, in MDA-MB-231 there was significant upregulation of *CDH1* upon TRIM24 knockdown, however no significant changes in other EMT markers were observed. Notably, siRNA mediated knock down of TRIM24 in MCF10A cells over-expressing TRIM24 reversed this effect, as shown by reduced expression of *FN1*, *SNAI2* and slightly increased expression of *CDH1* (Fig. 26C).

In order to determine if TRIM24 expression functionally impacts epithelial cell migration, Boyden-chamber based migration assays were performed. As expected, TRIM24-OE MCF10A cells had significantly higher migration as compared to Control MCF10A cells and consistent with this there was significant reduction in migration of shTRIM24 MDA-MB-231 cells as compared to shControl MDA-MB-231 cells (Fig. 27A-B).

### 4.3 EMT-related pathways are significantly enriched upon TRIM24-overexpression in MCF10A cells

To understand the mechanisms of TRIM24-induced transformation of MCF10A, we analyzed the gene expression profiles of 2560 cancer-associated genes using the HTG EdgeSeq Oncology biomarker assay and identified 501 genes (20%) whose expression was significantly altered, compared to vector only cells. TRIM24 overexpression resulted in activation of 223 (44%) and repression of 278 (56%) genes (Fig. 28A). For a complete list of deregulated genes, please see Appendix 9. Molecular signature hallmark analysis (GSEA) revealed that TRIM24-induced expression of genes altered

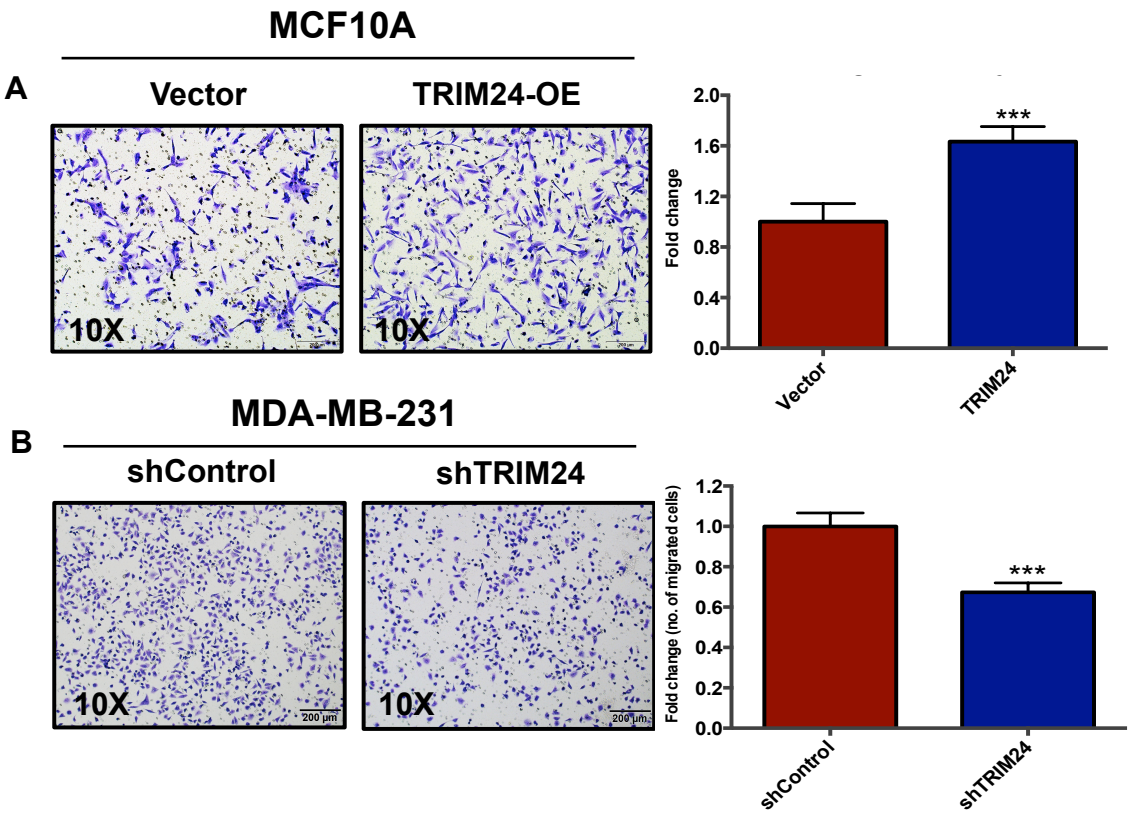


**Figure 27: TRIM24 regulates migration of breast cancer cells**

A & B, Boyden chamber-based migration assay of MCF10A (vector and TRIM24-OE, A) and MDA-MB-231 (shControl and shTRIM24, B). The data are averages from two replicates ± SD. *p < 0.05; **p < 0.01; ***p < 0.001.

A

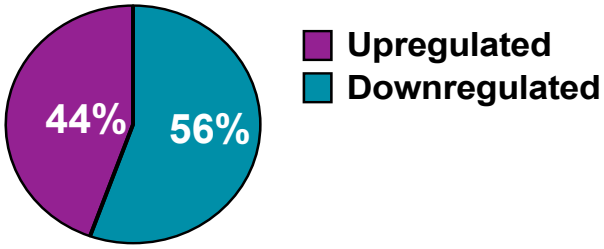


B

| Upregulated genes | | P-value |
|---|---|---|
| Hallmarks | Apoptosis | 1.13 e-19 |
| | Epithelial mesenchymal transition (EMT) | 5.82 e-18 |
| | TGF-beta signaling | 2.21 e-7 |
| Curated gene sets | Upregulated E-cadherin targets | 1.28 e-22 |
| | Upregulated BMP2 targets | 3.68e-19 |
| | Upregulated in Invasive Ductal carcinoma | 2.67e-18 |

| Downregulated genes | | P-value |
|---|---|---|
| Curated gene sets | Downregulated E-cadherin targets | 1.28 e-22 |
| | Downregulated in Metastasis in malignant melanoma | 3.68e-19 |

**Figure 28: EMT-related pathways are significantly enriched in TRIM24-OE MCF10A cells**

A, Pie-chart showing percentage of up-regulated and down-regulated genes upon TRIM24 over-expression as compared to Vector in MCF10A cells. B, Molecular Signature database-based pathway analysis of up-regulated and down-regulated genes upon TRIM24 over-expression as compared to Vector in MCF10A cells.

various hallmarks including apoptosis, epithelial mesenchymal transition (EMT) and TGF-beta signaling (Fig. 28B). Interestingly, TRIM24-activated genes include genes upregulated upon E-cadherin knockdown in HMLE (human mammary epithelial cells) cells, genes upregulated by BMP2 and genes upregulated in invasive ductal carcinoma (IDC) by using curative gene set search of molecular signature database. Similarly, TRIM24-repressed genes include genes downregulated upon E-cadherin knockdown in HMLE cells and genes downregulated in metastatic melanoma (Fig. 28B). For a complete list of enriched pathways, please see Appendix 10.

### 4.4 TRIM24 directly binds to several EMT-target genes

To elucidate critical targets of TRIM24-induced transformation, previously published TRIM24 ChIP-seq data (from MCF7 cells) was intersected with the transcriptional signature obtained after TRIM24-overexpression in MCF10A. Interestingly, several differentially regulated EMT genes were bound by TRIM24. Recruitment of TRIM24 at several of these EMT genes was confirmed by TRIM24-ChIP followed by qPCR in MDA-MB-468 cells. As shown in Fig. 29A, TRIM24 is recruited at several EMT genes such as *CDH1* and *MMP2*.

As previously mentioned TRIM24 via it's C-terminal Bromo domain acts as a histone reader and binds with highest affinity to an H3K23ac signature but also has the capacity to bind H3K9me2 signature [55]. To confirm the presence of an H3K23ac histone signature at TRIM24 bound sites on EMT genes, ChIP analysis of H3K23ac was performed. As shown in Fig. 29B, an H3K23ac signature is enriched at several EMT genes such as *CDH1* and *MMP2* at TRIM24-bound sites. Hence, it is clear that

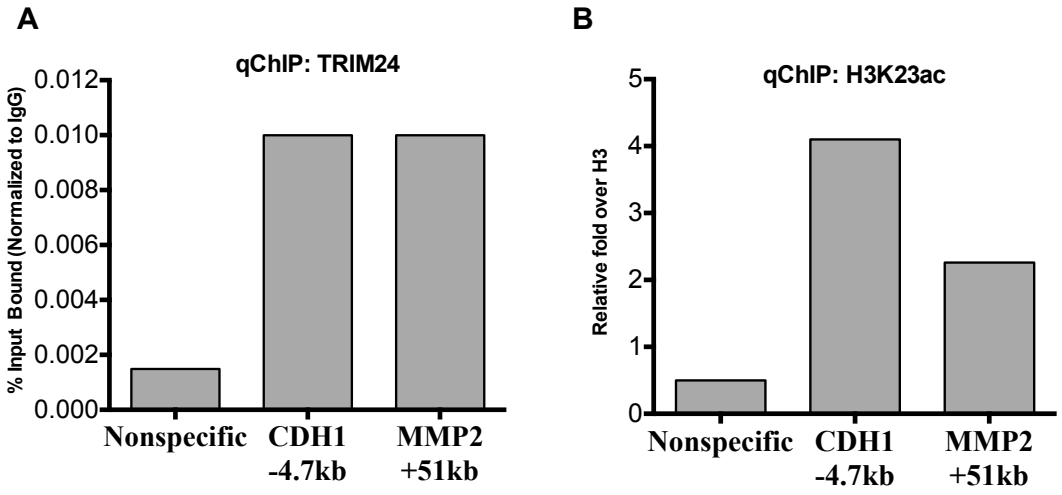


**Figure 29: TRIM24 ChIP in MDA-MB-468 cells**

A & B, TRIM24 and H3K23Ac ChIP confirms recruitment of TRIM24 at various EMT genes such as *CDH1* and *MMP2* along with previous assessment of gene expression to show direct impact of TRIM24 binding. (TRIM24 ChIP done by Roxsan Manshouri).

CDH1 and MMP2 are direct TRIM24 targets and bromo-domain dependent histone reader function may be important for recruitment of TRIM24 at these EMT genes.

### 4.5 TRIM24 over-expression inhibits acini formation

Primary mouse and human mammary epithelial cells, when grown on basement membrane gels, exhibit morphogenic changes to form polarized structures with a hollow lumen known as acini. Engelbreth-Holm-Swarm (EHS) tumor or matrigel (BD Biosciences) basement membrane is composed of matrix components such as laminin, collagen IV and entactin. MCF10A cells when cultured in matrigel-based 3D culture for about 10-12 days form acinar structures and retain several properties of glandular epithelial cells found *in vivo*. They exhibit extremely low levels of cell proliferation and are highly consistent with respect to size of acinar and cell number (8,9). Inhibition of cell proliferation and disruption of morphogenic events during acini formation is an important characteristic to investigate the effects of oncogenes and/or tumor suppressors on MCF10A morphogenesis.

Strikingly, when the TRIM24-OE MCF10A were subjected to 3D culture on growth-factor reduced matrigel they fail to form acini, whereas the vector cells formed distinct acini by Day 10 (Fig. 30A). By confocal microscopy analysis, it was further confirmed that TRIM24-OE MCF10A cells have very low expression of CDH1, whereas the vector cells have distinct CDH1 expression at cell-to-cell boundaries (Fig. 30B). As shown here, TRIM24-OE cells have very low expression of CDH1 and unlikely able to build proper cell-to-cell adhesion contacts, thus affecting MCF10A morphogenesis to form acinar structures. In future, CDH1 rescue studies will be performed to determine if CDH1 over-expression is sufficient ton rescue the loss of acinar phenotype in TRIM24-

OE MCF10A cells or if a more complex network of TRIM24-dependent gene targets are involved.

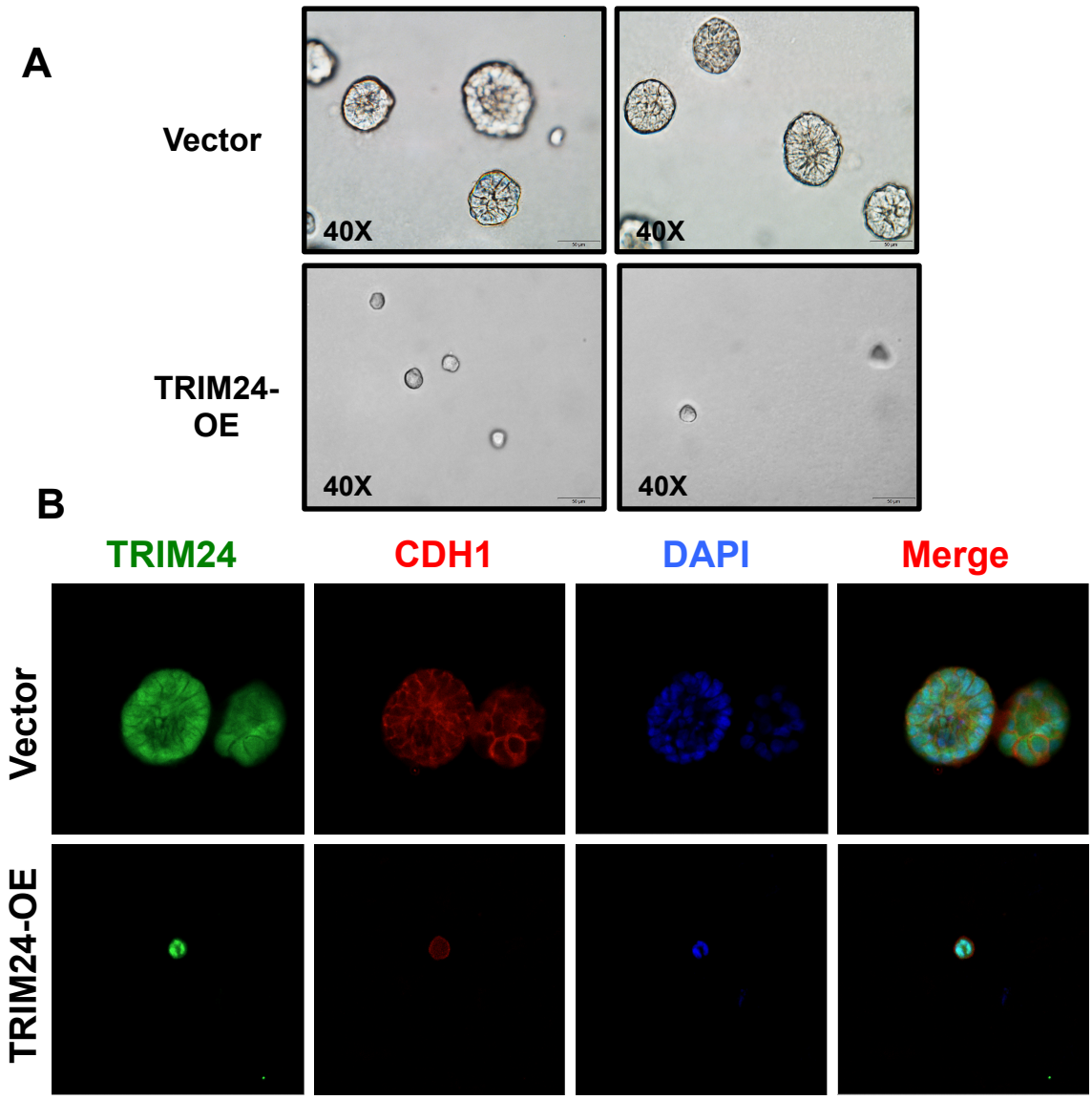


**Figure 30: TRIM24 over-expression suppresses acini formation**

A, Bright field images of acini formed by Vector and TRIM24-OE MCF10A cells.

B, Confocal images of Immunofluorescence for TRIM24 and CDH1 in acini formed by Vector and TRIM24-OE MCF10A cells (Confocal microscopy done by Erin Williams).

# Chapter 5: Discussion and Future directions

# Chapter 5: Discussion and Future directions

## 5.1 TRIM24 - a keystone to cancer metabolism

TRIM24 over-expression in immortalized human mammary epithelial cells induces oncogenic transformation coupled with an array of transcriptional and functional effects. In association with TRIM24-induced breast tumorigenesis, there is deregulation of multiple cancer related pathways including glucose metabolism. To the best of our knowledge, this is the first report of recognition of TRIM24 as one of the prime regulators of cancer metabolism. Over-expression of TRIM24 induces malignant transformation of iHMECs and when these cells are injecting sub-cutaneously into nude mice, a majority of tumors formed by TRIM24-iHMECs were either intermediate or high grade. Interestingly, tumors formed by TRIM24-iHMECs had about 40% epithelial cells with abnormally larger nuclei and this significantly correlated with TRIM24 expression.

In addition to glucose metabolism multiple growth-stimulating pathways such as the insulin [98], ErbB [99] and MAPK [100] that are linked with breast tumor development and progression were also significantly induced upon TRIM24-overexpression in iHMECs. The induction of both glycolysis and TCA cycle in TRIM24-iHMECs was confirmed by mRNA and protein analysis in addition to increased glucose uptake. Of note, Sea-horse analysis also showed that the Extracellular acidification rate (ECAR is rate of glycolysis) and Oxygen consumption rate (OCR is rate of TCA cycle) were higher in TRIM24-iHMECs. To determine whether a correlation between TRIM24 expression and various metabolic pathways existed, a Gene set enrichment analysis (GSEA) using gene expression datasets of invasive breast tumors (n =1008) was performed. The glucose transport pathway was identified as one of the top ten

pathways that correlated positively with TRIM24 expression in invasive breast carcinoma patients from the TCGA database.

One of the key emerging hallmarks of cancer is metabolic reprograming [26]. Otto Warburg reported that cancer cells intake high amounts of glucose and produce higher lactate even in the presence of oxygen, the phenomenon was termed as 'aerobic glycolysis' or Warburg effect [27]. Although it is quite clear that epigenetic, oncogenic and tumor suppressor mechanisms play a crucial role in regulating metabolic reprogramming of cancer cells, the key molecules involved in regulation of cancer metabolism and their role in oncogenesis are not very well understood. As mentioned previously, TRIM24 overexpression in iHMECs caused induction of not only glycolysis but also the TCA cycle pathway. Although this is in disagreement with the conventional Warburg effect, similar to TRIM24 iHMECs there are several reports of certain cancer cells that preferentially use only OXPHOS or a mix of glycolysis and OXPHOS to produce energy [101]. Several recent reports provide ample genetic evidence that mitochondria are indeed essential for tumorigenesis [34]. It is hypothesized that tumors are metabolically heterogeneous. A majority of tumor cells, exhibit aerobic glycolysis (Warburg effect), however, a small population of slow-cycling tumorigenic cells are dependent on OXPHOS activity. These slow-cycling cells are proposed to be the cells that are resistant to various cytotoxic treatments [35].

The schematic in the Figure 31 depicts how we think TRIM24 might regulate metabolism in breast cancer. As shown previously, TRIM24 is over-expressed in breast cancer and TRIM24 targets p53 for proteasomal-mediated degradation. TRIM24 is recruited to promoters of several metabolic and cell proliferation related genes such as GLUT1, IDH1/2 and c-Myc and it induces their gene expression. Since p53 is degraded it can no longer suppress the expression of glucose transporters. Increased GLUT1

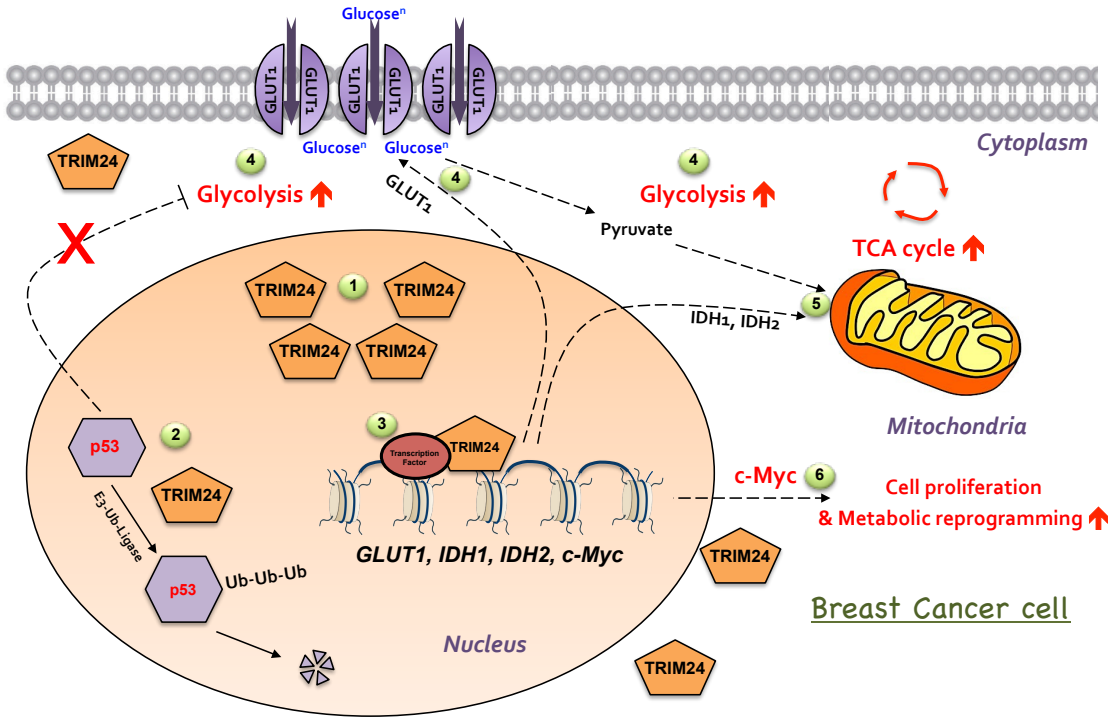


**Figure 31: Schematic for role TRIM24 in regulating cancer metabolism in breast cancer**

(1) TRIM24 is over-expressed in breast cancer, (2) TRIM24 targets p53 for degradation, (3) TRIM24 is recruited to promoters of metabolic and cell proliferation related genes (GLUT1, IDH1 & c-Myc) and it induces their expression, (4) p53 can no longer block Glycolysis & Increased GLUT1 expression causes increased glucose uptake and Glycolysis, (5) Increased IDH1/IDH2 causes increase in TCA cycle, (6) Increased c-Myc has multiple effects including increased glycolysis and TCA cycle and increased cell proliferation, ultimately leading to breast cancer.

expression causes increased glucose uptake and glycolysis. Increased IDH1/IDH2 causes increase in TCA cycle. Higher c-Myc levels have multiple effects including increased glycolysis and TCA cycle and increased cell proliferation, ultimately leading to breast cancer.

It is plausible that abnormal TRIM24 expression in cancer might affect cellular homeostasis by virtue of its epigenetic functions. Research has shown that cross talk between cellular metabolism and epigenetics might be very crucial in cancer progression [102]. The metabolic status of a cell is directly affected by epigenetic alterations that regulate gene expression of enzymes associated with metabolism, thus contributing to metabolic reprogramming in cancer. On the other hand, almost every known epigenetic enzyme relies on metabolites as cofactors or substrates, such as acetyl CoA. Thus, metabolic reprogramming in cancer can affect epigenetic status and ultimately alter the gene expression of oncogenes as well as tumor suppressors [102].

Of note, several metabolic enzymes are reportedly mutated in various cancers. One prominent example of cancer-associated mutation in metabolic enzymes is IDH1/IDH2 mutations found frequently in low-grade gliomas, that exhibit a gain of function by catalyzing the conversion of a-ketoglutarate (a-KG) to 2-hydroxy glutarate (2-HG), resulting in 100-fold higher intracellular concentration of 2-HG as compared to wild-type cells. 2-HG is a competitive inhibitor of a-KG dependent dioxygenases, including TET2 and the Jumonji C domain containing histone demethylases [103]. Further, various metabolic enzymes are mutated in several cancers for e.g. fumarate dehydrogenase (FH), succinate dehydrogenase (SDH) and phospho-glycerate dehydrogenase (PHGDH) [102].

A key question in the cancer metabolism field is whether an alteration in metabolism is the cause or consequence of oncogenic transformation. In the current

study, we show that TRIM24 induces oncogenic transformation of iHMECs in concert with metabolic adaptations and it is plausible that TRIM24-mediated metabolic reprogramming is more likely a driver event in breast tumorigenesis. Given the enhanced expression profile of TRIM24 not only in breast cancer but also in various other cancers, it is expected that loss of TRIM24 would oppose cancer development in mouse models. Surprisingly, it was found that complete or liver specific loss of TRIM24 in mouse models causes hepatocellular carcinoma. In the TRIM24 null mice, there was increased expression of lipase and inflammatory signaling genes, along with repression of de novo lipogenesis, steroid and lipid metabolism, and lipid transport. The TRIM24 null phenotype of increased inflammation, fibrosis and lipid accumulation in the liver was very similar to human non-alcoholic fatty liver disease (NAFLD) and non-obese non-alcoholic steatosis (NASH).

These contrasting phenotypes may be a result of differential interaction of TRIM24 with tissue-specific transcriptional complexes and target genes and/or tissue-specific response to deregulated p53 levels. In future, these questions may be answered by generating conditional TRIM24-over expression mouse models (breast or liver specific) along with mechanistic studies to determine key functional domains of TRIM24 and transcriptional complexes critical in order to orchestrate metabolic reprogramming by TRIM24.

### 5.2 Is the molecular interaction between TRIM24 and PPARγ critical for metabolic reprogramming in breast cancer?

As discussed previously, upon performing transcription factor affinity prediction (TRAP) analysis of TRIM24-ChIP binding sites it was found that Peroxisome

Proliferator Activated Receptor-γ (PPARγ) was among the top-three enriched transcription factors (Fig. 21). PPARγ is among the key players that regulate adipogenesis and whole-body lipid metabolism [92]. It regulates glucose homeostasis by inducing GLUT4 and c-Cbl associated protein (CAP) expression [92]. Its role in breast cancer is highly controversial. Based on studies in various breast cancer cell lines and mouse models, certain reports propose that PPARγ suppresses cell proliferation, induces differentiation and programmed cell death. In DMBA-induced breast cancer mouse models, PPARγ agonists have been reported to block breast cancer [104]. In contrast, when PPARγ transgenic mice (breast-specific) are crossed with MMTV-neu mouse model, they display severely accelerated rate of breast cancer propensity [105].

Intriguingly, in breast cancer cells ER-α physically associates with PPARγ and functionally interferes with PPARγ signaling [93]. As discussed previously, TRIM24 binds ER-α and chromatin (at specific histone modifications mentioned above) to activate estrogen-dependent genes associated with tumor development and cell proliferation [55]. Future studies will investigate the crosstalk between TRIM24, PPARγ and ER-α by co-immunoprecipitation studies in breast cancer cells. TRIM24 and PPARγ ChIP assays will be performed to confirm their co-recruitment and mechanism of action at various metabolic genes. Effects of PPARγ knockdown and over-expression on TRIM24-induced metabolic reprogramming in breast cancer cells will be assessed. Ultimately, these experiments will address if PPARγ and TRIM24 association or dissociation is critical to induce metabolic reprogramming in breast cancer.

### 5.3 TRIM24 a novel regulator of EMT in breast cancer

Our preliminary analysis shows that TRIM24 is a driver of EMT in breast epithelial cells. Upon TRIM24 over-expression the MCF10A cells, exhibit mesenchymal-like morphology with decreased clustering and loss of cell-to-cell contacts. The TRIM24 over-expressing MCF10A cells exhibited various markers consistent with EMT program, i. e. loss of CDH1 and increased expression of CDH2, VIM1, FN1, SNAI1 and SNAI2. Similarly, upon TRIM24 knockdown in several triple-negative breast epithelial cells a suppression of EMT program consistent with decrease in migration is observed.

Gene expression profiling of 2560 cancer-associated genes in TRIM24-OE MCF10A cells revealed that various hallmarks of cancer including apoptosis, epithelial mesenchymal transition and TGF-beta signaling were significantly altered. Molecular signature pathway analysis of TRIM24-activated genes revealed that these genes were upregulated in invasive ductal carcinoma; whereas TRIM24-repressed genes were among the genes that were downregulated in metastatic melanoma. In order to uncover the epigenetic mechanism of EMT regulation, we determined if TRIM24 was recruited to EMT genes. We found that TRIM24 is directly recruited to several EMT genes such as CDH1 and MMP2 and the TRIM24-bound sites have H3K23ac signature at these sites by ChIP analyses.

A major contributor of EMT is E-cadherin promoter methylation, resulting in suppression of E-cadherin expression, a key EMT signature. Amongst other mechanisms, methylation of histone H3 on lysine 9 (H3K9me2) by G9a is essential for DNA methylation of E-cadherin promoter in multiple breast cancer models [106]. Intriguingly, our laboratory has shown that the PHD and Bromo domains of TRIM24 can bind to H3K9me2 modification by performing *in vitro* GST-pull down assays [55].

Additionally, based on TRIM24-pulldown and mass-spectrometry analysis in MCF7 cells, TRIM24 interacts with G9a (EHMT2) (unpublished data). In the future, I will determine whether G9a and H3K9me2 histone signature are present at sites of TRIM24 enrichment at the *CDH1* promoter to uncover an epigenetic mechanism by which TRIM24 regulates E-cadherin expression. ChIP-PCR will be used to assess corecruitment of G9a (Transcription factor Y, Figure 32) and TRIM24 near *CDH1* promoter. In addition, effects of G9a knockdown of TRIM24 recruitment near *CDH1* promoter and vice-versa in MDA-MB-436 cells will be determined.

Future studies will examine the role of TRIM24 in invasion/metastasis by *in vivo* modeling. To determine the role of TRIM24 in regulation of metastasis, RFP/Luciferase labeled MDA-MB-231 cells will be generated with/without TRIM24 knockdown (shControl versus shTRIM24). Approximately, 0.5 x $10^6$ cells will be injected via the tail vein of SCID mice and the presence of lung metastasis will be monitored every week using bioluminescent imaging. After an appropriate time, tumors will be harvested and tumor tissue and number of lung metastatic nodules will be determined. Metastatic tumors will be characterized by H&E staining and IHC for RFP and for expression of various metastatic markers. I expect that mice harboring TRIM24-depleted MDA-MB-231 cells (shTRIM24) will show reduced tumor invasion/metastasis as compared to control cells (shControl).

**5.4 TRIM24-domain functional characterization for regulation of EMT:**

Previous work from our laboratory has showed that histone reader TRIM24 not only negatively regulates p53 as an E3-ubiquitin ligase but also interacts with and recruits transcription factors, such as estrogen receptor, to chromatin via a tandem

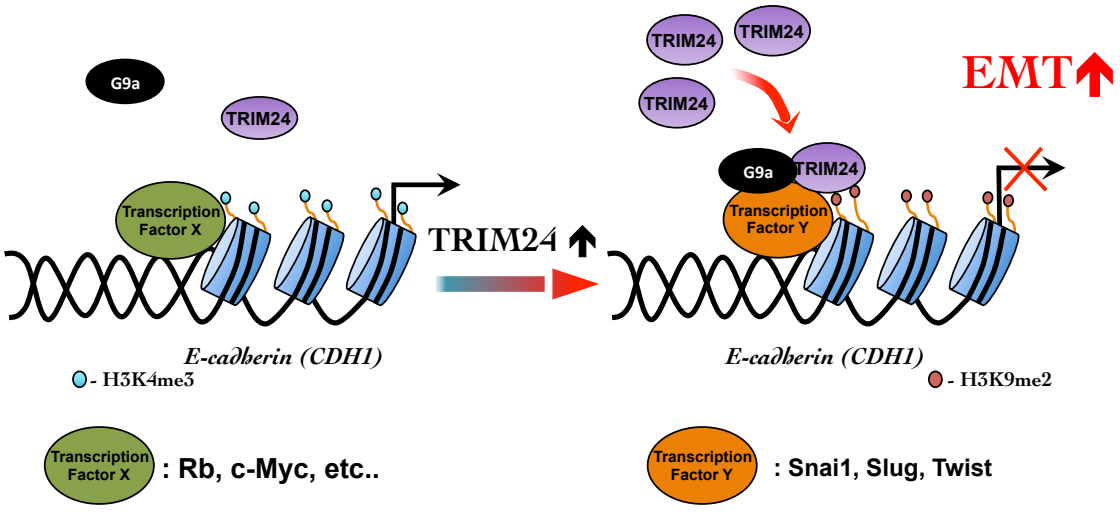


**Figure 32: Proposed model for TRIM24 as a novel regulator of EMT in breast cancer**

PHD-Bromo domains that binds unmethylated lysine 4 and acetylated lysine 23 of histone H3 (H3K4me0/H3K23ac). The question remains, which of the aforementioned functions is/are critical in regulation of TRIM24-mediated induction of EMT.

To test whether TRIM24-mediated EMT requires its histone reader, p53 regulation, ER-interaction or any subset of these functions, MCF10A-stable cell lines that over express TRIM24 with site-specific mutations in PHD and/or Bromo, p53-regulating RING domains, or LXXLL motifs will be generated. Stable cells will be characterized for various hallmarks of EMT such as change in morphology, gene expression changes and migration properties. Additionally, as part of a drug-discovery program we also have a TRIM24-bromodomain specific small molecule inhibitor (IACS9571). A titration of the IACS9571 inhibitor, guided by known IC50 level, will be used to assess how TRIM24-overexpressing cell lines respond at the level of EMT markers, proliferation and migration/invasion. Its effects will be compared to the phenotype of the TRIM24-Bromodomain point mutant rescue line. These studies may support use of combinations of epigenetic inhibitors that oppose EMT in breast cancers.

# Chapter 6: Conclusions

## Chapter 6: Conclusions

Since our laboratory's initial report showing TRIM24 over expression correlates with poor survival of breast cancer patients [55], several studies reported roles of TRIM24 in multiple cancers such as in prostate cancer [47], breast cancer [55, 56], non-small cell lung cancer [57], head and neck carcinoma [58], colorectal cancer [59], gastric cancer [60], glioblastoma [61] and human hepatocellular carcinoma [63]. However, except for the glioblastoma study, none of the other studies uncovered the mechanism of TRIM24-mediated oncogenesis. It was found that TRIM24 is up regulated in early stages of breast cancer progression not only in clinical human breast cancer tissues but also in an isogenic human mammary epithelial cell (iHMEC) model system consisting of cells from various stages of breast cancer. Exogenous over-expression of TRIM24 promoted oncogenic transformation of immortalized human mammary epithelial cells (TRIM24-iHMECs) and efficient growth of high-grade tumors in nude mice upon performing xenograft studies.

Gene expression analysis of TRIM24-iHMECs uncovered that aerobic glycolysis and tricarboxylic acid cycle was activated in addition increased glucose uptake was confirmed. In TRIM24-iHMECs, increased c-Myc expression and a decrease in p53 protein levels were observed. c-Myc and p53 play key roles in regulating cellular metabolism, hence, we proposed that these could be the possible mediators of TRIM24-induced metabolic reprogramming. Additionally, TRIM24 is recruited to the promoters of several metabolic genes such as *GLUT1, IDH1* and *IDH2*. Further, upon treatment of MCF7 breast cancer cells with a TRIM24-bromodomain inhibitor I found that several glucose metabolism genes were down regulated. Hence, it can be concluded that TRIM24 induces oncogenic transformation coupled with metabolic

reprogramming in breast cancer and TRIM24-bromodomain function may be critical for malignant transformation.

As mentioned before, TRIM24 is reported to be over-expressed in several cancers; however, a detailed analysis of how TRIM24 promotes tumorigenesis with progression to metastasis has not been elucidated. Our preliminary analysis shows that TRIM24 is a driver of epithelial to mesenchymal transition (EMT) in breast cancer. It was found that upon TRIM24 over-expression in MCF10A cells, there is mesenchymal-like change in the cellular morphology. As observed in a classical EMT program, TRIM24-MCF10A cells exhibit marked loss of E-cadherin and acquisition of various mesenchymal markers such as N-cadherin, fibronectin and vimentin. Further, TRIM24-knockdown in MDA-MB-231 and MDA-MB-468, there is reversal of EMT gene signature. HTG Oncology gene expression analysis of TRIM24-OE MCF10A cells further confirmed the EMT was among the top pathways that were enriched. TRIM24 may be involved in transcriptional regulation of EMT genes as confirmed by TRIM24-ChIP analysis and the presence of H3K23ac signature at several EMT genes in MDA-MB-468 cells. Our hypothesis is that aberrant expression of TRIM24 impacts a network of transcription regulatory factors and signaling pathways to induce EMT and metastasis in breast cancer.

Approximately 90% of breast cancer-related deaths are caused by metastasis not by primary tumor [13]. Hence, for effective reduction of cancer mortality, it is very critical to intervene in the critical transition of non-invasive ductal carcinoma to extremely lethal invasive breast cancer. The proposed research holds great promise to identify a unique role of TRIM24 in metastasis and mechanisms involving EMT. These studies will provide a better understanding of molecular mechanisms that drive EMT

and will pave the way for developing therapeutic opportunities for metastatic tumors by targeting the epigenetic regulator TRIM24.

## List of Appendices

## Appendix 1: List of primers for cloning and qPCR

| Cloning Primers | | | |
|---|---|---|---|
| **TRIM24-F1** | ATTTTACACGTGATGGAGGTGGCGGTGGAGAA | | |
| **TRIM24-R1** | CGGGGCTCTAGATTATTTAAGCAACTGGCGTT | | |
| **qRT-PCR primers** | | | |
| **Gene** | **Species** | **Forward primer** | **Reverse primer** |
| TRIM24 | Human | GCGCCTACT TTTATTTCTTTACTG | TTTGTCAAGAAAGGGTGTAA CG |
| β-ACTIN | Human | GGACTTCGAGCAAGAGA TGG | AGCACTGTGTTGGCGTACAG |
| TP53 | Human | AAAGAAGAAACCACTGGATG | ATTCAGCTCTCGGAACAT |
| GLUT1 | Human | CCA GCT GCC ATT GCC GTT | GAC GTA GGG ACC ACA CAG TTGC |
| GLUT4 | Human | GTCGGGCTTCCAACAGATAG | ACCCCAATGTTGTACCCAAA |
| HK2 | Human | ATG AGG GGC GGA TGT GTA TCA | GGT TCA GTG AGC CCA TGT CAA |
| ENO1 | Human | AAA GCT GGT GCC GTT GAG AAG | AGC ATG AGA ACC GCC ATT GAT |
| ALDO-A | Human | GGG TGT CAT CCT CTT CCA TGA | GAC CAC GCC CTT GTC TAC CTT |
| PGM1 | Human | ACC CAC TCC CTT CAT ACA ATC | CTC CTC ACT GGT CAT GGC TTA |
| PDK1 | Human | CCG CTC TCC ATG AAG CAG TT | TTG CCG CAG AAA CAT AAA TGA G |
| GPI | Human | GGT ACA CAG GCA AGA CCA TC | GTT TTG GCA ATG TGA GTT CC |
| PKM1 | Human | CGAGCCTCAAGTCACTCCAC | GTGAGCAGACCTGCCAGACT |
| PKM2 | Human | ATTATTTGAGGAACTCCGCC GCCT | ATTCCGGGTCACAGCAATGA TGG |
| LDHC | Human | CCTCTTGGGCTATTGGACTG | GCCTCCTCCTCAGAATTCAA |
| ACO1 | Human | TTGGAGGATTCAAGATATGG | ACTCATCACAATTCCGAAT |
| DLAT | Human | GTTCCTACAGGTGTCTTC | AAGGTAATAATGAGGTAT GGT |
| IDH1 | Human | GAGATAACCTACACACCA AGT | AACACCACCACCTTCTTC |
| IDH2 | Human | GATGGATGGTGATGAGAT | AAATACTTTAGCTGGATGTC |

| | | | |
|---|---|---|---|
| MDH2 | Human | TGTGATGTGGTAGTTATTCC | ATTGGTGTTGAACAGGTC |
| OGDH | Human | AATGTCATCAGGAAGGAG | GGTGGTACTTCACATCTC |
| PDHA1 | Human | ATGTATGCCAAGAACTTC | ATTATACTTACAGGCTAGAG |
| PDHB | Human | AGGAGTTGAATGTGAGGTGATAA | ATGACACTGGCTTCTATGGT |
| SDHA | Human | ATGCCATCCACTACATGA | ATAAATCTTCCCATCTTCAGTT |
| SDHB | Human | GACACCAACCTCAATAAG | GATTCATCCTTCTTCTTCAA |
| SDHD | Human | ACCGACCTATCCCAGAATG | CAGCCTTGGAGCCAGAAT |
| FH | Human | TTAAGATTGGAGGTGTGA | CATAATCCTGGTTTACTTCA |
| TWIST1 | Human | GCCGGAGACCTAGATGTCATT | CCCACGCCCTGTTTCTTTGA |
| TGFB | Human | CTTTGGATGCGGCCTATTGC | TAAGCTCAGGACCCTGCTGT |
| CDH1 | Human | TGCCCAGAAAATGAAAAAGG | GTGTATGTGGCAATGCGTTC |
| CDH2 | Human | ACAATCCTCCAGAGTTAC | CTTATCGGTCAGAGTTAGA |
| VIM | Human | AAGTGGAATGCCCTTAAAG | ATAGTGTCTTGGTAGTTAGC |
| SNAI2 | Human | TCCTGGTCAAAGAAGCATT | ATCTCTGGTTGTGGTATGA |

**Appendix 2: List of antibodies used for Immunoblotting**

| Antibody details (Catalog) | Species | Company | Application |
|---|---|---|---|
| TRIM24 (NB100-2597) | Rabbit | Novus Biologicals | Western |
| TRIM24 (14208-1-AP) | Rabbit | Protein tech | IHC |
| p53(DO1)-HRP (sc-126) | Mouse | Santa Cruz | Western |
| b-Actin- HRP (5125) | Rabbit | Cell Signaling | Western |
| Hexokinase II (2687) | Rabbit | Cell Signaling | Western |
| Aldolase (3188) | Rabbit | Cell Signaling | Western |
| Enolase -1 (3810) | Rabbit | Cell Signaling | Western |
| PDHK1 (3820) | Rabbit | Cell Signaling | Western |
| LDHA/ LDHC (3538) | Rabbit | Cell Signaling | Western |
| PGM1 (ab55616) | Mouse | Abcam | Western |
| | | | |
| | | | |
| | | | |
| | | | |
| | | | |
| | | | |
| | | | |
| | | | |
| | | | |

**Appendix 3: All red score data for TRIM24 staining in Human breast tissue array**

| Status | Levels | TRIM24 (Number of patients) | | | Total | Chi-square | P-value |
|---|---|---|---|---|---|---|---|
| | | Low | Medium | High | | | |
| ER status | Low | 15 | 22 | 6 | 43 | | |
| | High | 3 | 12 | 14 | 29 | 11.87 | 0.0026 |
| | Total | 18 | 34 | 20 | 72 | | |
| | | TRIM24 | | | Total | | |
| | | Low | Medium | High | | | |
| PR status | Low | 14 | 24 | 10 | 48 | | |
| | High | 4 | 10 | 10 | 24 | 3.74 | 0.1541 |
| | Total | 18 | 34 | 20 | 72 | | |
| | | TRIM24 | | | Total | | |
| | | Low | Medium | High | | | |
| HER2 status | Low | 14 | 8 | 0 | 22 | | |
| | High | 4 | 26 | 20 | 50 | 28.51 | <.0001 |
| | Total | 18 | 34 | 20 | 72 | | |
| | | TRIM24 | | | Total | | |
| | | Low | Medium | High | | | |
| P53 | Low | 12 | 16 | 12 | 40 | | |
| | High | 6 | 18 | 8 | 32 | 2.05 | 0.3588 |
| | Total | 18 | 34 | 20 | 72 | | |
| | | TRIM24 | | | Total | | |
| | | Low | Medium | High | | | |
| Ki67 | Low | 8 | 7 | 7 | 22 | | |
| | High | 10 | 27 | 13 | 50 | 3.41 | 0.1818 |
| | Total | 18 | 34 | 20 | 72 | | |

| Key to All Red score | | |
|---|---|---|
| TRIM24 | ER/PR | HER2 |
| Low (0-2) | Low (0-3) | Low (0-1) |
| Medium (3-5) | High (3-8) | High (2-3) |
| High (6-8) | | |

**Appendix 4: List of deregulated genes in TRIM24-iHMECs by nanostring analysis**

| Upregulated genes | | | | | | | | |
|---|---|---|---|---|---|---|---|---|
| | Control | | | TRIM24 | | | | |
| Gene | A | B | C | A | B | C | t-test | Fold change |
| TRIM39 | 0.00 | 167.49 | 132.51 | 605.68 | 572.34 | 591.15 | 0.00 | 5.9 |
| PDE4DIP | 0.00 | 219.12 | 80.88 | 833.22 | 376.66 | 408.42 | 0.05 | 5.4 |
| GLS2 | 236.96 | 35.30 | 27.74 | 518.79 | 374.78 | 469.60 | 0.01 | 4.5 |
| PRKCI | 91.91 | 92.75 | 115.34 | 397.29 | 440.82 | 450.99 | 0.00 | 4.3 |
| PRKCH | 75.47 | 97.49 | 127.04 | 369.65 | 389.17 | 473.85 | 0.00 | 4.1 |
| CAMKK2 | 117.28 | 87.50 | 95.22 | 462.87 | 391.28 | 374.84 | 0.00 | 4.1 |
| SgK494 | 0.00 | 202.37 | 97.63 | 525.91 | 415.23 | 285.19 | 0.03 | 4.1 |
| TESK2 | 0.00 | 84.47 | 215.53 | 370.71 | 330.23 | 496.93 | 0.02 | 4.0 |
| MYC | 84.91 | 106.26 | 108.84 | 336.89 | 370.51 | 392.51 | 0.00 | 3.7 |
| MAPKAPK5 | 70.14 | 94.23 | 135.63 | 331.82 | 317.40 | 397.15 | 0.00 | 3.5 |
| STRADA | 21.47 | 168.55 | 109.99 | 285.93 | 384.41 | 290.46 | 0.01 | 3.2 |
| ME3 | 17.33 | 172.80 | 109.87 | 310.73 | 288.43 | 353.48 | 0.01 | 3.2 |
| FGFR2 | 100.45 | 114.59 | 84.96 | 273.19 | 277.81 | 358.25 | 0.00 | 3.0 |
| TTL | 84.61 | 111.39 | 104.00 | 293.80 | 305.09 | 309.23 | 0.00 | 3.0 |
| DDX5 | 90.50 | 124.69 | 84.81 | 357.23 | 258.22 | 290.89 | 0.00 | 3.0 |
| TRIM26 | 44.07 | 142.46 | 113.47 | 260.31 | 272.90 | 327.49 | 0.01 | 2.9 |
| CEBPA | 90.19 | 111.15 | 98.66 | 266.75 | 298.82 | 274.99 | 0.00 | 2.8 |
| TRIM37 | 85.26 | 113.30 | 101.44 | 292.72 | 278.46 | 264.67 | 0.00 | 2.8 |
| TRIM39 | 84.33 | 116.55 | 99.12 | 296.83 | 235.94 | 284.93 | 0.00 | 2.7 |
| MTOR | 57.47 | 135.06 | 107.47 | 218.24 | 306.41 | 280.85 | 0.01 | 2.7 |
| PIK3CA | 63.52 | 93.07 | 143.41 | 254.09 | 241.62 | 309.69 | 0.01 | 2.7 |
| BIRC3 | 98.26 | 102.09 | 99.65 | 288.82 | 256.61 | 243.06 | 0.00 | 2.6 |
| PTPN11 | 80.24 | 120.97 | 98.80 | 238.57 | 259.67 | 286.49 | 0.00 | 2.6 |
| PFKFB2 | 57.89 | 122.72 | 119.40 | 216.86 | 265.92 | 299.32 | 0.01 | 2.6 |
| EPHA1 | 86.47 | 88.62 | 124.92 | 274.97 | 203.83 | 302.21 | 0.01 | 2.6 |
| TTK | 103.65 | 88.67 | 107.68 | 238.36 | 225.32 | 295.02 | 0.00 | 2.5 |
| YES1 | 80.08 | 109.47 | 110.45 | 240.24 | 247.23 | 272.17 | 0.00 | 2.5 |
| NEK6 | 99.98 | 87.87 | 112.15 | 256.38 | 207.41 | 255.11 | 0.00 | 2.4 |
| NADK | 80.59 | 132.86 | 86.55 | 193.31 | 240.18 | 272.71 | 0.01 | 2.4 |
| STK38L | 108.16 | 97.62 | 94.22 | 229.55 | 233.62 | 228.09 | 0.00 | 2.3 |
| CDKN2A | 189.02 | 74.63 | 36.35 | 217.37 | 229.33 | 240.38 | 0.05 | 2.3 |
| ERN1 | 78.27 | 133.34 | 88.39 | 265.59 | 213.98 | 203.27 | 0.01 | 2.3 |
| SDHD | 96.31 | 83.77 | 119.92 | 210.35 | 205.87 | 264.55 | 0.00 | 2.3 |
| TNK2 | 88.53 | 97.96 | 113.52 | 201.61 | 234.60 | 243.05 | 0.00 | 2.3 |
| LGR5 | 162.81 | 64.29 | 72.90 | 176.33 | 251.31 | 206.28 | 0.04 | 2.1 |
| COX6C | 96.44 | 102.71 | 100.85 | 207.39 | 198.92 | 224.80 | 0.00 | 2.1 |

| | | | | | | | | |
|---|---|---|---|---|---|---|---|---|
| TSC1 | 80.94 | 107.44 | 111.62 | 220.08 | 174.18 | 231.16 | 0.01 | 2.1 |
| STK38 | 71.10 | 105.05 | 123.85 | 198.54 | 203.43 | 215.53 | 0.00 | 2.1 |
| TRIM59 | 73.62 | 115.41 | 110.97 | 207.78 | 203.48 | 203.30 | 0.00 | 2.1 |
| PIP4K2A | 80.18 | 116.42 | 103.40 | 211.78 | 196.78 | 182.02 | 0.00 | 2.0 |
| BRCA1 | 61.92 | 123.09 | 115.00 | 190.10 | 195.23 | 195.77 | 0.01 | 1.9 |
| SIX4 | 117.49 | 84.35 | 98.17 | 166.19 | 214.52 | 202.52 | 0.01 | 1.9 |
| SIK3 | 97.85 | 116.82 | 85.33 | 189.45 | 199.08 | 193.78 | 0.00 | 1.9 |
| MASTL | 63.29 | 121.37 | 115.34 | 197.64 | 184.52 | 198.17 | 0.01 | 1.9 |
| ADRBK1 | 98.21 | 95.03 | 106.76 | 176.92 | 204.95 | 197.93 | 0.00 | 1.9 |
| MAP3K5 | 101.84 | 103.09 | 95.07 | 208.56 | 139.72 | 227.76 | 0.03 | 1.9 |
| SUFU | 112.01 | 99.86 | 88.12 | 168.24 | 211.29 | 196.43 | 0.00 | 1.9 |
| RPIA | 104.92 | 102.65 | 92.43 | 152.23 | 192.15 | 221.93 | 0.01 | 1.9 |
| EZH2 | 78.28 | 98.23 | 123.49 | 211.74 | 164.89 | 187.48 | 0.01 | 1.9 |
| BRD3 | 66.22 | 104.59 | 129.19 | 194.66 | 160.63 | 189.77 | 0.02 | 1.8 |
| PFKFB3 | 100.47 | 114.40 | 85.13 | 186.71 | 186.88 | 170.40 | 0.00 | 1.8 |
| TRIM8 | 110.66 | 97.48 | 91.86 | 160.42 | 184.29 | 189.82 | 0.00 | 1.8 |
| GNAQ | 114.66 | 96.08 | 89.26 | 192.33 | 166.22 | 174.53 | 0.00 | 1.8 |
| DLAT | 88.02 | 116.26 | 95.71 | 157.99 | 208.15 | 163.98 | 0.01 | 1.8 |
| SUZ12 | 96.47 | 92.31 | 111.22 | 162.27 | 156.41 | 208.20 | 0.01 | 1.8 |
| RPS6KB1 | 109.51 | 99.07 | 91.42 | 167.09 | 187.02 | 165.46 | 0.00 | 1.7 |
| TUBB | 97.55 | 95.46 | 106.99 | 175.70 | 162.12 | 179.90 | 0.00 | 1.7 |
| CSK | 74.68 | 117.18 | 108.14 | 149.28 | 207.10 | 160.90 | 0.03 | 1.7 |
| AURKB | 86.51 | 111.06 | 102.43 | 161.71 | 188.84 | 164.13 | 0.00 | 1.7 |
| HPRT1 | 103.22 | 87.37 | 109.41 | 171.22 | 164.29 | 179.41 | 0.00 | 1.7 |
| ACLY | 88.10 | 95.11 | 116.79 | 171.95 | 156.01 | 185.87 | 0.00 | 1.7 |
| VEGFA | 96.71 | 95.72 | 107.56 | 161.44 | 162.53 | 182.52 | 0.00 | 1.7 |
| SDHB | 88.47 | 96.21 | 115.32 | 159.71 | 157.81 | 183.03 | 0.00 | 1.7 |
| SNX16 | 110.81 | 94.84 | 94.35 | 175.13 | 151.39 | 174.28 | 0.00 | 1.7 |
| PIK3R4 | 76.17 | 113.25 | 110.58 | 159.56 | 168.70 | 163.27 | 0.01 | 1.6 |
| EXOSC10 | 103.90 | 92.24 | 103.86 | 182.68 | 151.99 | 153.98 | 0.00 | 1.6 |
| DDR1 | 117.47 | 98.22 | 84.31 | 163.14 | 146.66 | 177.28 | 0.01 | 1.6 |
| TIAM1 | 139.77 | 86.31 | 73.93 | 163.60 | 150.38 | 173.17 | 0.04 | 1.6 |
| CSNK1D | 75.44 | 119.51 | 105.05 | 149.96 | 171.24 | 160.75 | 0.01 | 1.6 |
| DNMT3A | 119.72 | 82.23 | 98.05 | 151.03 | 154.57 | 177.99 | 0.01 | 1.6 |
| NRAS | 83.60 | 121.47 | 94.93 | 163.56 | 167.72 | 152.35 | 0.01 | 1.6 |
| MELK | 87.94 | 104.29 | 107.77 | 137.44 | 163.73 | 174.99 | 0.01 | 1.6 |
| GSG2 | 88.51 | 106.43 | 105.06 | 160.65 | 153.49 | 164.00 | 0.00 | 1.6 |
| KRAS | 72.02 | 113.59 | 114.40 | 163.79 | 159.94 | 150.47 | 0.02 | 1.6 |
| PAK2 | 87.05 | 101.44 | 111.51 | 143.84 | 161.38 | 161.67 | 0.00 | 1.6 |
| PANK4 | 85.52 | 100.27 | 114.21 | 162.11 | 159.11 | 147.79 | 0.00 | 1.6 |
| GMPS | 88.50 | 103.49 | 108.01 | 157.02 | 147.45 | 161.72 | 0.00 | 1.6 |
| CHEK1 | 95.68 | 101.35 | 102.97 | 166.56 | 147.35 | 150.39 | 0.00 | 1.6 |
| PDP1 | 104.21 | 84.35 | 111.44 | 147.34 | 148.89 | 165.52 | 0.01 | 1.5 |

| | | | | | | | | |
|---|---|---|---|---|---|---|---|---|
| SGK1 | 111.61 | 97.68 | 90.71 | 170.02 | 146.22 | 142.16 | 0.01 | 1.5 |
| MAPK8 | 106.53 | 101.84 | 91.63 | 144.52 | 149.29 | 163.98 | 0.00 | 1.5 |
| RIOK1 | 100.31 | 106.32 | 93.37 | 142.94 | 154.84 | 156.08 | 0.00 | 1.5 |
| BUB1B | 103.13 | 90.63 | 106.24 | 167.40 | 138.12 | 140.39 | 0.01 | 1.5 |
| HIPK1 | 106.47 | 97.06 | 96.47 | 151.93 | 148.97 | 146.76 | 0.00 | 1.5 |
| DYRK1A | 95.03 | 110.40 | 94.57 | 126.29 | 173.39 | 144.49 | 0.03 | 1.5 |
| SDHA | 115.02 | 87.55 | 97.43 | 159.51 | 137.58 | 146.76 | 0.01 | 1.5 |
| HK1 | 69.60 | 108.27 | 122.13 | 139.79 | 145.81 | 156.05 | 0.05 | 1.5 |
| LGR4 | 92.55 | 101.35 | 106.10 | 174.12 | 134.23 | 128.84 | 0.04 | 1.5 |
| PRKAR2A | 108.79 | 96.03 | 95.18 | 138.54 | 153.30 | 143.89 | 0.00 | 1.5 |
| SRPK1 | 77.14 | 124.73 | 98.13 | 134.12 | 147.25 | 151.52 | 0.04 | 1.4 |
| MARK2 | 112.57 | 85.94 | 101.49 | 128.35 | 137.62 | 167.43 | 0.03 | 1.4 |
| BRD8 | 95.25 | 113.48 | 91.27 | 129.06 | 142.60 | 159.09 | 0.02 | 1.4 |
| INPP4A | 123.68 | 92.94 | 83.37 | 162.34 | 131.32 | 135.13 | 0.05 | 1.4 |
| GPR172A | 110.01 | 92.75 | 97.24 | 150.82 | 140.09 | 134.87 | 0.00 | 1.4 |
| PAFAH1B2 | 97.27 | 92.88 | 109.85 | 131.99 | 140.01 | 151.57 | 0.01 | 1.4 |
| NLK | 114.80 | 83.74 | 101.46 | 146.56 | 140.69 | 133.29 | 0.01 | 1.4 |
| MAP3K7 | 111.10 | 103.76 | 85.14 | 139.29 | 139.75 | 138.50 | 0.01 | 1.4 |
| CS | 119.50 | 92.02 | 88.48 | 157.98 | 128.22 | 130.72 | 0.05 | 1.4 |
| P2RY2 | 90.52 | 92.84 | 116.64 | 137.82 | 134.08 | 145.78 | 0.01 | 1.4 |
| KIAA1524 | 106.11 | 94.53 | 99.36 | 146.37 | 145.96 | 124.19 | 0.01 | 1.4 |
| AK3 | 88.50 | 112.84 | 98.65 | 133.79 | 134.47 | 146.39 | 0.01 | 1.4 |
| BRD2 | 92.84 | 105.03 | 102.13 | 138.39 | 148.03 | 127.62 | 0.01 | 1.4 |
| ABL1 | 100.00 | 104.92 | 95.08 | 116.72 | 158.40 | 134.39 | 0.04 | 1.4 |
| SH3BP5 | 85.21 | 107.66 | 107.13 | 137.75 | 138.42 | 132.58 | 0.01 | 1.4 |
| BRD7 | 88.56 | 108.28 | 103.16 | 116.82 | 138.78 | 148.61 | 0.04 | 1.4 |
| C17orf75 | 102.12 | 94.30 | 103.58 | 120.93 | 145.56 | 131.93 | 0.01 | 1.3 |
| PI4K2B | 81.40 | 114.94 | 103.65 | 137.73 | 127.26 | 131.01 | 0.04 | 1.3 |
| MDH2 | 106.64 | 99.58 | 93.78 | 132.61 | 136.44 | 125.99 | 0.00 | 1.3 |
| SMARCB1 | 89.38 | 105.81 | 104.81 | 115.12 | 141.11 | 135.71 | 0.03 | 1.3 |
| BRD9 | 109.05 | 100.42 | 90.53 | 144.25 | 128.72 | 120.62 | 0.02 | 1.3 |
| MAPK14 | 89.74 | 110.37 | 99.89 | 133.47 | 127.90 | 127.64 | 0.01 | 1.3 |
| VHL | 111.08 | 98.47 | 90.45 | 136.91 | 135.91 | 112.84 | 0.04 | 1.3 |
| CSNK2B | 87.32 | 101.10 | 111.58 | 120.88 | 135.08 | 131.34 | 0.02 | 1.3 |
| MAPK9 | 93.30 | 103.48 | 103.23 | 116.71 | 134.68 | 136.63 | 0.02 | 1.3 |
| FH | 88.01 | 103.30 | 108.69 | 116.95 | 122.93 | 134.12 | 0.04 | 1.3 |
| RIPK2 | 107.86 | 93.78 | 98.36 | 128.03 | 118.96 | 127.05 | 0.01 | 1.3 |
| RB1 | 100.30 | 99.01 | 100.69 | 127.90 | 127.04 | 119.56 | 0.00 | 1.2 |
| MAPK6 | 89.31 | 101.11 | 109.58 | 112.56 | 134.50 | 123.49 | 0.05 | 1.2 |
| MAP2K4 | 106.21 | 87.45 | 106.34 | 113.59 | 124.80 | 128.78 | 0.04 | 1.2 |
| TGFBR1 | 106.30 | 96.83 | 96.87 | 123.82 | 125.83 | 116.76 | 0.01 | 1.2 |
| MET | 100.36 | 97.04 | 102.60 | 117.81 | 120.36 | 123.81 | 0.00 | 1.2 |
| ACO1 | 91.31 | 106.02 | 102.67 | 116.76 | 121.04 | 122.48 | 0.01 | 1.2 |

| | | | | | | | | |
|---|---|---|---|---|---|---|---|---|
| GPI | 98.78 | 108.12 | 93.10 | 125.55 | 118.94 | 111.49 | 0.04 | 1.2 |
| RAF1 | 100.61 | 102.72 | 96.68 | 114.38 | 109.57 | 131.47 | 0.05 | 1.2 |
| CDK4 | 101.71 | 103.23 | 95.06 | 113.55 | 113.40 | 125.26 | 0.02 | 1.2 |
| CDK1 | 94.53 | 104.79 | 100.68 | 113.34 | 112.18 | 125.61 | 0.03 | 1.2 |
| PTEN | 104.69 | 102.38 | 92.93 | 118.46 | 113.63 | 114.01 | 0.02 | 1.2 |
| **Down-Regulated Genes** | | | | | | | | |
| CANT1 | 102.26 | 102.13 | 95.61 | 74.26 | 77.76 | 72.82 | 0.00 | 0.7 |
| RPS6KA4 | 89.61 | 112.76 | 97.63 | 67.81 | 80.92 | 74.18 | 0.03 | 0.7 |
| ATIC | 92.36 | 103.75 | 103.90 | 69.51 | 72.44 | 77.62 | 0.00 | 0.7 |
| RPS6KC1 | 97.65 | 110.53 | 91.82 | 63.45 | 84.16 | 71.48 | 0.03 | 0.7 |
| PRKAR1A | 99.04 | 100.29 | 100.67 | 68.68 | 72.59 | 76.65 | 0.00 | 0.7 |
| RIPK1 | 100.25 | 95.01 | 104.74 | 63.70 | 69.64 | 83.27 | 0.01 | 0.7 |
| BRCA2 | 94.16 | 106.10 | 99.74 | 68.15 | 71.34 | 77.11 | 0.00 | 0.7 |
| PDXK | 95.39 | 105.72 | 98.89 | 73.37 | 69.33 | 73.59 | 0.00 | 0.7 |
| LATS2 | 109.68 | 106.83 | 83.49 | 76.02 | 66.31 | 71.03 | 0.03 | 0.7 |
| AURKA | 94.64 | 113.24 | 92.13 | 71.74 | 65.29 | 75.09 | 0.02 | 0.7 |
| SPTAN1 | 94.90 | 102.35 | 102.74 | 68.42 | 69.69 | 72.68 | 0.00 | 0.7 |
| CAMK2D | 85.56 | 115.08 | 99.36 | 69.50 | 65.52 | 74.53 | 0.03 | 0.7 |
| BMPR1A | 109.26 | 103.28 | 87.46 | 65.26 | 71.55 | 69.21 | 0.01 | 0.7 |
| TKT | 94.42 | 106.27 | 99.31 | 65.99 | 67.99 | 70.86 | 0.00 | 0.7 |
| SGK196 | 86.59 | 112.34 | 101.08 | 72.34 | 66.83 | 65.30 | 0.01 | 0.7 |
| LIMK2 | 101.43 | 93.63 | 104.94 | 69.47 | 68.76 | 64.83 | 0.00 | 0.7 |
| FBXW7 | 106.32 | 104.96 | 88.72 | 72.23 | 65.27 | 65.31 | 0.01 | 0.7 |
| SRPK2 | 94.96 | 101.78 | 103.26 | 71.26 | 63.48 | 65.17 | 0.00 | 0.7 |
| SMAD4 | 106.16 | 95.81 | 98.03 | 58.31 | 63.28 | 74.85 | 0.00 | 0.7 |
| PIP5K1A | 97.04 | 106.67 | 96.29 | 65.90 | 68.32 | 62.03 | 0.00 | 0.7 |
| CARS | 109.98 | 104.43 | 85.59 | 63.52 | 60.63 | 65.80 | 0.01 | 0.6 |
| BRD1 | 120.83 | 90.76 | 88.41 | 65.75 | 63.12 | 60.99 | 0.03 | 0.6 |
| PDK1 | 103.94 | 109.44 | 86.61 | 73.79 | 60.17 | 53.65 | 0.01 | 0.6 |
| H6PD | 124.34 | 78.77 | 96.89 | 54.75 | 70.57 | 60.73 | 0.05 | 0.6 |
| RUNX1 | 110.51 | 88.95 | 100.54 | 60.45 | 62.33 | 62.23 | 0.00 | 0.6 |
| PIKFYVE | 105.65 | 89.69 | 104.66 | 65.22 | 53.00 | 66.37 | 0.00 | 0.6 |
| PRKD2 | 114.02 | 96.97 | 89.01 | 59.53 | 57.54 | 66.06 | 0.01 | 0.6 |
| NF2 | 104.52 | 97.14 | 98.34 | 60.72 | 64.47 | 57.76 | 0.00 | 0.6 |
| JUN | 110.79 | 105.36 | 83.84 | 60.50 | 58.71 | 62.61 | 0.01 | 0.6 |
| BMPR2 | 102.34 | 97.17 | 100.49 | 61.37 | 54.70 | 63.72 | 0.00 | 0.6 |
| CCND1 | 107.49 | 97.78 | 94.73 | 58.79 | 58.02 | 61.48 | 0.00 | 0.6 |
| CDH1 | 93.28 | 106.31 | 100.41 | 58.32 | 61.00 | 58.15 | 0.00 | 0.6 |
| TRIB1 | 114.51 | 88.92 | 96.56 | 58.70 | 54.87 | 63.68 | 0.01 | 0.6 |
| ABL2 | 110.03 | 101.83 | 88.14 | 54.74 | 62.36 | 58.45 | 0.00 | 0.6 |
| NPM1 | 96.75 | 104.96 | 98.29 | 54.00 | 54.00 | 56.62 | 0.00 | 0.5 |
| ETNK2 | 95.16 | 87.67 | 117.17 | 44.66 | 52.02 | 66.98 | 0.01 | 0.5 |
| JAK1 | 70.16 | 104.17 | 125.66 | 55.93 | 54.15 | 51.56 | 0.05 | 0.5 |

| | | | | | | | | |
|---|---|---|---|---|---|---|---|---|
| PLXNB2 | 107.81 | 99.81 | 92.38 | 53.14 | 49.49 | 57.30 | 0.00 | 0.5 |
| NEK7 | 106.05 | 94.44 | 99.51 | 50.83 | 55.51 | 53.60 | 0.00 | 0.5 |
| HERC4 | 101.72 | 105.21 | 93.07 | 53.40 | 50.35 | 53.23 | 0.00 | 0.5 |
| RIOK3 | 114.66 | 102.70 | 82.64 | 52.09 | 41.01 | 62.60 | 0.01 | 0.5 |
| ATF2 | 93.99 | 107.22 | 98.78 | 38.01 | 56.30 | 58.19 | 0.00 | 0.5 |
| APC | 93.07 | 133.46 | 73.47 | 54.11 | 50.09 | 48.61 | 0.05 | 0.5 |
| PIK3R1 | 71.49 | 110.08 | 118.43 | 55.74 | 41.38 | 52.83 | 0.03 | 0.5 |
| TNIK | 92.42 | 118.61 | 88.97 | 48.05 | 40.12 | 59.52 | 0.01 | 0.5 |
| CXCR7 | 96.52 | 94.33 | 109.15 | 52.16 | 52.47 | 38.81 | 0.00 | 0.5 |
| GNAS | 99.34 | 98.90 | 101.76 | 48.50 | 47.80 | 48.36 | 0.00 | 0.5 |
| PKN1 | 104.60 | 88.72 | 106.68 | 45.31 | 46.34 | 47.45 | 0.00 | 0.5 |
| LPAR1 | 93.72 | 116.63 | 89.65 | 36.29 | 49.87 | 48.58 | 0.00 | 0.4 |
| PIK3C2B | 101.12 | 103.81 | 95.08 | 56.94 | 39.02 | 38.43 | 0.00 | 0.4 |
| IRAK2 | 85.32 | 108.56 | 106.12 | 42.10 | 56.71 | 35.03 | 0.00 | 0.4 |
| TGFBR2 | 87.37 | 113.03 | 99.60 | 37.35 | 40.70 | 43.57 | 0.00 | 0.4 |
| CALM3 | 88.83 | 102.81 | 108.35 | 36.49 | 43.15 | 36.87 | 0.00 | 0.4 |
| HRAS | 69.46 | 116.39 | 114.15 | 38.16 | 35.63 | 41.85 | 0.02 | 0.4 |
| IDH1 | 106.85 | 109.69 | 83.46 | 37.03 | 29.78 | 47.63 | 0.00 | 0.4 |
| MAGI2 | 133.29 | 92.11 | 74.60 | 43.31 | 45.01 | 21.11 | 0.03 | 0.4 |
| FLT3 | 122.76 | 113.11 | 64.13 | 26.59 | 47.37 | 34.56 | 0.03 | 0.4 |
| PRKCQ | 101.45 | 100.14 | 98.41 | 32.96 | 35.88 | 39.27 | 0.00 | 0.4 |
| ILK | 96.77 | 106.34 | 96.88 | 29.07 | 34.35 | 42.80 | 0.00 | 0.4 |
| INPP4B | 92.55 | 107.86 | 99.59 | 36.86 | 29.67 | 37.83 | 0.00 | 0.3 |
| PLK2 | 97.54 | 92.11 | 110.35 | 30.90 | 32.64 | 37.50 | 0.00 | 0.3 |
| AURKC | 122.94 | 116.51 | 60.55 | 21.30 | 37.95 | 41.54 | 0.03 | 0.3 |
| FLNB | 105.10 | 95.84 | 99.05 | 32.87 | 31.05 | 28.04 | 0.00 | 0.3 |
| EPHB6 | 121.89 | 96.25 | 81.86 | 26.40 | 39.20 | 25.74 | 0.01 | 0.3 |
| NTRK1 | 119.13 | 109.76 | 71.12 | 25.80 | 22.99 | 41.93 | 0.01 | 0.3 |
| TGFBR3 | 149.12 | 84.11 | 66.77 | 36.91 | 32.88 | 17.99 | 0.05 | 0.3 |
| TRIM5 | 119.21 | 101.99 | 78.80 | 22.75 | 26.84 | 35.36 | 0.00 | 0.3 |
| HKDC1 | 98.24 | 135.77 | 65.98 | 26.60 | 33.17 | 20.75 | 0.02 | 0.3 |
| TBX22 | 130.75 | 120.46 | 48.79 | 28.32 | 33.64 | 18.41 | 0.05 | 0.3 |
| HOXB7 | 118.67 | 96.82 | 84.51 | 24.45 | 31.31 | 19.46 | 0.00 | 0.3 |
| MST1R | 104.36 | 103.37 | 92.27 | 22.22 | 24.91 | 26.15 | 0.00 | 0.2 |
| MYLK4 | 69.48 | 137.18 | 93.33 | 30.10 | 26.81 | 14.67 | 0.02 | 0.2 |
| MRGPRX3 | 118.30 | 93.42 | 88.28 | 25.62 | 22.83 | 16.65 | 0.00 | 0.2 |
| ALK | 104.07 | 102.73 | 93.20 | 22.54 | 20.08 | 21.98 | 0.00 | 0.2 |
| INSR | 99.84 | 92.06 | 108.09 | 13.64 | 17.95 | 29.07 | 0.00 | 0.2 |
| LRP1B | 119.97 | 126.32 | 53.71 | 0.00 | 15.43 | 33.78 | 0.03 | 0.2 |
| EPHA4 | 128.80 | 106.80 | 64.40 | 20.46 | 14.91 | 12.69 | 0.01 | 0.2 |
| ERBB4 | 98.24 | 135.77 | 65.98 | 10.64 | 18.96 | 10.37 | 0.01 | 0.1 |
| ROBO1 | 103.32 | 95.99 | 100.69 | 14.48 | 12.90 | 11.55 | 0.00 | 0.1 |
| STK32A | 84.10 | 121.76 | 94.14 | 10.12 | 16.23 | 7.89 | 0.00 | 0.1 |

| | | | | | | | | |
|---|---|---|---|---|---|---|---|---|
| MAP2K6 | 98.31 | 109.99 | 91.70 | 10.65 | 15.81 | 6.92 | 0.00 | 0.1 |
| RPS6KA6 | 143.73 | 83.17 | 73.10 | 14.01 | 10.05 | 7.98 | 0.02 | 0.1 |
| ANGPTL4 | 120.81 | 95.40 | 83.79 | 9.35 | 12.90 | 7.06 | 0.00 | 0.1 |
| FYN | 82.16 | 118.31 | 99.54 | 8.37 | 8.39 | 9.18 | 0.00 | 0.1 |
| PRKD1 | 74.75 | 114.38 | 110.87 | 6.07 | 9.01 | 9.87 | 0.00 | 0.1 |
| SMO | 120.56 | 92.82 | 86.62 | 0.00 | 15.95 | 0.00 | 0.00 | 0.1 |
| AKT3 | 88.61 | 105.97 | 105.42 | 3.84 | 4.88 | 5.35 | 0.00 | 0.0 |
| TP53 | 110.82 | 99.07 | 90.11 | 4.99 | 3.59 | 2.62 | 0.00 | 0.0 |
| CDK14 | 118.73 | 90.53 | 90.74 | 3.55 | 5.53 | 1.73 | 0.00 | 0.0 |
| ROS1 | 92.87 | 100.01 | 107.11 | 2.13 | 1.90 | 3.86 | 0.00 | 0.0 |
| HCK | 100.78 | 126.35 | 72.87 | 0.00 | 0.00 | 0.00 | 0.00 | 0.0 |

**Appendix 5: GO pathway analysis of deregulated genes in TRIM24-iHMECs**

| Upregulated Genes | | | |
|---|---|---|---|
| **Term** | **Count** | **%** | **P-Value** |
| GO:0006468~protein amino acid phosphorylation | 52 | 41.3 | 4.83E-37 |
| GO:0016310~phosphorylation | 55 | 43.7 | 1.13E-36 |
| GO:0006793~phosphorus metabolic process | 57 | 45.2 | 1.61E-34 |
| GO:0006796~phosphate metabolic process | 57 | 45.2 | 1.61E-34 |
| GO:0007242~intracellular signaling cascade | 38 | 30.2 | 2.28E-12 |
| GO:0043549~regulation of kinase activity | 19 | 15.1 | 7.45E-10 |
| GO:0042325~regulation of phosphorylation | 21 | 16.7 | 1.28E-09 |
| GO:0051338~regulation of transferase activity | 19 | 15.1 | 1.44E-09 |
| GO:0019220~regulation of phosphate metabolic process | 21 | 16.7 | 2.55E-09 |
| GO:0051174~regulation of phosphorus metabolic process | 21 | 16.7 | 2.55E-09 |
| GO:0045859~regulation of protein kinase activity | 18 | 14.3 | 3.28E-09 |
| GO:0006084~acetyl-CoA metabolic process | 8 | 6.3 | 4.92E-09 |
| GO:0007243~protein kinase cascade | 18 | 14.3 | 9.35E-09 |
| GO:0009060~aerobic respiration | 8 | 6.3 | 1.23E-08 |
| GO:0046356~acetyl-CoA catabolic process | 7 | 5.6 | 2.53E-08 |
| GO:0006099~tricarboxylic acid cycle | 7 | 5.6 | 2.53E-08 |
| GO:0006732~coenzyme metabolic process | 12 | 9.5 | 5.32E-08 |
| GO:0009109~coenzyme catabolic process | 7 | 5.6 | 5.66E-08 |
| GO:0051187~cofactor catabolic process | 7 | 5.6 | 1.75E-07 |
| GO:0042127~regulation of cell proliferation | 23 | 18.3 | 4.02E-07 |
| GO:0046777~protein amino acid autophosphorylation | 9 | 7.1 | 4.86E-07 |
| GO:0042981~regulation of apoptosis | 23 | 18.3 | 5.78E-07 |
| GO:0051186~cofactor metabolic process | 12 | 9.5 | 6.22E-07 |
| GO:0043067~regulation of programmed cell death | 23 | 18.3 | 6.83E-07 |
| GO:0010941~regulation of cell death | 23 | 18.3 | 7.27E-07 |
| GO:0000075~cell cycle checkpoint | 9 | 7.1 | 8.24E-07 |
| GO:0044093~positive regulation of molecular function | 19 | 15.1 | 1.41E-06 |
| GO:0043085~positive regulation of catalytic activity | 17 | 13.5 | 5.66E-06 |
| GO:0043066~negative regulation of apoptosis | 14 | 11.1 | 7.11E-06 |
| GO:0043648~dicarboxylic acid metabolic process | 6 | 4.8 | 8.17E-06 |
| GO:0043069~negative regulation of programmed cell death | 14 | 11.1 | 8.27E-06 |
| GO:0060548~negative regulation of cell death | 14 | 11.1 | 8.52E-06 |
| GO:0006091~generation of precursor metabolites and energy | 13 | 10.3 | 1.06E-05 |
| GO:0018107~peptidyl-threonine phosphorylation | 5 | 4.0 | 1.25E-05 |
| GO:0006917~induction of apoptosis | 13 | 10.3 | 1.33E-05 |
| GO:0012502~induction of programmed cell death | 13 | 10.3 | 1.37E-05 |
| GO:0045333~cellular respiration | 8 | 6.3 | 1.54E-05 |

| | | | |
|---|---|---|---|
| GO:0051726~regulation of cell cycle | 13 | 10.3 | 1.86E-05 |
| GO:0018210~peptidyl-threonine modification | 5 | 4.0 | 2.39E-05 |
| GO:0010033~response to organic substance | 19 | 15.1 | 2.46E-05 |
| GO:0019318~hexose metabolic process | 10 | 7.9 | 3.02E-05 |
| GO:0006915~apoptosis | 17 | 13.5 | 3.47E-05 |
| GO:0006006~glucose metabolic process | 9 | 7.1 | 3.92E-05 |
| GO:0012501~programmed cell death | 17 | 13.5 | 4.14E-05 |
| GO:0042770~DNA damage response, signal transduction | 7 | 5.6 | 5.14E-05 |
| GO:0043065~positive regulation of apoptosis | 14 | 11.1 | 5.49E-05 |
| GO:0043068~positive regulation of programmed cell death | 14 | 11.1 | 5.90E-05 |
| GO:0010942~positive regulation of cell death | 14 | 11.1 | 6.18E-05 |
| GO:0008219~cell death | 18 | 14.3 | 8.34E-05 |
| GO:0016265~death | 18 | 14.3 | 9.08E-05 |
| GO:0005996~monosaccharide metabolic process | 10 | 7.9 | 9.33E-05 |
| GO:0006007~glucose catabolic process | 6 | 4.8 | 1.15E-04 |
| GO:0007167~enzyme linked receptor protein signaling pathway | 12 | 9.5 | 1.24E-04 |
| GO:0033674~positive regulation of kinase activity | 10 | 7.9 | 1.26E-04 |
| GO:0000165~MAPKKK cascade | 9 | 7.1 | 1.43E-04 |
| | | | |
| **Down-regulated Genes** | | | |
| Term | Count | % | PValue |
| GO:0016310~phosphorylation | 50 | 54.9 | 5.39E-37 |
| GO:0006468~protein amino acid phosphorylation | 47 | 51.6 | 1.07E-36 |
| GO:0006793~phosphorus metabolic process | 50 | 54.9 | 5.99E-33 |
| GO:0006796~phosphate metabolic process | 50 | 54.9 | 5.99E-33 |
| GO:0007242~intracellular signaling cascade | 31 | 34.1 | 1.56E-10 |
| GO:0007167~enzyme linked receptor protein signaling pathway | 17 | 18.7 | 6.50E-10 |
| GO:0042325~regulation of phosphorylation | 19 | 20.9 | 1.07E-09 |
| GO:0051174~regulation of phosphorus metabolic process | 19 | 20.9 | 2.01E-09 |
| GO:0019220~regulation of phosphate metabolic process | 19 | 20.9 | 2.01E-09 |
| GO:0007243~protein kinase cascade | 17 | 18.7 | 2.03E-09 |
| GO:0042127~regulation of cell proliferation | 22 | 24.2 | 2.66E-08 |
| GO:0051094~positive regulation of developmental process | 14 | 15.4 | 3.07E-08 |
| GO:0044093~positive regulation of molecular function | 18 | 19.8 | 2.19E-07 |
| GO:0045597~positive regulation of cell differentiation | 12 | 13.2 | 2.95E-07 |
| GO:0045859~regulation of protein kinase activity | 14 | 15.4 | 3.77E-07 |
| GO:0043549~regulation of kinase activity | 14 | 15.4 | 5.57E-07 |
| GO:0010033~response to organic substance | 19 | 20.9 | 8.33E-07 |
| GO:0051338~regulation of transferase activity | 14 | 15.4 | 8.86E-07 |
| GO:0001932~regulation of protein amino acid phosphorylation | 10 | 11.0 | 1.96E-06 |

| | | | |
|---|---|---|---|
| GO:0007169~transmembrane receptor protein tyrosine kinase signaling pathway | 11 | 12.1 | 2.06E-06 |
| GO:0051130~positive regulation of cellular component organization | 10 | 11.0 | 2.85E-06 |
| GO:0008284~positive regulation of cell proliferation | 14 | 15.4 | 2.91E-06 |
| GO:0009725~response to hormone stimulus | 13 | 14.3 | 4.81E-06 |
| GO:0051098~regulation of binding | 9 | 9.9 | 7.25E-06 |
| GO:0007166~cell surface receptor linked signal transduction | 29 | 31.9 | 1.27E-05 |
| GO:0009719~response to endogenous stimulus | 13 | 14.3 | 1.30E-05 |
| GO:0051101~regulation of DNA binding | 8 | 8.8 | 1.45E-05 |
| GO:0045860~positive regulation of protein kinase activity | 10 | 11.0 | 1.55E-05 |
| GO:0033674~positive regulation of kinase activity | 10 | 11.0 | 2.05E-05 |
| GO:0008285~negative regulation of cell proliferation | 12 | 13.2 | 2.38E-05 |
| GO:0030097~hemopoiesis | 10 | 11.0 | 2.43E-05 |
| GO:0051347~positive regulation of transferase activity | 10 | 11.0 | 2.77E-05 |
| GO:0043085~positive regulation of catalytic activity | 14 | 15.4 | 3.33E-05 |
| GO:0032388~positive regulation of intracellular transport | 5 | 5.5 | 4.21E-05 |
| GO:0048534~hemopoietic or lymphoid organ development | 10 | 11.0 | 5.18E-05 |
| GO:0006275~regulation of DNA replication | 6 | 6.6 | 5.30E-05 |
| GO:0007569~cell aging | 5 | 5.5 | 6.19E-05 |
| GO:0044092~negative regulation of molecular function | 11 | 12.1 | 6.64E-05 |
| GO:0043408~regulation of MAPKKK cascade | 7 | 7.7 | 8.05E-05 |
| GO:0002520~immune system development | 10 | 11.0 | 8.21E-05 |
| GO:0007568~aging | 7 | 7.7 | 8.47E-05 |
| GO:0042493~response to drug | 9 | 9.9 | 8.64E-05 |
| GO:0007369~gastrulation | 6 | 6.6 | 9.51E-05 |
| GO:0043388~positive regulation of DNA binding | 6 | 6.6 | 9.51E-05 |
| GO:0032386~regulation of intracellular transport | 6 | 6.6 | 1.02E-04 |
| GO:0051050~positive regulation of transport | 9 | 9.9 | 1.08E-04 |
| GO:0030334~regulation of cell migration | 8 | 8.8 | 1.22E-04 |
| GO:0031399~regulation of protein modification process | 10 | 11.0 | 1.36E-04 |
| GO:0051259~protein oligomerization | 8 | 8.8 | 1.47E-04 |
| GO:0051092~positive regulation of NF-kappaB transcription factor activity | 5 | 5.5 | 1.47E-04 |
| GO:0051099~positive regulation of binding | 6 | 6.6 | 1.59E-04 |
| GO:0042306~regulation of protein import into nucleus | 5 | 5.5 | 1.94E-04 |
| GO:0010627~regulation of protein kinase cascade | 9 | 9.9 | 2.30E-04 |
| GO:0018108~peptidyl-tyrosine phosphorylation | 5 | 5.5 | 2.31E-04 |
| GO:0031346~positive regulation of cell projection organization | 5 | 5.5 | 2.52E-04 |
| GO:0040012~regulation of locomotion | 8 | 8.8 | 2.68E-04 |
| GO:0018212~peptidyl-tyrosine modification | 5 | 5.5 | 2.73E-04 |
| GO:0051270~regulation of cell motion | 8 | 8.8 | 2.77E-04 |

| | | | |
|---|---|---|---|
| GO:0032880~regulation of protein localization | 7 | 7.7 | 2.93E-04 |

**Appendix 6: KEGG pathway analysis of deregulated genes in TRIM24-iHMECs**

| Up-regulated Genes | | | | |
|---|---|---|---|---|
| **Term** | **Count** | **%** | **P-Value** | **Benjamini** |
| Citrate cycle (TCA cycle) | 9 | 7.1 | 2E-08 | 2E-06 |
| Pathways in cancer | 22 | 17.5 | 3E-08 | 2E-06 |
| ErbB signaling pathway | 12 | 9.5 | 1E-07 | 4E-06 |
| Chronic myeloid leukemia | 11 | 8.7 | 3E-07 | 6E-06 |
| Renal cell carcinoma | 10 | 7.9 | 2E-06 | 3E-05 |
| Pancreatic cancer | 10 | 7.9 | 2E-06 | 3E-05 |
| Bladder cancer | 8 | 6.3 | 4E-06 | 6E-05 |
| Neurotrophin signaling pathway | 12 | 9.5 | 4E-06 | 5E-05 |
| Glioma | 9 | 7.1 | 7E-06 | 7E-05 |
| Insulin signaling pathway | 12 | 9.5 | 1E-05 | 9E-05 |
| Melanoma | 9 | 7.1 | 2E-05 | 1E-04 |
| Acute myeloid leukemia | 8 | 6.3 | 4E-05 | 3E-04 |
| MAPK signaling pathway | 15 | 11.9 | 9E-05 | 6E-04 |
| Non-small cell lung cancer | 7 | 5.6 | 2E-04 | 2E-03 |
| Fc epsilon RI signaling pathway | 8 | 6.3 | 3E-04 | 2E-03 |
| T cell receptor signaling pathway | 9 | 7.1 | 3E-04 | 2E-03 |
| Colorectal cancer | 8 | 6.3 | 4E-04 | 2E-03 |
| Prostate cancer | 8 | 6.3 | 6E-04 | 3E-03 |
| Epithelial cell signaling in Helicobacter pylori infection | 7 | 5.6 | 8E-04 | 4E-03 |
| Cell cycle | 9 | 7.1 | 9E-04 | 4E-03 |
| GnRH signaling pathway | 8 | 6.3 | 1E-03 | 5E-03 |
| mTOR signaling pathway | 6 | 4.8 | 2E-03 | 6E-03 |
| Endometrial cancer | 6 | 4.8 | 2E-03 | 6E-03 |
| Progesterone-mediated oocyte maturation | 7 | 5.6 | 3E-03 | 1E-02 |
| Gap junction | 7 | 5.6 | 3E-03 | 1E-02 |
| NOD-like receptor signaling pathway | 6 | 4.8 | 3E-03 | 1E-02 |
| **Down-regulated Genes** | | | | |
| **Term** | **Count** | **%** | **P-Value** | **Benjamini** |
| Neurotrophin signaling pathway | 12 | 13.19 | 1.4E-07 | 1.2E-05 |
| Endometrial cancer | 8 | 8.79 | 2.0E-06 | 8.4E-05 |
| Pathways in cancer | 16 | 17.58 | 3.8E-06 | 1.1E-04 |
| Pancreatic cancer | 8 | 8.79 | 1.8E-05 | 3.8E-04 |
| Chronic myeloid leukemia | 8 | 8.79 | 2.4E-05 | 4.0E-04 |
| Colorectal cancer | 8 | 8.79 | 5.0E-05 | 7.0E-04 |
| Glioma | 7 | 7.69 | 8.4E-05 | 1.0E-03 |
| Thyroid cancer | 5 | 5.49 | 3.3E-04 | 3.5E-03 |
| Apoptosis | 7 | 7.69 | 5.0E-04 | 4.7E-03 |

| | | | | |
|---|---|---|---|---|
| ErbB signaling pathway | 7 | 7.69 | 5.0E-04 | 4.7E-03 |
| Acute myeloid leukemia | 6 | 6.59 | 5.5E-04 | 4.6E-03 |
| MAPK signaling pathway | 11 | 12.09 | 9.8E-04 | 7.6E-03 |
| Melanoma | 6 | 6.59 | 1.4E-03 | 9.8E-03 |
| T cell receptor signaling pathway | 7 | 7.69 | 1.6E-03 | 1.0E-02 |
| Phosphatidylinositol signaling system | 6 | 6.59 | 1.7E-03 | 1.2E-02 |
| Fc epsilon RI signaling pathway | 6 | 6.59 | 2.1E-03 | 1.9E-02 |
| Non-small cell lung cancer | 5 | 5.49 | 3.6E-03 | 1.9E-02 |
| Axon guidance | 7 | 7.69 | 3.9E-03 | 2.3E-02 |
| Fc gamma R-mediated phagocytosis | 6 | 6.59 | 5.0E-03 | 2.5E-02 |
| GnRH signaling pathway | 6 | 6.59 | 5.7E-03 | 3.7E-02 |
| Focal adhesion | 8 | 8.79 | 8.9E-03 | 5.0E-02 |
| Adherens junction | 5 | 5.49 | 1.2E-02 | 4.9E-02 |
| Bladder cancer | 4 | 4.40 | 1.3E-02 | 7.3E-02 |
| Prostate cancer | 5 | 5.49 | 2.0E-02 | 7.2E-02 |
| Insulin signaling pathway | 6 | 6.59 | 2.1E-02 | 8.3E-02 |
| Inositol phosphate metabolism | 4 | 4.40 | 2.5E-02 | 9.7E-02 |
| Toll-like receptor signaling pathway | 5 | 5.49 | 3.1E-02 | 9.7E-02 |
| Wnt signaling pathway | 6 | 6.59 | 3.2E-02 | 1.3E-01 |
| Long-term potentiation | 4 | 4.40 | 4.6E-02 | 1.4E-01 |

## Appendix 7: GSEA report for pathways positively correlating with TRIM24 expression in invasive carcinoma patients

| Pathways postively enriched with TRIM24 | | | | |
|---|---|---|---|---|
| **NAME** | **FDR q-val** | **ES** | **NES** | **NOM p-val** |
| KEGG_OOCYTE_MEIOSIS | 0.06408 | 0.52151 | 1.87444 | 0.00000 |
| REACTOME_DEADENYLATION_DEPENDENT_MRNA_DECAY | 0.06434 | 0.62592 | 1.87805 | 0.00382 |
| REACTOME_KINESINS | 0.06713 | 0.83314 | 1.87817 | 0.00192 |
| PID_AURORA_B_PATHWAY | 0.06795 | 0.71556 | 1.85762 | 0.00763 |
| REACTOME_TRANSPORT_OF_MATURE_MRNA_DERIVED_FROM_AN_INTRONLESS_TRANSCRIPT | 0.06845 | 0.71711 | 1.88203 | 0.00389 |
| REACTOME_ANTIGEN_PROCESSING_UBIQUITINATION_PROTEASOME_DEGRADATION | 0.07023 | 0.49987 | 1.85804 | 0.00186 |
| REACTOME_GLUCOSE_TRANSPORT | 0.07066 | 0.63171 | 1.88390 | 0.00186 |
| REACTOME_TRANSCRIPTION | 0.07192 | 0.55355 | 1.91430 | 0.00546 |
| REACTOME_MITOTIC_G2_G2_M_PHASES | 0.07214 | 0.56097 | 1.84754 | 0.00546 |
| REACTOME_NEP_NS2_INTERACTS_WITH_THE_CELLULAR_EXPORT_MACHINERY | 0.07263 | 0.75149 | 1.85856 | 0.00195 |
| REACTOME_ANTIVIRAL_MECHANISM_BY_IFN_STIMULATED_GENES | 0.07322 | 0.61327 | 1.88518 | 0.00000 |
| KEGG_RNA_DEGRADATION | 0.07602 | 0.59834 | 1.91539 | 0.00000 |
| REACTOME_REGULATION_OF_GLUCOKINASE_BY_GLUCOKINASE_REGULATORY_PROTEIN | 0.07690 | 0.71516 | 1.88557 | 0.00190 |
| REACTOME_TRANSPORT_OF_RIBONUCLEOPROTEINS_INTO_THE_HOST_NUCLEUS | 0.07828 | 0.75012 | 1.88901 | 0.00000 |
| REACTOME_LATE_PHASE_OF_HIV_LIFE_CYCLE | 0.07982 | 0.55328 | 1.83218 | 0.00570 |
| REACTOME_TRANSPORT_OF_MATURE_TRANSCRIPT_TO_CYTOPLASM | 0.08048 | 0.68610 | 1.89741 | 0.00388 |
| REACTOME_MEIOSIS | 0.08146 | 0.59509 | 1.91615 | 0.00000 |
| BIOCARTA_ATRBRCA_PATHWAY | 0.08189 | 0.76268 | 1.89002 | 0.00000 |
| REACTOME_MEIOTIC_RECOMBINATION | 0.08225 | 0.64034 | 1.82548 | 0.00188 |
| REACTOME_INTERACTIONS_OF_VPR_WITH_HOST_CELLULAR_PROTEINS | 0.08325 | 0.72806 | 1.92217 | 0.00195 |
| REACTOME_MRNA_3_END_PROCESSING | 0.08413 | 0.69132 | 1.81575 | 0.00586 |
| REACTOME_RNA_POL_II_TRANSCRIPTION | 0.08626 | 0.55333 | 1.80294 | 0.01095 |
| REACTOME_METABOLISM_OF_NON_CODING_RNA | 0.08628 | 0.66598 | 1.81632 | 0.00576 |
| REACTOME_TELOMERE_MAINTENANCE | 0.08643 | 0.68094 | 1.80537 | 0.01328 |
| REACTOME_HIV_LIFE_CYCLE | 0.08865 | 0.54442 | 1.80587 | 0.00949 |
| REACTOME_MEIOTIC_SYNAPSIS | 0.08981 | 0.62712 | 1.92364 | 0.00000 |
| PID_PLK1_PATHWAY | 0.09299 | 0.70542 | 1.93973 | 0.00366 |
| PID_BARD1PATHWAY | 0.09308 | 0.70553 | 1.79135 | 0.00593 |
| REACTOME_MITOTIC_M_M_G1_PHASES | 0.09489 | 0.67837 | 1.92756 | 0.00372 |
| REACTOME_CLEAVAGE_OF_GROWING_TRANSCRIPT_IN_THE_TERMINATION_REGION_ | 0.09509 | 0.67971 | 1.78624 | 0.00568 |
| PID_E2F_PATHWAY | 0.09586 | 0.53455 | 1.78174 | 0.00727 |
| REACTOME_G2_M_CHECKPOINTS | 0.09661 | 0.74742 | 1.77472 | 0.01326 |
| KEGG_CELL_CYCLE | 0.09687 | 0.55862 | 1.77733 | 0.01296 |
| REACTOME_LOSS_OF_NLP_FROM_MITOTIC_CENTROSOMES | 0.09713 | 0.54059 | 1.76872 | 0.00749 |
| REACTOME_CELL_CYCLE_MITOTIC | 0.09823 | 0.63418 | 2.01532 | 0.00366 |

| | | | | |
|---|---|---|---|---|
| PID_ATM_PATHWAY | 0.09938 | 0.62878 | 1.76889 | 0.00559 |
| REACTOME_G0_AND_EARLY_G1 | 0.09998 | 0.74488 | 1.76329 | 0.00765 |
| REACTOME_MRNA_PROCESSING | 0.10062 | 0.55231 | 1.75046 | 0.01527 |
| PID_P53REGULATIONPATHWAY | 0.10128 | 0.51186 | 1.75457 | 0.00384 |
| REACTOME_CELL_CYCLE_CHECKPOINTS | 0.10152 | 0.63477 | 1.75934 | 0.01498 |
| REACTOME_DEADENYLATION_OF_MRNA | 0.10189 | 0.67875 | 1.75146 | 0.00411 |
| REACTOME_DEPOSITION_OF_NEW_CENPA_CONTAINING_NUCLEOSOMES_AT_THE_CENTROMERE | 0.10204 | 0.71104 | 1.73884 | 0.01333 |
| REACTOME_MITOTIC_G1_G1_S_PHASES | 0.10254 | 0.59616 | 1.74061 | 0.01679 |
| REACTOME_ACTIVATION_OF_ATR_IN_RESPONSE_TO_REPLICATION_STRESS | 0.10291 | 0.76476 | 1.75521 | 0.01331 |
| REACTOME_FACTORS_INVOLVED_IN_MEGAKARYOCYTE_DEVELOPMENT_AND_PLATELET_PRODUCTION | 0.10315 | 0.44949 | 1.74232 | 0.00514 |
| REACTOME_SIGNALING_BY_TGF_BETA_RECEPTOR_COMPLEX | 0.10343 | 0.49065 | 1.74428 | 0.00179 |
| PID_ATR_PATHWAY | 0.10404 | 0.73865 | 1.94007 | 0.00185 |
| REACTOME_G1_S_TRANSITION | 0.10676 | 0.61844 | 1.73105 | 0.02052 |
| REACTOME_E2F_MEDIATED_REGULATION_OF_DNA_REPLICATION | 0.10906 | 0.67603 | 1.72596 | 0.02068 |
| REACTOME_REGULATION_OF_MITOTIC_CELL_CYCLE | 0.11120 | 0.63876 | 1.72137 | 0.02385 |
| PID_FANCONI_PATHWAY | 0.11789 | 0.73211 | 1.94110 | 0.00188 |
| REACTOME_PACKAGING_OF_TELOMERE_ENDS | 0.11850 | 0.68107 | 1.69037 | 0.02457 |
| REACTOME_TRANSCRIPTIONAL_ACTIVITY_OF_SMAD2_SMAD3_SMAD4_HETEROTRIMER | 0.11936 | 0.51551 | 1.69138 | 0.00549 |
| REACTOME_PROCESSING_OF_CAPPED_INTRON_CONTAINING_PRE_MRNA | 0.11967 | 0.55976 | 1.71013 | 0.02682 |
| REACTOME_DNA_STRAND_ELONGATION | 0.12033 | 0.76700 | 1.68599 | 0.01905 |
| KEGG_VIBRIO_CHOLERAE_INFECTION | 0.12037 | 0.51593 | 1.69642 | 0.01289 |
| REACTOME_DNA_REPAIR | 0.12056 | 0.51428 | 1.69222 | 0.02617 |
| REACTOME_DOUBLE_STRAND_BREAK_REPAIR | 0.12056 | 0.65993 | 1.69440 | 0.02574 |
| REACTOME_RNA_POL_I_RNA_POL_III_AND_MITOCHONDRIAL_TRANSCRIPTION | 0.12074 | 0.50434 | 1.68373 | 0.01842 |
| REACTOME_SYNTHESIS_OF_DNA | 0.12095 | 0.64069 | 1.69964 | 0.02578 |
| REACTOME_RECRUITMENT_OF_MITOTIC_CENTROSOME_PROTEINS_AND_COMPLEXES | 0.12103 | 0.50539 | 1.70437 | 0.00914 |
| REACTOME_S_PHASE | 0.12119 | 0.61692 | 1.69748 | 0.03142 |
| REACTOME_CHROMOSOME_MAINTENANCE | 0.12125 | 0.67446 | 2.02219 | 0.00000 |
| REACTOME_CLASS_I_MHC_MEDIATED_ANTIGEN_PROCESSING_PRESENTATION | 0.12180 | 0.44952 | 1.70082 | 0.00550 |
| REACTOME_DOWNREGULATION_OF_SMAD2_3_SMAD4_TRANSCRIPTIONAL_ACTIVITY | 0.12293 | 0.60638 | 1.70455 | 0.00787 |
| REACTOME_HIV_INFECTION | 0.12411 | 0.50023 | 1.67602 | 0.02421 |
| REACTOME_MITOTIC_PROMETAPHASE | 0.12438 | 0.70370 | 1.95132 | 0.00189 |
| PID_FOXOPATHWAY | 0.12481 | 0.48528 | 1.67349 | 0.00890 |
| REACTOME_PROCESSING_OF_CAPPED_INTRONLESS_PRE_MRNA | 0.12514 | 0.69404 | 1.67675 | 0.01934 |
| REACTOME_DNA_REPLICATION | 0.13022 | 0.68481 | 1.96305 | 0.00368 |
| REACTOME_ACTIVATION_OF_THE_PRE_REPLICATIVE_COMPLEX | 0.13127 | 0.77417 | 1.66250 | 0.01934 |
| KEGG_DNA_REPLICATION | 0.13129 | 0.71138 | 1.66065 | 0.03781 |
| PID_MYC_ACTIVPATHWAY | 0.13238 | 0.51319 | 1.66345 | 0.03825 |
| REACTOME_RNA_POL_I_TRANSCRIPTION | 0.13568 | 0.54073 | 1.65408 | 0.03097 |
| BIOCARTA_MPR_PATHWAY | 0.13574 | 0.53412 | 1.65234 | 0.01835 |
| PID_NFAT_3PATHWAY | 0.13881 | 0.45721 | 1.64747 | 0.01622 |

| | | | | |
|---|---|---|---|---|
| REACTOME_APC_CDC20_MEDIATED_DEGRADATION_OF_NEK2A | 0.14737 | 0.65242 | 1.63723 | 0.02985 |
| REACTOME_EXTENSION_OF_TELOMERES | 0.14908 | 0.71081 | 1.63372 | 0.03738 |
| KEGG_BASAL_TRANSCRIPTION_FACTORS | 0.15401 | 0.54087 | 1.62712 | 0.02124 |
| KEGG_PROGESTERONE_MEDIATED_OOCYTE_MATURATION | 0.16323 | 0.44447 | 1.61206 | 0.01068 |
| BIOCARTA_G2_PATHWAY | 0.16461 | 0.60109 | 1.61253 | 0.03137 |
| REACTOME_CELL_CYCLE | 0.16472 | 0.61694 | 2.03270 | 0.00361 |
| REACTOME_RNA_POL_II_PRE_TRANSCRIPTION_EVENTS | 0.16534 | 0.49104 | 1.60485 | 0.03683 |
| KEGG_MISMATCH_REPAIR | 0.16577 | 0.64843 | 1.61320 | 0.03512 |
| KEGG_NUCLEOTIDE_EXCISION_REPAIR | 0.16581 | 0.51854 | 1.60270 | 0.03795 |
| REACTOME_M_G1_TRANSITION | 0.16619 | 0.63197 | 1.60577 | 0.05639 |
| PID_CDC42_PATHWAY | 0.16620 | 0.44910 | 1.61468 | 0.01299 |
| PID_FOXM1PATHWAY | 0.16721 | 0.55348 | 1.60655 | 0.05128 |
| REACTOME_HOST_INTERACTIONS_OF_HIV_FACTORS | 0.16792 | 0.51664 | 1.59923 | 0.04135 |
| REACTOME_HOMOLOGOUS_RECOMBINATION_REPAIR_OF_REPLICATION_INDEPENDENT_DOUBLE_STRAND_BREAKS | 0.16930 | 0.65792 | 1.59629 | 0.03512 |
| REACTOME_LAGGING_STRAND_SYNTHESIS | 0.17241 | 0.71544 | 1.59174 | 0.04461 |
| REACTOME_APC_C_CDC20_MEDIATED_DEGRADATION_OF_MITOTIC_PROTEINS | 0.18120 | 0.60192 | 1.58256 | 0.07063 |
| REACTOME_APC_C_CDH1_MEDIATED_DEGRADATION_OF_CDC20_AND_OTHER_APC_C_CDH1_TARGETED_PROTEINS_IN_LATE_MITOSIS_EARLY_G1 | 0.19813 | 0.59770 | 1.56708 | 0.07421 |
| KEGG_SPLICEOSOME | 0.20514 | 0.51304 | 1.55945 | 0.06434 |
| KEGG_HOMOLOGOUS_RECOMBINATION | 0.20534 | 0.60543 | 1.55755 | 0.06180 |
| REACTOME_CYCLIN_E_ASSOCIATED_EVENTS_DURING_G1_S_TRANSITION_ | 0.21934 | 0.56082 | 1.54500 | 0.08736 |
| REACTOME_RNA_POL_I_PROMOTER_OPENING | 0.22835 | 0.64999 | 1.53680 | 0.06857 |
| PID_PI3KCIAKTPATHWAY | 0.23155 | 0.45818 | 1.53275 | 0.03018 |
| REACTOME_ORC1_REMOVAL_FROM_CHROMATIN | 0.23915 | 0.58463 | 1.52366 | 0.09888 |
| REACTOME_REGULATION_OF_MRNA_STABILITY_BY_PROTEINS_THAT_BIND_AU_RICH_ELEMENTS | 0.24074 | 0.51165 | 1.52429 | 0.07934 |
| BIOCARTA_PROTEASOME_PATHWAY | 0.24789 | 0.65029 | 1.51581 | 0.09478 |
| PID_TELOMERASEPATHWAY | 0.26377 | 0.41596 | 1.50312 | 0.02974 |
| PID_INSULIN_GLUCOSE_PATHWAY | 0.26954 | 0.48411 | 1.49755 | 0.06579 |
| REACTOME_SCFSKP2_MEDIATED_DEGRADATION_OF_P27_P21 | 0.27322 | 0.57794 | 1.48846 | 0.11359 |
| REACTOME_SIGNALING_BY_WNT | 0.27351 | 0.51564 | 1.49312 | 0.08679 |
| BIOCARTA_ACTINY_PATHWAY | 0.27415 | 0.59575 | 1.48946 | 0.06903 |
| REACTOME_ASSEMBLY_OF_THE_PRE_REPLICATIVE_COMPLEX | 0.27479 | 0.59730 | 1.49072 | 0.10841 |
| REACTOME_MHC_CLASS_II_ANTIGEN_PRESENTATION | 0.29102 | 0.41678 | 1.47185 | 0.07196 |
| SA_G1_AND_S_PHASES | 0.29140 | 0.59326 | 1.47326 | 0.08812 |
| PID_ECADHERIN_NASCENTAJ_PATHWAY | 0.29210 | 0.47020 | 1.47468 | 0.05321 |
| KEGG_UBIQUITIN_MEDIATED_PROTEOLYSIS | 0.29307 | 0.54255 | 2.04425 | 0.00188 |
| KEGG_PYRIMIDINE_METABOLISM | 0.29385 | 0.45504 | 1.46808 | 0.07547 |
| REACTOME_GENERIC_TRANSCRIPTION_PATHWAY | 0.29591 | 0.40078 | 1.46340 | 0.09464 |
| REACTOME_TRANSCRIPTION_COUPLED_NER_TC_NER | 0.29715 | 0.50489 | 1.46426 | 0.08969 |
| REACTOME_RNA_POL_I_TRANSCRIPTION_INITIATION | 0.30228 | 0.52275 | 1.45781 | 0.08364 |
| REACTOME_AUTODEGRADATION_OF_CDH1_BY_CDH1_APC_C | 0.30504 | 0.55141 | 1.45445 | 0.13197 |
| REACTOME_INSULIN_RECEPTOR_RECYCLING | 0.31323 | 0.55970 | 1.44766 | 0.11132 |

| | | | | |
|---|---|---|---|---|
| PID_AURORA_A_PATHWAY | 0.31582 | 0.48821 | 1.44424 | 0.08672 |
| REACTOME_ACTIVATION_OF_NF_KAPPAB_IN_B_CELLS | 0.32016 | 0.51224 | 1.43992 | 0.12037 |
| REACTOME_P53_DEPENDENT_G1_DNA_DAMAGE_RESPONSE | 0.32274 | 0.54136 | 1.43336 | 0.13458 |
| REACTOME_SCF_BETA_TRCP_MEDIATED_DEGRADATION_OF_EMI1 | 0.32282 | 0.57213 | 1.43491 | 0.13645 |
| REACTOME_NUCLEOTIDE_EXCISION_REPAIR | 0.32432 | 0.46860 | 1.43563 | 0.09830 |
| REACTOME_MRNA_SPLICING | 0.33122 | 0.48743 | 1.42301 | 0.11686 |
| REACTOME_RNA_POL_II_TRANSCRIPTION_PRE_INITIATION_AND_PROMOTER_OPENING | 0.33273 | 0.47377 | 1.42540 | 0.09641 |
| KEGG_PROTEASOME | 0.33354 | 0.59200 | 1.42326 | 0.15789 |
| KEGG_PROTEIN_EXPORT | 0.33894 | 0.58179 | 1.41684 | 0.12398 |
| BIOCARTA_G1_PATHWAY | 0.34162 | 0.46818 | 1.41175 | 0.09009 |
| PID_AJDISS_2PATHWAY | 0.34311 | 0.40989 | 1.41251 | 0.06944 |
| PID_MYC_PATHWAY | 0.34561 | 0.45365 | 1.40774 | 0.08663 |
| REACTOME_DOWNREGULATION_OF_TGF_BETA_RECEPTOR_SIGNALING | 0.34578 | 0.49901 | 1.40418 | 0.10638 |

**Appendix 8: Histopathological report of tumors obtained after injection of Control or TRIM24-HMECs**

| Group | CONTROL | | | | | | | | | | Summary |
|---|---|---|---|---|---|---|---|---|---|---|---|
| Animal ID | 2506 | | 2508 | | 2509 | | 2510 | | 2549 | 2550 | |
| Specie | Mouse | | Mouse | | Mouse | | Mouse | | Mouse | Mouse | |
| Genotype/Strain | C57/129 | | C57/129 | | C57/129 | | C57/129 | | C57/129 | C57/129 | |
| Organ Morphologic Diagnosis | Lesion Grade | | Lesion Grade | | Lesion Grade | | Lesion Grade | | Lesion Grade | Lesion Grade | Incidence or Average Score of lesions |
| Xenograft tissue sample on the slide | P | | P | | P | | P | | P | P | 6 |
| Dx: Fibrous tissue | P | | P | | | | | | P | | 3 |
| Dx: Epithelial cells intermixed with fibrous tissue | | | | | P | | P | | | P | 3 |
| Epithelial cells (percent of epithelial cells from the total tumor mass) | 0 | | 0 | | 1 | | 1 | | 0 | 1 | 0.5 |
| Fibrous tissue (percent fibrous tissue and collagen deposition from the total tumor mass) | 100 | | 100 | | 99 | | 99 | | 100 | 99 | 99.5 |
| Cellular atypia of neoplastic epithelial cells (grade 0-4) | | | | | 0 | | 0 | | | 0 | 0 |
| Anysokaryosis (grade 0-4) | | | | | 0 | | 0 | | | 0 | 0 |
| Mitotic rate (total number of mitotic epithelial cells within the xenograft tumor) | | | | | 0 | | 0 | | | 0 | 0 |
| Vascularization (grade 1-4) | 1 | | 1 | | 1 | | 1 | | 1 | 1 | 1 |
| Grade of malignancy (grade 0-3) | 0 | | 0 | | 0 | | 0 | | 0 | 0 | 0 |
| Inflammation | P | | P | | P | | P | | P | | 5 |
| Infiltration of Neutrophilis and/or Macrophages | 1 | | 1 | | 1 | | 1 | | 2 | | 1.2 |
| Infiltration of Lymphocytes | 0 | | 0 | | 0 | | 0 | | 0 | | 0 |

| Group | TRIM24-1 | | | | | | | | | | | | Summary |
|---|---|---|---|---|---|---|---|---|---|---|---|---|---|
| Animal ID | 2513 | 2515 | 2516 | 2517 | 2518 | 2519 | 2520 | 2531 | 2532 | 2533 | 2534 | 2535 | |
| Specie | Mouse | Mouse | Mouse | Mouse | Mouse | Mouse | Mouse | Mouse | Mouse | Mouse | Mouse | Mouse | |
| Genotype/Strain | C57/129 | C57/129 | C57/129 | C57/129 | C57/129 | C57/129 | C57/129 | C57/129 | C57/129 | C57/129 | C57/129 | C57/129 | |
| Organ<br>Morphologic Diagnosis | Lesion Grade | Lesion Grade | Lesion Grade | Lesion Grade | Lesion Grade | Lesion Grade | Lesion Grade | Lesion Grade | Lesion Grade | Lesion Grade | Lesion Grade | Lesion Grade | Incidence or Average Score of lesions |
| Xenograft tissue sample on the slide | P | P | P | P | P | P | P | P | P | P | P | P | 12 |
| Dx: Fibrous tissue | | | | | | | | | | | | | |
| Dx: Epithelial cells intermixed with fibrous tissue | P | P | P | P | P | P | P | P | P | P | P | P | 12 |
| Epithelial cells (percent of epithelial cells from the total tumor mass) | 5 | 25 | 35 | 30 | 40 | 40 | 30 | 35 | 20 | 35 | 1 | 2 | 24.8 |
| Fibrous tissue (percent fibrous tissue and collagen deposition from the total tumor mass) | 95 | 75 | 65 | 70 | 60 | 60 | 70 | 65 | 80 | 65 | 99 | 98 | 75.2 |
| Cellular atypia of neoplastic epithelial cells (grade 0-4) | 2 | 1 | 4 | 2 | 3 | 4 | 2 | 4 | 2 | 3 | 0 | 1 | 2.3 |
| Anysokaryosis (grade 0-4) | 1 | 1 | 3 | 2 | 3 | 3 | 2 | 3 | 3 | 3 | 0 | 2 | 2.2 |
| Mitotic rate (total number of mitotic epithelial cells within the xenograft tumor) | 1 | 0 | 3 | 0 | 2 | 2 | 0 | 0 | 0 | 1 | 0 | 1 | 0.8 |
| Vascularization (grade 1-4) | 1 | 2 | 2 | 1 | 2 | 2 | 2 | 2 | 2 | 2 | 2 | 2 | 1.8 |
| Grade of malignancy (grade 0-3) | 1 | 1 | 3 | 2 | 2 | 3 | 2 | 3 | 2 | 2 | 0 | 1 | 1.8 |
| Inflammation | P | P | P | P | P | P | P | P | P | P | P | P | 12 |
| Infiltration of Neutrophilis and/or Macrophages | 3 | 2 | 3 | 3 | 2 | 3 | 2 | 2 | 4 | 4 | 3 | 2 | 3 |
| Infiltration of Lymphocytes | 1 | 1 | 2 | 1 | 2 | 2 | 1 | 3 | 3 | 1 | 0 | 0 | 1 |

| Group | TRIM24-2 | | | | | | | | | | | | | Summary |
|---|---|---|---|---|---|---|---|---|---|---|---|---|---|---|
| Animal ID | 2528 | 2521 | 2522 | 2525 | 2526 | 2527 | 2529 | 2530 | 2536 | 2537 | 2540 | 2541 | 2542 | |
| Specie | Mouse | Mouse | Mouse | Mouse | Mouse | Mouse | Mouse | Mouse | Mouse | Mouse | Mouse | Mouse | Mouse | |
| Genotype/Strain | C57/129 | C57/129 | C57/129 | C57/129 | C57/129 | C57/129 | C57/129 | C57/129 | C57/129 | C57/129 | C57/129 | C57/129 | C57/129 | |
| Organ<br>Morphologic Diagnosis | Lesion Grade | Lesion Grade | Lesion Grade | Lesion Grade | Lesion Grade | Lesion Grade | Lesion Grade | Lesion Grade | Lesion Grade | Lesion Grade | Lesion Grade | Lesion Grade | Lesion Grade | Incidence or Average Score of lesions |
| Xenograft tissue sample on the slide | | P | P | P | P | P | P | P | P | P | P | P | P | 12 |
| Dx: Fibrous tissue | | | | | | | | | | | | | | 0 |
| Dx: Epithelial cells intermixed with fibrous tissue | | P | P | P | P | P | P | P | P | P | P | P | P | 12 |
| Epithelial cells (percent of epithelial cells from the total tumor mass) | | 50 | 40 | 35 | 20 | 35 | 1 | 35 | 20 | 25 | 35 | 60 | 25 | 31.8 |
| Fibrous tissue (percent fibrous tissue and collagen deposition from the total tumor mass) | | 50 | 60 | 65 | 80 | 65 | 99 | 65 | 80 | 75 | 65 | 40 | 75 | 68.3 |
| Cellular atypia of neoplastic epithelial cells (grade 0-4) | | 4 | 4 | 4 | 2 | 4 | 1 | 4 | 2 | 3 | 4 | 4 | 3 | 3.3 |
| Anysokaryosis (grade 0-4) | | 3 | 3 | 3 | 3 | 3 | 1 | 4 | 2 | 3 | 4 | 4 | 3 | 3.0 |
| Mitotic rate (total number of mitotic epithelial cells within the xenograft tumor) | | 0 | 2 | 2 | 1 | 0 | 0 | 0 | 0 | 2 | 0 | 0 | 0 | 0.6 |
| Vascularization (grade 1-4) | | 2 | 2 | 2 | 1 | 2 | 1 | 2 | 1 | 1 | 2 | 2 | 2 | 1.7 |
| Grade of malignancy (grade 0-3) | | 3 | 3 | 3 | 1 | 3 | 0 | 3 | 1 | 2 | 3 | 3 | 2 | 2.3 |
| Inflammation | | P | P | P | P | P | P | P | P | P | P | P | P | 12 |
| Infiltration of Neutrophilis and/or Macrophages | | 2 | 2 | 1 | 1 | 2 | 1 | 2 | 1 | 3 | 3 | 3 | 2 | 2 |
| Infiltration of Lymphocytes | | 3 | 2 | 2 | 1 | 0 | 0 | 0 | 0 | 1 | 3 | 0 | 2 | 1 |

## Appendix 9: List of deregulated genes in TRIM24-OE MCF10A cells by HTG Edgeseq analysis

| Upregulated genes | | | | | | | |
|---|---|---|---|---|---|---|---|
| | | **Vector** | Normalized | FC | WT | Normalized | FC |
| 1 | FYN | 18 | 0.001 | 1 | 101 | 0.005 | 6.19 |
| 2 | MMP2 | 197 | 0.010 | 1 | 978 | 0.053 | 5.47 |
| 3 | IGFBP2 | 90 | 0.004 | 1 | 423 | 0.023 | 5.18 |
| 4 | CITED2 | 1211 | 0.060 | 1 | 4958 | 0.270 | 4.51 |
| 5 | ITGAM | 3 | 0.000 | 1 | 12 | 0.001 | 4.41 |
| 6 | CCL17 | 11 | 0.001 | 1 | 43 | 0.002 | 4.31 |
| 7 | F2R | 117 | 0.006 | 1 | 448 | 0.024 | 4.22 |
| 8 | NOV | 5 | 0.000 | 1 | 19 | 0.001 | 4.19 |
| 9 | TIMP1 | 5089 | 0.251 | 1 | 18943 | 1.031 | 4.10 |
| 10 | STC1 | 19 | 0.001 | 1 | 62 | 0.003 | 3.60 |
| 11 | NEIL1 | 12 | 0.001 | 1 | 38 | 0.002 | 3.49 |
| 12 | BMP4 | 82 | 0.004 | 1 | 259 | 0.014 | 3.48 |
| 13 | DKK1 | 2435 | 0.120 | 1 | 7608 | 0.414 | 3.44 |
| 14 | HSF4 | 15 | 0.001 | 1 | 46 | 0.003 | 3.38 |
| 15 | ADRA2A | 4 | 0.000 | 1 | 12 | 0.001 | 3.31 |
| 16 | FCGR1A | 7 | 0.000 | 1 | 21 | 0.001 | 3.31 |
| 17 | LFNG | 13 | 0.001 | 1 | 39 | 0.002 | 3.31 |
| 18 | APBB1 | 12 | 0.001 | 1 | 34 | 0.002 | 3.12 |
| 19 | ANGPT1 | 202 | 0.010 | 1 | 572 | 0.031 | 3.12 |
| 20 | TXNRD1 | 1960 | 0.097 | 1 | 5528 | 0.301 | 3.11 |
| 21 | EFNA2 | 4 | 0.000 | 1 | 11 | 0.001 | 3.03 |
| 22 | FAT4 | 88 | 0.004 | 1 | 241 | 0.013 | 3.02 |
| 23 | PDCD1LG2 | 7 | 0.000 | 1 | 19 | 0.001 | 2.99 |
| 24 | IGFBP4 | 314 | 0.016 | 1 | 843 | 0.046 | 2.96 |
| 25 | IL27 | 3 | 0.000 | 1 | 8 | 0.000 | 2.94 |
| 26 | FBN1 | 309 | 0.015 | 1 | 797 | 0.043 | 2.84 |
| 27 | FOXO1 | 195 | 0.010 | 1 | 484 | 0.026 | 2.74 |
| 28 | GSTM1 | 27 | 0.001 | 1 | 66 | 0.004 | 2.69 |
| 29 | PRMT8 | 10 | 0.000 | 1 | 24 | 0.001 | 2.65 |
| 30 | HSP90AA1 | 15 | 0.001 | 1 | 36 | 0.002 | 2.65 |
| 31 | PBX1 | 80 | 0.004 | 1 | 192 | 0.010 | 2.65 |
| 32 | CARD11 | 33 | 0.002 | 1 | 77 | 0.004 | 2.57 |
| 33 | CLDN3 | 6 | 0.000 | 1 | 14 | 0.001 | 2.57 |
| 34 | TNFRSF8 | 12 | 0.001 | 1 | 28 | 0.002 | 2.57 |
| 35 | SLC7A11 | 110 | 0.005 | 1 | 256 | 0.014 | 2.57 |
| 36 | CD68 | 269 | 0.013 | 1 | 619 | 0.034 | 2.54 |
| 37 | RELN | 12 | 0.001 | 1 | 27 | 0.001 | 2.48 |
| 38 | SULT2A1 | 13 | 0.001 | 1 | 29 | 0.002 | 2.46 |
| 39 | HPSE | 123 | 0.006 | 1 | 272 | 0.015 | 2.44 |
| 40 | IRS1 | 134 | 0.007 | 1 | 295 | 0.016 | 2.43 |
| 41 | TAT | 12 | 0.001 | 1 | 26 | 0.001 | 2.39 |
| 42 | S100A4 | 497 | 0.025 | 1 | 1061 | 0.058 | 2.35 |
| 43 | DAPK1 | 65 | 0.003 | 1 | 137 | 0.007 | 2.32 |
| 44 | PPAP2B | 71 | 0.004 | 1 | 146 | 0.008 | 2.27 |
| 45 | WNT5A | 218 | 0.011 | 1 | 448 | 0.024 | 2.27 |
| 46 | ID4 | 5 | 0.000 | 1 | 10 | 0.001 | 2.20 |
| 47 | GNLY | 21 | 0.001 | 1 | 42 | 0.002 | 2.20 |
| 48 | BTC | 26 | 0.001 | 1 | 52 | 0.003 | 2.20 |
| 49 | TCL1A | 30 | 0.001 | 1 | 60 | 0.003 | 2.20 |
| 50 | PROK1 | 35 | 0.002 | 1 | 70 | 0.004 | 2.20 |
| 51 | MAF | 3 | 0.000 | 1 | 6 | 0.000 | 2.20 |
| 52 | PDPN | 49 | 0.002 | 1 | 98 | 0.005 | 2.20 |
| 53 | SIX1 | 41 | 0.002 | 1 | 81 | 0.004 | 2.18 |
| 54 | GADD45B | 407 | 0.020 | 1 | 800 | 0.044 | 2.17 |

| | | | | | | | |
|---|---|---|---|---|---|---|---|
| 55 | MAGEA4 | 26 | 0.001 | 1 | 51 | 0.003 | 2.16 |
| 56 | TSC1 | 51 | 0.003 | 1 | 99 | 0.005 | 2.14 |
| 57 | MYBL1 | 46 | 0.002 | 1 | 89 | 0.005 | 2.13 |
| 58 | MAP1LC3A | 85 | 0.004 | 1 | 164 | 0.009 | 2.13 |
| 59 | AXL | 348 | 0.017 | 1 | 669 | 0.036 | 2.12 |
| 60 | LTF | 25 | 0.001 | 1 | 48 | 0.003 | 2.12 |
| 61 | COL18A1 | 64 | 0.003 | 1 | 122 | 0.007 | 2.10 |
| 62 | GPER1 | 19 | 0.001 | 1 | 36 | 0.002 | 2.09 |
| 63 | IFNW1 | 18 | 0.001 | 1 | 34 | 0.002 | 2.08 |
| 64 | GAS6 | 637 | 0.031 | 1 | 1197 | 0.065 | 2.07 |
| 65 | HOXB13 | 16 | 0.001 | 1 | 30 | 0.002 | 2.07 |
| 66 | SYP | 30 | 0.001 | 1 | 56 | 0.003 | 2.06 |
| 67 | SCUBE1 | 7 | 0.000 | 1 | 13 | 0.001 | 2.05 |
| 68 | IL11 | 33 | 0.002 | 1 | 60 | 0.003 | 2.00 |
| 69 | TOP3B | 21 | 0.001 | 1 | 38 | 0.002 | 1.99 |
| 70 | GSN | 107 | 0.005 | 1 | 193 | 0.011 | 1.99 |
| 71 | CDKN2C | 67 | 0.003 | 1 | 120 | 0.007 | 1.97 |
| 72 | ABCC3 | 2222 | 0.110 | 1 | 3979 | 0.217 | 1.97 |
| 73 | CST6 | 57 | 0.003 | 1 | 102 | 0.006 | 1.97 |
| 74 | NQO1 | 6428 | 0.317 | 1 | 11484 | 0.625 | 1.97 |
| 75 | FLRT1 | 14 | 0.001 | 1 | 25 | 0.001 | 1.97 |
| 76 | CYR61 | 743 | 0.037 | 1 | 1316 | 0.072 | 1.95 |
| 77 | CDKN2D | 39 | 0.002 | 1 | 69 | 0.004 | 1.95 |
| 78 | FGF13 | 17 | 0.001 | 1 | 30 | 0.002 | 1.95 |
| 79 | IKBKG | 17 | 0.001 | 1 | 30 | 0.002 | 1.95 |
| 80 | KLF17 | 17 | 0.001 | 1 | 30 | 0.002 | 1.95 |
| 81 | EPS8 | 515 | 0.025 | 1 | 908 | 0.049 | 1.94 |
| 82 | BMF | 83 | 0.004 | 1 | 146 | 0.008 | 1.94 |
| 83 | SOX3 | 28 | 0.001 | 1 | 49 | 0.003 | 1.93 |
| 84 | FZD2 | 183 | 0.009 | 1 | 320 | 0.017 | 1.93 |
| 85 | DUSP10 | 132 | 0.007 | 1 | 230 | 0.013 | 1.92 |
| 86 | ZEB1 | 160 | 0.008 | 1 | 278 | 0.015 | 1.92 |
| 87 | S1PR1 | 34 | 0.002 | 1 | 59 | 0.003 | 1.91 |
| 88 | PFKFB1 | 44 | 0.002 | 1 | 76 | 0.004 | 1.90 |
| 89 | BNIP3L | 310 | 0.015 | 1 | 535 | 0.029 | 1.90 |
| 90 | MAOB | 46 | 0.002 | 1 | 79 | 0.004 | 1.89 |
| 91 | IGFBP6 | 653 | 0.032 | 1 | 1120 | 0.061 | 1.89 |
| 92 | GFAP | 28 | 0.001 | 1 | 48 | 0.003 | 1.89 |
| 93 | PRDM14 | 28 | 0.001 | 1 | 48 | 0.003 | 1.89 |
| 94 | CAMKK1 | 31 | 0.002 | 1 | 53 | 0.003 | 1.88 |
| 95 | STAT2 | 344 | 0.017 | 1 | 586 | 0.032 | 1.88 |
| 96 | DCK | 10 | 0.000 | 1 | 17 | 0.001 | 1.87 |
| 97 | DNAJC4 | 76 | 0.004 | 1 | 129 | 0.007 | 1.87 |
| 98 | PDCD1 | 29 | 0.001 | 1 | 49 | 0.003 | 1.86 |
| 99 | ACADS | 57 | 0.003 | 1 | 96 | 0.005 | 1.86 |
| 100 | CLIC3 | 119 | 0.006 | 1 | 199 | 0.011 | 1.84 |
| 101 | ARNT2 | 9 | 0.000 | 1 | 15 | 0.001 | 1.84 |
| 102 | FGF22 | 18 | 0.001 | 1 | 30 | 0.002 | 1.84 |
| 103 | PDZK1 | 53 | 0.003 | 1 | 88 | 0.005 | 1.83 |
| 104 | ZBTB16 | 449 | 0.022 | 1 | 745 | 0.041 | 1.83 |
| 105 | IDH2 | 315 | 0.016 | 1 | 522 | 0.028 | 1.83 |
| 106 | RPS6KB1 | 20 | 0.001 | 1 | 33 | 0.002 | 1.82 |
| 107 | SMAD7 | 134 | 0.007 | 1 | 221 | 0.012 | 1.82 |
| 108 | IL2RB | 37 | 0.002 | 1 | 61 | 0.003 | 1.82 |
| 109 | NUDT13 | 17 | 0.001 | 1 | 28 | 0.002 | 1.82 |
| 110 | SLCO2B1 | 17 | 0.001 | 1 | 28 | 0.002 | 1.82 |
| 111 | MAP3K1 | 198 | 0.010 | 1 | 326 | 0.018 | 1.82 |
| 112 | CALML5 | 39 | 0.002 | 1 | 64 | 0.003 | 1.81 |
| 113 | NRP1 | 204 | 0.010 | 1 | 334 | 0.018 | 1.80 |
| 114 | HSPA6 | 11 | 0.001 | 1 | 18 | 0.001 | 1.80 |
| 115 | DNAJB2 | 63 | 0.003 | 1 | 103 | 0.006 | 1.80 |
| 116 | TGFB1 | 49 | 0.002 | 1 | 80 | 0.004 | 1.80 |

| | | | | | | | |
|---|---|---|---|---|---|---|---|
| 117 | GZMH | 27 | 0.001 | 1 | 44 | 0.002 | 1.80 |
| 118 | RUNX3 | 27 | 0.001 | 1 | 44 | 0.002 | 1.80 |
| 119 | DMC1 | 8 | 0.000 | 1 | 13 | 0.001 | 1.79 |
| 120 | TIMP2 | 842 | 0.042 | 1 | 1368 | 0.074 | 1.79 |
| 121 | EYA1 | 34 | 0.002 | 1 | 55 | 0.003 | 1.78 |
| 122 | CTSD | 3612 | 0.178 | 1 | 5810 | 0.316 | 1.77 |
| 123 | CIDEA | 33 | 0.002 | 1 | 53 | 0.003 | 1.77 |
| 124 | BCL2L1 | 930 | 0.046 | 1 | 1489 | 0.081 | 1.76 |
| 125 | CREB5 | 25 | 0.001 | 1 | 40 | 0.002 | 1.76 |
| 126 | RAMP1 | 157 | 0.008 | 1 | 250 | 0.014 | 1.76 |
| 127 | NKX2_1 | 22 | 0.001 | 1 | 35 | 0.002 | 1.75 |
| 128 | AKR1C3 | 1864 | 0.092 | 1 | 2949 | 0.160 | 1.74 |
| 129 | ATP6V1G2 | 45 | 0.002 | 1 | 71 | 0.004 | 1.74 |
| 130 | TRADD | 158 | 0.008 | 1 | 249 | 0.014 | 1.74 |
| 131 | TMEFF1 | 14 | 0.001 | 1 | 22 | 0.001 | 1.73 |
| 132 | UTF1 | 14 | 0.001 | 1 | 22 | 0.001 | 1.73 |
| 133 | PPP2R1B | 44 | 0.002 | 1 | 69 | 0.004 | 1.73 |
| 134 | THBS1 | 12509 | 0.618 | 1 | 19505 | 1.061 | 1.72 |
| 135 | CYP2U1 | 104 | 0.005 | 1 | 162 | 0.009 | 1.72 |
| 136 | CNPY4 | 38 | 0.002 | 1 | 59 | 0.003 | 1.71 |
| 137 | MLPH | 154 | 0.008 | 1 | 239 | 0.013 | 1.71 |
| 138 | EFNA5 | 956 | 0.047 | 1 | 1483 | 0.081 | 1.71 |
| 139 | DNAJC22 | 60 | 0.003 | 1 | 93 | 0.005 | 1.71 |
| 140 | ID1 | 2794 | 0.138 | 1 | 4329 | 0.236 | 1.71 |
| 141 | PLAT | 473 | 0.023 | 1 | 732 | 0.040 | 1.71 |
| 142 | AHNAK2 | 145 | 0.007 | 1 | 224 | 0.012 | 1.70 |
| 143 | SPINK1 | 13 | 0.001 | 1 | 20 | 0.001 | 1.70 |
| 144 | FGFR1 | 160 | 0.008 | 1 | 246 | 0.013 | 1.69 |
| 145 | NOL3 | 54 | 0.003 | 1 | 83 | 0.005 | 1.69 |
| 146 | SQSTM1 | 3038 | 0.150 | 1 | 4652 | 0.253 | 1.69 |
| 147 | CLCF1 | 121 | 0.006 | 1 | 185 | 0.010 | 1.69 |
| 148 | COL1A2 | 19 | 0.001 | 1 | 29 | 0.002 | 1.68 |
| 149 | NCOA1 | 78 | 0.004 | 1 | 119 | 0.006 | 1.68 |
| 150 | CCL24 | 21 | 0.001 | 1 | 32 | 0.002 | 1.68 |
| 151 | HNF1B | 23 | 0.001 | 1 | 35 | 0.002 | 1.68 |
| 152 | MAGED1 | 493 | 0.024 | 1 | 745 | 0.041 | 1.67 |
| 153 | DAAM1 | 96 | 0.005 | 1 | 145 | 0.008 | 1.67 |
| 154 | NGFRAP1 | 49 | 0.002 | 1 | 74 | 0.004 | 1.66 |
| 155 | ZEB2 | 106 | 0.005 | 1 | 160 | 0.009 | 1.66 |
| 156 | APH1B | 95 | 0.005 | 1 | 143 | 0.008 | 1.66 |
| 157 | ID3 | 320 | 0.016 | 1 | 481 | 0.026 | 1.66 |
| 158 | LOX | 348 | 0.017 | 1 | 523 | 0.028 | 1.66 |
| 159 | CKMT2 | 40 | 0.002 | 1 | 60 | 0.003 | 1.65 |
| 160 | KLF12 | 70 | 0.003 | 1 | 105 | 0.006 | 1.65 |
| 161 | CCDC103 | 48 | 0.002 | 1 | 72 | 0.004 | 1.65 |
| 162 | FTH1 | 180468 | 8.909 | 1 | 270144 | 14.702 | 1.65 |
| 163 | ITGB2 | 168 | 0.008 | 1 | 251 | 0.014 | 1.65 |
| 164 | FAS | 61 | 0.003 | 1 | 91 | 0.005 | 1.64 |
| 165 | GLI2 | 31 | 0.002 | 1 | 46 | 0.003 | 1.64 |
| 166 | HECTD4 | 54 | 0.003 | 1 | 80 | 0.004 | 1.63 |
| 167 | DHH | 23 | 0.001 | 1 | 34 | 0.002 | 1.63 |
| 168 | FRS3 | 38 | 0.002 | 1 | 56 | 0.003 | 1.62 |
| 169 | IFNB1 | 17 | 0.001 | 1 | 25 | 0.001 | 1.62 |
| 170 | ADORA2A | 15 | 0.001 | 1 | 22 | 0.001 | 1.62 |
| 171 | PLG | 54 | 0.003 | 1 | 79 | 0.004 | 1.61 |
| 172 | COL11A1 | 26 | 0.001 | 1 | 38 | 0.002 | 1.61 |
| 173 | CD5 | 22 | 0.001 | 1 | 32 | 0.002 | 1.60 |
| 174 | FLJ10474 | 275 | 0.014 | 1 | 400 | 0.022 | 1.60 |
| 175 | PDGFC | 416 | 0.021 | 1 | 605 | 0.033 | 1.60 |
| 176 | CYP1B1 | 436 | 0.022 | 1 | 634 | 0.035 | 1.60 |
| 177 | TMEM45B | 20 | 0.001 | 1 | 29 | 0.002 | 1.60 |
| 178 | NUMBL | 55 | 0.003 | 1 | 79 | 0.004 | 1.58 |

| | | | | | | | |
|---|---|---|---|---|---|---|---|
| 179 | PIK3R1 | 786 | 0.039 | 1 | 1128 | 0.061 | 1.58 |
| 180 | CYCS | 23 | 0.001 | 1 | 33 | 0.002 | 1.58 |
| 181 | SLC10A1 | 26 | 0.001 | 1 | 37 | 0.002 | 1.57 |
| 182 | HSPB8 | 19 | 0.001 | 1 | 27 | 0.001 | 1.57 |
| 183 | PPP3R2 | 19 | 0.001 | 1 | 27 | 0.001 | 1.57 |
| 184 | TNFRSF1B | 38 | 0.002 | 1 | 54 | 0.003 | 1.57 |
| 185 | FGFRL1 | 278 | 0.014 | 1 | 395 | 0.021 | 1.57 |
| 186 | TMEM74B | 50 | 0.002 | 1 | 71 | 0.004 | 1.57 |
| 187 | HAVCR2 | 43 | 0.002 | 1 | 61 | 0.003 | 1.56 |
| 188 | TLR4 | 86 | 0.004 | 1 | 122 | 0.007 | 1.56 |
| 189 | CACNB4 | 12 | 0.001 | 1 | 17 | 0.001 | 1.56 |
| 190 | PRKCA | 169 | 0.008 | 1 | 239 | 0.013 | 1.56 |
| 191 | LIN28B | 29 | 0.001 | 1 | 41 | 0.002 | 1.56 |
| 192 | SPP1 | 29 | 0.001 | 1 | 41 | 0.002 | 1.56 |
| 193 | IL2RG | 49 | 0.002 | 1 | 69 | 0.004 | 1.55 |
| 194 | PCOLCE | 27 | 0.001 | 1 | 38 | 0.002 | 1.55 |
| 195 | MEF2C | 32 | 0.002 | 1 | 45 | 0.002 | 1.55 |
| 196 | EGR3 | 62 | 0.003 | 1 | 87 | 0.005 | 1.55 |
| 197 | CD3D | 40 | 0.002 | 1 | 56 | 0.003 | 1.54 |
| 198 | CCS | 183 | 0.009 | 1 | 255 | 0.014 | 1.54 |
| 199 | CCL18 | 41 | 0.002 | 1 | 57 | 0.003 | 1.53 |
| 200 | GAMT | 124 | 0.006 | 1 | 171 | 0.009 | 1.52 |
| 201 | PLK2 | 1449 | 0.072 | 1 | 1997 | 0.109 | 1.52 |
| 202 | LYN | 43 | 0.002 | 1 | 59 | 0.003 | 1.51 |
| 203 | MEIS1 | 43 | 0.002 | 1 | 59 | 0.003 | 1.51 |
| 204 | RPTOR | 43 | 0.002 | 1 | 59 | 0.003 | 1.51 |
| 205 | AQP4 | 35 | 0.002 | 1 | 48 | 0.003 | 1.51 |
| 206 | S100B | 35 | 0.002 | 1 | 48 | 0.003 | 1.51 |
| 207 | NR5A2 | 27 | 0.001 | 1 | 37 | 0.002 | 1.51 |
| 208 | LATS2 | 73 | 0.004 | 1 | 100 | 0.005 | 1.51 |
| 209 | RHOU | 141 | 0.007 | 1 | 193 | 0.011 | 1.51 |
| 210 | INSR | 57 | 0.003 | 1 | 78 | 0.004 | 1.51 |
| 211 | GSR | 949 | 0.047 | 1 | 1297 | 0.071 | 1.51 |
| 212 | PDK2 | 123 | 0.006 | 1 | 168 | 0.009 | 1.51 |
| 213 | CDH13 | 733 | 0.036 | 1 | 1000 | 0.054 | 1.50 |
| 214 | NOTCH4 | 11 | 0.001 | 1 | 15 | 0.001 | 1.50 |
| 215 | MKNK1 | 22 | 0.001 | 1 | 30 | 0.002 | 1.50 |
| 216 | CCL26 | 44 | 0.002 | 1 | 60 | 0.003 | 1.50 |
| 217 | BMP8B | 39 | 0.002 | 1 | 53 | 0.003 | 1.50 |
| 218 | ITM2A | 39 | 0.002 | 1 | 53 | 0.003 | 1.50 |
| 219 | ID2 | 67 | 0.003 | 1 | 91 | 0.005 | 1.50 |
| 220 | WISP2 | 109 | 0.005 | 1 | 148 | 0.008 | 1.50 |
| 221 | SLC38A2 | 4109 | 0.203 | 1 | 5577 | 0.304 | 1.50 |
| 222 | SLC7A7 | 28 | 0.001 | 1 | 38 | 0.002 | 1.50 |
| 223 | SIRT2 | 198 | 0.010 | 1 | 268 | 0.015 | 1.49 |
| 224 | SULT1A1 | 34 | 0.002 | 1 | 46 | 0.003 | 1.49 |
| 225 | ACSL5 | 20 | 0.001 | 1 | 27 | 0.001 | 1.49 |
| 226 | HSPB2 | 23 | 0.001 | 1 | 31 | 0.002 | 1.49 |
| 227 | NRG1 | 116 | 0.006 | 1 | 156 | 0.008 | 1.48 |
| 228 | CTGF | 644 | 0.032 | 1 | 866 | 0.047 | 1.48 |
| 229 | CFTR | 38 | 0.002 | 1 | 51 | 0.003 | 1.48 |
| 230 | GRN | 503 | 0.025 | 1 | 675 | 0.037 | 1.48 |
| 231 | NFATC3 | 117 | 0.006 | 1 | 157 | 0.009 | 1.48 |
| 232 | SHC3 | 44 | 0.002 | 1 | 59 | 0.003 | 1.48 |
| 233 | FMO5 | 53 | 0.003 | 1 | 71 | 0.004 | 1.48 |
| 234 | SERPINE1 | 3651 | 0.180 | 1 | 4874 | 0.265 | 1.47 |
| 235 | IGF1 | 18 | 0.001 | 1 | 24 | 0.001 | 1.47 |
| 236 | ABCB5 | 36 | 0.002 | 1 | 48 | 0.003 | 1.47 |
| 237 | NR1H3 | 45 | 0.002 | 1 | 60 | 0.003 | 1.47 |
| 238 | CMTM1 | 12 | 0.001 | 1 | 16 | 0.001 | 1.47 |
| 239 | RAD52 | 21 | 0.001 | 1 | 28 | 0.002 | 1.47 |
| 240 | SLCO1A2 | 27 | 0.001 | 1 | 36 | 0.002 | 1.47 |

| | | | | | | | |
|---|---|---|---|---|---|---|---|
| 241 | ABCC11 | 43 | 0.002 | 1 | 57 | 0.003 | 1.46 |
| 242 | ZNF189 | 86 | 0.004 | 1 | 114 | 0.006 | 1.46 |
| 243 | VEGFA | 160 | 0.008 | 1 | 212 | 0.012 | 1.46 |
| 244 | CCL13 | 37 | 0.002 | 1 | 49 | 0.003 | 1.46 |
| 245 | SERPINC1 | 37 | 0.002 | 1 | 49 | 0.003 | 1.46 |
| 246 | NCOA2 | 145 | 0.007 | 1 | 192 | 0.010 | 1.46 |
| 247 | ACVR2A | 59 | 0.003 | 1 | 78 | 0.004 | 1.46 |
| 248 | GATA2 | 56 | 0.003 | 1 | 74 | 0.004 | 1.46 |
| 249 | KRT8 | 4165 | 0.206 | 1 | 5501 | 0.299 | 1.46 |
| 250 | CEBPE | 22 | 0.001 | 1 | 29 | 0.002 | 1.45 |
| 251 | HDAC2 | 44 | 0.002 | 1 | 58 | 0.003 | 1.45 |
| 252 | SF3A1 | 104 | 0.005 | 1 | 137 | 0.007 | 1.45 |
| 253 | CREBBP | 120 | 0.006 | 1 | 158 | 0.009 | 1.45 |
| 254 | SALL4 | 98 | 0.005 | 1 | 129 | 0.007 | 1.45 |
| 255 | CDH2 | 541 | 0.027 | 1 | 712 | 0.039 | 1.45 |
| 256 | PMS2 | 362 | 0.018 | 1 | 476 | 0.026 | 1.45 |
| 257 | DACH1 | 35 | 0.002 | 1 | 46 | 0.003 | 1.45 |
| 258 | F8 | 83 | 0.004 | 1 | 109 | 0.006 | 1.45 |
| 259 | MESP1 | 32 | 0.002 | 1 | 42 | 0.002 | 1.45 |
| 260 | IGFBP7 | 224 | 0.011 | 1 | 294 | 0.016 | 1.45 |
| 261 | OR10J3 | 71 | 0.004 | 1 | 93 | 0.005 | 1.44 |
| 262 | CTSH | 343 | 0.017 | 1 | 449 | 0.024 | 1.44 |
| 263 | NRP2 | 230 | 0.011 | 1 | 301 | 0.016 | 1.44 |
| 264 | BDNF | 244 | 0.012 | 1 | 319 | 0.017 | 1.44 |
| 265 | GATA4 | 36 | 0.002 | 1 | 47 | 0.003 | 1.44 |
| 266 | CCT6B | 56 | 0.003 | 1 | 73 | 0.004 | 1.44 |
| 267 | FGF2 | 478 | 0.024 | 1 | 620 | 0.034 | 1.43 |
| 268 | IRAK3 | 27 | 0.001 | 1 | 35 | 0.002 | 1.43 |
| 269 | FEN1 | 115 | 0.006 | 1 | 149 | 0.008 | 1.43 |
| 270 | HIF1A | 2835 | 0.140 | 1 | 3673 | 0.200 | 1.43 |
| 271 | C1orf86 | 85 | 0.004 | 1 | 110 | 0.006 | 1.43 |
| 272 | BTG1 | 177 | 0.009 | 1 | 229 | 0.012 | 1.43 |
| 273 | PRICKLE1 | 86 | 0.004 | 1 | 111 | 0.006 | 1.42 |
| 274 | NPM1 | 52 | 0.003 | 1 | 67 | 0.004 | 1.42 |
| 275 | MGST1 | 6186 | 0.305 | 1 | 7968 | 0.434 | 1.42 |
| 276 | ANPEP | 3038 | 0.150 | 1 | 3911 | 0.213 | 1.42 |
| 277 | LAT | 7 | 0.000 | 1 | 9 | 0.000 | 1.42 |
| 278 | DDB2 | 70 | 0.003 | 1 | 90 | 0.005 | 1.42 |
| 279 | LRRK2 | 116 | 0.006 | 1 | 149 | 0.008 | 1.42 |
| 280 | TIPARP | 991 | 0.049 | 1 | 1272 | 0.069 | 1.41 |
| 281 | SUFU | 46 | 0.002 | 1 | 59 | 0.003 | 1.41 |
| 282 | TFDP2 | 235 | 0.012 | 1 | 301 | 0.016 | 1.41 |
| 283 | MCM7 | 25 | 0.001 | 1 | 32 | 0.002 | 1.41 |
| 284 | DMD | 43 | 0.002 | 1 | 55 | 0.003 | 1.41 |
| 285 | MT1A | 18 | 0.001 | 1 | 23 | 0.001 | 1.41 |
| 286 | NRG3 | 18 | 0.001 | 1 | 23 | 0.001 | 1.41 |
| 287 | RUNX2 | 310 | 0.015 | 1 | 396 | 0.022 | 1.41 |
| 288 | MLF1 | 44 | 0.002 | 1 | 56 | 0.003 | 1.40 |
| 289 | SLC22A9 | 44 | 0.002 | 1 | 56 | 0.003 | 1.40 |
| 290 | SNAI2 | 228 | 0.011 | 1 | 290 | 0.016 | 1.40 |
| 291 | STK32A | 37 | 0.002 | 1 | 47 | 0.003 | 1.40 |
| 292 | GATA3 | 248 | 0.012 | 1 | 315 | 0.017 | 1.40 |
| 293 | HMOX1 | 89 | 0.004 | 1 | 113 | 0.006 | 1.40 |
| 294 | LETMD1 | 293 | 0.014 | 1 | 372 | 0.020 | 1.40 |
| 295 | FLNC | 79 | 0.004 | 1 | 100 | 0.005 | 1.40 |
| 296 | CHI3L1 | 121 | 0.006 | 1 | 153 | 0.008 | 1.39 |
| 297 | PRF1 | 38 | 0.002 | 1 | 48 | 0.003 | 1.39 |
| 298 | LRP2 | 42 | 0.002 | 1 | 53 | 0.003 | 1.39 |
| 299 | SLC10A2 | 65 | 0.003 | 1 | 82 | 0.004 | 1.39 |
| 300 | PF4 | 50 | 0.002 | 1 | 63 | 0.003 | 1.39 |
| 301 | HOXA11 | 27 | 0.001 | 1 | 34 | 0.002 | 1.39 |
| 302 | NTRK1 | 27 | 0.001 | 1 | 34 | 0.002 | 1.39 |

| 303 | LIN28A | 35 | 0.002 | 1 | 44 | 0.002 | 1.39 |
|---|---|---|---|---|---|---|---|
| 304 | ITGB8 | 494 | 0.024 | 1 | 620 | 0.034 | 1.38 |
| 305 | CD40LG | 59 | 0.003 | 1 | 74 | 0.004 | 1.38 |
| 306 | ENDOD1 | 244 | 0.012 | 1 | 306 | 0.017 | 1.38 |
| 307 | DLC1 | 185 | 0.009 | 1 | 232 | 0.013 | 1.38 |
| 308 | NOS2 | 4 | 0.000 | 1 | 5 | 0.000 | 1.38 |
| 309 | COL9A3 | 16 | 0.001 | 1 | 20 | 0.001 | 1.38 |
| 310 | TOLLIP | 20 | 0.001 | 1 | 25 | 0.001 | 1.38 |
| 311 | KLK2 | 36 | 0.002 | 1 | 45 | 0.002 | 1.38 |
| 312 | DES | 12 | 0.001 | 1 | 15 | 0.001 | 1.38 |
| 313 | NPPB | 28 | 0.001 | 1 | 35 | 0.002 | 1.38 |
| 314 | PRKACG | 28 | 0.001 | 1 | 35 | 0.002 | 1.38 |
| 315 | DNAJC12 | 57 | 0.003 | 1 | 71 | 0.004 | 1.37 |
| 316 | CDK5 | 322 | 0.016 | 1 | 401 | 0.022 | 1.37 |
| 317 | XCL2 | 49 | 0.002 | 1 | 61 | 0.003 | 1.37 |
| 318 | DNAJB12 | 239 | 0.012 | 1 | 297 | 0.016 | 1.37 |
| 319 | ACKR3 | 33 | 0.002 | 1 | 41 | 0.002 | 1.37 |
| 320 | PECAM1 | 58 | 0.003 | 1 | 72 | 0.004 | 1.37 |
| 321 | CAPNS1 | 1055 | 0.052 | 1 | 1309 | 0.071 | 1.37 |
| 322 | CCL7 | 25 | 0.001 | 1 | 31 | 0.002 | 1.37 |
| 323 | CDH3 | 50 | 0.002 | 1 | 62 | 0.003 | 1.37 |
| 324 | GHR | 63 | 0.003 | 1 | 78 | 0.004 | 1.36 |
| 325 | PARP3 | 21 | 0.001 | 1 | 26 | 0.001 | 1.36 |
| 326 | LY96 | 38 | 0.002 | 1 | 47 | 0.003 | 1.36 |
| 327 | NR0B1 | 17 | 0.001 | 1 | 21 | 0.001 | 1.36 |
| 328 | CYBA | 51 | 0.003 | 1 | 63 | 0.003 | 1.36 |
| 329 | SLC22A2 | 47 | 0.002 | 1 | 58 | 0.003 | 1.36 |
| 330 | PTGR1 | 270 | 0.013 | 1 | 333 | 0.018 | 1.36 |
| 331 | PPP2R2B | 52 | 0.003 | 1 | 64 | 0.003 | 1.36 |
| 332 | NEIL3 | 139 | 0.007 | 1 | 171 | 0.009 | 1.36 |
| 333 | ITGB4 | 2049 | 0.101 | 1 | 2518 | 0.137 | 1.35 |
| 334 | OSM | 44 | 0.002 | 1 | 54 | 0.003 | 1.35 |
| 335 | ATF1 | 194 | 0.010 | 1 | 238 | 0.013 | 1.35 |
| 336 | ETV1 | 75 | 0.004 | 1 | 92 | 0.005 | 1.35 |
| 337 | CPT1C | 40 | 0.002 | 1 | 49 | 0.003 | 1.35 |
| 338 | TRAF3 | 80 | 0.004 | 1 | 98 | 0.005 | 1.35 |
| 339 | ORM2 | 49 | 0.002 | 1 | 60 | 0.003 | 1.35 |
| 340 | PIK3R2 | 640 | 0.032 | 1 | 783 | 0.043 | 1.35 |
| 341 | DNAJB5 | 36 | 0.002 | 1 | 44 | 0.002 | 1.35 |
| 342 | RPA3 | 36 | 0.002 | 1 | 44 | 0.002 | 1.35 |
| 343 | CTSB | 494 | 0.024 | 1 | 603 | 0.033 | 1.35 |
| 344 | MCM4 | 23 | 0.001 | 1 | 28 | 0.002 | 1.34 |
| 345 | IRF2 | 92 | 0.005 | 1 | 112 | 0.006 | 1.34 |
| 346 | MAP2K6 | 37 | 0.002 | 1 | 45 | 0.002 | 1.34 |
| 347 | SIRT4 | 42 | 0.002 | 1 | 51 | 0.003 | 1.34 |
| 348 | UBE2Z | 257 | 0.013 | 1 | 312 | 0.017 | 1.34 |
| 349 | TWIST1 | 234 | 0.012 | 1 | 284 | 0.015 | 1.34 |
| 350 | IFIT2 | 61 | 0.003 | 1 | 74 | 0.004 | 1.34 |
| 351 | CYLD | 90 | 0.004 | 1 | 109 | 0.006 | 1.34 |
| 352 | LGALS3 | 488 | 0.024 | 1 | 591 | 0.032 | 1.34 |
| 353 | EPOR | 38 | 0.002 | 1 | 46 | 0.003 | 1.33 |
| 354 | PRMT6 | 48 | 0.002 | 1 | 58 | 0.003 | 1.33 |
| 355 | MAP3K8 | 87 | 0.004 | 1 | 105 | 0.006 | 1.33 |
| 356 | IL18 | 1042 | 0.051 | 1 | 1257 | 0.068 | 1.33 |
| 357 | PAG1 | 39 | 0.002 | 1 | 47 | 0.003 | 1.33 |
| 358 | TEP1 | 39 | 0.002 | 1 | 47 | 0.003 | 1.33 |
| 359 | CES2 | 205 | 0.010 | 1 | 247 | 0.013 | 1.33 |
| 360 | PAF1 | 183 | 0.009 | 1 | 220 | 0.012 | 1.33 |
| 361 | NFAT5 | 213 | 0.011 | 1 | 256 | 0.014 | 1.32 |
| 362 | EXT1 | 763 | 0.038 | 1 | 917 | 0.050 | 1.32 |
| 363 | GLUD1 | 774 | 0.038 | 1 | 930 | 0.051 | 1.32 |
| 364 | FRMD6 | 973 | 0.048 | 1 | 1168 | 0.064 | 1.32 |

| | | | | | | | |
|---|---|---|---|---|---|---|---|
| 365 | F2 | 5 | 0.000 | 1 | 6 | 0.000 | 1.32 |
| 366 | TEK | 5 | 0.000 | 1 | 6 | 0.000 | 1.32 |
| 367 | UGT2B7 | 20 | 0.001 | 1 | 24 | 0.001 | 1.32 |
| 368 | CAPN3 | 70 | 0.003 | 1 | 84 | 0.005 | 1.32 |
| 369 | CD63 | 6672 | 0.329 | 1 | 7991 | 0.435 | 1.32 |
| 370 | HHAT | 51 | 0.003 | 1 | 61 | 0.003 | 1.32 |
| 371 | WNT10A | 46 | 0.002 | 1 | 55 | 0.003 | 1.32 |
| 372 | DNAJB14 | 115 | 0.006 | 1 | 137 | 0.007 | 1.31 |
| 373 | TTF1 | 63 | 0.003 | 1 | 75 | 0.004 | 1.31 |
| 374 | CAPN5 | 116 | 0.006 | 1 | 138 | 0.008 | 1.31 |
| 375 | ERG | 27 | 0.001 | 1 | 32 | 0.002 | 1.31 |
| 376 | ERCC6 | 254 | 0.013 | 1 | 301 | 0.016 | 1.31 |
| 377 | FGF9 | 38 | 0.002 | 1 | 45 | 0.002 | 1.31 |
| 378 | SOCS5 | 478 | 0.024 | 1 | 566 | 0.031 | 1.31 |
| 379 | OTX2 | 49 | 0.002 | 1 | 58 | 0.003 | 1.30 |
| 380 | COL4A5 | 60 | 0.003 | 1 | 71 | 0.004 | 1.30 |
| 381 | MAP3K5 | 224 | 0.011 | 1 | 265 | 0.014 | 1.30 |
| 382 | CKB | 44 | 0.002 | 1 | 52 | 0.003 | 1.30 |
| 383 | C1QA | 50 | 0.002 | 1 | 59 | 0.003 | 1.30 |
| 384 | TERF2IP | 179 | 0.009 | 1 | 211 | 0.011 | 1.30 |
| 385 | MAP1B | 247 | 0.012 | 1 | 291 | 0.016 | 1.30 |
| 386 | SH2B1 | 225 | 0.011 | 1 | 265 | 0.014 | 1.30 |
| 387 | SELM | 467 | 0.023 | 1 | 550 | 0.030 | 1.30 |
| 388 | NOG | 17 | 0.001 | 1 | 20 | 0.001 | 1.30 |
| 389 | FN1 | 31349 | 1.548 | 1 | 36875 | 2.007 | 1.30 |
| | | | | | | | |

**Down-regulated genes**

| | | **Vector** | Normalized | FC | WT | Normalized | FC |
|---|---|---|---|---|---|---|---|
| 1 | OLIG2 | 37 | 0.002 | 1 | 27 | 0.001 | 0.80 |
| 2 | SLC15A1 | 37 | 0.002 | 1 | 27 | 0.001 | 0.80 |
| 3 | SLC25A4 | 85 | 0.004 | 1 | 62 | 0.003 | 0.80 |
| 4 | NR1I2 | 48 | 0.002 | 1 | 35 | 0.002 | 0.80 |
| 5 | PRKG1 | 48 | 0.002 | 1 | 35 | 0.002 | 0.80 |
| 6 | RAD23B | 3379 | 0.167 | 1 | 2462 | 0.134 | 0.80 |
| 7 | RBX1 | 1001 | 0.049 | 1 | 729 | 0.040 | 0.80 |
| 8 | POLD3 | 187 | 0.009 | 1 | 136 | 0.007 | 0.80 |
| 9 | MIA | 11 | 0.001 | 1 | 8 | 0.000 | 0.80 |
| 10 | ERBB4 | 22 | 0.001 | 1 | 16 | 0.001 | 0.80 |
| 11 | GDF3 | 33 | 0.002 | 1 | 24 | 0.001 | 0.80 |
| 12 | PFKFB4 | 77 | 0.004 | 1 | 56 | 0.003 | 0.80 |
| 13 | DNAJC10 | 1052 | 0.052 | 1 | 765 | 0.042 | 0.80 |
| 14 | AIFM1 | 359 | 0.018 | 1 | 261 | 0.014 | 0.80 |
| 15 | RAD51B | 183 | 0.009 | 1 | 133 | 0.007 | 0.80 |
| 16 | RAB25 | 84 | 0.004 | 1 | 61 | 0.003 | 0.80 |
| 17 | IL12B | 51 | 0.003 | 1 | 37 | 0.002 | 0.80 |
| 18 | EMP1 | 3160 | 0.156 | 1 | 2291 | 0.125 | 0.80 |
| 19 | CASP4 | 457 | 0.023 | 1 | 331 | 0.018 | 0.80 |
| 20 | CX3CL1 | 29 | 0.001 | 1 | 21 | 0.001 | 0.80 |
| 21 | XRCC3 | 174 | 0.009 | 1 | 126 | 0.007 | 0.80 |
| 22 | WHSC1 | 756 | 0.037 | 1 | 547 | 0.030 | 0.80 |
| 23 | AICDA | 47 | 0.002 | 1 | 34 | 0.002 | 0.80 |
| 24 | FOXA2 | 47 | 0.002 | 1 | 34 | 0.002 | 0.80 |
| 25 | MPO | 36 | 0.002 | 1 | 26 | 0.001 | 0.80 |
| 26 | NCOA3 | 928 | 0.046 | 1 | 670 | 0.036 | 0.80 |
| 27 | BAMBI | 212 | 0.010 | 1 | 153 | 0.008 | 0.80 |
| 28 | LTA4H | 825 | 0.041 | 1 | 595 | 0.032 | 0.80 |
| 29 | COX5A | 1697 | 0.084 | 1 | 1223 | 0.067 | 0.79 |
| 30 | POU5F1 | 243 | 0.012 | 1 | 175 | 0.010 | 0.79 |
| 31 | IL20RB | 443 | 0.022 | 1 | 319 | 0.017 | 0.79 |
| 32 | FZD1 | 100 | 0.005 | 1 | 72 | 0.004 | 0.79 |
| 33 | CSNK1A1 | 2277 | 0.112 | 1 | 1639 | 0.089 | 0.79 |
| 34 | RAD17 | 339 | 0.017 | 1 | 244 | 0.013 | 0.79 |

| | | | | | | | |
|---|---|---|---|---|---|---|---|
| 35 | CDKL5 | 57 | 0.003 | 1 | 41 | 0.002 | 0.79 |
| 36 | SFRP2 | 57 | 0.003 | 1 | 41 | 0.002 | 0.79 |
| 37 | KNG1 | 32 | 0.002 | 1 | 23 | 0.001 | 0.79 |
| 38 | AIMP2 | 312 | 0.015 | 1 | 224 | 0.012 | 0.79 |
| 39 | HSPA8 | 19076 | 0.942 | 1 | 13686 | 0.745 | 0.79 |
| 40 | CRTC2 | 473 | 0.023 | 1 | 339 | 0.018 | 0.79 |
| 41 | BCR | 522 | 0.026 | 1 | 374 | 0.020 | 0.79 |
| 42 | SLC22A7 | 74 | 0.004 | 1 | 53 | 0.003 | 0.79 |
| 43 | EXOC3 | 155 | 0.008 | 1 | 111 | 0.006 | 0.79 |
| 44 | SMAD5 | 859 | 0.042 | 1 | 614 | 0.033 | 0.79 |
| 45 | TGFBR2 | 1537 | 0.076 | 1 | 1098 | 0.060 | 0.79 |
| 46 | IL12A | 35 | 0.002 | 1 | 25 | 0.001 | 0.79 |
| 47 | IL22RA1 | 42 | 0.002 | 1 | 30 | 0.002 | 0.79 |
| 48 | PIK3CG | 49 | 0.002 | 1 | 35 | 0.002 | 0.79 |
| 49 | POLD1 | 63 | 0.003 | 1 | 45 | 0.002 | 0.79 |
| 50 | ERCC8 | 289 | 0.014 | 1 | 206 | 0.011 | 0.79 |
| 51 | CDK2 | 452 | 0.022 | 1 | 322 | 0.018 | 0.79 |
| 52 | RBPMS2 | 66 | 0.003 | 1 | 47 | 0.003 | 0.79 |
| 53 | ABCB4 | 59 | 0.003 | 1 | 42 | 0.002 | 0.78 |
| 54 | DAPL1 | 45 | 0.002 | 1 | 32 | 0.002 | 0.78 |
| 55 | WNT1 | 45 | 0.002 | 1 | 32 | 0.002 | 0.78 |
| 56 | FLOT2 | 1306 | 0.064 | 1 | 928 | 0.051 | 0.78 |
| 57 | AFF1 | 228 | 0.011 | 1 | 162 | 0.009 | 0.78 |
| 58 | TP53 | 677 | 0.033 | 1 | 481 | 0.026 | 0.78 |
| 59 | ITGA5 | 556 | 0.027 | 1 | 395 | 0.021 | 0.78 |
| 60 | MIF | 4457 | 0.220 | 1 | 3165 | 0.172 | 0.78 |
| 61 | CARM1 | 959 | 0.047 | 1 | 681 | 0.037 | 0.78 |
| 62 | ACSL3 | 438 | 0.022 | 1 | 311 | 0.017 | 0.78 |
| 63 | FZD9 | 31 | 0.002 | 1 | 22 | 0.001 | 0.78 |
| 64 | SIN3B | 234 | 0.012 | 1 | 166 | 0.009 | 0.78 |
| 65 | NTF3 | 55 | 0.003 | 1 | 39 | 0.002 | 0.78 |
| 66 | HSPA12A | 48 | 0.002 | 1 | 34 | 0.002 | 0.78 |
| 67 | RASGRF1 | 48 | 0.002 | 1 | 34 | 0.002 | 0.78 |
| 68 | BNIP2 | 1265 | 0.062 | 1 | 896 | 0.049 | 0.78 |
| 69 | CXCL10 | 65 | 0.003 | 1 | 46 | 0.003 | 0.78 |
| 70 | RTN1 | 65 | 0.003 | 1 | 46 | 0.003 | 0.78 |
| 71 | TFPI2 | 65 | 0.003 | 1 | 46 | 0.003 | 0.78 |
| 72 | SMC4 | 328 | 0.016 | 1 | 232 | 0.013 | 0.78 |
| 73 | WNT6 | 58 | 0.003 | 1 | 41 | 0.002 | 0.78 |
| 74 | LIFR | 133 | 0.007 | 1 | 94 | 0.005 | 0.78 |
| 75 | MECOM | 92 | 0.005 | 1 | 65 | 0.004 | 0.78 |
| 76 | RHOA | 3524 | 0.174 | 1 | 2488 | 0.135 | 0.78 |
| 77 | HAND1 | 85 | 0.004 | 1 | 60 | 0.003 | 0.78 |
| 78 | CD74 | 102 | 0.005 | 1 | 72 | 0.004 | 0.78 |
| 79 | PML | 469 | 0.023 | 1 | 331 | 0.018 | 0.78 |
| 80 | KEAP1 | 122 | 0.006 | 1 | 86 | 0.005 | 0.78 |
| 81 | HMGB1 | 850 | 0.042 | 1 | 599 | 0.033 | 0.78 |
| 82 | NRIP1 | 816 | 0.040 | 1 | 575 | 0.031 | 0.78 |
| 83 | ACTR2 | 5221 | 0.258 | 1 | 3679 | 0.200 | 0.78 |
| 84 | IL33 | 71 | 0.004 | 1 | 50 | 0.003 | 0.78 |
| 85 | NRG2 | 27 | 0.001 | 1 | 19 | 0.001 | 0.78 |
| 86 | AP2B1 | 1088 | 0.054 | 1 | 765 | 0.042 | 0.78 |
| 87 | FZD3 | 138 | 0.007 | 1 | 97 | 0.005 | 0.77 |
| 88 | CES1 | 84 | 0.004 | 1 | 59 | 0.003 | 0.77 |
| 89 | DNAJC7 | 225 | 0.011 | 1 | 158 | 0.009 | 0.77 |
| 90 | DLK1 | 47 | 0.002 | 1 | 33 | 0.002 | 0.77 |
| 91 | ZIC1 | 47 | 0.002 | 1 | 33 | 0.002 | 0.77 |
| 92 | ZNF420 | 104 | 0.005 | 1 | 73 | 0.004 | 0.77 |
| 93 | PPARD | 181 | 0.009 | 1 | 127 | 0.007 | 0.77 |
| 94 | SPRY1 | 67 | 0.003 | 1 | 47 | 0.003 | 0.77 |
| 95 | IRF3 | 757 | 0.037 | 1 | 531 | 0.029 | 0.77 |
| 96 | MOB1B | 442 | 0.022 | 1 | 310 | 0.017 | 0.77 |

| | | | | | | | |
|---|---|---|---|---|---|---|---|
| 97 | ATG7 | 147 | 0.007 | 1 | 103 | 0.006 | 0.77 |
| 98 | BRIP1 | 197 | 0.010 | 1 | 138 | 0.008 | 0.77 |
| 99 | FUS | 1865 | 0.092 | 1 | 1306 | 0.071 | 0.77 |
| 100 | CTLA4 | 30 | 0.001 | 1 | 21 | 0.001 | 0.77 |
| 101 | LRP1B | 40 | 0.002 | 1 | 28 | 0.002 | 0.77 |
| 102 | RB1CC1 | 50 | 0.002 | 1 | 35 | 0.002 | 0.77 |
| 103 | PHB2 | 3448 | 0.170 | 1 | 2412 | 0.131 | 0.77 |
| 104 | RAD23A | 998 | 0.049 | 1 | 698 | 0.038 | 0.77 |
| 105 | BIRC5 | 156 | 0.008 | 1 | 109 | 0.006 | 0.77 |
| 106 | USMG5 | 3786 | 0.187 | 1 | 2643 | 0.144 | 0.77 |
| 107 | CCNF | 139 | 0.007 | 1 | 97 | 0.005 | 0.77 |
| 108 | CNTFR | 33 | 0.002 | 1 | 23 | 0.001 | 0.77 |
| 109 | CYP2C19 | 56 | 0.003 | 1 | 39 | 0.002 | 0.77 |
| 110 | PIAS3 | 658 | 0.032 | 1 | 458 | 0.025 | 0.77 |
| 111 | COL4A2 | 1036 | 0.051 | 1 | 721 | 0.039 | 0.77 |
| 112 | FES | 23 | 0.001 | 1 | 16 | 0.001 | 0.77 |
| 113 | SLC11A1 | 46 | 0.002 | 1 | 32 | 0.002 | 0.77 |
| 114 | PDGFRB | 59 | 0.003 | 1 | 41 | 0.002 | 0.77 |
| 115 | CMKLR1 | 36 | 0.002 | 1 | 25 | 0.001 | 0.77 |
| 116 | PHF6 | 436 | 0.022 | 1 | 302 | 0.016 | 0.76 |
| 117 | PRL | 52 | 0.003 | 1 | 36 | 0.002 | 0.76 |
| 118 | SCN3A | 52 | 0.003 | 1 | 36 | 0.002 | 0.76 |
| 119 | SEC61G | 1832 | 0.090 | 1 | 1268 | 0.069 | 0.76 |
| 120 | CAD | 341 | 0.017 | 1 | 236 | 0.013 | 0.76 |
| 121 | BAG4 | 201 | 0.010 | 1 | 139 | 0.008 | 0.76 |
| 122 | UBE2I | 1147 | 0.057 | 1 | 793 | 0.043 | 0.76 |
| 123 | BCAT1 | 68 | 0.003 | 1 | 47 | 0.003 | 0.76 |
| 124 | NUP62 | 680 | 0.034 | 1 | 470 | 0.026 | 0.76 |
| 125 | PIM2 | 97 | 0.005 | 1 | 67 | 0.004 | 0.76 |
| 126 | FASLG | 42 | 0.002 | 1 | 29 | 0.002 | 0.76 |
| 127 | CEBPB | 3662 | 0.181 | 1 | 2528 | 0.138 | 0.76 |
| 128 | CDK7 | 358 | 0.018 | 1 | 247 | 0.013 | 0.76 |
| 129 | NDC80 | 216 | 0.011 | 1 | 149 | 0.008 | 0.76 |
| 130 | AQP7 | 303 | 0.015 | 1 | 209 | 0.011 | 0.76 |
| 131 | C5AR1 | 58 | 0.003 | 1 | 40 | 0.002 | 0.76 |
| 132 | SRSF1 | 1184 | 0.058 | 1 | 815 | 0.044 | 0.76 |
| 133 | ADRA2B | 93 | 0.005 | 1 | 64 | 0.003 | 0.76 |
| 134 | DISP2 | 64 | 0.003 | 1 | 44 | 0.002 | 0.76 |
| 135 | PRKAR1B | 80 | 0.004 | 1 | 55 | 0.003 | 0.76 |
| 136 | NR1H4 | 48 | 0.002 | 1 | 33 | 0.002 | 0.76 |
| 137 | PIK3CA | 466 | 0.023 | 1 | 320 | 0.017 | 0.76 |
| 138 | GPI | 3807 | 0.188 | 1 | 2611 | 0.142 | 0.76 |
| 139 | SLCO2A1 | 108 | 0.005 | 1 | 74 | 0.004 | 0.76 |
| 140 | ATP5A1 | 6316 | 0.312 | 1 | 4327 | 0.235 | 0.76 |
| 141 | FOXRED1 | 200 | 0.010 | 1 | 137 | 0.007 | 0.76 |
| 142 | FBP1 | 19 | 0.001 | 1 | 13 | 0.001 | 0.75 |
| 143 | CACYBP | 133 | 0.007 | 1 | 91 | 0.005 | 0.75 |
| 144 | XAB2 | 550 | 0.027 | 1 | 376 | 0.020 | 0.75 |
| 145 | CCNT1 | 395 | 0.020 | 1 | 270 | 0.015 | 0.75 |
| 146 | IRAK1 | 771 | 0.038 | 1 | 527 | 0.029 | 0.75 |
| 147 | CD80 | 60 | 0.003 | 1 | 41 | 0.002 | 0.75 |
| 148 | DENND4A | 230 | 0.011 | 1 | 157 | 0.009 | 0.75 |
| 149 | EIF4E | 107 | 0.005 | 1 | 73 | 0.004 | 0.75 |
| 150 | ITPKB | 343 | 0.017 | 1 | 234 | 0.013 | 0.75 |
| 151 | PER1 | 686 | 0.034 | 1 | 468 | 0.025 | 0.75 |
| 152 | EN2 | 22 | 0.001 | 1 | 15 | 0.001 | 0.75 |
| 153 | CXCR6 | 66 | 0.003 | 1 | 45 | 0.002 | 0.75 |
| 154 | THEM4 | 198 | 0.010 | 1 | 135 | 0.007 | 0.75 |
| 155 | PSMD7 | 1049 | 0.052 | 1 | 715 | 0.039 | 0.75 |
| 156 | CASP8AP2 | 226 | 0.011 | 1 | 154 | 0.008 | 0.75 |
| 157 | PORCN | 47 | 0.002 | 1 | 32 | 0.002 | 0.75 |
| 158 | PPP2CB | 772 | 0.038 | 1 | 524 | 0.029 | 0.75 |

| | | | | | | | |
|---|---|---|---|---|---|---|---|
| 159 | DNAJA4 | 28 | 0.001 | 1 | 19 | 0.001 | 0.75 |
| 160 | TLR5 | 56 | 0.003 | 1 | 38 | 0.002 | 0.75 |
| 161 | DNAJB1 | 578 | 0.029 | 1 | 392 | 0.021 | 0.75 |
| 162 | VAPA | 2858 | 0.141 | 1 | 1938 | 0.105 | 0.75 |
| 163 | SOCS2 | 31 | 0.002 | 1 | 21 | 0.001 | 0.75 |
| 164 | POLD2 | 638 | 0.031 | 1 | 432 | 0.024 | 0.75 |
| 165 | MAOA | 65 | 0.003 | 1 | 44 | 0.002 | 0.75 |
| 166 | EI24 | 1742 | 0.086 | 1 | 1179 | 0.064 | 0.75 |
| 167 | ZNF552 | 68 | 0.003 | 1 | 46 | 0.003 | 0.75 |
| 168 | PRC1 | 241 | 0.012 | 1 | 163 | 0.009 | 0.75 |
| 169 | GYS2 | 37 | 0.002 | 1 | 25 | 0.001 | 0.74 |
| 170 | ALDOC | 151 | 0.007 | 1 | 102 | 0.006 | 0.74 |
| 171 | NFE2L2 | 40 | 0.002 | 1 | 27 | 0.001 | 0.74 |
| 172 | PAK1IP1 | 163 | 0.008 | 1 | 110 | 0.006 | 0.74 |
| 173 | MAGEB3 | 43 | 0.002 | 1 | 29 | 0.002 | 0.74 |
| 174 | STK3 | 162 | 0.008 | 1 | 109 | 0.006 | 0.74 |
| 175 | CNOT3 | 605 | 0.030 | 1 | 407 | 0.022 | 0.74 |
| 176 | RPS6KA6 | 55 | 0.003 | 1 | 37 | 0.002 | 0.74 |
| 177 | NPC1 | 116 | 0.006 | 1 | 78 | 0.004 | 0.74 |
| 178 | MAPK14 | 265 | 0.013 | 1 | 178 | 0.010 | 0.74 |
| 179 | FUBP1 | 2343 | 0.116 | 1 | 1573 | 0.086 | 0.74 |
| 180 | PAICS | 3065 | 0.151 | 1 | 2057 | 0.112 | 0.74 |
| 181 | LPCAT1 | 76 | 0.004 | 1 | 51 | 0.003 | 0.74 |
| 182 | HSP90B1 | 8492 | 0.419 | 1 | 5693 | 0.310 | 0.74 |
| 183 | APP | 5840 | 0.288 | 1 | 3912 | 0.213 | 0.74 |
| 184 | KIF14 | 118 | 0.006 | 1 | 79 | 0.004 | 0.74 |
| 185 | JUNB | 1520 | 0.075 | 1 | 1017 | 0.055 | 0.74 |
| 186 | MYCN | 18 | 0.001 | 1 | 12 | 0.001 | 0.73 |
| 187 | CX3CR1 | 33 | 0.002 | 1 | 22 | 0.001 | 0.73 |
| 188 | LRMP | 39 | 0.002 | 1 | 26 | 0.001 | 0.73 |
| 189 | PLA2G5 | 45 | 0.002 | 1 | 30 | 0.002 | 0.73 |
| 190 | MRE11A | 51 | 0.003 | 1 | 34 | 0.002 | 0.73 |
| 191 | DNAJB9 | 69 | 0.003 | 1 | 46 | 0.003 | 0.73 |
| 192 | IRF9 | 81 | 0.004 | 1 | 54 | 0.003 | 0.73 |
| 193 | FLRT3 | 144 | 0.007 | 1 | 96 | 0.005 | 0.73 |
| 194 | NCK2 | 156 | 0.008 | 1 | 104 | 0.006 | 0.73 |
| 195 | CD276 | 306 | 0.015 | 1 | 204 | 0.011 | 0.73 |
| 196 | PDIA4 | 462 | 0.023 | 1 | 308 | 0.017 | 0.73 |
| 197 | PAK7 | 3 | 0.000 | 1 | 2 | 0.000 | 0.73 |
| 198 | WWOX | 24 | 0.001 | 1 | 16 | 0.001 | 0.73 |
| 199 | KL | 27 | 0.001 | 1 | 18 | 0.001 | 0.73 |
| 200 | IL23A | 75 | 0.004 | 1 | 50 | 0.003 | 0.73 |
| 201 | SLIT2 | 174 | 0.009 | 1 | 116 | 0.006 | 0.73 |
| 202 | SNCA | 249 | 0.012 | 1 | 166 | 0.009 | 0.73 |
| 203 | HSPA9 | 1807 | 0.089 | 1 | 1204 | 0.066 | 0.73 |
| 204 | KRT18 | 8025 | 0.396 | 1 | 5344 | 0.291 | 0.73 |
| 205 | STAG2 | 670 | 0.033 | 1 | 446 | 0.024 | 0.73 |
| 206 | CHD1 | 603 | 0.030 | 1 | 401 | 0.022 | 0.73 |
| 207 | DNAJC11 | 337 | 0.017 | 1 | 224 | 0.012 | 0.73 |
| 208 | GPAM | 146 | 0.007 | 1 | 97 | 0.005 | 0.73 |
| 209 | SRSF2 | 2771 | 0.137 | 1 | 1839 | 0.100 | 0.73 |
| 210 | PHB | 1672 | 0.083 | 1 | 1109 | 0.060 | 0.73 |
| 211 | ATR | 487 | 0.024 | 1 | 323 | 0.018 | 0.73 |
| 212 | CCT7 | 2444 | 0.121 | 1 | 1620 | 0.088 | 0.73 |
| 213 | HJURP | 240 | 0.012 | 1 | 159 | 0.009 | 0.73 |
| 214 | SERPINF1 | 74 | 0.004 | 1 | 49 | 0.003 | 0.73 |
| 215 | PSMD2 | 876 | 0.043 | 1 | 580 | 0.032 | 0.73 |
| 216 | POLE2 | 133 | 0.007 | 1 | 88 | 0.005 | 0.73 |
| 217 | FAF1 | 443 | 0.022 | 1 | 293 | 0.016 | 0.73 |
| 218 | STAT5A | 56 | 0.003 | 1 | 37 | 0.002 | 0.73 |
| 219 | GPC4 | 53 | 0.003 | 1 | 35 | 0.002 | 0.73 |
| 220 | CALM1 | 471 | 0.023 | 1 | 311 | 0.017 | 0.73 |

| | | | | | | | |
|---|---|---|---|---|---|---|---|
| 221 | SERTAD1 | 250 | 0.012 | 1 | 165 | 0.009 | 0.73 |
| 222 | EAF2 | 91 | 0.004 | 1 | 60 | 0.003 | 0.73 |
| 223 | WWC1 | 91 | 0.004 | 1 | 60 | 0.003 | 0.73 |
| 224 | CLIC1 | 4551 | 0.225 | 1 | 3000 | 0.163 | 0.73 |
| 225 | MAPK10 | 88 | 0.004 | 1 | 58 | 0.003 | 0.73 |
| 226 | CRYAA | 82 | 0.004 | 1 | 54 | 0.003 | 0.73 |
| 227 | TAP1 | 158 | 0.008 | 1 | 104 | 0.006 | 0.73 |
| 228 | MAGEA1 | 38 | 0.002 | 1 | 25 | 0.001 | 0.73 |
| 229 | OPCML | 38 | 0.002 | 1 | 25 | 0.001 | 0.73 |
| 230 | TNKS2 | 225 | 0.011 | 1 | 148 | 0.008 | 0.73 |
| 231 | LTN1 | 594 | 0.029 | 1 | 390 | 0.021 | 0.72 |
| 232 | LPL | 32 | 0.002 | 1 | 21 | 0.001 | 0.72 |
| 233 | DNAJA3 | 850 | 0.042 | 1 | 557 | 0.030 | 0.72 |
| 234 | GRP | 58 | 0.003 | 1 | 38 | 0.002 | 0.72 |
| 235 | TNFSF8 | 84 | 0.004 | 1 | 55 | 0.003 | 0.72 |
| 236 | CCL23 | 55 | 0.003 | 1 | 36 | 0.002 | 0.72 |
| 237 | CXCL12 | 52 | 0.003 | 1 | 34 | 0.002 | 0.72 |
| 238 | SHC2 | 46 | 0.002 | 1 | 30 | 0.002 | 0.72 |
| 239 | CALML3 | 69 | 0.003 | 1 | 45 | 0.002 | 0.72 |
| 240 | GPSM2 | 634 | 0.031 | 1 | 413 | 0.022 | 0.72 |
| 241 | PTCH1 | 109 | 0.005 | 1 | 71 | 0.004 | 0.72 |
| 242 | BCL2L2 | 478 | 0.024 | 1 | 311 | 0.017 | 0.72 |
| 243 | MAFF | 552 | 0.027 | 1 | 359 | 0.020 | 0.72 |
| 244 | CCNH | 40 | 0.002 | 1 | 26 | 0.001 | 0.72 |
| 245 | EGF | 60 | 0.003 | 1 | 39 | 0.002 | 0.72 |
| 246 | MSI1 | 120 | 0.006 | 1 | 78 | 0.004 | 0.72 |
| 247 | CXCL16 | 180 | 0.009 | 1 | 117 | 0.006 | 0.72 |
| 248 | MYCL | 37 | 0.002 | 1 | 24 | 0.001 | 0.72 |
| 249 | TNXB | 74 | 0.004 | 1 | 48 | 0.003 | 0.72 |
| 250 | CIDEB | 54 | 0.003 | 1 | 35 | 0.002 | 0.71 |
| 251 | SORT1 | 695 | 0.034 | 1 | 450 | 0.024 | 0.71 |
| 252 | RPS4X | 3881 | 0.192 | 1 | 2511 | 0.137 | 0.71 |
| 253 | ADM | 1281 | 0.063 | 1 | 828 | 0.045 | 0.71 |
| 254 | E2F1 | 82 | 0.004 | 1 | 53 | 0.003 | 0.71 |
| 255 | ATP6V0C | 814 | 0.040 | 1 | 526 | 0.029 | 0.71 |
| 256 | HMGB2 | 1119 | 0.055 | 1 | 723 | 0.039 | 0.71 |
| 257 | SYNCRIP | 1355 | 0.067 | 1 | 875 | 0.048 | 0.71 |
| 258 | CRYAB | 79 | 0.004 | 1 | 51 | 0.003 | 0.71 |
| 259 | ATG3 | 976 | 0.048 | 1 | 630 | 0.034 | 0.71 |
| 260 | AXIN1 | 138 | 0.007 | 1 | 89 | 0.005 | 0.71 |
| 261 | ADIPOR1 | 2580 | 0.127 | 1 | 1663 | 0.091 | 0.71 |
| 262 | TP53BP2 | 244 | 0.012 | 1 | 157 | 0.009 | 0.71 |
| 263 | SEC22C | 157 | 0.008 | 1 | 101 | 0.005 | 0.71 |
| 264 | PDGFRA | 56 | 0.003 | 1 | 36 | 0.002 | 0.71 |
| 265 | NOD2 | 42 | 0.002 | 1 | 27 | 0.001 | 0.71 |
| 266 | SRM | 1150 | 0.057 | 1 | 739 | 0.040 | 0.71 |
| 267 | MAP3K4 | 494 | 0.024 | 1 | 317 | 0.017 | 0.71 |
| 268 | KRAS | 533 | 0.026 | 1 | 342 | 0.019 | 0.71 |
| 269 | PYCARD | 92 | 0.005 | 1 | 59 | 0.003 | 0.71 |
| 270 | ASPM | 1201 | 0.059 | 1 | 769 | 0.042 | 0.71 |
| 271 | CSF2 | 25 | 0.001 | 1 | 16 | 0.001 | 0.71 |
| 272 | GJA1 | 75 | 0.004 | 1 | 48 | 0.003 | 0.71 |
| 273 | SMC3 | 789 | 0.039 | 1 | 504 | 0.027 | 0.70 |
| 274 | CCL21 | 83 | 0.004 | 1 | 53 | 0.003 | 0.70 |
| 275 | CBX5 | 1687 | 0.083 | 1 | 1077 | 0.059 | 0.70 |
| 276 | FGF3 | 47 | 0.002 | 1 | 30 | 0.002 | 0.70 |
| 277 | GTF2H3 | 290 | 0.014 | 1 | 185 | 0.010 | 0.70 |
| 278 | HSPA4 | 2941 | 0.145 | 1 | 1875 | 0.102 | 0.70 |
| 279 | GSK3B | 1354 | 0.067 | 1 | 863 | 0.047 | 0.70 |
| 280 | SACS | 583 | 0.029 | 1 | 371 | 0.020 | 0.70 |
| 281 | RIPK1 | 225 | 0.011 | 1 | 143 | 0.008 | 0.70 |
| 282 | XRCC1 | 85 | 0.004 | 1 | 54 | 0.003 | 0.70 |

| | | | | | | | |
|---|---|---|---|---|---|---|---|
| 283 | RASD1 | 52 | 0.003 | 1 | 33 | 0.002 | 0.70 |
| 284 | FBXW11 | 1088 | 0.054 | 1 | 689 | 0.037 | 0.70 |
| 285 | CXCL6 | 79 | 0.004 | 1 | 50 | 0.003 | 0.70 |
| 286 | FANCE | 117 | 0.006 | 1 | 74 | 0.004 | 0.70 |
| 287 | TNFRSF10A | 185 | 0.009 | 1 | 117 | 0.006 | 0.70 |
| 288 | ZHX2 | 141 | 0.007 | 1 | 89 | 0.005 | 0.70 |
| 289 | FZD5 | 65 | 0.003 | 1 | 41 | 0.002 | 0.70 |
| 290 | PARP2 | 241 | 0.012 | 1 | 152 | 0.008 | 0.70 |
| 291 | ETV5 | 268 | 0.013 | 1 | 169 | 0.009 | 0.70 |
| 292 | NOLC1 | 522 | 0.026 | 1 | 329 | 0.018 | 0.69 |
| 293 | DKC1 | 868 | 0.043 | 1 | 547 | 0.030 | 0.69 |
| 294 | MTMR2 | 762 | 0.038 | 1 | 480 | 0.026 | 0.69 |
| 295 | CUL2 | 578 | 0.029 | 1 | 364 | 0.020 | 0.69 |
| 296 | NOD1 | 54 | 0.003 | 1 | 34 | 0.002 | 0.69 |
| 297 | IRAK2 | 97 | 0.005 | 1 | 61 | 0.003 | 0.69 |
| 298 | EIF5B | 288 | 0.014 | 1 | 181 | 0.010 | 0.69 |
| 299 | FOXP1 | 304 | 0.015 | 1 | 191 | 0.010 | 0.69 |
| 300 | FLRT2 | 191 | 0.009 | 1 | 120 | 0.007 | 0.69 |
| 301 | DUSP5 | 320 | 0.016 | 1 | 201 | 0.011 | 0.69 |
| 302 | PPP2R4 | 486 | 0.024 | 1 | 305 | 0.017 | 0.69 |
| 303 | ATP7B | 51 | 0.003 | 1 | 32 | 0.002 | 0.69 |
| 304 | FGF14 | 51 | 0.003 | 1 | 32 | 0.002 | 0.69 |
| 305 | CAV2 | 2812 | 0.139 | 1 | 1764 | 0.096 | 0.69 |
| 306 | TOP3A | 142 | 0.007 | 1 | 89 | 0.005 | 0.69 |
| 307 | S100A2 | 163 | 0.008 | 1 | 102 | 0.006 | 0.69 |
| 308 | CD55 | 1228 | 0.061 | 1 | 768 | 0.042 | 0.69 |
| 309 | MAG | 8 | 0.000 | 1 | 5 | 0.000 | 0.69 |
| 310 | CAMKK2 | 72 | 0.004 | 1 | 45 | 0.002 | 0.69 |
| 311 | RELB | 56 | 0.003 | 1 | 35 | 0.002 | 0.69 |
| 312 | JUN | 671 | 0.033 | 1 | 419 | 0.023 | 0.69 |
| 313 | SERPINH1 | 1864 | 0.092 | 1 | 1163 | 0.063 | 0.69 |
| 314 | CHEK2 | 170 | 0.008 | 1 | 106 | 0.006 | 0.69 |
| 315 | TNFRSF10B | 1561 | 0.077 | 1 | 973 | 0.053 | 0.69 |
| 316 | RPL13 | 138 | 0.007 | 1 | 86 | 0.005 | 0.69 |
| 317 | PRKAG3 | 53 | 0.003 | 1 | 33 | 0.002 | 0.69 |
| 318 | CD209 | 151 | 0.007 | 1 | 94 | 0.005 | 0.69 |
| 319 | CRLF2 | 45 | 0.002 | 1 | 28 | 0.002 | 0.69 |
| 320 | CCL19 | 37 | 0.002 | 1 | 23 | 0.001 | 0.69 |
| 321 | NUF2 | 459 | 0.023 | 1 | 285 | 0.016 | 0.68 |
| 322 | PLA2G4C | 58 | 0.003 | 1 | 36 | 0.002 | 0.68 |
| 323 | PIM3 | 303 | 0.015 | 1 | 188 | 0.010 | 0.68 |
| 324 | ECT2 | 740 | 0.037 | 1 | 459 | 0.025 | 0.68 |
| 325 | GYS1 | 158 | 0.008 | 1 | 98 | 0.005 | 0.68 |
| 326 | DNAJB11 | 752 | 0.037 | 1 | 466 | 0.025 | 0.68 |
| 327 | NUPR1 | 744 | 0.037 | 1 | 461 | 0.025 | 0.68 |
| 328 | HSPD1 | 6857 | 0.339 | 1 | 4248 | 0.231 | 0.68 |
| 329 | KRT13 | 76 | 0.004 | 1 | 47 | 0.003 | 0.68 |
| 330 | AK3 | 186 | 0.009 | 1 | 115 | 0.006 | 0.68 |
| 331 | CENPF | 1733 | 0.086 | 1 | 1071 | 0.058 | 0.68 |
| 332 | ADIPOR2 | 709 | 0.035 | 1 | 438 | 0.024 | 0.68 |
| 333 | FGF1 | 34 | 0.002 | 1 | 21 | 0.001 | 0.68 |
| 334 | SLC16A1 | 1543 | 0.076 | 1 | 953 | 0.052 | 0.68 |
| 335 | FZD10 | 47 | 0.002 | 1 | 29 | 0.002 | 0.68 |
| 336 | PRKAA1 | 394 | 0.019 | 1 | 243 | 0.013 | 0.68 |
| 337 | BAK1 | 621 | 0.031 | 1 | 383 | 0.021 | 0.68 |
| 338 | NME1 | 1803 | 0.089 | 1 | 1111 | 0.060 | 0.68 |
| 339 | HRAS | 614 | 0.030 | 1 | 378 | 0.021 | 0.68 |
| 340 | BMP1 | 554 | 0.027 | 1 | 341 | 0.019 | 0.68 |
| 341 | RASSF1 | 26 | 0.001 | 1 | 16 | 0.001 | 0.68 |
| 342 | HSPB3 | 39 | 0.002 | 1 | 24 | 0.001 | 0.68 |
| 343 | PALM2_AKAP2 | 65 | 0.003 | 1 | 40 | 0.002 | 0.68 |
| 344 | GNG4 | 122 | 0.006 | 1 | 75 | 0.004 | 0.68 |

| | | | | | | | |
|---|---|---|---|---|---|---|---|
| 345 | CRY1 | 96 | 0.005 | 1 | 59 | 0.003 | 0.68 |
| 346 | RUNDC1 | 272 | 0.013 | 1 | 167 | 0.009 | 0.68 |
| 347 | ACKR4 | 44 | 0.002 | 1 | 27 | 0.001 | 0.68 |
| 348 | DNAJC5G | 44 | 0.002 | 1 | 27 | 0.001 | 0.68 |
| 349 | YWHAZ | 15370 | 0.759 | 1 | 9414 | 0.512 | 0.68 |
| 350 | EVL | 420 | 0.021 | 1 | 257 | 0.014 | 0.67 |
| 351 | XIAP | 170 | 0.008 | 1 | 104 | 0.006 | 0.67 |
| 352 | BTG3 | 703 | 0.035 | 1 | 430 | 0.023 | 0.67 |
| 353 | MAPKAPK5 | 36 | 0.002 | 1 | 22 | 0.001 | 0.67 |
| 354 | FGF7 | 77 | 0.004 | 1 | 47 | 0.003 | 0.67 |
| 355 | SPC25 | 136 | 0.007 | 1 | 83 | 0.005 | 0.67 |
| 356 | TXNL4B | 141 | 0.007 | 1 | 86 | 0.005 | 0.67 |
| 357 | BCL2L10 | 123 | 0.006 | 1 | 75 | 0.004 | 0.67 |
| 358 | NCOR1 | 361 | 0.018 | 1 | 220 | 0.012 | 0.67 |
| 359 | ACKR2 | 64 | 0.003 | 1 | 39 | 0.002 | 0.67 |
| 360 | NFKB1 | 471 | 0.023 | 1 | 287 | 0.016 | 0.67 |
| 361 | GUCY1A3 | 69 | 0.003 | 1 | 42 | 0.002 | 0.67 |
| 362 | C17orf53 | 194 | 0.010 | 1 | 118 | 0.006 | 0.67 |
| 363 | SHC4 | 74 | 0.004 | 1 | 45 | 0.002 | 0.67 |
| 364 | RIF1 | 630 | 0.031 | 1 | 383 | 0.021 | 0.67 |
| 365 | TMEM123 | 51 | 0.003 | 1 | 31 | 0.002 | 0.67 |
| 366 | ZFP42 | 51 | 0.003 | 1 | 31 | 0.002 | 0.67 |
| 367 | NEIL2 | 79 | 0.004 | 1 | 48 | 0.003 | 0.67 |
| 368 | MKI67 | 981 | 0.048 | 1 | 596 | 0.032 | 0.67 |
| 369 | GADD45A | 1908 | 0.094 | 1 | 1159 | 0.063 | 0.67 |
| 370 | FAM117B | 191 | 0.009 | 1 | 116 | 0.006 | 0.67 |
| 371 | BOD1 | 84 | 0.004 | 1 | 51 | 0.003 | 0.67 |
| 372 | DUSP8 | 117 | 0.006 | 1 | 71 | 0.004 | 0.67 |
| 373 | CBX3 | 4206 | 0.208 | 1 | 2551 | 0.139 | 0.67 |
| 374 | CPT1B | 269 | 0.013 | 1 | 163 | 0.009 | 0.67 |
| 375 | IDH1 | 2504 | 0.124 | 1 | 1516 | 0.083 | 0.67 |
| 376 | GSTP1 | 10353 | 0.511 | 1 | 6267 | 0.341 | 0.67 |
| 377 | CDC14A | 119 | 0.006 | 1 | 72 | 0.004 | 0.67 |
| 378 | KPNA2 | 2244 | 0.111 | 1 | 1357 | 0.074 | 0.67 |
| 379 | MAGEE1 | 43 | 0.002 | 1 | 26 | 0.001 | 0.67 |
| 380 | SMC1A | 1084 | 0.054 | 1 | 655 | 0.036 | 0.67 |
| 381 | JAG2 | 106 | 0.005 | 1 | 64 | 0.003 | 0.67 |
| 382 | HHEX | 121 | 0.006 | 1 | 73 | 0.004 | 0.67 |
| 383 | RRM2 | 1951 | 0.096 | 1 | 1177 | 0.064 | 0.67 |
| 384 | SNRPB | 2786 | 0.138 | 1 | 1680 | 0.091 | 0.66 |
| 385 | PRKAR2B | 73 | 0.004 | 1 | 44 | 0.002 | 0.66 |
| 386 | DNAJC17 | 479 | 0.024 | 1 | 288 | 0.016 | 0.66 |
| 387 | MBL2 | 15 | 0.001 | 1 | 9 | 0.000 | 0.66 |
| 388 | TERT | 35 | 0.002 | 1 | 21 | 0.001 | 0.66 |
| 389 | TNFSF15 | 40 | 0.002 | 1 | 24 | 0.001 | 0.66 |
| 390 | HSPH1 | 45 | 0.002 | 1 | 27 | 0.001 | 0.66 |
| 391 | ALDH4A1 | 50 | 0.002 | 1 | 30 | 0.002 | 0.66 |
| 392 | TNFSF13B | 60 | 0.003 | 1 | 36 | 0.002 | 0.66 |
| 393 | CCT2 | 1535 | 0.076 | 1 | 920 | 0.050 | 0.66 |
| 394 | USF2 | 112 | 0.006 | 1 | 67 | 0.004 | 0.66 |
| 395 | BID | 393 | 0.019 | 1 | 235 | 0.013 | 0.66 |
| 396 | SLC25A13 | 393 | 0.019 | 1 | 235 | 0.013 | 0.66 |
| 397 | CTPS1 | 455 | 0.022 | 1 | 272 | 0.015 | 0.66 |
| 398 | MCM6 | 595 | 0.029 | 1 | 355 | 0.019 | 0.66 |
| 399 | GNAQ | 585 | 0.029 | 1 | 349 | 0.019 | 0.66 |
| 400 | CTSS | 99 | 0.005 | 1 | 59 | 0.003 | 0.66 |
| 401 | TNKS | 47 | 0.002 | 1 | 28 | 0.002 | 0.66 |
| 402 | TAZ | 185 | 0.009 | 1 | 110 | 0.006 | 0.66 |
| 403 | PROK2 | 37 | 0.002 | 1 | 22 | 0.001 | 0.66 |
| 404 | ATP5G1 | 1383 | 0.068 | 1 | 822 | 0.045 | 0.66 |
| 405 | IHH | 32 | 0.002 | 1 | 19 | 0.001 | 0.65 |
| 406 | KDM5B | 987 | 0.049 | 1 | 586 | 0.032 | 0.65 |

| | | | | | | | |
|---|---|---|---|---|---|---|---|
| 407 | HK2 | 155 | 0.008 | 1 | 92 | 0.005 | 0.65 |
| 408 | GNL3 | 1813 | 0.090 | 1 | 1076 | 0.059 | 0.65 |
| 409 | PDGFA | 258 | 0.013 | 1 | 153 | 0.008 | 0.65 |
| 410 | RRM1 | 1153 | 0.057 | 1 | 683 | 0.037 | 0.65 |
| 411 | AKAP1 | 884 | 0.044 | 1 | 523 | 0.028 | 0.65 |
| 412 | AR | 44 | 0.002 | 1 | 26 | 0.001 | 0.65 |
| 413 | TLR7 | 44 | 0.002 | 1 | 26 | 0.001 | 0.65 |
| 414 | XRCC5 | 83 | 0.004 | 1 | 49 | 0.003 | 0.65 |
| 415 | RUNX1 | 432 | 0.021 | 1 | 255 | 0.014 | 0.65 |
| 416 | CASP9 | 39 | 0.002 | 1 | 23 | 0.001 | 0.65 |
| 417 | PCNA | 2358 | 0.116 | 1 | 1390 | 0.076 | 0.65 |
| 418 | FGF12 | 56 | 0.003 | 1 | 33 | 0.002 | 0.65 |
| 419 | RASA1 | 503 | 0.025 | 1 | 296 | 0.016 | 0.65 |
| 420 | HUS1 | 204 | 0.010 | 1 | 120 | 0.007 | 0.65 |
| 421 | CCR8 | 34 | 0.002 | 1 | 20 | 0.001 | 0.65 |
| 422 | VIPR1 | 34 | 0.002 | 1 | 20 | 0.001 | 0.65 |
| 423 | SLC7A9 | 68 | 0.003 | 1 | 40 | 0.002 | 0.65 |
| 424 | ARMC1 | 631 | 0.031 | 1 | 371 | 0.020 | 0.65 |
| 425 | MDC1 | 150 | 0.007 | 1 | 88 | 0.005 | 0.65 |
| 426 | TYMS | 1982 | 0.098 | 1 | 1162 | 0.063 | 0.65 |
| 427 | MYBL2 | 449 | 0.022 | 1 | 263 | 0.014 | 0.65 |
| 428 | FGF5 | 41 | 0.002 | 1 | 24 | 0.001 | 0.65 |
| 429 | COL5A1 | 82 | 0.004 | 1 | 48 | 0.003 | 0.65 |
| 430 | FEM1B | 598 | 0.030 | 1 | 350 | 0.019 | 0.65 |
| 431 | IL15 | 118 | 0.006 | 1 | 69 | 0.004 | 0.64 |
| 432 | CASP10 | 77 | 0.004 | 1 | 45 | 0.002 | 0.64 |
| 433 | MAP7D1 | 125 | 0.006 | 1 | 73 | 0.004 | 0.64 |
| 434 | DNAJC16 | 72 | 0.004 | 1 | 42 | 0.002 | 0.64 |
| 435 | BMP2 | 12 | 0.001 | 1 | 7 | 0.000 | 0.64 |
| 436 | LTB | 24 | 0.001 | 1 | 14 | 0.001 | 0.64 |
| 437 | MT1X | 1247 | 0.062 | 1 | 727 | 0.040 | 0.64 |
| 438 | AGER | 115 | 0.006 | 1 | 67 | 0.004 | 0.64 |
| 439 | TUBB3 | 184 | 0.009 | 1 | 107 | 0.006 | 0.64 |
| 440 | SLC19A3 | 43 | 0.002 | 1 | 25 | 0.001 | 0.64 |
| 441 | DHCR24 | 2919 | 0.144 | 1 | 1697 | 0.092 | 0.64 |
| 442 | ALPL | 93 | 0.005 | 1 | 54 | 0.003 | 0.64 |
| 443 | CELSR2 | 100 | 0.005 | 1 | 58 | 0.003 | 0.64 |
| 444 | PPP3CB | 383 | 0.019 | 1 | 222 | 0.012 | 0.64 |
| 445 | TPD52 | 1077 | 0.053 | 1 | 624 | 0.034 | 0.64 |
| 446 | SPHK1 | 95 | 0.005 | 1 | 55 | 0.003 | 0.64 |
| 447 | TMSB10 | 59206 | 2.923 | 1 | 34272 | 1.865 | 0.64 |
| 448 | GREM1 | 64 | 0.003 | 1 | 37 | 0.002 | 0.64 |
| 449 | SUV39H2 | 362 | 0.018 | 1 | 209 | 0.011 | 0.64 |
| 450 | NUMB | 291 | 0.014 | 1 | 168 | 0.009 | 0.64 |
| 451 | PLA2G4A | 279 | 0.014 | 1 | 161 | 0.009 | 0.64 |
| 452 | EOMES | 59 | 0.003 | 1 | 34 | 0.002 | 0.64 |
| 453 | HMGXB3 | 177 | 0.009 | 1 | 102 | 0.006 | 0.64 |
| 454 | TRIP13 | 750 | 0.037 | 1 | 432 | 0.024 | 0.63 |
| 455 | FRZB | 33 | 0.002 | 1 | 19 | 0.001 | 0.63 |
| 456 | BAG1 | 233 | 0.012 | 1 | 134 | 0.007 | 0.63 |
| 457 | ZNF589 | 127 | 0.006 | 1 | 73 | 0.004 | 0.63 |
| 458 | ITGAV | 674 | 0.033 | 1 | 387 | 0.021 | 0.63 |
| 459 | OLR1 | 54 | 0.003 | 1 | 31 | 0.002 | 0.63 |
| 460 | RIPK2 | 218 | 0.011 | 1 | 125 | 0.007 | 0.63 |
| 461 | SLC38A5 | 82 | 0.004 | 1 | 47 | 0.003 | 0.63 |
| 462 | KCNIP1 | 89 | 0.004 | 1 | 51 | 0.003 | 0.63 |
| 463 | PLEK2 | 124 | 0.006 | 1 | 71 | 0.004 | 0.63 |
| 464 | CCR10 | 49 | 0.002 | 1 | 28 | 0.002 | 0.63 |
| 465 | CDH5 | 56 | 0.003 | 1 | 32 | 0.002 | 0.63 |
| 466 | IL4 | 63 | 0.003 | 1 | 36 | 0.002 | 0.63 |
| 467 | CCNE1 | 189 | 0.009 | 1 | 108 | 0.006 | 0.63 |
| 468 | ALDH2 | 21 | 0.001 | 1 | 12 | 0.001 | 0.63 |

| | | | | | | | |
|---|---|---|---|---|---|---|---|
| 469 | MMP7 | 42 | 0.002 | 1 | 24 | 0.001 | 0.63 |
| 470 | TNNI3 | 42 | 0.002 | 1 | 24 | 0.001 | 0.63 |
| 471 | MOS | 84 | 0.004 | 1 | 48 | 0.003 | 0.63 |
| 472 | HSF2 | 175 | 0.009 | 1 | 100 | 0.005 | 0.63 |
| 473 | MELK | 562 | 0.028 | 1 | 321 | 0.017 | 0.63 |
| 474 | SORD | 810 | 0.040 | 1 | 462 | 0.025 | 0.63 |
| 475 | ANXA1 | 6621 | 0.327 | 1 | 3771 | 0.205 | 0.63 |
| 476 | PLCG2 | 58 | 0.003 | 1 | 33 | 0.002 | 0.63 |
| 477 | MAP3K3 | 109 | 0.005 | 1 | 62 | 0.003 | 0.63 |
| 478 | PTPN11 | 814 | 0.040 | 1 | 463 | 0.025 | 0.63 |
| 479 | DNAJC9 | 405 | 0.020 | 1 | 230 | 0.013 | 0.63 |
| 480 | TINF2 | 127 | 0.006 | 1 | 72 | 0.004 | 0.62 |
| 481 | SMS | 2142 | 0.106 | 1 | 1213 | 0.066 | 0.62 |
| 482 | E2F5 | 152 | 0.008 | 1 | 86 | 0.005 | 0.62 |
| 483 | VDAC1 | 8163 | 0.403 | 1 | 4618 | 0.251 | 0.62 |
| 484 | BUB1 | 1117 | 0.055 | 1 | 631 | 0.034 | 0.62 |
| 485 | TRAF6 | 232 | 0.011 | 1 | 131 | 0.007 | 0.62 |
| 486 | SUSD3 | 62 | 0.003 | 1 | 35 | 0.002 | 0.62 |
| 487 | CXCL5 | 39 | 0.002 | 1 | 22 | 0.001 | 0.62 |
| 488 | DUSP2 | 39 | 0.002 | 1 | 22 | 0.001 | 0.62 |
| 489 | SLC31A1 | 314 | 0.016 | 1 | 177 | 0.010 | 0.62 |
| 490 | TPX2 | 641 | 0.032 | 1 | 361 | 0.020 | 0.62 |
| 491 | CDCA7 | 112 | 0.006 | 1 | 63 | 0.003 | 0.62 |
| 492 | RAD51 | 217 | 0.011 | 1 | 122 | 0.007 | 0.62 |
| 493 | CKS2 | 2946 | 0.145 | 1 | 1655 | 0.090 | 0.62 |
| 494 | PLK1 | 1053 | 0.052 | 1 | 591 | 0.032 | 0.62 |
| 495 | GMPS | 1290 | 0.064 | 1 | 724 | 0.039 | 0.62 |
| 496 | CXCL14 | 98 | 0.005 | 1 | 55 | 0.003 | 0.62 |
| 497 | RUVBL1 | 1645 | 0.081 | 1 | 923 | 0.050 | 0.62 |
| 498 | PLK4 | 423 | 0.021 | 1 | 237 | 0.013 | 0.62 |
| 499 | YBX3 | 981 | 0.048 | 1 | 549 | 0.030 | 0.62 |
| 500 | MYC | 1496 | 0.074 | 1 | 837 | 0.046 | 0.62 |
| 501 | ERO1L | 717 | 0.035 | 1 | 401 | 0.022 | 0.62 |
| 502 | DBI | 6117 | 0.302 | 1 | 3421 | 0.186 | 0.62 |
| 503 | MAPK8 | 93 | 0.005 | 1 | 52 | 0.003 | 0.62 |
| 504 | CKS1B | 1720 | 0.085 | 1 | 960 | 0.052 | 0.62 |
| 505 | TLR8 | 52 | 0.003 | 1 | 29 | 0.002 | 0.61 |
| 506 | PDK1 | 296 | 0.015 | 1 | 165 | 0.009 | 0.61 |
| 507 | CD22 | 79 | 0.004 | 1 | 44 | 0.002 | 0.61 |
| 508 | SKP2 | 670 | 0.033 | 1 | 373 | 0.020 | 0.61 |
| 509 | MAP2K3 | 291 | 0.014 | 1 | 162 | 0.009 | 0.61 |
| 510 | NASP | 812 | 0.040 | 1 | 452 | 0.025 | 0.61 |
| 511 | DNMT1 | 922 | 0.046 | 1 | 513 | 0.028 | 0.61 |
| 512 | PLCG1 | 283 | 0.014 | 1 | 157 | 0.009 | 0.61 |
| 513 | PAK1 | 193 | 0.010 | 1 | 107 | 0.006 | 0.61 |
| 514 | CENPN | 74 | 0.004 | 1 | 41 | 0.002 | 0.61 |
| 515 | TSHR | 65 | 0.003 | 1 | 36 | 0.002 | 0.61 |
| 516 | PSRC1 | 318 | 0.016 | 1 | 176 | 0.010 | 0.61 |
| 517 | NOX1 | 47 | 0.002 | 1 | 26 | 0.001 | 0.61 |
| 518 | NCL | 17179 | 0.848 | 1 | 9503 | 0.517 | 0.61 |
| 519 | CCNB1 | 2627 | 0.130 | 1 | 1453 | 0.079 | 0.61 |
| 520 | PTTG2 | 2554 | 0.126 | 1 | 1412 | 0.077 | 0.61 |
| 521 | FBXW7 | 123 | 0.006 | 1 | 68 | 0.004 | 0.61 |
| 522 | MAPT | 29 | 0.001 | 1 | 16 | 0.001 | 0.61 |
| 523 | MNAT1 | 167 | 0.008 | 1 | 92 | 0.005 | 0.61 |
| 524 | EFNB1 | 109 | 0.005 | 1 | 60 | 0.003 | 0.61 |
| 525 | COL11A2 | 40 | 0.002 | 1 | 22 | 0.001 | 0.61 |
| 526 | JPH3 | 82 | 0.004 | 1 | 45 | 0.002 | 0.60 |
| 527 | TIFA | 359 | 0.018 | 1 | 197 | 0.011 | 0.60 |
| 528 | BCL10 | 966 | 0.048 | 1 | 530 | 0.029 | 0.60 |
| 529 | MAP3K2 | 301 | 0.015 | 1 | 165 | 0.009 | 0.60 |
| 530 | RAB27B | 301 | 0.015 | 1 | 165 | 0.009 | 0.60 |

| | | | | | | | |
|---|---|---|---|---|---|---|---|
| 531 | HSPA2 | 73 | 0.004 | 1 | 40 | 0.002 | 0.60 |
| 532 | MSH6 | 482 | 0.024 | 1 | 264 | 0.014 | 0.60 |
| 533 | CTNND2 | 42 | 0.002 | 1 | 23 | 0.001 | 0.60 |
| 534 | CHSY1 | 170 | 0.008 | 1 | 93 | 0.005 | 0.60 |
| 535 | DLGAP5 | 850 | 0.042 | 1 | 465 | 0.025 | 0.60 |
| 536 | RAG1 | 64 | 0.003 | 1 | 35 | 0.002 | 0.60 |
| 537 | XBP1 | 715 | 0.035 | 1 | 391 | 0.021 | 0.60 |
| 538 | KRT16 | 236 | 0.012 | 1 | 129 | 0.007 | 0.60 |
| 539 | CCT4 | 2101 | 0.104 | 1 | 1147 | 0.062 | 0.60 |
| 540 | HHIP | 44 | 0.002 | 1 | 24 | 0.001 | 0.60 |
| 541 | BBC3 | 90 | 0.004 | 1 | 49 | 0.003 | 0.60 |
| 542 | TTK | 421 | 0.021 | 1 | 229 | 0.012 | 0.60 |
| 543 | GBP2 | 114 | 0.006 | 1 | 62 | 0.003 | 0.60 |
| 544 | ADRA1A | 92 | 0.005 | 1 | 50 | 0.003 | 0.60 |
| 545 | CCNO | 116 | 0.006 | 1 | 63 | 0.003 | 0.60 |
| 546 | PRKCZ | 70 | 0.003 | 1 | 38 | 0.002 | 0.60 |
| 547 | TAP2 | 144 | 0.007 | 1 | 78 | 0.004 | 0.60 |
| 548 | NAT8L | 24 | 0.001 | 1 | 13 | 0.001 | 0.60 |
| 549 | RELA | 48 | 0.002 | 1 | 26 | 0.001 | 0.60 |
| 550 | WNT16 | 48 | 0.002 | 1 | 26 | 0.001 | 0.60 |
| 551 | HMGA1 | 2257 | 0.111 | 1 | 1222 | 0.067 | 0.60 |
| 552 | FUT8 | 352 | 0.017 | 1 | 190 | 0.010 | 0.60 |
| 553 | WNT8A | 63 | 0.003 | 1 | 34 | 0.002 | 0.59 |
| 554 | NOTCH1 | 126 | 0.006 | 1 | 68 | 0.004 | 0.59 |
| 555 | CACNA1G | 39 | 0.002 | 1 | 21 | 0.001 | 0.59 |
| 556 | PTCHD1 | 39 | 0.002 | 1 | 21 | 0.001 | 0.59 |
| 557 | HNF1A | 52 | 0.003 | 1 | 28 | 0.002 | 0.59 |
| 558 | TNFRSF9 | 52 | 0.003 | 1 | 28 | 0.002 | 0.59 |
| 559 | WNT9A | 225 | 0.011 | 1 | 121 | 0.007 | 0.59 |
| 560 | CCL2 | 80 | 0.004 | 1 | 43 | 0.002 | 0.59 |
| 561 | MFNG | 41 | 0.002 | 1 | 22 | 0.001 | 0.59 |
| 562 | TGFBR1 | 427 | 0.021 | 1 | 229 | 0.012 | 0.59 |
| 563 | MCM5 | 735 | 0.036 | 1 | 394 | 0.021 | 0.59 |
| 564 | AKR1B1 | 6825 | 0.337 | 1 | 3658 | 0.199 | 0.59 |
| 565 | MUC1 | 1394 | 0.069 | 1 | 747 | 0.041 | 0.59 |
| 566 | DNAJC5B | 43 | 0.002 | 1 | 23 | 0.001 | 0.59 |
| 567 | RASGRF2 | 60 | 0.003 | 1 | 32 | 0.002 | 0.59 |
| 568 | PHGDH | 818 | 0.040 | 1 | 436 | 0.024 | 0.59 |
| 569 | DPPA4 | 154 | 0.008 | 1 | 82 | 0.004 | 0.59 |
| 570 | TMEM57 | 216 | 0.011 | 1 | 115 | 0.006 | 0.59 |
| 571 | SIAH1 | 299 | 0.015 | 1 | 159 | 0.009 | 0.59 |
| 572 | IRF1 | 79 | 0.004 | 1 | 42 | 0.002 | 0.59 |
| 573 | TNFRSF17 | 49 | 0.002 | 1 | 26 | 0.001 | 0.58 |
| 574 | FOXC1 | 17 | 0.001 | 1 | 9 | 0.000 | 0.58 |
| 575 | HOXA10 | 17 | 0.001 | 1 | 9 | 0.000 | 0.58 |
| 576 | POLD4 | 51 | 0.003 | 1 | 27 | 0.001 | 0.58 |
| 577 | SPI1 | 68 | 0.003 | 1 | 36 | 0.002 | 0.58 |
| 578 | NLRP3 | 85 | 0.004 | 1 | 45 | 0.002 | 0.58 |
| 579 | TNFAIP2 | 85 | 0.004 | 1 | 45 | 0.002 | 0.58 |
| 580 | ACLY | 2291 | 0.113 | 1 | 1212 | 0.066 | 0.58 |
| 581 | MCM2 | 465 | 0.023 | 1 | 245 | 0.013 | 0.58 |
| 582 | MMS19 | 380 | 0.019 | 1 | 200 | 0.011 | 0.58 |
| 583 | LIG1 | 333 | 0.016 | 1 | 175 | 0.010 | 0.58 |
| 584 | PMAIP1 | 198 | 0.010 | 1 | 104 | 0.006 | 0.58 |
| 585 | GPR160 | 40 | 0.002 | 1 | 21 | 0.001 | 0.58 |
| 586 | CNPY3 | 128 | 0.006 | 1 | 67 | 0.004 | 0.58 |
| 587 | CCT5 | 1811 | 0.089 | 1 | 947 | 0.052 | 0.58 |
| 588 | CYP1A2 | 44 | 0.002 | 1 | 23 | 0.001 | 0.58 |
| 589 | FOXD3 | 23 | 0.001 | 1 | 12 | 0.001 | 0.58 |
| 590 | PLA2G4E | 69 | 0.003 | 1 | 36 | 0.002 | 0.58 |
| 591 | CDC20 | 2422 | 0.120 | 1 | 1262 | 0.069 | 0.57 |
| 592 | PRLR | 48 | 0.002 | 1 | 25 | 0.001 | 0.57 |

| | | | | | | | |
|---|---|---|---|---|---|---|---|
| 593 | RORC | 73 | 0.004 | 1 | 38 | 0.002 | 0.57 |
| 594 | PTP4A1 | 892 | 0.044 | 1 | 464 | 0.025 | 0.57 |
| 595 | TMPRSS2 | 25 | 0.001 | 1 | 13 | 0.001 | 0.57 |
| 596 | MMP14 | 777 | 0.038 | 1 | 404 | 0.022 | 0.57 |
| 597 | ABCA4 | 77 | 0.004 | 1 | 40 | 0.002 | 0.57 |
| 598 | SLC45A3 | 231 | 0.011 | 1 | 120 | 0.007 | 0.57 |
| 599 | BTG2 | 617 | 0.030 | 1 | 320 | 0.017 | 0.57 |
| 600 | TIAM1 | 108 | 0.005 | 1 | 56 | 0.003 | 0.57 |
| 601 | IL7R | 195 | 0.010 | 1 | 101 | 0.005 | 0.57 |
| 602 | MADCAM1 | 56 | 0.003 | 1 | 29 | 0.002 | 0.57 |
| 603 | TNFRSF25 | 114 | 0.006 | 1 | 59 | 0.003 | 0.57 |
| 604 | EPGN | 892 | 0.044 | 1 | 461 | 0.025 | 0.57 |
| 605 | KLRG1 | 60 | 0.003 | 1 | 31 | 0.002 | 0.57 |
| 606 | CCNA2 | 1026 | 0.051 | 1 | 530 | 0.029 | 0.57 |
| 607 | MAD2L1 | 775 | 0.038 | 1 | 400 | 0.022 | 0.57 |
| 608 | SMO | 64 | 0.003 | 1 | 33 | 0.002 | 0.57 |
| 609 | BIRC7 | 97 | 0.005 | 1 | 50 | 0.003 | 0.57 |
| 610 | DDIT3 | 33 | 0.002 | 1 | 17 | 0.001 | 0.57 |
| 611 | GNAZ | 66 | 0.003 | 1 | 34 | 0.002 | 0.57 |
| 612 | RFC4 | 439 | 0.022 | 1 | 226 | 0.012 | 0.57 |
| 613 | BUB1B | 212 | 0.010 | 1 | 109 | 0.006 | 0.57 |
| 614 | TYMP | 395 | 0.020 | 1 | 203 | 0.011 | 0.57 |
| 615 | MRPL13 | 477 | 0.024 | 1 | 245 | 0.013 | 0.57 |
| 616 | IGF2 | 37 | 0.002 | 1 | 19 | 0.001 | 0.57 |
| 617 | FPR1 | 417 | 0.021 | 1 | 214 | 0.012 | 0.57 |
| 618 | LIG3 | 154 | 0.008 | 1 | 79 | 0.004 | 0.57 |
| 619 | DICER1 | 525 | 0.026 | 1 | 269 | 0.015 | 0.56 |
| 620 | PA2G4 | 3074 | 0.152 | 1 | 1575 | 0.086 | 0.56 |
| 621 | CHD7 | 256 | 0.013 | 1 | 131 | 0.007 | 0.56 |
| 622 | MAPK13 | 86 | 0.004 | 1 | 44 | 0.002 | 0.56 |
| 623 | RFC3 | 507 | 0.025 | 1 | 259 | 0.014 | 0.56 |
| 624 | FANCB | 186 | 0.009 | 1 | 95 | 0.005 | 0.56 |
| 625 | PPARGC1B | 237 | 0.012 | 1 | 121 | 0.007 | 0.56 |
| 626 | HNRNPA2B1 | 2706 | 0.134 | 1 | 1379 | 0.075 | 0.56 |
| 627 | GEMIN2 | 263 | 0.013 | 1 | 134 | 0.007 | 0.56 |
| 628 | AURKA | 1727 | 0.085 | 1 | 879 | 0.048 | 0.56 |
| 629 | CD86 | 63 | 0.003 | 1 | 32 | 0.002 | 0.56 |
| 630 | PPP2R2C | 203 | 0.010 | 1 | 103 | 0.006 | 0.56 |
| 631 | C3 | 2949 | 0.146 | 1 | 1494 | 0.081 | 0.56 |
| 632 | ITLN2 | 79 | 0.004 | 1 | 40 | 0.002 | 0.56 |
| 633 | MDM2 | 2824 | 0.139 | 1 | 1429 | 0.078 | 0.56 |
| 634 | SLK | 832 | 0.041 | 1 | 421 | 0.023 | 0.56 |
| 635 | MAP2K4 | 319 | 0.016 | 1 | 161 | 0.009 | 0.56 |
| 636 | CMC2 | 465 | 0.023 | 1 | 234 | 0.013 | 0.55 |
| 637 | REL | 211 | 0.010 | 1 | 106 | 0.006 | 0.55 |
| 638 | GTSE1 | 237 | 0.012 | 1 | 119 | 0.006 | 0.55 |
| 639 | SLC3A2 | 1103 | 0.054 | 1 | 553 | 0.030 | 0.55 |
| 640 | HIST1H3H | 3524 | 0.174 | 1 | 1764 | 0.096 | 0.55 |
| 641 | HGF | 8 | 0.000 | 1 | 4 | 0.000 | 0.55 |
| 642 | COMP | 26 | 0.001 | 1 | 13 | 0.001 | 0.55 |
| 643 | TBX21 | 30 | 0.001 | 1 | 15 | 0.001 | 0.55 |
| 644 | MAGEB2 | 42 | 0.002 | 1 | 21 | 0.001 | 0.55 |
| 645 | PRKAG2 | 66 | 0.003 | 1 | 33 | 0.002 | 0.55 |
| 646 | PTCHD2 | 72 | 0.004 | 1 | 36 | 0.002 | 0.55 |
| 647 | NGFR | 86 | 0.004 | 1 | 43 | 0.002 | 0.55 |
| 648 | BCL2 | 94 | 0.005 | 1 | 47 | 0.003 | 0.55 |
| 649 | BRCA2 | 202 | 0.010 | 1 | 101 | 0.005 | 0.55 |
| 650 | CAPN1 | 586 | 0.029 | 1 | 293 | 0.016 | 0.55 |
| 651 | XRCC6BP1 | 24 | 0.001 | 1 | 12 | 0.001 | 0.55 |
| 652 | ATG13 | 50 | 0.002 | 1 | 25 | 0.001 | 0.55 |
| 653 | BMP8A | 74 | 0.004 | 1 | 37 | 0.002 | 0.55 |
| 654 | IGF1R | 200 | 0.010 | 1 | 100 | 0.005 | 0.55 |

| 655 | RPS6KA1 | 417 | 0.021 | 1 | 208 | 0.011 | 0.55 |
|---|---|---|---|---|---|---|---|
| 656 | CASP1 | 524 | 0.026 | 1 | 261 | 0.014 | 0.55 |
| 657 | CTSC | 2319 | 0.114 | 1 | 1154 | 0.063 | 0.55 |
| 658 | ZAK | 561 | 0.028 | 1 | 278 | 0.015 | 0.55 |
| 659 | DFFA | 271 | 0.013 | 1 | 134 | 0.007 | 0.55 |
| 660 | DAB2IP | 393 | 0.019 | 1 | 194 | 0.011 | 0.54 |
| 661 | LEF1 | 67 | 0.003 | 1 | 33 | 0.002 | 0.54 |
| 662 | LIPE | 61 | 0.003 | 1 | 30 | 0.002 | 0.54 |
| 663 | GRIA3 | 57 | 0.003 | 1 | 28 | 0.002 | 0.54 |
| 664 | KCTD11 | 55 | 0.003 | 1 | 27 | 0.001 | 0.54 |
| 665 | MAPRE2 | 108 | 0.005 | 1 | 53 | 0.003 | 0.54 |
| 666 | LRG1 | 53 | 0.003 | 1 | 26 | 0.001 | 0.54 |
| 667 | CACNG1 | 51 | 0.003 | 1 | 25 | 0.001 | 0.54 |
| 668 | KDM5C | 737 | 0.036 | 1 | 361 | 0.020 | 0.54 |
| 669 | SNAI3 | 45 | 0.002 | 1 | 22 | 0.001 | 0.54 |
| 670 | HSPE1 | 7143 | 0.353 | 1 | 3492 | 0.190 | 0.54 |
| 671 | SMPDL3B | 119 | 0.006 | 1 | 58 | 0.003 | 0.54 |
| 672 | TCP1 | 3441 | 0.170 | 1 | 1675 | 0.091 | 0.54 |
| 673 | ADAM17 | 405 | 0.020 | 1 | 197 | 0.011 | 0.54 |
| 674 | MAP2K1 | 999 | 0.049 | 1 | 485 | 0.026 | 0.54 |
| 675 | CDX2 | 64 | 0.003 | 1 | 31 | 0.002 | 0.53 |
| 676 | DLL3 | 60 | 0.003 | 1 | 29 | 0.002 | 0.53 |
| 677 | LMO2 | 60 | 0.003 | 1 | 29 | 0.002 | 0.53 |
| 678 | DNAJB13 | 58 | 0.003 | 1 | 28 | 0.002 | 0.53 |
| 679 | NKX3_1 | 114 | 0.006 | 1 | 55 | 0.003 | 0.53 |
| 680 | NOS3 | 27 | 0.001 | 1 | 13 | 0.001 | 0.53 |
| 681 | PABPC1 | 81 | 0.004 | 1 | 39 | 0.002 | 0.53 |
| 682 | CDC7 | 192 | 0.009 | 1 | 92 | 0.005 | 0.53 |
| 683 | TNFRSF14 | 46 | 0.002 | 1 | 22 | 0.001 | 0.53 |
| 684 | PROM1 | 67 | 0.003 | 1 | 32 | 0.002 | 0.53 |
| 685 | NT5E | 289 | 0.014 | 1 | 138 | 0.008 | 0.53 |
| 686 | TNFRSF21 | 267 | 0.013 | 1 | 127 | 0.007 | 0.52 |
| 687 | CCR3 | 61 | 0.003 | 1 | 29 | 0.002 | 0.52 |
| 688 | ANAPC2 | 179 | 0.009 | 1 | 85 | 0.005 | 0.52 |
| 689 | CEACAM7 | 59 | 0.003 | 1 | 28 | 0.002 | 0.52 |
| 690 | BLM | 133 | 0.007 | 1 | 63 | 0.003 | 0.52 |
| 691 | ORC6 | 169 | 0.008 | 1 | 80 | 0.004 | 0.52 |
| 692 | BAG3 | 656 | 0.032 | 1 | 310 | 0.017 | 0.52 |
| 693 | TRIP4 | 91 | 0.004 | 1 | 43 | 0.002 | 0.52 |
| 694 | HSPA4L | 377 | 0.019 | 1 | 178 | 0.010 | 0.52 |
| 695 | GM2A | 303 | 0.015 | 1 | 143 | 0.008 | 0.52 |
| 696 | NKD1 | 34 | 0.002 | 1 | 16 | 0.001 | 0.52 |
| 697 | FAM162A | 253 | 0.012 | 1 | 119 | 0.006 | 0.52 |
| 698 | FGFR2 | 47 | 0.002 | 1 | 22 | 0.001 | 0.52 |
| 699 | TDG | 691 | 0.034 | 1 | 323 | 0.018 | 0.52 |
| 700 | FOS | 2531 | 0.125 | 1 | 1181 | 0.064 | 0.51 |
| 701 | MCM3 | 533 | 0.026 | 1 | 248 | 0.013 | 0.51 |
| 702 | PPID | 570 | 0.028 | 1 | 265 | 0.014 | 0.51 |
| 703 | EZR | 994 | 0.049 | 1 | 462 | 0.025 | 0.51 |
| 704 | VAMP8 | 1070 | 0.053 | 1 | 494 | 0.027 | 0.51 |
| 705 | TIE1 | 52 | 0.003 | 1 | 24 | 0.001 | 0.51 |
| 706 | ORM1 | 91 | 0.004 | 1 | 42 | 0.002 | 0.51 |
| 707 | MCL1 | 4472 | 0.221 | 1 | 2064 | 0.112 | 0.51 |
| 708 | NRAS | 404 | 0.020 | 1 | 186 | 0.010 | 0.51 |
| 709 | ANXA8 | 1838 | 0.091 | 1 | 846 | 0.046 | 0.51 |
| 710 | SREBF1 | 1489 | 0.074 | 1 | 685 | 0.037 | 0.51 |
| 711 | ACTR3B | 50 | 0.002 | 1 | 23 | 0.001 | 0.51 |
| 712 | BOC | 37 | 0.002 | 1 | 17 | 0.001 | 0.51 |
| 713 | THPO | 85 | 0.004 | 1 | 39 | 0.002 | 0.51 |
| 714 | NODAL | 83 | 0.004 | 1 | 38 | 0.002 | 0.50 |
| 715 | TSPAN14 | 996 | 0.049 | 1 | 456 | 0.025 | 0.50 |
| 716 | NR4A1 | 142 | 0.007 | 1 | 65 | 0.004 | 0.50 |

| | | | | | | | |
|---|---|---|---|---|---|---|---|
| 717 | LYZ | 59 | 0.003 | 1 | 27 | 0.001 | 0.50 |
| 718 | MLLT4 | 306 | 0.015 | 1 | 140 | 0.008 | 0.50 |
| 719 | RALA | 460 | 0.023 | 1 | 210 | 0.011 | 0.50 |
| 720 | CASP14 | 57 | 0.003 | 1 | 26 | 0.001 | 0.50 |
| 721 | LAG3 | 112 | 0.006 | 1 | 51 | 0.003 | 0.50 |
| 722 | ITGB7 | 66 | 0.003 | 1 | 30 | 0.002 | 0.50 |
| 723 | ETV4 | 55 | 0.003 | 1 | 25 | 0.001 | 0.50 |
| 724 | PFKFB2 | 405 | 0.020 | 1 | 183 | 0.010 | 0.50 |
| 725 | CCL28 | 186 | 0.009 | 1 | 84 | 0.005 | 0.50 |
| 726 | CDC25A | 182 | 0.009 | 1 | 82 | 0.004 | 0.50 |
| 727 | RAC3 | 188 | 0.009 | 1 | 84 | 0.005 | 0.49 |
| 728 | AQP1 | 18 | 0.001 | 1 | 8 | 0.000 | 0.49 |
| 729 | MUTYH | 54 | 0.003 | 1 | 24 | 0.001 | 0.49 |
| 730 | PKMYT1 | 302 | 0.015 | 1 | 134 | 0.007 | 0.49 |
| 731 | MTFP1 | 230 | 0.011 | 1 | 102 | 0.006 | 0.49 |
| 732 | EGFR | 954 | 0.047 | 1 | 423 | 0.023 | 0.49 |
| 733 | SLC2A1 | 1039 | 0.051 | 1 | 460 | 0.025 | 0.49 |
| 734 | SLC7A5 | 615 | 0.030 | 1 | 271 | 0.015 | 0.49 |
| 735 | PF4V1 | 84 | 0.004 | 1 | 37 | 0.002 | 0.49 |
| 736 | CEP55 | 50 | 0.002 | 1 | 22 | 0.001 | 0.49 |
| 737 | TAGLN | 1082 | 0.053 | 1 | 476 | 0.026 | 0.48 |
| 738 | IL2RA | 41 | 0.002 | 1 | 18 | 0.001 | 0.48 |
| 739 | ACACA | 647 | 0.032 | 1 | 284 | 0.015 | 0.48 |
| 740 | STAT6 | 498 | 0.025 | 1 | 218 | 0.012 | 0.48 |
| 741 | VCAM1 | 64 | 0.003 | 1 | 28 | 0.002 | 0.48 |
| 742 | SLCO3A1 | 96 | 0.005 | 1 | 42 | 0.002 | 0.48 |
| 743 | AURKB | 605 | 0.030 | 1 | 264 | 0.014 | 0.48 |
| 744 | TNFSF14 | 94 | 0.005 | 1 | 41 | 0.002 | 0.48 |
| 745 | RAD9A | 101 | 0.005 | 1 | 44 | 0.002 | 0.48 |
| 746 | ESR1 | 74 | 0.004 | 1 | 32 | 0.002 | 0.48 |
| 747 | XRCC4 | 74 | 0.004 | 1 | 32 | 0.002 | 0.48 |
| 748 | HOXD1 | 58 | 0.003 | 1 | 25 | 0.001 | 0.48 |
| 749 | GABBR2 | 72 | 0.004 | 1 | 31 | 0.002 | 0.47 |
| 750 | TNC | 144 | 0.007 | 1 | 62 | 0.003 | 0.47 |
| 751 | ANGPT2 | 7 | 0.000 | 1 | 3 | 0.000 | 0.47 |
| 752 | RIPK3 | 7 | 0.000 | 1 | 3 | 0.000 | 0.47 |
| 753 | TREX1 | 49 | 0.002 | 1 | 21 | 0.001 | 0.47 |
| 754 | MYOD1 | 42 | 0.002 | 1 | 18 | 0.001 | 0.47 |
| 755 | DSC2 | 173 | 0.009 | 1 | 74 | 0.004 | 0.47 |
| 756 | PELP1 | 131 | 0.006 | 1 | 56 | 0.003 | 0.47 |
| 757 | CSNK2A1 | 797 | 0.039 | 1 | 340 | 0.019 | 0.47 |
| 758 | RPS6KB2 | 455 | 0.022 | 1 | 194 | 0.011 | 0.47 |
| 759 | PFKFB3 | 176 | 0.009 | 1 | 75 | 0.004 | 0.47 |
| 760 | SPEF1 | 47 | 0.002 | 1 | 20 | 0.001 | 0.47 |
| 761 | XCR1 | 47 | 0.002 | 1 | 20 | 0.001 | 0.47 |
| 762 | TCF7L1 | 26 | 0.001 | 1 | 11 | 0.001 | 0.47 |
| 763 | DDX58 | 346 | 0.017 | 1 | 146 | 0.008 | 0.47 |
| 764 | NDRG1 | 524 | 0.026 | 1 | 221 | 0.012 | 0.46 |
| 765 | EPO | 57 | 0.003 | 1 | 24 | 0.001 | 0.46 |
| 766 | PFDN2 | 3443 | 0.170 | 1 | 1449 | 0.079 | 0.46 |
| 767 | CCR6 | 50 | 0.002 | 1 | 21 | 0.001 | 0.46 |
| 768 | PRKX | 360 | 0.018 | 1 | 151 | 0.008 | 0.46 |
| 769 | SLCO4A1 | 31 | 0.002 | 1 | 13 | 0.001 | 0.46 |
| 770 | HES1 | 117 | 0.006 | 1 | 49 | 0.003 | 0.46 |
| 771 | SLC7A8 | 79 | 0.004 | 1 | 33 | 0.002 | 0.46 |
| 772 | CCNB2 | 84 | 0.004 | 1 | 35 | 0.002 | 0.46 |
| 773 | RAD51C | 192 | 0.009 | 1 | 80 | 0.004 | 0.46 |
| 774 | FST | 118 | 0.006 | 1 | 49 | 0.003 | 0.46 |
| 775 | CCL5 | 94 | 0.005 | 1 | 39 | 0.002 | 0.46 |
| 776 | TLR2 | 82 | 0.004 | 1 | 34 | 0.002 | 0.46 |
| 777 | TRAF2 | 70 | 0.003 | 1 | 29 | 0.002 | 0.46 |
| 778 | CD70 | 298 | 0.015 | 1 | 123 | 0.007 | 0.46 |

| | | | | | | | |
|---|---|---|---|---|---|---|---|
| 779 | STEAP4 | 80 | 0.004 | 1 | 33 | 0.002 | 0.45 |
| 780 | CCT6A | 3304 | 0.163 | 1 | 1361 | 0.074 | 0.45 |
| 781 | ESM1 | 17 | 0.001 | 1 | 7 | 0.000 | 0.45 |
| 782 | HLA_B | 1665 | 0.082 | 1 | 685 | 0.037 | 0.45 |
| 783 | ADORA2B | 825 | 0.041 | 1 | 339 | 0.018 | 0.45 |
| 784 | GPD2 | 677 | 0.033 | 1 | 277 | 0.015 | 0.45 |
| 785 | KSR1 | 27 | 0.001 | 1 | 11 | 0.001 | 0.45 |
| 786 | CCL22 | 59 | 0.003 | 1 | 24 | 0.001 | 0.45 |
| 787 | HSPB7 | 32 | 0.002 | 1 | 13 | 0.001 | 0.45 |
| 788 | NR4A3 | 47 | 0.002 | 1 | 19 | 0.001 | 0.45 |
| 789 | SYK | 124 | 0.006 | 1 | 50 | 0.003 | 0.44 |
| 790 | CDK8 | 362 | 0.018 | 1 | 145 | 0.008 | 0.44 |
| 791 | MAPK8IP2 | 5 | 0.000 | 1 | 2 | 0.000 | 0.44 |
| 792 | LECT1 | 40 | 0.002 | 1 | 16 | 0.001 | 0.44 |
| 793 | CHGA | 60 | 0.003 | 1 | 24 | 0.001 | 0.44 |
| 794 | SOCS3 | 65 | 0.003 | 1 | 26 | 0.001 | 0.44 |
| 795 | XRCC2 | 501 | 0.025 | 1 | 200 | 0.011 | 0.44 |
| 796 | HMGCR | 540 | 0.027 | 1 | 215 | 0.012 | 0.44 |
| 797 | CMTM2 | 73 | 0.004 | 1 | 29 | 0.002 | 0.44 |
| 798 | CAPN6 | 43 | 0.002 | 1 | 17 | 0.001 | 0.44 |
| 799 | PRKCB | 43 | 0.002 | 1 | 17 | 0.001 | 0.44 |
| 800 | FANCA | 86 | 0.004 | 1 | 34 | 0.002 | 0.44 |
| 801 | CCL3 | 81 | 0.004 | 1 | 32 | 0.002 | 0.44 |
| 802 | ABCA3 | 119 | 0.006 | 1 | 47 | 0.003 | 0.44 |
| 803 | SLC2A3 | 193 | 0.010 | 1 | 76 | 0.004 | 0.43 |
| 804 | EIF4EBP1 | 1104 | 0.055 | 1 | 434 | 0.024 | 0.43 |
| 805 | PTCHD3 | 56 | 0.003 | 1 | 22 | 0.001 | 0.43 |
| 806 | EIF4A1 | 13513 | 0.667 | 1 | 5285 | 0.288 | 0.43 |
| 807 | HSPA14 | 77 | 0.004 | 1 | 30 | 0.002 | 0.43 |
| 808 | CCNA1 | 95 | 0.005 | 1 | 37 | 0.002 | 0.43 |
| 809 | DKK2 | 67 | 0.003 | 1 | 26 | 0.001 | 0.43 |
| 810 | WASL | 49 | 0.002 | 1 | 19 | 0.001 | 0.43 |
| 811 | CD8A | 80 | 0.004 | 1 | 31 | 0.002 | 0.43 |
| 812 | NMU | 411 | 0.020 | 1 | 159 | 0.009 | 0.43 |
| 813 | VCAN | 539 | 0.027 | 1 | 208 | 0.011 | 0.43 |
| 814 | FHIT | 127 | 0.006 | 1 | 49 | 0.003 | 0.43 |
| 815 | IL10RA | 70 | 0.003 | 1 | 27 | 0.001 | 0.43 |
| 816 | ICAM1 | 172 | 0.008 | 1 | 66 | 0.004 | 0.42 |
| 817 | LTA | 34 | 0.002 | 1 | 13 | 0.001 | 0.42 |
| 818 | PAX8 | 68 | 0.003 | 1 | 26 | 0.001 | 0.42 |
| 819 | DEFB1 | 97 | 0.005 | 1 | 37 | 0.002 | 0.42 |
| 820 | EBF4 | 21 | 0.001 | 1 | 8 | 0.000 | 0.42 |
| 821 | PTPN5 | 42 | 0.002 | 1 | 16 | 0.001 | 0.42 |
| 822 | ANGPTL4 | 651 | 0.032 | 1 | 248 | 0.013 | 0.42 |
| 823 | RBBP8 | 541 | 0.027 | 1 | 206 | 0.011 | 0.42 |
| 824 | PIDD1 | 305 | 0.015 | 1 | 116 | 0.006 | 0.42 |
| 825 | CDC6 | 500 | 0.025 | 1 | 190 | 0.010 | 0.42 |
| 826 | EDN1 | 129 | 0.006 | 1 | 49 | 0.003 | 0.42 |
| 827 | PCSK6 | 140 | 0.007 | 1 | 53 | 0.003 | 0.42 |
| 828 | SMUG1 | 107 | 0.005 | 1 | 40 | 0.002 | 0.41 |
| 829 | CXCR2 | 27 | 0.001 | 1 | 10 | 0.001 | 0.41 |
| 830 | TLR9 | 46 | 0.002 | 1 | 17 | 0.001 | 0.41 |
| 831 | SLC29A1 | 112 | 0.006 | 1 | 41 | 0.002 | 0.40 |
| 832 | SLC29A2 | 389 | 0.019 | 1 | 142 | 0.008 | 0.40 |
| 833 | CDC25B | 1251 | 0.062 | 1 | 456 | 0.025 | 0.40 |
| 834 | MT2A | 45572 | 2.250 | 1 | 16510 | 0.899 | 0.40 |
| 835 | FOXE1 | 58 | 0.003 | 1 | 21 | 0.001 | 0.40 |
| 836 | ATXN1 | 61 | 0.003 | 1 | 22 | 0.001 | 0.40 |
| 837 | TIMP3 | 272 | 0.013 | 1 | 98 | 0.005 | 0.40 |
| 838 | BBS4 | 25 | 0.001 | 1 | 9 | 0.000 | 0.40 |
| 839 | DUSP6 | 304 | 0.015 | 1 | 109 | 0.006 | 0.40 |
| 840 | UBE2C | 112 | 0.006 | 1 | 40 | 0.002 | 0.39 |

| | | | | | | | |
|---|---|---|---|---|---|---|---|
| 841 | EXO1 | 266 | 0.013 | 1 | 95 | 0.005 | 0.39 |
| 842 | ETV7 | 79 | 0.004 | 1 | 28 | 0.002 | 0.39 |
| 843 | NFKB2 | 173 | 0.009 | 1 | 61 | 0.003 | 0.39 |
| 844 | KIF2C | 323 | 0.016 | 1 | 112 | 0.006 | 0.38 |
| 845 | SERPINB5 | 1068 | 0.053 | 1 | 370 | 0.020 | 0.38 |
| 846 | CD83 | 137 | 0.007 | 1 | 47 | 0.003 | 0.38 |
| 847 | VEGFC | 248 | 0.012 | 1 | 85 | 0.005 | 0.38 |
| 848 | MTSS1 | 187 | 0.009 | 1 | 64 | 0.003 | 0.38 |
| 849 | PLAUR | 702 | 0.035 | 1 | 235 | 0.013 | 0.37 |
| 850 | DLL4 | 9 | 0.000 | 1 | 3 | 0.000 | 0.37 |
| 851 | AQP2 | 18 | 0.001 | 1 | 6 | 0.000 | 0.37 |
| 852 | BCL2L11 | 66 | 0.003 | 1 | 22 | 0.001 | 0.37 |
| 853 | PTHLH | 78 | 0.004 | 1 | 26 | 0.001 | 0.37 |
| 854 | IFI27 | 138 | 0.007 | 1 | 46 | 0.003 | 0.37 |
| 855 | PGC | 3 | 0.000 | 1 | 1 | 0.000 | 0.37 |
| 856 | PTCRA | 3 | 0.000 | 1 | 1 | 0.000 | 0.37 |
| 857 | IFNA2 | 24 | 0.001 | 1 | 8 | 0.000 | 0.37 |
| 858 | TWIST2 | 334 | 0.016 | 1 | 111 | 0.006 | 0.37 |
| 859 | KLF4 | 112 | 0.006 | 1 | 37 | 0.002 | 0.36 |
| 860 | HMGB3 | 185 | 0.009 | 1 | 61 | 0.003 | 0.36 |
| 861 | ANXA3 | 1693 | 0.084 | 1 | 558 | 0.030 | 0.36 |
| 862 | ODC1 | 405 | 0.020 | 1 | 132 | 0.007 | 0.36 |
| 863 | IL1RAP | 384 | 0.019 | 1 | 125 | 0.007 | 0.36 |
| 864 | CCR1 | 40 | 0.002 | 1 | 13 | 0.001 | 0.36 |
| 865 | FOXA1 | 253 | 0.012 | 1 | 82 | 0.004 | 0.36 |
| 866 | RSPO1 | 71 | 0.004 | 1 | 23 | 0.001 | 0.36 |
| 867 | F11R | 466 | 0.023 | 1 | 150 | 0.008 | 0.35 |
| 868 | CSF3 | 1298 | 0.064 | 1 | 417 | 0.023 | 0.35 |
| 869 | MST1R | 131 | 0.006 | 1 | 42 | 0.002 | 0.35 |
| 870 | PTTG1 | 163 | 0.008 | 1 | 52 | 0.003 | 0.35 |
| 871 | IL4R | 895 | 0.044 | 1 | 283 | 0.015 | 0.35 |
| 872 | CTNNBIP1 | 54 | 0.003 | 1 | 17 | 0.001 | 0.35 |
| 873 | TNF | 54 | 0.003 | 1 | 17 | 0.001 | 0.35 |
| 874 | SOX9 | 732 | 0.036 | 1 | 229 | 0.012 | 0.34 |
| 875 | PPP1R15A | 252 | 0.012 | 1 | 78 | 0.004 | 0.34 |
| 876 | SPATA2 | 88 | 0.004 | 1 | 27 | 0.001 | 0.34 |
| 877 | MACC1 | 170 | 0.008 | 1 | 52 | 0.003 | 0.34 |
| 878 | PRDM1 | 247 | 0.012 | 1 | 75 | 0.004 | 0.33 |
| 879 | EFNA1 | 449 | 0.022 | 1 | 136 | 0.007 | 0.33 |
| 880 | DSP | 1596 | 0.079 | 1 | 482 | 0.026 | 0.33 |
| 881 | KRT5 | 9363 | 0.462 | 1 | 2827 | 0.154 | 0.33 |
| 882 | FASN | 2096 | 0.103 | 1 | 632 | 0.034 | 0.33 |
| 883 | HEY1 | 10 | 0.000 | 1 | 3 | 0.000 | 0.33 |
| 884 | NFKBIA | 433 | 0.021 | 1 | 129 | 0.007 | 0.33 |
| 885 | NFKBIE | 195 | 0.010 | 1 | 58 | 0.003 | 0.33 |
| 886 | SOX7 | 350 | 0.017 | 1 | 104 | 0.006 | 0.33 |
| 887 | TSPAN13 | 288 | 0.014 | 1 | 85 | 0.005 | 0.33 |
| 888 | SGK2 | 17 | 0.001 | 1 | 5 | 0.000 | 0.32 |
| 889 | FAM213A | 252 | 0.012 | 1 | 74 | 0.004 | 0.32 |
| 890 | FGF17 | 75 | 0.004 | 1 | 22 | 0.001 | 0.32 |
| 891 | VDR | 550 | 0.027 | 1 | 161 | 0.009 | 0.32 |
| 892 | CCNC | 225 | 0.011 | 1 | 65 | 0.004 | 0.32 |
| 893 | EPCAM | 111 | 0.005 | 1 | 32 | 0.002 | 0.32 |
| 894 | IER3 | 1443 | 0.071 | 1 | 413 | 0.022 | 0.32 |
| 895 | CRTAC1 | 56 | 0.003 | 1 | 16 | 0.001 | 0.31 |
| 896 | BHLHE40 | 1330 | 0.066 | 1 | 380 | 0.021 | 0.31 |
| 897 | PLAU | 704 | 0.035 | 1 | 200 | 0.011 | 0.31 |
| 898 | C1orf106 | 554 | 0.027 | 1 | 157 | 0.009 | 0.31 |
| 899 | GADD45G | 50 | 0.002 | 1 | 14 | 0.001 | 0.31 |
| 900 | PIK3R5 | 43 | 0.002 | 1 | 12 | 0.001 | 0.31 |
| 901 | BMP6 | 18 | 0.001 | 1 | 5 | 0.000 | 0.31 |
| 902 | MMP3 | 36 | 0.002 | 1 | 10 | 0.001 | 0.31 |

| | | | | | | | |
|---|---|---|---|---|---|---|---|
| 903 | HMGA2 | 500 | 0.025 | 1 | 138 | 0.008 | 0.30 |
| 904 | CTSV | 240 | 0.012 | 1 | 66 | 0.004 | 0.30 |
| 905 | PLK3 | 603 | 0.030 | 1 | 165 | 0.009 | 0.30 |
| 906 | RAMP3 | 59 | 0.003 | 1 | 16 | 0.001 | 0.30 |
| 907 | CDK6 | 451 | 0.022 | 1 | 122 | 0.007 | 0.30 |
| 908 | NFKBIZ | 832 | 0.041 | 1 | 224 | 0.012 | 0.30 |
| 909 | ASNS | 399 | 0.020 | 1 | 106 | 0.006 | 0.29 |
| 910 | RAD54L | 35 | 0.002 | 1 | 9 | 0.000 | 0.28 |
| 911 | PRR15L | 176 | 0.009 | 1 | 45 | 0.002 | 0.28 |
| 912 | FGFR3 | 157 | 0.008 | 1 | 40 | 0.002 | 0.28 |
| 913 | GALNT3 | 838 | 0.041 | 1 | 213 | 0.012 | 0.28 |
| 914 | CKMT1A | 489 | 0.024 | 1 | 124 | 0.007 | 0.28 |
| 915 | VSNL1 | 214 | 0.011 | 1 | 54 | 0.003 | 0.28 |
| 916 | KRT14 | 350 | 0.017 | 1 | 88 | 0.005 | 0.28 |
| 917 | KCND2 | 4 | 0.000 | 1 | 1 | 0.000 | 0.28 |
| 918 | PAX3 | 20 | 0.001 | 1 | 5 | 0.000 | 0.28 |
| 919 | CCR7 | 28 | 0.001 | 1 | 7 | 0.000 | 0.28 |
| 920 | GPR126 | 145 | 0.007 | 1 | 36 | 0.002 | 0.27 |
| 921 | TTC9 | 57 | 0.003 | 1 | 14 | 0.001 | 0.27 |
| 922 | TLR1 | 114 | 0.006 | 1 | 28 | 0.002 | 0.27 |
| 923 | DDR1 | 961 | 0.047 | 1 | 235 | 0.013 | 0.27 |
| 924 | CAMK2B | 174 | 0.009 | 1 | 42 | 0.002 | 0.27 |
| 925 | FGF19 | 46 | 0.002 | 1 | 11 | 0.001 | 0.26 |
| 926 | GDF6 | 26 | 0.001 | 1 | 6 | 0.000 | 0.25 |
| 927 | FZD8 | 57 | 0.003 | 1 | 13 | 0.001 | 0.25 |
| 928 | EXOSC8 | 53 | 0.003 | 1 | 12 | 0.001 | 0.25 |
| 929 | TICAM1 | 55 | 0.003 | 1 | 12 | 0.001 | 0.24 |
| 930 | CXXC4 | 33 | 0.002 | 1 | 7 | 0.000 | 0.23 |
| 931 | IDO1 | 24 | 0.001 | 1 | 5 | 0.000 | 0.23 |
| 932 | ITGA2 | 882 | 0.044 | 1 | 181 | 0.010 | 0.23 |
| 933 | KIT | 5 | 0.000 | 1 | 1 | 0.000 | 0.22 |
| 934 | ALB | 20 | 0.001 | 1 | 4 | 0.000 | 0.22 |
| 935 | AREG | 9999 | 0.494 | 1 | 1984 | 0.108 | 0.22 |
| 936 | BIRC3 | 1138 | 0.056 | 1 | 218 | 0.012 | 0.21 |
| 937 | IL20RA | 63 | 0.003 | 1 | 12 | 0.001 | 0.21 |
| 938 | PTGS2 | 280 | 0.014 | 1 | 53 | 0.003 | 0.21 |
| 939 | RBL1 | 228 | 0.011 | 1 | 43 | 0.002 | 0.21 |
| 940 | CD24 | 869 | 0.043 | 1 | 162 | 0.009 | 0.21 |
| 941 | FCER2 | 11 | 0.001 | 1 | 2 | 0.000 | 0.20 |
| 942 | LIF | 890 | 0.044 | 1 | 154 | 0.008 | 0.19 |
| 943 | SOD2 | 7007 | 0.346 | 1 | 1174 | 0.064 | 0.18 |
| 944 | GNGT2 | 12 | 0.001 | 1 | 2 | 0.000 | 0.18 |
| 945 | OAS1 | 12 | 0.001 | 1 | 2 | 0.000 | 0.18 |
| 946 | ABCC2 | 157 | 0.008 | 1 | 26 | 0.001 | 0.18 |
| 947 | TMEM132A | 222 | 0.011 | 1 | 36 | 0.002 | 0.18 |
| 948 | KCNK5 | 32 | 0.002 | 1 | 5 | 0.000 | 0.17 |
| 949 | TNNI2 | 270 | 0.013 | 1 | 42 | 0.002 | 0.17 |
| 950 | KRT6A | 262 | 0.013 | 1 | 40 | 0.002 | 0.17 |
| 951 | JAG1 | 606 | 0.030 | 1 | 92 | 0.005 | 0.17 |
| 952 | FAM83B | 291 | 0.014 | 1 | 43 | 0.002 | 0.16 |
| 953 | CXCL3 | 901 | 0.044 | 1 | 133 | 0.007 | 0.16 |
| 954 | LAMB3 | 1577 | 0.078 | 1 | 229 | 0.012 | 0.16 |
| 955 | BECN1 | 69 | 0.003 | 1 | 10 | 0.001 | 0.16 |
| 956 | TGFA | 410 | 0.020 | 1 | 58 | 0.003 | 0.16 |
| 957 | BIK | 310 | 0.015 | 1 | 43 | 0.002 | 0.15 |
| 958 | CCND2 | 544 | 0.027 | 1 | 72 | 0.004 | 0.15 |
| 959 | ALDH1A3 | 4918 | 0.243 | 1 | 642 | 0.035 | 0.14 |
| 960 | INPP5J | 23 | 0.001 | 1 | 3 | 0.000 | 0.14 |
| 961 | CLCA2 | 529 | 0.026 | 1 | 66 | 0.004 | 0.14 |
| 962 | ITGA6 | 1676 | 0.083 | 1 | 209 | 0.011 | 0.14 |
| 963 | TP63 | 303 | 0.015 | 1 | 37 | 0.002 | 0.13 |
| 964 | KRT17 | 2669 | 0.132 | 1 | 314 | 0.017 | 0.13 |

| | | | | | | | |
|---|---|---|---|---|---|---|---|
| 965 | COL1A1 | 69 | 0.003 | 1 | 8 | 0.000 | 0.13 |
| 966 | CXCL2 | 1589 | 0.078 | 1 | 178 | 0.010 | 0.12 |
| 967 | CCL15 | 18 | 0.001 | 1 | 2 | 0.000 | 0.12 |
| 968 | ELMO1 | 27 | 0.001 | 1 | 3 | 0.000 | 0.12 |
| 969 | TNFAIP3 | 614 | 0.030 | 1 | 68 | 0.004 | 0.12 |
| 970 | INHBA | 222 | 0.011 | 1 | 22 | 0.001 | 0.11 |
| 971 | SOX15 | 298 | 0.015 | 1 | 29 | 0.002 | 0.11 |
| 972 | IL1B | 377 | 0.019 | 1 | 36 | 0.002 | 0.11 |
| 973 | SERPINB2 | 233 | 0.012 | 1 | 22 | 0.001 | 0.10 |
| 974 | CXCL1 | 640 | 0.032 | 1 | 59 | 0.003 | 0.10 |
| 975 | CXCL8 | 653 | 0.032 | 1 | 58 | 0.003 | 0.10 |
| 976 | DLL1 | 24 | 0.001 | 1 | 2 | 0.000 | 0.09 |
| 977 | SFRP1 | 648 | 0.032 | 1 | 51 | 0.003 | 0.09 |
| 978 | SFN | 6460 | 0.319 | 1 | 507 | 0.028 | 0.09 |
| 979 | CBLC | 188 | 0.009 | 1 | 13 | 0.001 | 0.08 |
| 980 | CDH1 | 1637 | 0.081 | 1 | 113 | 0.006 | 0.08 |
| 981 | HBEGF | 75 | 0.004 | 1 | 5 | 0.000 | 0.07 |
| 982 | LAMA3 | 1951 | 0.096 | 1 | 126 | 0.007 | 0.07 |
| 983 | LAMC2 | 4464 | 0.220 | 1 | 277 | 0.015 | 0.07 |
| 984 | KLK5 | 311 | 0.015 | 1 | 19 | 0.001 | 0.07 |
| 985 | ACTA2 | 17 | 0.001 | 1 | 1 | 0.000 | 0.06 |
| 986 | ARHGEF16 | 55 | 0.003 | 1 | 3 | 0.000 | 0.06 |
| 987 | IL1A | 1331 | 0.066 | 1 | 57 | 0.003 | 0.05 |
| 988 | FGFBP1 | 2307 | 0.114 | 1 | 81 | 0.004 | 0.04 |
| 989 | DSG3 | 978 | 0.048 | 1 | 28 | 0.002 | 0.03 |
| 990 | ITGB6 | 415 | 0.020 | 1 | 3 | 0.000 | 0.01 |
| 991 | COL17A1 | 517 | 0.026 | 1 | 3 | 0.000 | 0.01 |

## Appendix 10: List of deregulated pathways in TRIM24-OE MCF10A cells by HTG Edgeseq analysis


### Hallmarks analysis for Upregulated genes

| Gene Set Name [# Genes (K)] | Description | # Genes in Overlap (k) | k/K | p-value | FDR q-value |
|---|---|---|---|---|---|
| HALLMARK_APOPTOSIS [161] | Genes mediating programmed cell death (apoptosis) by activation of caspases. | 18 | | $1.13\ e^{-19}$ | $5.65\ e^{-18}$ |
| HALLMARK_EPITHELIAL_MESENCHYMAL_TRANSITION [200] | Genes defining epithelial-mesenchymal transition, as in wound healing, fibrosis and metastasis. | 18 | | $5.82\ e^{-18}$ | $1.46\ e^{-16}$ |
| HALLMARK_UV_RESPONSE_DN [144] | Genes down-regulated in response to ultraviolet (UV) radiation. | 12 | | $5.43\ e^{-12}$ | $9.04\ e^{-11}$ |
| HALLMARK_COMPLEMENT [200] | Genes encoding components of the complement system, which is part of the innate immune system. | 12 | | $2.54\ e^{-10}$ | $2.54\ e^{-9}$ |
| HALLMARK_KRAS_SIGNALING_UP [200] | Genes up-regulated by KRAS activation. | 12 | | $2.54\ e^{-10}$ | $2.54\ e^{-9}$ |
| HALLMARK_ALLOGRAFT_REJECTION [200] | Genes up-regulated during transplant rejection. | 11 | | $3.59\ e^{-9}$ | $2.99\ e^{-8}$ |
| HALLMARK_ANGIOGENESIS [36] | Genes up-regulated during formation of blood vessels (angiogenesis). | 6 | | $1.79\ e^{-8}$ | $1.28\ e^{-7}$ |
| HALLMARK_ESTROGEN_RESPONSE_LATE [200] | Genes defining late response to estrogen. | 10 | | $4.61\ e^{-8}$ | $2.56\ e^{-7}$ |
| HALLMARK_P53_PATHWAY [200] | Genes involved in p53 pathways and networks. | 10 | | $4.61\ e^{-8}$ | $2.56\ e^{-7}$ |
| HALLMARK_TGF_BETA_SIGNALING [54] | Genes up-regulated in response to TGFB1 [GeneID=7040]. | 6 | | $2.21\ e^{-7}$ | $1.11\ e^{-6}$ |

MSigDB
Molecular Signatures Database

# Pathway analysis for Upregulated genes

| Gene Set Name [# Genes (K)] | Description | # Genes in Overlap (k) | k/K | p-value | FDR q-value |
|---|---|---|---|---|---|
| ONDER_CDH1_TARGETS_2_UP [256] | Genes up-regulated in HMLE cells (immortalized nontransformed mammary epithelium) after E-cadhedrin (CDH1) [GeneID=999] knockdown by RNAi. | 23 | | $1.28\ e^{-22}$ | $4.33\ e^{-19}$ |
| SENESE_HDAC1_TARGETS_DN [260] | Genes down-regulated in U2OS cells (osteosarcoma) upon knockdown of HDAC1 [GeneID=3065] by RNAi. | 21 | | $8.83\ e^{-20}$ | $1.5\ e^{-16}$ |
| VART_KSHV_INFECTION_ANGIOGENIC_MARKERS ERS_UP [165] | Angiogenic markers up-regulated in lymph endothelial cells upon infection with KSHV (Kaposi's sarcoma herpes virus). | 18 | | $1.77\ e^{-19}$ | $2.01\ e^{-16}$ |
| LEE_BMP2_TARGETS_UP [745] | Genes up-regulated in uterus upon knockout of BMP2 [GeneID=650]. | 30 | | $3.68\ e^{-19}$ | $3.12\ e^{-16}$ |
| KOKKINAKIS_METHIONINE_DEPRIVATION_96HR 6HR_UP [117] | Genes up-regulated in MEWO cells (melanoma) after 96 h of methionine [PubChem=876] deprivation. | 16 | | $4.61\ e^{-19}$ | $3.13\ e^{-16}$ |
| SCHUETZ_BREAST_CANCER_DUCTAL_INVASIVE_ VE_UP [351] | Genes up-regulated in invasive ductal carcinoma (IDC) relative to ductal carcinoma in situ (DCIS, non-invasive). | 22 | | $2.67\ e^{-18}$ | $1.51\ e^{-15}$ |

MSigDB
Molecular Signatures Database

# Pathway analysis for Downregulated genes

| Gene Set Name [# Genes (K)] | Description | # Genes in Overlap (k) | k/K | p-value | FDR q-value |
|---|---|---|---|---|---|
| ONDER_CDH1_TARGETS_2_DN [464] | Genes down-regulated in HMLE cells (immortalized nontransformed mammary epithelium) after E-cadhedrin (CDH1) [GeneID=999] knockdown by RNAi. | 80 | | $1.28\ e^{-93}$ | $6.79\ e^{-90}$ |
| SMID_BREAST_CANCER_LUMINAL_B_DN [564] | Genes down-regulated in the luminal B subtype of breast cancer. | 54 | | $2.96\ e^{-48}$ | $7.84\ e^{-45}$ |
| SMID_BREAST_CANCER_BASAL_UP [648] | Genes up-regulated in basal subtype of breast cancer samles. | 55 | | $2.67\ e^{-46}$ | $4.71\ e^{-43}$ |
| CHARAFE_BREAST_CANCER_LUMINAL_VS_BASAL SAL_DN [455] | Genes down-regulated in luminal-like breast cancer cell lines compared to the basal-like ones. | 43 | | $3.78\ e^{-38}$ | $5.01\ e^{-35}$ |
| ZWANG_CLASS_3_TRANSIENTLY_INDUCED_BY_E Y_EGF [222] | Class III of genes transiently induced by EGF [GeneID =1950] in 184A1 cells (mammary epithelium). | 34 | | $1.49\ e^{-37}$ | $1.58\ e^{-34}$ |
| LEI_MYB_TARGETS [318] | Myb-regulated genes in MCF7 (breast cancer) and lung epithelial cell lines overexpressing MYBL2, MYBL1 or MYB [GeneID=4605;4603;4602]. | 36 | | $7.55\ e^{-35}$ | $6.67\ e^{-32}$ |
| DELYS_THYROID_CANCER_UP [443] | Genes up-regulated in papillary thyroid carcinoma (PTC) compared to normal tissue. | 40 | | $1.01\ e^{-34}$ | $7.64\ e^{-32}$ |
| GSE9988_LOW_LPS_VS_CTRL_TREATED_MONOCY OCYTE_UP [200] | Genes up-regulated in comparison of monocytes treated with 1 ng/ml LPS (TLR4 agonist) versus monocytes treated with control IgG. | 31 | | $1.78\ e^{-34}$ | $1.18\ e^{-31}$ |
| JAEGER_METASTASIS_DN [258] | Genes down-regulated in metastases from malignant melanoma compared to the primary tumors. | 33 | | $8.66\ e^{-34}$ | $5.11\ e^{-31}$ |

## References


1. Gradishar WJ, Anderson BO, Balassanian R, Blair SL, Burstein HJ, Cyr A, Elias AD, Farrar WB, Forero A, Giordano SH, Goetz M, Goldstein LJ, Hudis CA, Isakoff SJ, Marcom PK, Mayer IA, et al. Breast Cancer Version 2.2015. Journal of the National Comprehensive Cancer Network : JNCCN. 2015; 13(4):448-475.
2. Dai X, Li T, Bai Z, Yang Y, Liu X, Zhan J and Shi B. Breast cancer intrinsic subtype classification, clinical use and future trends. American journal of cancer research. 2015; 5(10):2929-2943.
3. Cancer Genome Atlas N. Comprehensive molecular portraits of human breast tumours. Nature. 2012; 490(7418):61-70.
4. Higgins MJ and Baselga J. Targeted therapies for breast cancer. The Journal of clinical investigation. 2011; 121(10):3797-3803.
5. Gradishar WJ. Adjuvant endocrine therapy for early breast cancer: the story so far. Cancer Invest. 28(4):433-442.
6. Altundag K and Ibrahim NK. Aromatase inhibitors in breast cancer: an overview. Oncologist. 2006; 11(6):553-562.
7. Baum M. The ATAC (Arimidex, Tamoxifen, Alone or in Combination) adjuvant breast cancer trial in postmenopausal patients: factors influencing the success of patient recruitment. Eur J Cancer. 2002; 38(15):1984-1986.
8. Crivellari D, Sun Z, Coates AS, Price KN, Thurlimann B, Mouridsen H, Mauriac L, Forbes JF, Paridaens RJ, Castiglione-Gertsch M, Gelber RD, Colleoni M, Lang I, Del Mastro L, Gladieff L, Rabaglio M, et al. Letrozole compared with tamoxifen for elderly patients with endocrine-responsive early breast cancer: the BIG 1-98 trial. J Clin Oncol. 2008; 26(12):1972-1979.
9. Hassan MS, Ansari J, Spooner D and Hussain SA. Chemotherapy for breast cancer (Review). Oncology reports. 2010; 24(5):1121-1131.
10. Jahanzeb M. Adjuvant trastuzumab therapy for HER2-positive breast cancer. Clinical breast cancer. 2008; 8(4):324-333.
11. De Craene B and Berx G. Regulatory networks defining EMT during cancer initiation and progression. Nature reviews Cancer. 2013; 13(2):97-110.
12. Paget S. The distribution of secondary growths in cancer of the breast. 1889. Cancer metastasis reviews. 1989; 8(2):98-101.
13. Wang Y and Zhou BP. Epithelial-mesenchymal transition in breast cancer progression and metastasis. Chinese journal of cancer. 2011; 30(9):603-611.
14. Woodhouse EC, Chuaqui RF and Liotta LA. General mechanisms of metastasis. Cancer. 1997; 80(8 Suppl):1529-1537.
15. Bill R and Christofori G. The relevance of EMT in breast cancer metastasis: Correlation or causality? FEBS letters. 2015; 589(14):1577-1587.
16. Lu J, Guo H, Treekitkarnmongkol W, Li P, Zhang J, Shi B, Ling C, Zhou X, Chen T, Chiao PJ, Feng X, Seewaldt VL, Muller WJ, Sahin A, Hung MC and Yu D. 14-3-3zeta Cooperates with ErbB2 to promote ductal carcinoma in situ progression to invasive breast cancer by inducing epithelial-mesenchymal transition. Cancer cell. 2009; 16(3):195-207.
17. Singh A and Settleman J. EMT, cancer stem cells and drug resistance: an emerging axis of evil in the war on cancer. Oncogene. 2010; 29(34):4741-4751.
18. Thiery JP, Acloque H, Huang RY and Nieto MA. Epithelial-mesenchymal transitions in development and disease. Cell. 2009; 139(5):871-890.

19. Ye X and Weinberg RA. Epithelial-Mesenchymal Plasticity: A Central Regulator of Cancer Progression. Trends in cell biology. 2015.
20. Lamouille S, Xu J and Derynck R. Molecular mechanisms of epithelial-mesenchymal transition. Nature reviews Molecular cell biology. 2014; 15(3):178-196.
21. Yang F, Sun L, Li Q, Han X, Lei L, Zhang H and Shang Y. SET8 promotes epithelial-mesenchymal transition and confers TWIST dual transcriptional activities. The EMBO journal. 2012; 31(1):110-123.
22. Yang MH, Hsu DS, Wang HW, Wang HJ, Lan HY, Yang WH, Huang CH, Kao SY, Tzeng CH, Tai SK, Chang SY, Lee OK and Wu KJ. Bmi1 is essential in Twist1-induced epithelial-mesenchymal transition. Nature cell biology. 2010; 12(10):982-992.
23. Yang MH, Wu MZ, Chiou SH, Chen PM, Chang SY, Liu CJ, Teng SC and Wu KJ. Direct regulation of TWIST by HIF-1alpha promotes metastasis. Nature cell biology. 2008; 10(3):295-305.
24. Sanchez-Tillo E, Lazaro A, Torrent R, Cuatrecasas M, Vaquero EC, Castells A, Engel P and Postigo A. ZEB1 represses E-cadherin and induces an EMT by recruiting the SWI/SNF chromatin-remodeling protein BRG1. Oncogene. 2010; 29(24):3490-3500.
25. Postigo AA, Depp JL, Taylor JJ and Kroll KL. Regulation of Smad signaling through a differential recruitment of coactivators and corepressors by ZEB proteins. The EMBO journal. 2003; 22(10):2453-2462.
26. Hanahan D and Weinberg RA. Hallmarks of cancer: the next generation. Cell. 2011; 144(5):646-674.
27. Warburg O. On the origin of cancer cells. Science. 1956; 123(3191):309-314.
28. DeBerardinis RJ, Lum JJ, Hatzivassiliou G and Thompson CB. The biology of cancer: metabolic reprogramming fuels cell growth and proliferation. Cell metabolism. 2008; 7(1):11-20.
29. Deberardinis RJ, Sayed N, Ditsworth D and Thompson CB. Brick by brick: metabolism and tumor cell growth. Current opinion in genetics & development. 2008; 18(1):54-61.
30. Jones RG and Thompson CB. Tumor suppressors and cell metabolism: a recipe for cancer growth. Genes & development. 2009; 23(5):537-548.
31. Dang CV. The interplay between MYC and HIF in the Warburg effect. Ernst Schering Foundation symposium proceedings. 2007; (4):35-53.
32. Schwartzenberg-Bar-Yoseph F, Armoni M and Karnieli E. The tumor suppressor p53 down-regulates glucose transporters GLUT1 and GLUT4 gene expression. Cancer research. 2004; 64(7):2627-2633.
33. Bensaad K, Tsuruta A, Selak MA, Vidal MN, Nakano K, Bartrons R, Gottlieb E and Vousden KH. TIGAR, a p53-inducible regulator of glycolysis and apoptosis. Cell. 2006; 126(1):107-120.
34. Weinberg SE and Chandel NS. Targeting mitochondria metabolism for cancer therapy. Nature chemical biology. 2015; 11(1):9-15.
35. Viale A, Corti D and Draetta GF. Tumors and mitochondrial respiration: a neglected connection. Cancer research. 2015; 75(18):3685-3686.
36. Hatakeyama S. TRIM proteins and cancer. Nature reviews Cancer. 2011; 11(11):792-804.
37. Herquel B, Ouararhni K and Davidson I. The TIF1alpha-related TRIM cofactors couple chromatin modifications to transcriptional regulation, signaling and tumor suppression. Transcription. 2011; 2(5):231-236.

38. Zeng L and Zhou MM. Bromodomain: an acetyl-lysine binding domain. FEBS letters. 2002; 513(1):124-128.
39. Wysocka J, Swigut T, Xiao H, Milne TA, Kwon SY, Landry J, Kauer M, Tackett AJ, Chait BT, Badenhorst P, Wu C and Allis CD. A PHD finger of NURF couples histone H3 lysine 4 trimethylation with chromatin remodelling. Nature. 2006; 442(7098):86-90.
40. Le Douarin B, Zechel C, Garnier JM, Lutz Y, Tora L, Pierrat P, Heery D, Gronemeyer H, Chambon P and Losson R. The N-terminal part of TIF1, a putative mediator of the ligand-dependent activation function (AF-2) of nuclear receptors, is fused to B-raf in the oncogenic protein T18. The EMBO journal. 1995; 14(9):2020-2033.
41. Le Douarin B, Nielsen AL, Garnier JM, Ichinose H, Jeanmougin F, Losson R and Chambon P. A possible involvement of TIF1 alpha and TIF1 beta in the epigenetic control of transcription by nuclear receptors. The EMBO journal. 1996; 15(23):6701-6715.
42. Venturini L, You J, Stadler M, Galien R, Lallemand V, Koken MH, Mattei MG, Ganser A, Chambon P, Losson R and de The H. TIF1gamma, a novel member of the transcriptional intermediary factor 1 family. Oncogene. 1999; 18(5):1209-1217.
43. Beckstead R, Ortiz JA, Sanchez C, Prokopenko SN, Chambon P, Losson R and Bellen HJ. Bonus, a Drosophila homolog of TIF1 proteins, interacts with nuclear receptors and can inhibit betaFTZ-F1-dependent transcription. Mol Cell. 2001; 7(4):753-765.
44. Remboutsika E, Lutz Y, Gansmuller A, Vonesch JL, Losson R and Chambon P. The putative nuclear receptor mediator TIF1alpha is tightly associated with euchromatin. J Cell Sci. 1999; 112 ( Pt 11):1671-1683.
45. Teyssier C, Ou CY, Khetchoumian K, Losson R and Stallcup MR. Transcriptional intermediary factor 1alpha mediates physical interaction and functional synergy between the coactivator-associated arginine methyltransferase 1 and glucocorticoid receptor-interacting protein 1 nuclear receptor coactivators. Mol Endocrinol. 2006; 20(6):1276-1286.
46. Torres-Padilla ME and Zernicka-Goetz M. Role of TIF1alpha as a modulator of embryonic transcription in the mouse zygote. J Cell Biol. 2006; 174(3):329-338.
47. Kikuchi M, Okumura F, Tsukiyama T, Watanabe M, Miyajima N, Tanaka J, Imamura M and Hatakeyama S. TRIM24 mediates ligand-dependent activation of androgen receptor and is repressed by a bromodomain-containing protein, BRD7, in prostate cancer cells. Biochim Biophys Acta. 2009; 1793(12):1828-1836.
48. Khetchoumian K, Teletin M, Tisserand J, Mark M, Herquel B, Ignat M, Zucman-Rossi J, Cammas F, Lerouge T, Thibault C, Metzger D, Chambon P and Losson R. Loss of Trim24 (Tif1alpha) gene function confers oncogenic activity to retinoic acid receptor alpha. Nature genetics. 2007; 39(12):1500-1506.
49. Tisserand J, Khetchoumian K, Thibault C, Dembele D, Chambon P and Losson R. Tripartite motif 24 (Trim24/Tif1alpha) tumor suppressor protein is a novel negative regulator of interferon (IFN)/signal transducers and activators of transcription (STAT) signaling pathway acting through retinoic acid receptor alpha (Raralpha) inhibition. J Biol Chem. 2011; 286(38):33369-33379.
50. Herquel B, Ouararhni K, Martianov I, Le Gras S, Ye T, Keime C, Lerouge T, Jost B, Cammas F, Losson R and Davidson I. Trim24-repressed VL30 retrotransposons regulate gene expression by producing noncoding RNA. Nature structural & molecular biology. 2013; 20(3):339-346.
51. Jiang S, Minter LC, Stratton SA, Yang P, Abbas HA, Akdemir ZC, Pant V, Post S, Gagea M, Lee RG, Lozano G and Barton MC. TRIM24 suppresses development of spontaneous

hepatic lipid accumulation and hepatocellular carcinoma in mice. Journal of hepatology. 2015; 62(2):371-379.
52. Fraser RA, Heard DJ, Adam S, Lavigne AC, Le Douarin B, Tora L, Losson R, Rochette-Egly C and Chambon P. The putative cofactor TIF1alpha is a protein kinase that is hyperphosphorylated upon interaction with liganded nuclear receptors. J Biol Chem. 1998; 273(26):16199-16204.
53. Allton K, Jain AK, Herz HM, Tsai WW, Jung SY, Qin J, Bergmann A, Johnson RL and Barton MC. Trim24 targets endogenous p53 for degradation. Proc Natl Acad Sci U S A. 2009; 106(28):11612-11616.
54. Jain AK, Allton K, Duncan AD and Barton MC. TRIM24 is a p53-induced E3-ubiquitin ligase that undergoes ATM-mediated phosphorylation and autodegradation during DNA damage. Mol Cell Biol. 2014; 34(14):2695-2709.
55. Tsai WW, Wang Z, Yiu TT, Akdemir KC, Xia W, Winter S, Tsai CY, Shi X, Schwarzer D, Plunkett W, Aronow B, Gozani O, Fischle W, Hung MC, Patel DJ and Barton MC. TRIM24 links a non-canonical histone signature to breast cancer. Nature. 2010; 468(7326):927-932.
56. Chambon M, Orsetti B, Berthe ML, Bascoul-Mollevi C, Rodriguez C, Duong V, Gleizes M, Thenot S, Bibeau F, Theillet C and Cavailles V. Prognostic significance of TRIM24/TIF-1alpha gene expression in breast cancer. Am J Pathol. 2011; 178(4):1461-1469.
57. Li H, Sun L, Tang Z, Fu L, Xu Y, Li Z, Luo W, Qiu X and Wang E. Overexpression of TRIM24 correlates with tumor progression in non-small cell lung cancer. PloS one. 2012; 7(5):e37657.
58. Cui Z, Cao W, Li J, Song X, Mao L and Chen W. TRIM24 overexpression is common in locally advanced head and neck squamous cell carcinoma and correlates with aggressive malignant phenotypes. PloS one. 2013; 8(5):e63887.
59. Wang J, Zhu J, Dong M, Yu H, Dai X and Li K. Knockdown of tripartite motif containing 24 by lentivirus suppresses cell growth and induces apoptosis in human colorectal cancer cells. Oncol Res. 2014; 22(1):39-45.
60. Miao ZF, Wang ZN, Zhao TT, Xu YY, Wu JH, Liu XY, Xu H, You Y and Xu HM. TRIM24 is upregulated in human gastric cancer and promotes gastric cancer cell growth and chemoresistance. Virchows Arch. 2015; 466(5):525-532.
61. Zhang LH, Yin AA, Cheng JX, Huang HY, Li XM, Zhang YQ, Han N and Zhang X. TRIM24 promotes glioma progression and enhances chemoresistance through activation of the PI3K/Akt signaling pathway. Oncogene. 2015; 34(5):600-610.
62. Xue D, Zhang X, Zhang X, Liu J, Li N, Liu C, Liu Y and Wang P. Clinical significance and biological roles of TRIM24 in human bladder carcinoma. Tumour Biol. 2015; 36(9):6849-6855.
63. Liu X, Huang Y, Yang D, Li X, Liang J, Lin L, Zhang M, Zhong K, Liang B and Li J. Overexpression of TRIM24 is associated with the onset and progress of human hepatocellular carcinoma. PloS one. 2014; 9(1):e85462.
64. Rivlin N, Katz S, Doody M, Sheffer M, Horesh S, Molchadsky A, Koifman G, Shetzer Y, Goldfinger N, Rotter V and Geiger T. Rescue of embryonic stem cells from cellular transformation by proteomic stabilization of mutant p53 and conversion into WT conformation. Proc Natl Acad Sci U S A. 2014; 111(19):7006-7011.
65. Garbe JC, Bhattacharya S, Merchant B, Bassett E, Swisshelm K, Feiler HS, Wyrobek AJ and Stampfer MR. Molecular distinctions between stasis and telomere attrition senescence barriers shown by long-term culture of normal human mammary epithelial cells. Cancer research. 2009; 69(19):7557-7568.

66. Stampfer MR and Bartley JC. Induction of transformation and continuous cell lines from normal human mammary epithelial cells after exposure to benzo[a]pyrene. Proc Natl Acad Sci U S A. 1985; 82(8):2394-2398.
67. Stampfer MR, Garbe J, Nijjar T, Wigington D, Swisshelm K and Yaswen P. Loss of p53 function accelerates acquisition of telomerase activity in indefinite lifespan human mammary epithelial cell lines. Oncogene. 2003; 22(34):5238-5251.
68. Debnath J, Muthuswamy SK and Brugge JS. Morphogenesis and oncogenesis of MCF-10A mammary epithelial acini grown in three-dimensional basement membrane cultures. Methods. 2003; 30(3):256-268.
69. Campeau E, Ruhl VE, Rodier F, Smith CL, Rahmberg BL, Fuss JO, Campisi J, Yaswen P, Cooper PK and Kaufman PD. A versatile viral system for expression and depletion of proteins in mammalian cells. PloS one. 2009; 4(8):e6529.
70. Geiss GK, Bumgarner RE, Birditt B, Dahl T, Dowidar N, Dunaway DL, Fell HP, Ferree S, George RD, Grogan T, James JJ, Maysuria M, Mitton JD, Oliveri P, Osborn JL, Peng T, et al. Direct multiplexed measurement of gene expression with color-coded probe pairs. Nat Biotechnol. 2008; 26(3):317-325.
71. Dennis G, Jr., Sherman BT, Hosack DA, Yang J, Gao W, Lane HC and Lempicki RA. DAVID: Database for Annotation, Visualization, and Integrated Discovery. Genome Biol. 2003; 4(5):P3.
72. Allred DC, Harvey JM, Berardo M and Clark GM. Prognostic and predictive factors in breast cancer by immunohistochemical analysis. Mod Pathol. 1998; 11(2):155-168.
73. Ferrick DA, Neilson A and Beeson C. Advances in measuring cellular bioenergetics using extracellular flux. Drug discovery today. 2008; 13(5-6):268-274.
74. Wen H, Li Y, Xi Y, Jiang S, Stratton S, Peng D, Tanaka K, Ren Y, Xia Z, Wu J, Li B, Barton MC, Li W, Li H and Shi X. ZMYND11 links histone H3.3K36me3 to transcription elongation and tumour suppression. Nature. 2014; 508(7495):263-268.
75. Subramanian A, Tamayo P, Mootha VK, Mukherjee S, Ebert BL, Gillette MA, Paulovich A, Pomeroy SL, Golub TR, Lander ES and Mesirov JP. Gene set enrichment analysis: a knowledge-based approach for interpreting genome-wide expression profiles. Proc Natl Acad Sci U S A. 2005; 102(43):15545-15550.
76. Jain AK, Allton K, Iacovino M, Mahen E, Milczarek RJ, Zwaka TP, Kyba M and Barton MC. p53 regulates cell cycle and microRNAs to promote differentiation of human embryonic stem cells. PLoS biology. 2012; 10(2):e1001268.
77. Parker JS, Mullins M, Cheang MC, Leung S, Voduc D, Vickery T, Davies S, Fauron C, He X, Hu Z, Quackenbush JF, Stijleman IJ, Palazzo J, Marron JS, Nobel AB, Mardis E, et al. Supervised risk predictor of breast cancer based on intrinsic subtypes. J Clin Oncol. 2009; 27(8):1160-1167.
78. Novak P, Jensen TJ, Garbe JC, Stampfer MR and Futscher BW. Stepwise DNA methylation changes are linked to escape from defined proliferation barriers and mammary epithelial cell immortalization. Cancer research. 2009; 69(12):5251-5258.
79. Stampfer M, LaBarge M and Garbe J. (2013). An Integrated Human Mammary Epithelial Cell Culture System for Studying Carcinogenesis and Aging. In: Schatten H, ed. Cell and Molecular Biology of Breast Cancer: Humana Press), pp. 323-361.
80. Brenner AJ, Stampfer MR and Aldaz CM. Increased p16 expression with first senescence arrest in human mammary epithelial cells and extended growth capacity with p16 inactivation. Oncogene. 1998; 17(2):199-205.

81. Garbe JC, Holst CR, Bassett E, Tlsty T and Stampfer MR. Inactivation of p53 function in cultured human mammary epithelial cells turns the telomere-length dependent senescence barrier from agonescence into crisis. Cell Cycle. 2007; 6(15):1927-1936.
82. Pierce JH, Arnstein P, DiMarco E, Artrip J, Kraus MH, Lonardo F, Di Fiore PP and Aaronson SA. Oncogenic potential of erbB-2 in human mammary epithelial cells. Oncogene. 1991; 6(7):1189-1194.
83. Chen JQ and Russo J. Dysregulation of glucose transport, glycolysis, TCA cycle and glutaminolysis by oncogenes and tumor suppressors in cancer cells. Biochim Biophys Acta. 2012; 1826(2):370-384.
84. Diers AR, Broniowska KA, Chang CF and Hogg N. Pyruvate fuels mitochondrial respiration and proliferation of breast cancer cells: effect of monocarboxylate transporter inhibition. The Biochemical journal. 2012; 444(3):561-571.
85. Zhang C, Liu J, Liang Y, Wu R, Zhao Y, Hong X, Lin M, Yu H, Liu L, Levine AJ, Hu W and Feng Z. Tumour-associated mutant p53 drives the Warburg effect. Nat Commun. 2013; 4:2935.
86. Kawauchi K, Araki K, Tobiume K and Tanaka N. p53 regulates glucose metabolism through an IKK-NF-kappaB pathway and inhibits cell transformation. Nature cell biology. 2008; 10(5):611-618.
87. Kim HR, Roe JS, Lee JE, Cho EJ and Youn HD. p53 regulates glucose metabolism by miR-34a. Biochem Biophys Res Commun. 2013; 437(2):225-231.
88. Yeung SJ, Pan J and Lee MH. Roles of p53, MYC and HIF-1 in regulating glycolysis - the seventh hallmark of cancer. Cell Mol Life Sci. 2008; 65(24):3981-3999.
89. Wise DR, DeBerardinis RJ, Mancuso A, Sayed N, Zhang XY, Pfeiffer HK, Nissim I, Daikhin E, Yudkoff M, McMahon SB and Thompson CB. Myc regulates a transcriptional program that stimulates mitochondrial glutaminolysis and leads to glutamine addiction. Proc Natl Acad Sci U S A. 2008; 105(48):18782-18787.
90. Gao P, Tchernyshyov I, Chang TC, Lee YS, Kita K, Ochi T, Zeller KI, De Marzo AM, Van Eyk JE, Mendell JT and Dang CV. c-Myc suppression of miR-23a/b enhances mitochondrial glutaminase expression and glutamine metabolism. Nature. 2009; 458(7239):762-765.
91. Li F, Wang Y, Zeller KI, Potter JJ, Wonsey DR, O'Donnell KA, Kim JW, Yustein JT, Lee LA and Dang CV. Myc stimulates nuclearly encoded mitochondrial genes and mitochondrial biogenesis. Mol Cell Biol. 2005; 25(14):6225-6234.
92. Ahmadian M, Suh JM, Hah N, Liddle C, Atkins AR, Downes M and Evans RM. PPARgamma signaling and metabolism: the good, the bad and the future. Nature medicine. 2013; 19(5):557-566.
93. Bonofiglio D, Gabriele S, Aquila S, Catalano S, Gentile M, Middea E, Giordano F and Ando S. Estrogen receptor alpha binds to peroxisome proliferator-activated receptor response element and negatively interferes with peroxisome proliferator-activated receptor gamma signaling in breast cancer cells. Clinical cancer research : an official journal of the American Association for Cancer Research. 2005; 11(17):6139-6147.
94. Filippakopoulos P, Qi J, Picaud S, Shen Y, Smith WB, Fedorov O, Morse EM, Keates T, Hickman TT, Felletar I, Philpott M, Munro S, McKeown MR, Wang Y, Christie AL, West N, et al. Selective inhibition of BET bromodomains. Nature. 2010; 468(7327):1067-1073.
95. Palmer WS, Poncet-Montange G, Liu G, Petrocchi A, Reyna N, Subramanian G, Theroff J, Yau A, Kost-Alimova M, Bardenhagen JP, Leo E, Shepard HE, Tieu TN, Shi X, Zhan Y, Zhao S, et al. Structure-Guided Design of IACS-9571, a Selective High-Affinity Dual TRIM24-BRPF1 Bromodomain Inhibitor. J Med Chem. 2015.

96. Thakkar KN, Stratton SA and Barton MC. Tissue-specific metabolism and TRIM24. Aging. 2015.
97. Pathiraja TN, Thakkar KN, Jiang S, Stratton S, Liu Z, Gagea M, Shi X, Shah PK, Phan L, Lee MH, Andersen J, Stampfer M and Barton MC. TRIM24 links glucose metabolism with transformation of human mammary epithelial cells. Oncogene. 2015; 34(22):2836-2845.
98. Werner H and Bruchim I. IGF-1 and BRCA1 signalling pathways in familial cancer. The lancet oncology. 2012; 13(12):e537-544.
99. Arteaga CL, Sliwkowski MX, Osborne CK, Perez EA, Puglisi F and Gianni L. Treatment of HER2-positive breast cancer: current status and future perspectives. Nature reviews Clinical oncology. 2012; 9(1):16-32.
100. Zhu C, Qi X, Chen Y, Sun B, Dai Y and Gu Y. PI3K/Akt and MAPK/ERK1/2 signaling pathways are involved in IGF-1-induced VEGF-C upregulation in breast cancer. Journal of cancer research and clinical oncology. 2011; 137(11):1587-1594.
101. Moreno-Sanchez R, Rodriguez-Enriquez S, Marin-Hernandez A and Saavedra E. Energy metabolism in tumor cells. The FEBS journal. 2007; 274(6):1393-1418.
102. Yun J, Johnson JL, Hanigan CL and Locasale JW. Interactions between epigenetics and metabolism in cancers. Frontiers in oncology. 2012; 2:163.
103. Lu C and Thompson CB. Metabolic regulation of epigenetics. Cell metabolism. 2012; 16(1):9-17.
104. Mehta RG, Williamson E, Patel MK and Koeffler HP. A ligand of peroxisome proliferator-activated receptor gamma, retinoids, and prevention of preneoplastic mammary lesions. J Natl Cancer Inst. 2000; 92(5):418-423.
105. Saez E, Rosenfeld J, Livolsi A, Olson P, Lombardo E, Nelson M, Banayo E, Cardiff RD, Izpisua-Belmonte JC and Evans RM. PPAR gamma signaling exacerbates mammary gland tumor development. Genes & development. 2004; 18(5):528-540.
106. Dong C, Wu Y, Yao J, Wang Y, Yu Y, Rychahou PG, Evers BM and Zhou BP. G9a interacts with Snail and is critical for Snail-mediated E-cadherin repression in human breast cancer. The Journal of clinical investigation. 2012; 122(4):1469-1486.

## Vita

Kaushik Thakkar was born in Pune, in the state of Maharashtra, India. He was born on 13th May 1986 to Mr. Narendra Thakkar and Mrs. Lata Thakkar. After completing his high school at S.V Union High School, Kaushik, continued his college education at A.S.D.B Dadawala College of Sciences, University of Pune, Pune from 2003-2006. Kaushik graduated from college with a First class and obtained his Bachelor's in Science (B. Sc) majoring in Microbiology. Following his undergraduate training, Kaushik continued to pursue his Master's of Science majoring in Microbiology at Abasaheb Garware college, Pune from 2006-2008. Kaushik completed his Master's dissertation project titled "Synthesis, characterization and antimicrobial activity of extracellular crystalline silver nanoparticles (AgNPs) from *Morganella* sp." under the mentorship of Dr. Yogesh Shouche. After graduating from University of Pune in 2008, Kaushik worked at two Drug discovery companies, Piramal Life Sciences Limited and Lupin Limited as Research Associate (2008-2010). Kaushik joined the PhD graduate program at the Graduate School of Biomedical Sciences, a joint venture of The University of Texas Health Science Center at Houston and The University of Texas MD Anderson Cancer Center, Houston in August, 2010. Kaushik, joined the lab of Dr. Michelle C. Barton to pursue his PhD dissertation project. His project focuses on understanding the role of histone reader TRIM24 in regulating metabolic reprogramming and EMT in breast cancer.